

Chemical characterization of atmospheric organic
aerosol using ultrahigh resolution mass spectrometry
and molecular evidence for the association with
reactive oxygen species formation

Dissertation

for attaining the academic degree of “Doctor rerum naturalium”
(Dr. rer. nat.) at the Chemistry Department,
Faculty of Chemistry, Pharmaceutical Sciences, Geography and Geosciences
of the Johannes Gutenberg-University, Mainz

by

Yun Zhang

born in Tianjin, China



JOHANNES GUTENBERG
UNIVERSITÄT MAINZ

Mainz, March 2021

Faculty director: Prof. Dr. Tobias Reich
1st supervisor: Prof. Dr. Thorsten Hoffmann
2nd supervisor: Prof. Dr. Ulrich Pöschl

Date of Examination: 07/06/2021

D77-Dissertation of the Johannes Gutenberg University, Mainz

I hereby declare that I wrote the dissertation submitted without any unauthorized external assistance and used only sources acknowledged in the work. All textual passages which are appropriated verbatim or paraphrased from published and unpublished texts as well as all information obtained from oral sources are duly indicated and listed in accordance with bibliographical rules. In carrying out this research, I complied with the rules of standard scientific practice as formulated in the statutes of Johannes Gutenberg-University Mainz to insure standard scientific practice.

Mainz, March 2021

“格物致知”

“Extension of knowledge lies in the investigation of things”

《大学》

《Great Learning》

Zusammenfassung

Atmosphärische Aerosolpartikel sind stark mit dem globalen Klima, der Luftqualität und der menschlichen Gesundheit verbunden. Sie beeinflussen die Strahlungsbilanz der Erde direkt, indem sie die solare und terrestrische Strahlung streuen oder absorbieren, oder indirekt, indem sie als Wolkenkondensationskerne und Eiskerne dienen. Darüber hinaus kann die Ablagerung von eingeatmeten Aerosolpartikeln in den menschlichen Atemwegen zur Bildung von reaktiven Sauerstoffspezies (ROS) führen, die möglicherweise oxidativen Stress und Zellschäden verursachen. Insbesondere organisches Aerosol (OA) macht oft einen erheblichen Anteil der Partikelmasse aus und sein Beitrag zur partikelinduzierten Toxizität hat in den letzten Jahren mehr und mehr Aufmerksamkeit erhalten. Aufgrund der komplexen chemischen Zusammensetzung von Feinstaub (PM) ist das derzeitige Wissen jedoch unzureichend um die gesundheitsrelevanten Auswirkungen abschließend zu beurteilen.

Das Ziel dieser Arbeit war i) die chemische Zusammensetzung von OA-Proben, die in verschiedenen Regionen gesammelt wurden, basierend auf ultrahochauflösender Massenspektrometrie (UHRMS) zu charakterisieren und ii) molekulare Hinweise auf den Zusammenhang zwischen der ROS-Bildung und partikelgetragenen organischen Verbindungen zu untersuchen. Insbesondere wurde eine neue Metrik, das "Maximum Carbonyl Ratio (MCR)" vorgeschlagen, um die UHRMS-Daten zu interpretieren.

Der erste Teil dieser Arbeit befasst sich mit in der Entwicklung einer Methode zur Analyse von atmosphärischen Aerosolpartikeln mit Durchmessern $\leq 2,5 \mu\text{m}$ ($\text{PM}_{2,5}$) und von im Labor erzeugten Proben von sekundären organischen Aerosolen (SOA). Die $\text{PM}_{2,5}$ -Aerosolproben wurden in vier chinesischen Megastädten (Peking, Shanghai, Guangzhou und Xi'an), einer mitteleuropäischen Stadt (Mainz, Deutschland) und einer abgelegenen Region (Hyytiälä, Finnland) gesammelt, während die SOA-Proben durch Ozonolyse von α -Pinen, β -Pinen und Limonen in einem Strömungsrohr bzw. durch Photooxidation von Isopren und Naphthalin in einer Smogkammer erzeugt wurden. Ultrahochleistungs-Flüssigkeitschromatographie (UHPLC) gekoppelt an ein Orbitrap-Massenspektrometer mit Elektrospray-Ionisation (ESI) wurde angewendet, um Tausende von organischen Verbindungen auf molekularer Ebene zu charakterisieren. Die Ergebnisse zeigen deutliche Unterschiede in der chemischen Zusammensetzung der organischen Verbindungen in den Proben aus den verschiedenen Regionen sowie in den SOA-Proben, die aus verschiedenen Vorläufern gebildet wurden. Beispielsweise wurden mehr aromatische organische Verbindungen und eine beträchtliche Anzahl von Organosulfaten mit langer Kohlenstoffkette und niedrigem Ungesättigtheitsgrad in Pekinger OA im Vergleich zu OA in Mainz beobachtet.

Der zweite Teil dieser Studie konzentriert sich auf die Anwendung der neuen Metrik MCR, die auf der Grundlage der aus den UHRMS-Daten gewonnenen molekularen Zusammensetzung berechnet und zur Abschätzung der maximalen Anzahl von Carbonylgruppen in einem Molekül verwendet werden kann. Darüber hinaus wurde durch die Kombination des MCR-Wertes mit dem traditionellen VK-Diagramm das MCR-Van Krevelen (MCR-VK)-Diagramm, ein aktualisiertes Visualisierungswerkzeug entwickelt. Entsprechend der Position typischer SOA-Verbindungen im MCR-VK-Diagramm (z. B. Pinonsäure oder 2-Methyl-Tetrole) wurde das Diagramm in fünf

spezifische Regionen unterteilt und zwar, sehr stark oxidierte organische Verbindungen, stark oxidierte organische Verbindungen, mittelmäßig oxidierte organische Verbindungen, oxidierte ungesättigte organische Verbindungen und stark ungesättigte organische Verbindungen. Anschließend wurde dieser Ansatz angewandt, um die Aerosolproben aus den verschiedenen Städten und den im Labor erzeugten SOA-Proben zu klassifizieren. Die Verteilung von Hyytiälä-OA im MCR-VK-Diagramm war dabei ähnlich wie die von α -Pinen-SOA und β -Pinen-SOA, was darauf hindeutet, dass Monoterpene die primäre OA-Quelle an diesem Standort im borealen Wald sind. Darüber hinaus wurden in Hyytiälä OA mehr sehr hoch oxidierte organische Verbindungen und hoch oxidierte organische Verbindungen im Vergleich zu denen in α und β -Pinen SOA beobachtet, was darauf hindeutet, dass die Partikel in der Umgebungsatmosphäre komplexere Oxidationsprozesse im Vergleich zu im Labor erzeugtem SOA durchlaufen haben. Dies deutet darauf hin, dass die Anwendung der MCR-Metrik und des MCR-VK-Diagramms helfen kann, die Quellen und Entstehungsprozesse der atmosphärischen OA-Komponenten, die mit dem UHRMS erfasst wurden, besser zu verstehen.

Schließlich wurden die vorgeschlagene MCR-Metrik und das MCR-VK-Diagramm verwendet, um gegebenenfalls auch gesundheitsrelevante organische Komponenten zu identifizieren, da die MCR-Werte Informationen über die Häufigkeit von hoch oxidierten Nicht-Carbonyl-Organismen (niedrige MCR-Werte, die oxidativen Stress verursachen können) und hoch elektrophilen organischen Verbindungen (hohe MCR-Werte, die elektrophilen Stress verursachen können) liefern. Die von PM_{2,5}-Proben aus der Umgebung und von im Labor erzeugten SOA-Proben in Wasser produzierten ROS wurden als Index zur Bewertung der Toxizität von Aerosolpartikeln quantifiziert. Die Ausbeute an ROS bezog sich auf die Summe der H₂O₂-Ausbeute und der Radikalausbeute, die mit einer fluorometrischen Sonde bzw. mit der paramagnetischen Elektronenresonanz gemessen wurden. Die Ergebnisse deuten darauf hin, dass die Gesamtintensität der oxidierten organischen Verbindungen (d.h. sehr hoch oxidierte organische Verbindungen, hoch oxidierte organische Verbindungen, intermediär oxidierte organische Verbindungen) in städtischen PM_{2,5}-Proben und im Labor erzeugten SOA signifikant positiv mit der ROS-Ausbeute korreliert, was darauf hindeutet, dass diese oxidierten organischen Verbindungen einen erheblichen Beitrag zur ROS-Bildung leisten.

Zusammenfassend lässt sich festhalten, dass die in dieser Arbeit entwickelte UHPLC-Orbitrap-MS-Methode sich als effektiv erwiesen hat, um die komplexe chemische Zusammensetzung in OA besser zu verstehen. Die vorgeschlagene MCR-Metrik und das Visualisierungstool des MCR-VK-Diagramms können zur Verbesserung der Klassifizierung von OA und zur Identifizierung der gesundheitsrelevanten organischen Komponenten verwendet werden. Dies liefert neue Einblicke, um die chemische Zusammensetzung, die Bildungsprozesse und die gesundheitlichen Auswirkungen von atmosphärischen Aerosolen besser zu verstehen.

Abstract

Atmospheric aerosol particles are strongly associated with global climate, air quality, and human health. They influence the Earth's radiative balance directly by scattering or absorbing solar and terrestrial radiation, or indirectly by serving as cloud condensation nuclei and ice nuclei. Moreover, the deposition of inhaled aerosol particles in the human respiratory tract can lead to the formation of reactive oxygen species (ROS), potentially causing oxidative stress and cell damage. Particularly, organic aerosol (OA) often accounts for a substantial fraction of particulate mass, and its contribution to particle-induced toxicity has received more attention. However, due to the complex chemical composition of fine particulate matter (PM), current knowledge is insufficient for qualitative characterization of the health-related organic compounds.

The aim of this work was i) to characterize the chemical composition of OA samples collected in ambient regions by using ultrahigh resolution mass spectrometry (UHRMS) and ii) to explore the molecular evidence for the association of ROS formation with organic compounds. In particular, a new metric 'maximum carbonyl ratio (MCR)' was proposed to interpret the UHRMS data by unveiling the information of carbonyl functional groups in the structures of these organic compounds.

The first part of this study was development of an analytical method for analysis of ambient particulate aerosol samples with diameters of $PM \leq 2.5 \mu m$ ($PM_{2.5}$) and laboratory-generated secondary organic aerosol (SOA) samples. The ambient $PM_{2.5}$ samples were collected in four Chinese megacities (Beijing, Shanghai, Guangzhou, and Xi'an), a central European city (Mainz, Germany), and a remote region (Hyytiälä, Finland), whereas SOA samples were generated by ozonolysis of α -pinene, β -pinene, and limonene in a flow tube, respectively and photo-oxidation of isoprene and naphthalene in a smog chamber, respectively. Ultrahigh performance liquid chromatography (UHPLC) coupled to the UHRMS-Orbitrap with electrospray ionization (ESI) was applied to characterize thousands of organic compounds at the molecular level. The results showed clear differences in the chemical composition of organic compounds in ambient samples from different regions as well as in SOA samples derived from different precursors, e.g., more aromatic organic compounds and a substantial number of organosulfates with long-carbon chain and low degree of unsaturation were observed in Beijing OA compared to OA in Mainz. It indicates that sources probably play important roles in the chemical processes of OA formation.

The second part of this study focused on the application of the new metric of MCR, which can be calculated based on the molecular composition obtained from the UHRMS data and be used to estimate the maximum number of carbonyl groups in a molecule. Furthermore, the MCR-Van Krevelen (MCR-VK) diagram, an updated visualization tool, was developed by the combination of the MCR value and the traditional VK diagram. According to the location of typical SOA compounds (e.g., pinonic acid and 2-methyl-tetrols) in the MCR-VK diagram, MCR-VK diagram was divided into five specific regions corresponding to very highly oxidized organic compounds, highly oxidized organic compounds, intermediately oxidized organic compounds, oxidized unsaturated organic compounds, and highly unsaturated organic compounds, respectively. Then, this approach was applied to classify the organic compounds observed in the ambient aerosol samples and laboratory-generated SOA samples and their distributions in the MCR-VK diagram

were obtained. The distribution of Hyytiälä OA in the MCR-VK diagram was similar with that of α -pinene SOA and β -pinene SOA, indicating that monoterpenes may be the primary OA source at this boreal forest site. Furthermore, more very highly oxidized organic compounds and highly oxidized organic compounds were observed in Hyytiälä OA compared to those in α/β -pinene SOA, indicating that the particles in the ambient atmosphere experienced more complex oxidation processes compared to the laboratory-generated SOA. This suggests that the application of MCR metric and MCR-VK diagram can help to better understand the sources and formation processes of atmospheric OA components detected by the UHRMS.

Finally, the proposed MCR metric and MCR-VK diagram were utilized to identify the health-relevant organics components, since the MCR values give the information about the abundance of highly oxidized non-carbonyl organics (low MCR values, which are able to cause oxidative stress) and highly electrophilic organic compounds (high MCR values, which can induce electrophilic stress). The ROS produced by ambient PM_{2.5} samples and laboratory-generated SOA samples in water was quantified as an index of assessing the toxicity of aerosol particles. The yield of ROS referred to the sum of H₂O₂ yield and radical yield, which were measured using a fluorometric probe and electron paramagnetic resonance, respectively. The results suggest that the total intensity of oxidized organic compounds (i.e., very highly oxidized organic compounds, highly oxidized organic compounds, intermediately oxidized organic compounds) in ambient urban PM_{2.5} samples and laboratory-generated SOA both had significantly positive correlations with the ROS yield, indicating that these oxidized organic compounds made considerable contribution to the ROS formation.

In conclusion, the UHPLC-Orbitrap MS method developed in this work has been proved to be effective to identify the complex chemical composition in OA. The proposed metric of MCR and the visualization tool of MCR-VK diagram can be used to improve the classification of OA and to identify the health-related organic components. This provides a new insight to better understand the chemical composition, formation processes, and health effects of atmospheric aerosols.

Table of contents

Zusammenfassung	I
Abstract	III
1 Introduction	1
1.1 Atmospheric aerosol	1
1.2 Secondary organic aerosol	5
1.2.1 Formation mechanisms	5
1.2.2 Gas-particle partitioning	7
1.2.3 Condensed phase chemistry	8
1.3 Mass spectrometry for the analysis of atmospheric aerosol	9
1.3.1 Online and offline mass spectrometry techniques	10
1.3.2 Ionization method	11
1.3.2.1 Electrospray ionization	12
1.3.3 High resolution mass spectrometer	14
1.3.3.1 Q-Exactive hybrid quadrupole-orbitrap mass spectrometer	16
1.3.4 Data analysis and visualization	17
1.4 Formation of reactive oxygen species by particulate matter	22
1.4.1 Endogenous formation of ROS	22
1.4.2 Components in PM related to ROS formation	24
1.5 Thesis objectives and outline	26
2 Analytical method development and chemical characterization of OA using ultrahigh resolution mass spectrometry	29
2.1 Introduction	30

2.2 Methodology	32
2.2.1 Sample collection and preparation	32
2.2.2 UHRMS analysis	33
2.2.3 UHRMS data processing.....	33
2.3 Results and discussion.....	35
2.3.1 General characteristics.....	35
2.3.2 CHO compounds.....	39
2.3.3 CHON compounds.....	43
2.3.4 CHN compounds.....	46
2.3.5 Sulfur compounds (CHOS and CHONS subgroups).....	48
2.4 Conclusion and implication.....	48
2.5 Additional information and results.....	50
2.5.1 Difference of chemical composition between ACN/H ₂ O and H ₂ O extraction method	50
3 The maximum carbonyl ratio as a metric for the structural classification of OA.....	53
3.1 Introduction	54
3.2 Material and methods	58
3.2.1 Laboratory SOA generation and collection	58
3.2.2 Ambient PM sampling	59
3.2.3 Sample preparation and UHRMS analysis	59
3.2.4 Data processing	60
3.3 Results and discussion.....	60
3.3.1 Definition of maximum carbonyl ratio (MCR).....	60
3.3.2 MCR-VK diagram	62
3.3.3 MCR-VK diagram application on aerosol samples.....	65

3.4 Conclusion and implication.....	68
4 Molecular evidence for the association of reactive oxygen species yield with oxidized organic compounds	71
4.1 Introduction	72
4.2 Material and methods	74
4.2.2 Laboratory SOA formation	75
4.2.3 UHRMS measurements and data processing	75
4.2.4 Quantification of H ₂ O ₂ yield.....	76
4.2.5 Measurement of radical yield by EPR	77
4.3 Results and discussion.....	77
4.3.1 MCR-VK diagram	77
4.3.2 Contribution of OOC and UOC in ambient and laboratory particulate aerosol samples.....	80
4.3.3 Yield and formation potential of ROS by ambient PM.....	81
4.3.4 Correlation between R _{OOC/UOC} and ROS yield	84
4.4 Conclusion and implication.....	87
5 Conclusions and Outlook.....	89
6 References	91
7 Appendix.....	107

1 Introduction

1.1 Atmospheric aerosol

Atmospheric aerosols, defined as solid or liquid particles suspended in air, are ubiquitous in Earth's atmosphere. They play a key role in many environmental processes and impact the climate (Pöschl, 2005; Seinfeld and Pandis, 2006). Aerosol particles influence the Earth's radiative balance directly by scattering and absorbing solar and terrestrial radiation, or indirectly by acting in the formation of clouds and precipitation as cloud condensation nuclei (CCN) and ice nuclei (IN) (Pöschl, 2005; Hallquist et al., 2009). Participating in heterogeneous chemical reactions and multiphase processes may affect the distribution and abundance of atmospheric trace gases (Pöschl, 2005; George et al., 2015). Moreover, atmospheric aerosol particles can have adverse effects on human health by entering and damaging the respiratory and cardiovascular system or causing infectious and allergic diseases (Pöschl, 2005; Brüggemann, 2015; Pöschl and Shiraiwa, 2015).

According to their origin, atmospheric aerosols can be classified as primary and secondary aerosols. Primary aerosols are directly emitted into the air from natural and anthropogenic sources, including biomass burning, combustion of fossil fuels, volcanic eruptions, wind-driven or traffic-related suspension of soil and dust, sea spray, and biological materials (plant and animal debris, microorganisms, pollen, spore, etc.). Secondary aerosols, on the other hand, are formed in the atmosphere by chemical reactions of gaseous precursors and gas-to-particle conversion (Pöschl, 2005; Seinfeld and Pandis, 2006). Figure 1.1.1 represents the formation, growth, and processing of atmospheric aerosols.

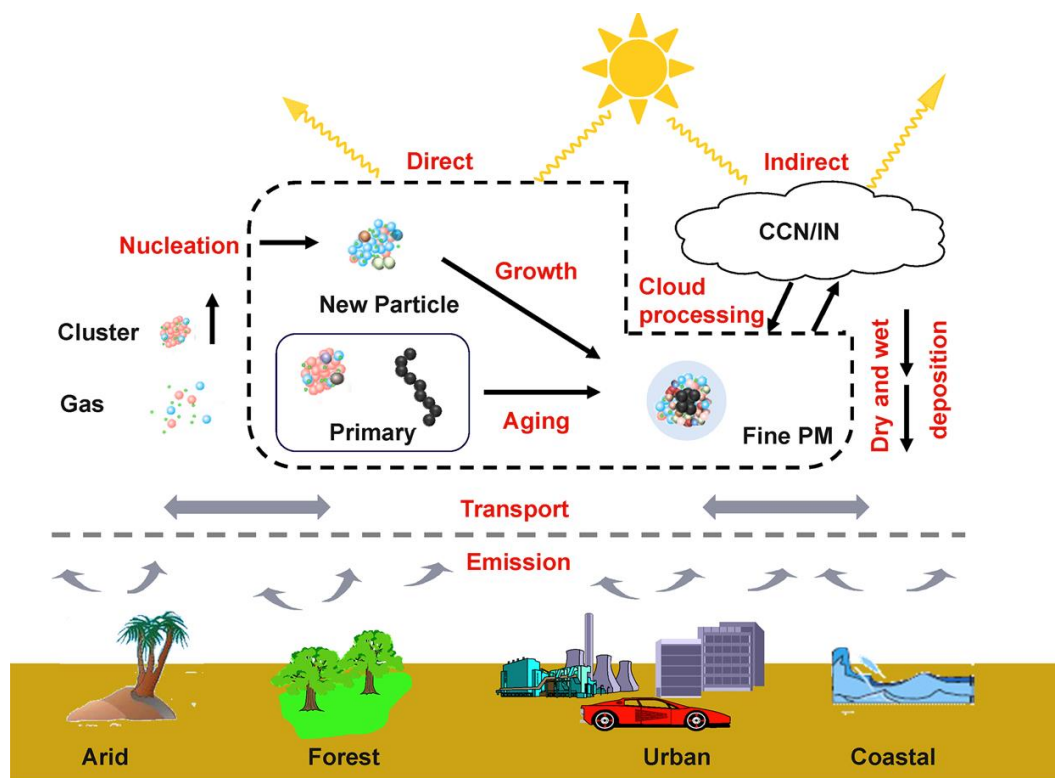


Figure 1.1.1: Schematic representation of the formation, growth and processing of atmospheric aerosols (Zhang et al., 2015).

The size of aerosol particles is mainly determined by their formation mechanisms. Particles larger than $1\ \mu\text{m}$ in diameter (coarse mode) are usually primary in nature and contribute largely to the mass of aerosol populations. Due to fast gravitational setting, long-range transport of these particles is rather limited resulting in short atmospheric lifetimes (Seinfeld and Pandis, 2006). Despite of their large size and low number concentration, primary particles in the coarse mode are essentially important for the formation of clouds and precipitation due to the ability to act as IN (Cantrell and Heymsfield, 2005; Seinfeld and Pandis, 2006; Vogel, 2014; Brüggemann, 2015). Particles smaller than $1\ \mu\text{m}$ in diameter, generally defined as fine mode, are typically secondary in nature and contribute largely to the number and surface area of particle populations. The fine mode can be further divided into accumulation mode ($0.1\text{--}1\ \mu\text{m}$), Aitken mode ($0.01\text{--}0.1\ \mu\text{m}$), and nucleation mode ($<0.01\ \mu\text{m}$) (Seinfeld and Pandis, 2006). Particles in the nucleation and the Aitken mode, formed by the condensation of low volatile compounds onto thermodynamically stable clusters, usually grow rapidly to the accumulation mode with the longest atmospheric lifetimes through condensation of vapors or coagulation with other particle (Kulmala et al., 2016). Fine particles are mainly removed from the atmosphere by wet deposition. Figure 1.1.2 provides an

overview of the size range and composition of atmospheric particles as well as the major types of multiphase chemical processes in the atmosphere.

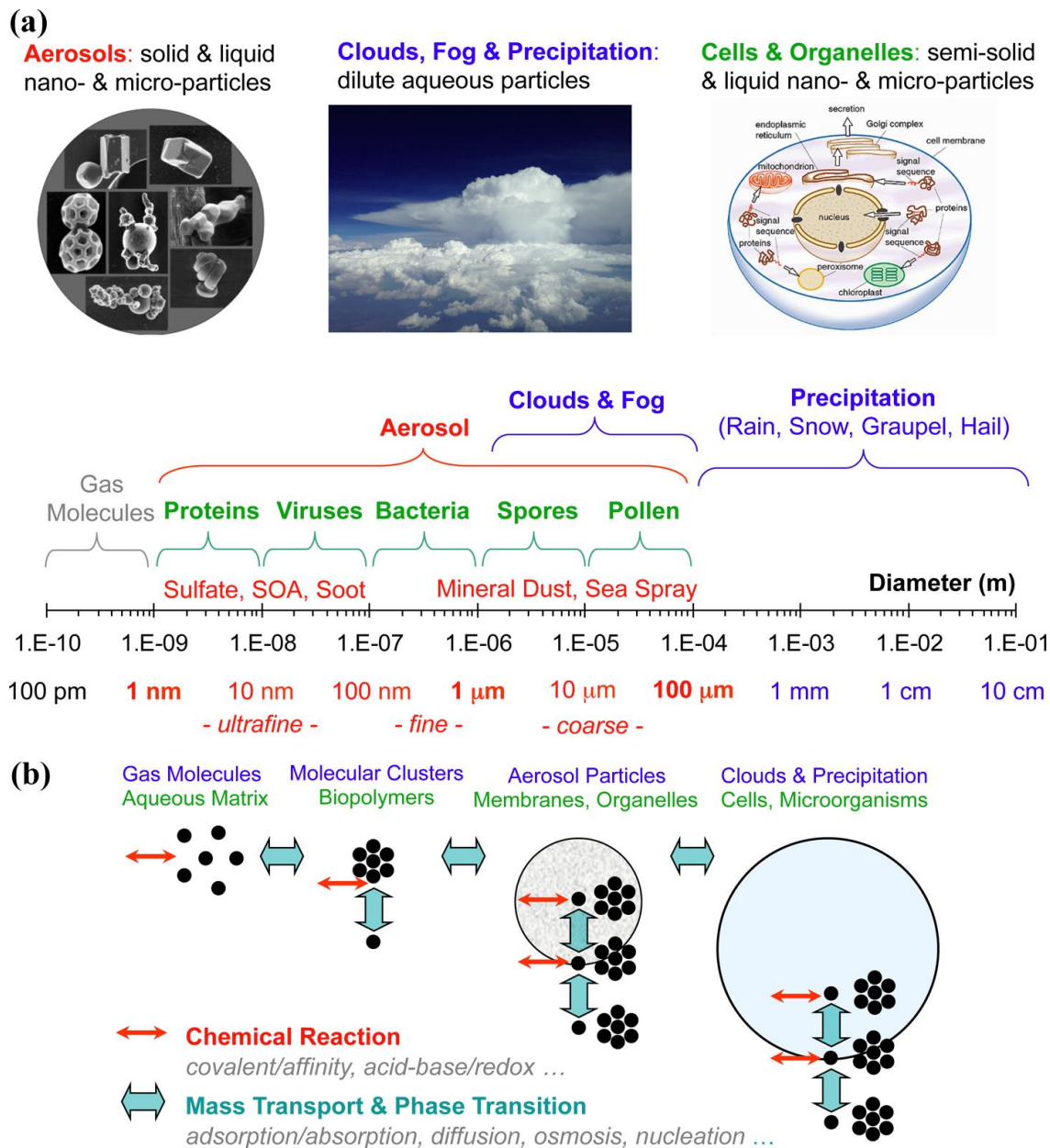


Figure 1.1.2: Overview of atmospheric aerosol particles: (a) Size range of aerosols, hydrometeors, cells and organelles. (b) Chemical reactions in the gas phase, at the interface, and in the particle bulk; mass transformation and phase transition in and between the gas phase, clusters, aerosols, cloud, and precipitation particles (Pöschl and Shiraiwa, 2015).

Atmospheric aerosol represents highly dynamic and complex system with a huge temporal and spatial variability in terms of chemical composition and size distribution. Concerning the chemical composition, atmospheric aerosols are complete mixtures consisting of inorganics and organics. The inorganic species have been observed with relatively high concentration in submicrometer aerosols at multiple locations around the world (Jimenez et al., 2009). The common inorganics include sulfate, nitrate, and ammonium, formed via the oxidation and neutralization of sulfur dioxide (SO_2), nitrogen oxides (NO_x) and ammonia (NH_3) (Koo et al., 2003; Fu et al., 2016). Organic components in atmospheric aerosol include hydrocarbons, alcohols, aldehydes, carboxylic acids, organosulfates, and organonitrates (Jimenez et al., 2009; Rincón et al., 2012; Wang et al., 2018). The knowledge of organic aerosols (OA) is still limited due to a variety and complexity of organic species in atmospheric aerosol. Figure 1.1.3 shows an overview of the inorganic species and organic components in atmospheric aerosols in the Northern Hemisphere, observed using aerosol mass spectrometer (AMS) measurements.

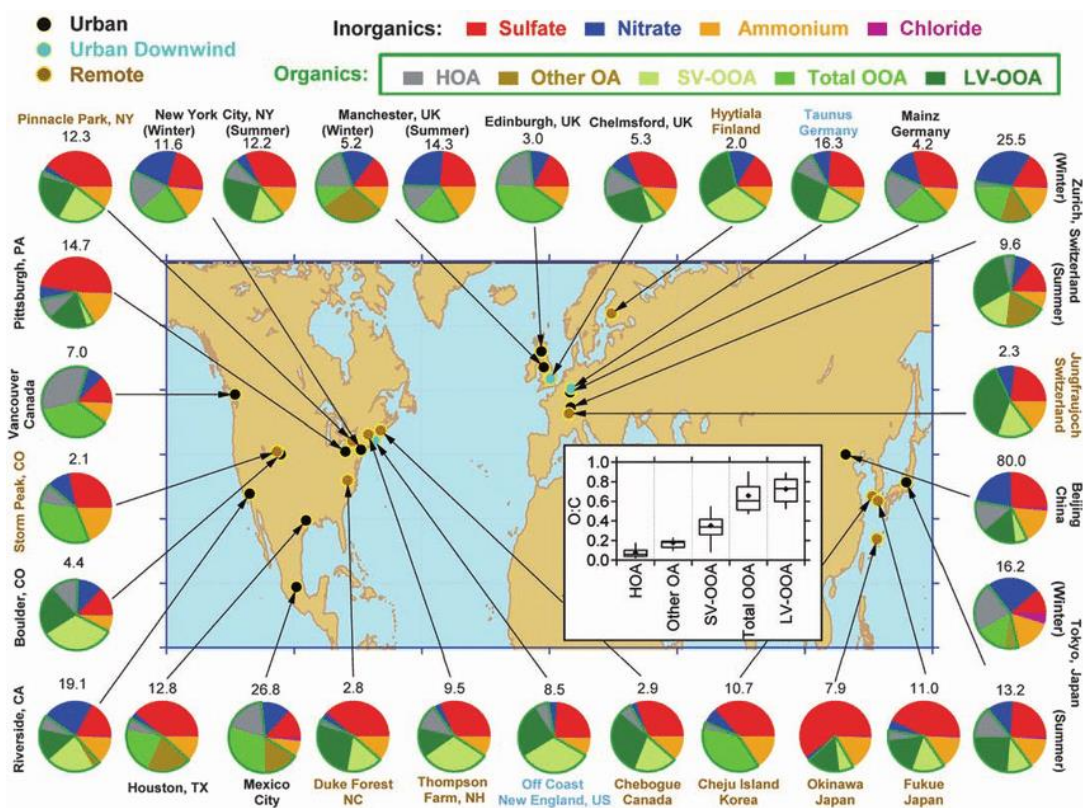


Figure 1.1.3: Total mass concentration ($\mu\text{g m}^{-3}$) and mass fractions of nonrefractory inorganic species and organic components in submicrometer aerosols at multi surface locations on the Northern Hemisphere. Organic aerosols are classified into hydrocarbon-like OA (HOA), semi-volatile oxygenated OA (SV-OOA) and low-volatile oxygenated OA (LV-OOA) (Jimenez et al., 2009).

1.2 Secondary organic aerosol

Organic aerosol (OA) constitutes 20–90% of tropospheric aerosol and there is increasing evidence that a major fraction of OA can be attributed to secondary organic aerosol (SOA) (Heald et al., 2005; Kroll and Seinfeld, 2008; Jimenez et al., 2009; Hallquist et al., 2009). SOA is formed by chemical reaction and gas-to-particle conversion of volatile organic compounds (VOCs) in the atmosphere, which may proceed through different pathways, as discussed in the following sections.

1.2.1 Formation mechanisms

The formation of secondary organic aerosol (SOA) starts with the emission of volatile organic compounds (VOCs) into the atmosphere, which are biogenic and anthropogenic in origin. On a global scale, the dominant precursors for SOA generation are biogenic VOCs, such as isoprene (C_5H_8), monoterpene ($C_{10}H_{16}$: α - and β -pinene, limonene, etc.), and sesquiterpenes ($C_{15}H_{24}$). Large amounts of biogenic VOCs emitted over forested areas like the Amazon rainforest and the boreal forest contribute to an increasing SOA fraction of local aerosol populations. Compared to the biogenic emissions, emissions of anthropogenic VOCs (e.g., alkanes and aromatics) are almost one order of magnitude smaller, however, they play a key role on local or regional scales (Atkinson & Arey, 2003; Goldstein and Galbally, 2007). VOCs release into the air and then react with atmospheric oxidants, such as hydroxyl radical ($\bullet OH$), ozone (O_3) and nitrate radical (NO_3). The produced condensable organic vapors form SOA by gas-to-particle conversion (i.e., condensation on pre-existing particles or nucleation). Figure 1.2.1 displays the formation mechanisms of atmospheric aerosols (Hoffmann et al., 2011).

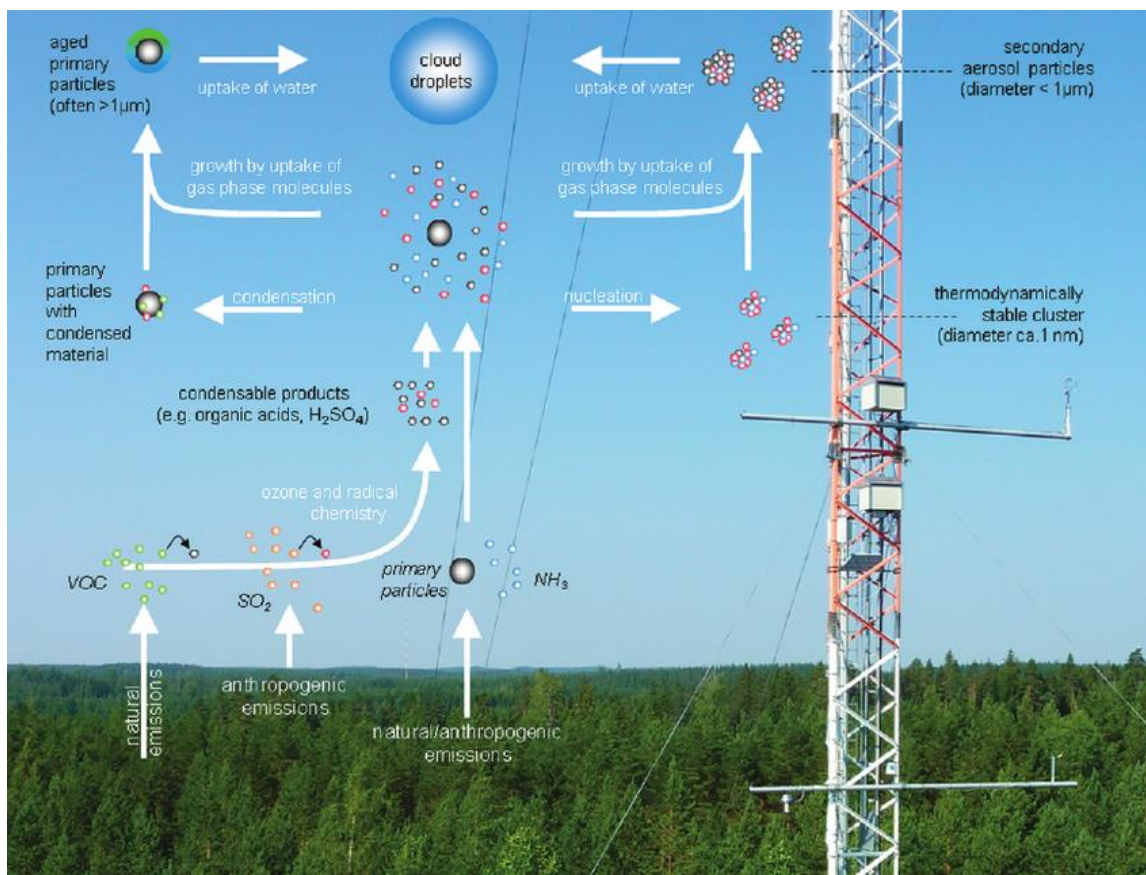


Figure 1.2.1 Formation mechanisms of atmospheric aerosols (Hoffmann et al., 2011).

VOCs react with $\bullet\text{OH}$, NO_3 , and O_3 in an initial step and form an alkyl radical which further react with oxygen producing an alkylperoxy radical (RO_2). Depending on the concentration of NO_x , HO_2 , and RO_2 , the RO_2 radicals recombine to products such as alcohols, hydroperoxides, peroxy nitrates or organic nitrates. Moreover, the RO_2 radicals can react with NO forming alkoxy radical (RO) which can isomerize or dissociate resulting again in an alkyl radical or react with oxygen to produce a carbonyl (Kroll and Seinfeld, 2008). Additionally, recent studies suggested that a class of extremely low-volatile organic compounds (ELVOCs) can be formed via further oxidation of alkylperoxy radicals. Intramolecular hydrogen shifts of an RO_2 radical followed by an autoxidation process involving oxygen addition at the alkyl radical site results in forming a more oxidized peroxy radical ($\text{R}_{\text{ELVOC}}\text{O}_2$) (Brüggemann, 2015; Jokinen et al., 2015; Mentel et al., 2015). Subsequently, ongoing H-shifts and oxygen additions lead to gas-phase formation of ELVOCs in dimer-, monomer-, and organic nitrate (in the presence of NO) channels (Ehn et al., 2014; Jokinen et al., 2014). Figure 1.2.2 shows a simplified schematic initial gas-phase oxidation of VOCs and formation of ELVOCs.

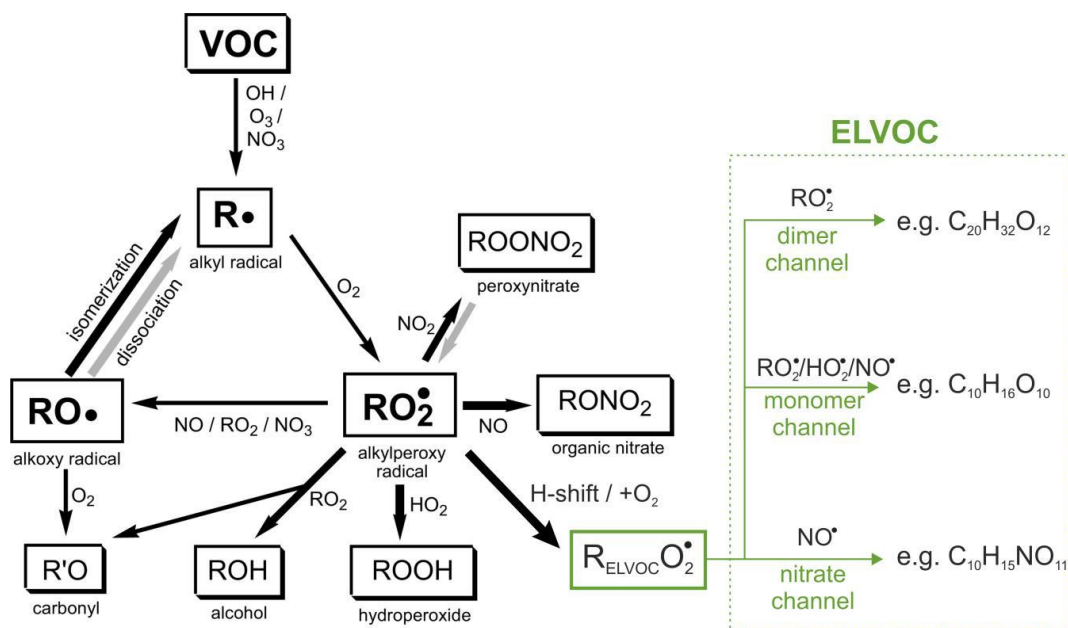


Figure 1.2.2: Simplified schematic of initial gas-phase oxidation of VOCs and formation of ELVOCs (green frames). The black arrows denote reactions that can lead to a volatility decrease, whereas the gray arrows denote reactions that can lead to a volatility increase (Brüggemann, 2015; Wang, 2018).

1.2.2 Gas-particle partitioning

SOA comprises large amounts of organic compounds with higher vapor pressure, considered as semi-volatile organic compounds (SVOCs), typically partition between the gas phase and the particle phase. Theoretical foundation on gas-particle partitioning of organic compounds was developed by Pankow (Pankow, 1994a, 1994b) and extended by Odum to SOA formation (Odum et al., 1996). Partitioning of each SVOCs is described by the equilibrium partitioning coefficient $K_{p,i}$ ($\text{m}^3 \mu\text{g}^{-1}$) or the saturation vapor concentration C_i^* ($\mu\text{g m}^{-3}$) (Donahue et al., 2006) as described by equation 1.1:

$$\frac{C_i^p}{C_i^g} = K_{p,i} C_{OA} = \frac{C_{OA}}{C_i^*} \quad (1.1)$$

where C_i^g and C_i^p represent the mass concentrations of species i per unit volume of air ($\mu\text{g m}^{-3}$) in the gas phase and in the particle phase, respectively, and C_{OA} is the mass concentration per unit volume of air ($\mu\text{g m}^{-3}$) of the total absorbing particle phase. As long as the absorbing mass is present, some fraction of a given SVOC will partition into the particle phase, even if its gas phase

concentration is below its saturation concentration, C_i^* . Moreover, the fraction F_i of a semi-volatile compound in the particle phase can be obtained via equation 1.1 (Hallquist et al., 2009), and depicted in the following equation 1.2:

$$F_i = \frac{C_i^p}{C_i^p + C_i^g} = \frac{C_{OA} * K_{p,i}}{1 + C_{OA} * K_{p,i}} = \frac{1}{1 + C_i^*/C_{OA}} \quad (1.2)$$

This hypothesis implies that compounds of greater volatility will increasingly partition into the particle phase as the amount of C_{OA} increases. When $C_{OA} = C_i^*$, half of the semivolatile mass of the compounds distribute in the particle phase. Whereas, if $C_{OA} >> C_i^*$, the compound will reside essentially in the particle phase.

This partitioning theory is limited due to the wide range of C_{OA} in the atmosphere and the ongoing oxidation of SVOCs in both the gas and particle phases. Donahue et al. proposed the approach of “volatility basis set” (VBS) (Donahue et al., 2006; Presto and Donahue, 2006; Pathak et al., 2007). Using the VBS, semi-volatile compounds can be mapped into the sets of bins with predefined value of C_i^* . Moreover, they suggested that oxidation of numerous intermediate volatility vapors may contribute significantly to ambient SOA formation.

1.2.3 Condensed phase chemistry

Organic compounds may undergo particle phase reactions in the condensed phase, affecting their chemical properties and volatility. These reactions, which include both heterogeneous and multiphase reactions, can be either non-oxidative or oxidative (Kroll & Seinfeld, 2008). The oligomeric and high-molecular-weight species can be formed via non-oxidative association reactions (also termed "accretion reactions"), in which the oxidation state of the total carbon is unchanged. (Barsanti & Pankow, 2004) Due to the vapor pressure will decrease significantly, such reactions can play an important role in the formation of SOA. Another mechanism of chemical evolution of organic aerosols is the oxidation of particle-phase organics by atmospheric oxidants (OH, NO₃, O₃, etc.), which often refers to “aerosol aging” (Rudich et al., 2007). Although the oxidative mechanisms in the particle phase are generally the same as those in the gas phase, the large difference of branching ratios among the various pathways may significantly affect on the vapor pressures of the oxidation products. Furthermore, photolytic processes may also influence the the oxidation state and volatility of particle-phase organics.

1.3 Mass spectrometry for the analysis of atmospheric aerosol

To assess the impact of atmospheric aerosols on the environment and human health, detailed information of their chemical composition and physical properties is required. This challenging task drives the development and application of analytical techniques for aerosol measurements. There are different types of analytical techniques used and developed for the analysis of atmospheric organic compounds, as shown in Figure 1.3.1 (Nozière et al., 2015). Therein, mass spectrometry (MS) is a powerful tool in the chemical characterization in aerosol research. Due to its high sensitivity with fast response time, MS offers a great potential for qualitative and quantitative analysis of a broad range of chemical components in OA (Farmer and Jimenez, 2010; Vogel, 2014; Brüggemann, 2015; Laskin, 2018). Until now, many of the significant advances in our understanding of atmospheric aerosols can be attributed to the applications of mass spectrometry (Pratt & Prather, 2012a; Pratt & Prather, 2012b).

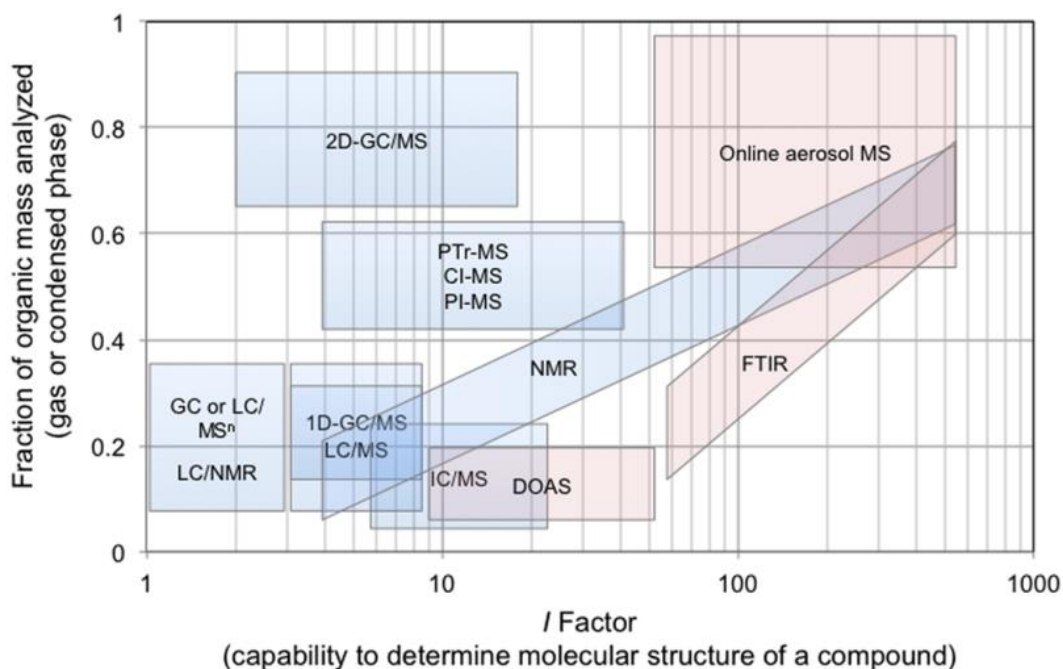


Figure 1.3.1: Summary of analytical techniques used to characterize atmospheric organic compounds. A decreasing *I* factor describes the increasing ability of a technique to identify the molecular structure of a compound, whereas the y-axis describes the fraction of the total organic mass of aerosol samples analyzed by a technique (Nozière et al., 2015).

The following will give a brief overview of online and offline MS techniques, and then introduce the applied MS technique as well as parameters and visualization tools used for data analysis in this dissertation. More detailed description of the application and recent development of MS analysis in atmospheric chemistry can be found in published reviews by Pratt and Prather (2012a, 2012b), Nizkorodov (2011) and Laskin (2018).

1.3.1 Online and offline mass spectrometry techniques

Generally, the MS techniques can be divided into online and offline techniques. Online MS is performed on introduced particles in or near real time, thereby providing high time resolution for insighting the chemical changes in atmospheric aerosol populations on short timescales, and eliminating potential artifacts associated with offline analysis methods, such as evaporation and chemical reactions during long sample collection and analysis time (Pratt & Prather, 2012b). In contrast, offline MS is performed on collected particles, requiring sample collection over hours to days and sample preparation prior to the analysis by mass spectrometer. However, much more information of chemical composition and structural speciation can be observed by the offline techniques compared to those obtained by online techniques (Pratt and Prather, 2012a).

Online MS techniques can be subdivided into two categories: bulk aerosol measurements which obtain statistical information on the average chemical composition of particle ensembles and single-particle measurements which measure the chemistry of individual particles. The general principle of online mass spectrometry techniques is to introduce airborne particles into the instrument, vaporize and ionize the species, and then analyze the ions using mass spectrometer (Hoffmann, 2011). Commonly, bulk aerosol measurements thermally vaporize particles prior to ionization, whereas single-particle measurements desorb particles one at a time using pulsed laser techniques (Pratt & Prather, 2012b; Brüggemann, 2015; Zuth, 2018). The Aerodyne aerosol mass spectrometer (AMS) is the main instrument used for bulk measurements, providing real-time MS analysis of size-resolved mass concentration of non-refractory aerosol species (e.g., most organics, ammonium, sulfate, and nitrate), for chemical characterization of bulk aerosol particles (Canagaratna et al., 2007; Pratt & Prather, 2012b). Recent approaches utilized online atmospheric pressure chemical ionization mass spectrometry (APCI-MS) for the analysis of ambient SOA particles (Vogel et al., 2013; Brüggemann et al., 2014; Zuth et al. 2018). Furthermore, the aerosol flowing atmospheric-pressure afterglow mass spectrometry (AeroFAPA-MS) measurements were also applied for the real time analysis of OA particles (Brüggemann et al., 2015; Brüggemann et al., 2017).

Offline MS techniques are preferred in cases when it is impractical to bring the instrument to the measurement location or when time-averaged composition of aerosol particles is needed (Laskin et al., 2018). In such cases, particles are collected traditionally on quartz or polytetrafluoroethylene-coated fiber filters. Alternatively, particles can be sampled by cascade impactors and separated based on size when particles transverse a series of impaction plates. Gases are mostly sampled by suitable sorbents or in gas-tight containers. Prior to the offline analysis, the samples are mostly processed by extraction, sonication, or derivatization in the laboratory (Brüggemann, 2015; Laskin et al., 2018; Zuth, 2018). The aerosol samples are usually analyzed by the separation techniques followed by MS detection.

The characterization of single or multiple individual aerosol constituents at the molecular level in highly complex mixtures generally requires chromatographic separation, of which the two most employed techniques are gas chromatography (GC) and liquid chromatography (LC) (Hallquist et al., 2009; Nozière et al., 2015; Brüggemann, 2015; Zuth, 2018). LC/MS is a commonly analytical method for the chemical characterization and quantification of moderately polar to polar organic analytes (Nozière et al., 2015). Nowadays, LC/MS analysis has been used to investigate the formation and aging of SOA from a series of precursors (e.g., glyoxal and acetic acid) (Surratt et al., 2008; Nozière et al., 2015). The selection of LC or high performance liquid chromatography (HPLC) columns and separation conditions requires knowledge of the properties of OA compounds. In most cases, reversed phase columns (e.g., C18 and C8 columns) are employed for separation of the analytes, whereas hydrophilic interaction liquid chromatography (HILIC) columns provide successful separation of atmospherically relevant monosaccharide anhydrides (e.g., levoglucosan, galactosan, and mannosan) (Hallquist et al., 2009; Laskin et al., 2018).

1.3.2 Ionization method

Among the ionization methods, the hard ionization techniques such as electron ionization (EI) or laser desorption ionization (LDI) mostly lead to the high degree of fragmentation, thus the identification power is generally low for individual particle phase organics (Hoffmann et al., 2011; Nozière et al., 2015).

By contrast, soft ionization techniques convert the precursor molecules into positive or negative ions without fragmentation, is a key prerequisite for the molecular assignment of organic compounds (Nizkorodov et al., 2011). Atmospheric pressure chemical ionization (APCI), frequently used in atmospheric mass spectrometry, is sensitive to nonpolar compounds such as PAHs, even be used for very labile analytes (e.g., hydroperoxides) (Hoffmann et al., 2011; Nozière

et. al., 2015; Laskin et al., 2018; Zuth, 2018). Electrospray ionization (ESI) is another widespread used ionization technique for aerosol samples, which performed at atmospheric pressure. In contrast to APCI, ESI is well-suited for the analysis of polar molecules (Müller-Tautges, 2014; Nozière et. al., 2015; Laskin et al., 2018; Zuth, 2018; Wang, 2019). The use of a light source is also a possibility technique to softly ionize organics, for instance, vacuum ultraviolet photoionization or atmospheric pressure photoionization (APPI) (Müller-Tautges, 2014; Nozière et. al., 2015; Zuth, 2018; Wang, 2019). An overview of the application range of different ionization techniques is given in Figure 1.3.2 (Müller-Tautges, 2014; Wang, 2019).

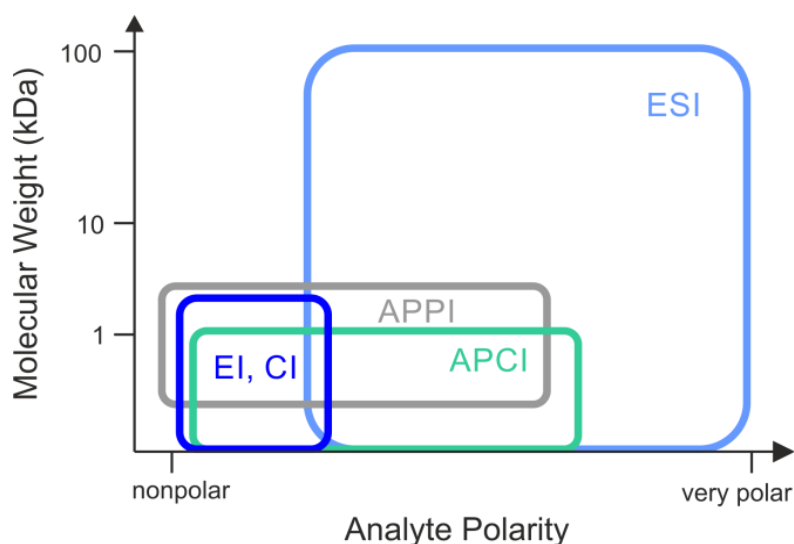


Figure 1.3.2: An overview of application range of different ionization techniques as function of analyte polarity and molecular weight (Müller-Tautges, 2014).

1.3.2.1 Electrospray ionization

ESI uses electrical energy to assist the transfer of ions from solution into the gaseous phase prior to mass spectrometric analysis. Neutral compounds can be converted to ionic form in solution or in gaseous phase by protonation or cationization (Ho et al., 2003). The ESI process involves three steps: (1) dispersal of a fine spray of charge droplets, followed by (2) solvent evaporation and (3) the formation of gaseous ions (Ho et al., 2003; Müller-Tautges, 2014; Wang, 2018).

Within an ESI source, a continuous stream of sample solution is pumped through a stainless steel or quartz silica capillary with a very low flow rate (0.1–10 $\mu\text{L}/\text{min}$). An either negative or positive high voltage (2–5 kV) is applied on the tip of the capillary, which can provide the electric

field gradient required to produce charge separation on the surface of the liquid droplets. This leads to the generation of a mist of highly charged droplets with the same polarity as the capillary voltage. The liquid protrudes from the capillary tip forming the “Taylor cone”. The charged droplets pass down a pressure gradient and potential gradient toward the analyzer region of the mass spectrometer. With the aid of a sheath gas stream (usually nitrogen drying gas) and/or an elevated ESI-source temperature, the solvent of the charged droplets is continuously evaporated, leading to a decrease of droplets size and an increase of surface charge density. When the Coulombic repulsion of the surface charge exceeds the surface tension of the charged droplets, they reach the Rayleigh limit and disintegrate into smaller droplets, which is called droplet jet fission process (Cech and Enke, 2001; Ho et al., 2003; Müller-Tautges, 2014; Wang, 2018).

The generation of gaseous ions can be explained by two proposed mechanisms: (1) The ion evaporation model (IEM) assumes that the increased charge density due to solvent evaporation causes Coulombic repulsion to overcome the surface tension of liquid, resulting in a release of ions from droplet surfaces (Iribarne & Thomson, 1976). This model is suitable for describing the ionization of small molecules. (2) The charge residue model (CRM) assumes that the increased charge density through desolvation causes the large droplets to divide into smaller and smaller droplets and eventually consist only of single ions (Dole et al., 1968). This model is well suited for describing the ionization of large molecules (Cech and Enke, 2001; Müller-Tautges, 2014; Wang, 2018). Figure 1.3.3 illustrates the electrospray ionization process.

The typical ions generated in ESI source are deprotonated ions in the negative mode ($[M-H]^-$ with $M = \text{molecule}$). Positive mode ESI spectra typically contain protonated ions ($[M+H]^+$) or adducts ($[M+Na]^+$, $[M+K]^+$, and $[M+NH_4]^+$) (Müller-Tautges, 2014; Wang, 2018). The heated electrospray ionization (HESI) source, developed by Thermo Scientific, is applied in this work. HESI transforms ions in solution into ions in the gas phase by using ESI in combination with heated auxiliary gas, providing better desolvation and nebulization performance (Müller-Tautges, 2014).

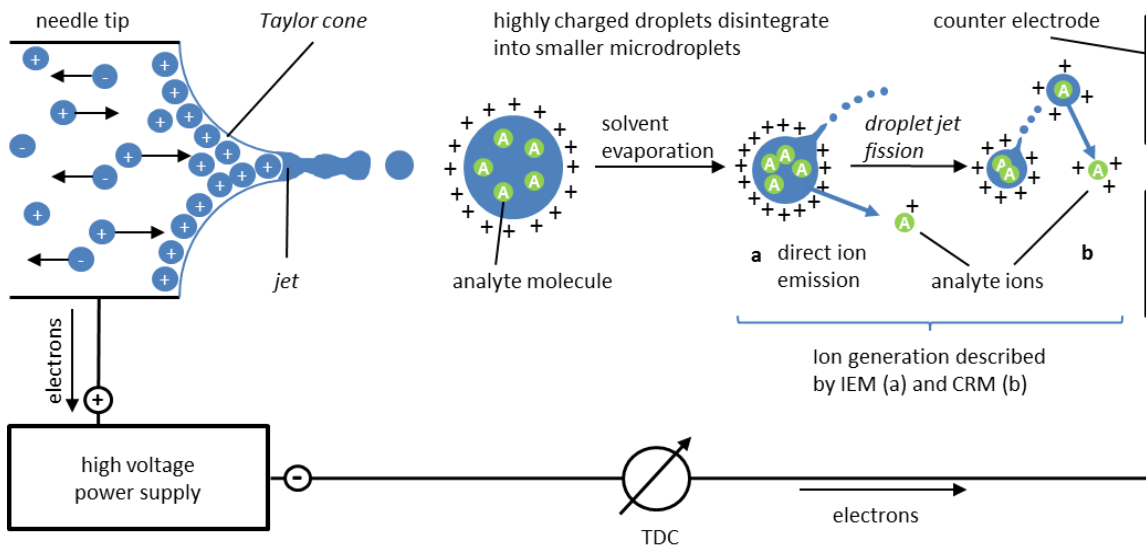


Figure 1.3.3: Schematic illustration of electrospray ionization process (Müller-Tautges, 2014).

1.3.3 High resolution mass spectrometer

High resolution mass spectrometry (HRMS) or ultrahigh resolution mass spectrometry (UHRMS) is a powerful tool for chemical characterization at molecular level with features of high resolution and high mass accuracy (Stock, 2017; Hoffmann et al., 2011; Nizkorodov et al., 2011; Laskin et al., 2018; Wang, 2018). Mass accuracy is defined as the difference between the measured and theoretical mass (equation 1.3), and usually expressed in parts per million (ppm).

$$\text{Mass accuracy} = \left(\frac{\frac{m}{z}_{\text{experimental}} - \frac{m}{z}_{\text{theoretical}}}{\frac{m}{z}_{\text{theoretical}}} \right) \times 10^6 \quad (1.3)$$

For instance, the mass measurement error of 0.001 mass-to-charge (m/z) for a singly charged ion at m/z 500 corresponds to mass accuracy of 2 ppm (Nizkorodov et al., 2011; Nozière et al., 2015). Resolving power (R) is defined as the ratio of the peak position to its full width at half maximum (equation 1.4):

$$R = (m/z) / \text{peak full width at half maximum} \quad (1.4)$$

which determines the ability of the instrument to separate two adjacent peaks on the m/z scale (Nizkorodov et al., 2011; Nozière et al., 2015). High accuracy coupled with high resolution allows one to determine unambiguous elemental formulas for each ion peak, in turn can be used to characterize thousands of organic compounds present in complex atmospheric aerosol samples.

Three major types of HRMS are well-suited for complex samples analysis: (1) high resolution quadrupole time-of-flight (HR-Q-TOF) mass spectrometers which have a resolving power of up to 40,000 across a m/z 100–500 mass range; (2) the Orbitrap mass spectrometers which have higher resolving power in excess of 1,000,000 at $m/z < 300$ –400 within a 3 seconds detection time making it compatible with several types of chromatographic separations; (3) the Fourier transform ion cyclotron (FTICR) mass spectrometers which provide the highest mass resolution and mass accuracy of all existing MS technologies, offering the best resolution power with a record resolution of 40,000,000 at m/z 609 at a magnetic field of 7 T (Nozière et al., 2015; Wang, 2018). Figure 1.3.4 illustrates the advantages of high resolving power for OA analysis, and the comparison of different types of HRMS.

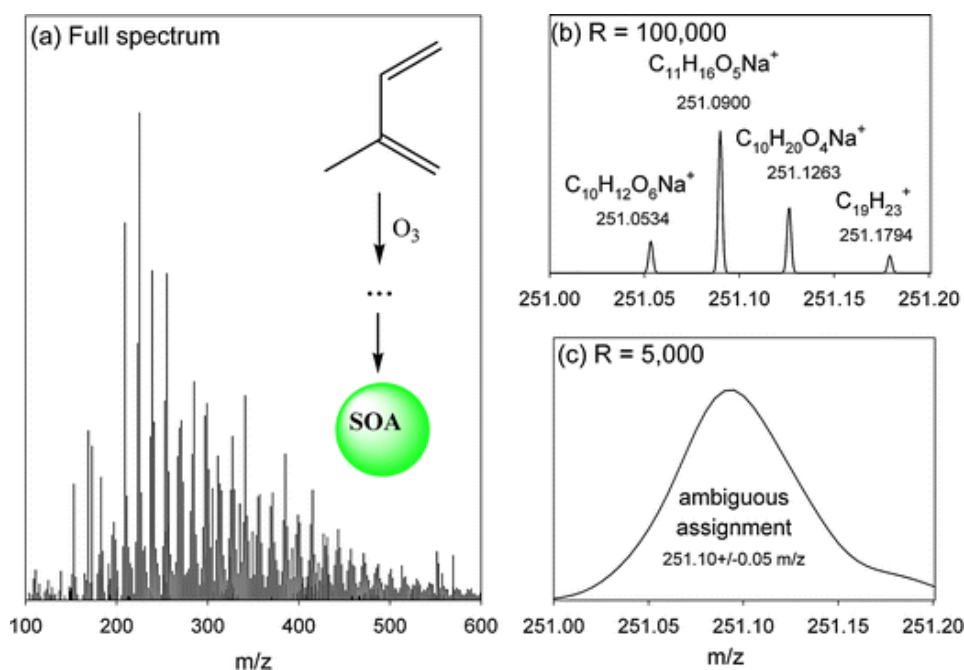


Figure 1.3.4: (a) An ESI mass spectrum of isoprene/ozonide SOA. (b) peaks around m/z 251 recorded at the Orbitrap resolving power of $R = 100,000$. (c) how the same mass range would look like if recorded at a typical resolving power of a reflection-TOF instrument with $R = 5,000$ (Nizkorodov et al., 2011).

In last years, HRMS coupled with the soft ionization sources (e.g., ESI and APCI) has been successfully used for detailed chemical characterization of atmospheric aerosols (Nizkorodov et al., 2011; Lin et al., 2012a; Lin et al., 2012b; Rincón et al., 2012; Kourtchev et al., 2014; Nozière et al., 2015; Kourtchev et al., 2016; Wang et al., 2016; Wang et al., 2017; Laskin et al., 2018; Wang et al., 2018; Wang et al., 2019). In this study, the Orbitrap MS is applied for the identification of chemical composition of OA and described in the following chapter.

1.3.3.1 Q-Exactive hybrid quadrupole-orbitrap mass spectrometer

The roots of the Orbitrap analyzer can be traced back to 1923 when the Kingdon trap was developed, later improved by Makarov and finally commercialized by Thermo Fisher Scientific in 2005 (Makarov, 2000; Zubarev and Makarov, 2013). In this study, the Q-Exactive hybrid quadrupole-orbitrap mass spectrometer (built by Thermo Fisher Scientific in 2011) was applied. The instrument has a maximum resolution of 140,000 at m/z 200 and a mass accuracy <3 ppm (external calibration) and <1 ppm (internal calibration). Figure 1.3.7 displays the schematic of the Q-Exactive hybrid quadrupole-orbitrap mass spectrometer.

The ions generated in an ion source (commonly ESI or APCI) are focused by a lens stack and further transmitted by a bent flatapole to a quadrupole for optional precursor ion selection. Subsequently, the ions enter a curved linear trap (C-Trap), where ions are focused by collisional cooling. After that, ions are either transmitted directly to the Orbitrap mass analyzer for detection or led into the higher-energy collisional dissociation (HCD) cell for fragmentation. For MS^2 analysis, the fragmented product ions are again focused in the C-Trap and then transmitted to the Orbitrap for detection (Scigelova and Makarov, 2006; Müller-Tautges, 2014; Zuth, 2018; Wang, 2018).

The Orbitrap consists of a spindle-shaped electrode in the center and an outer barrel-shaped electrode, which is split in the middle by a ceramic ring (see Figure 1.3.5). The ions are injected into the Orbitrap essentially perpendicular to the z -axis and trapped by means of an electrostatic field between the central and out electrodes. A radial electric field bends the ions trajectory toward the central electrode whereas tangential velocity creates an opposing centrifugal force, forcing the ions to a rotational movement around the central electrode, which is like the trajectory of a planet in the solar system. At the same time, the axial electric field caused by the special conical shape of electrodes pushes ions toward the widest part of the trap, initiating a harmonic axial oscillation. The frequency (ω_{axial}) of the axial oscillation does not depend on the tangential velocity or the distribution of the circulating ions, but on the m/z ratios of the ions as described by equation 1.5:

$$\omega_{axial} = \sqrt{k \left(\frac{z}{m_i} \right)} \quad (1.5)$$

where k is the force constant of the electrical potential. The frequency of the harmonic axial oscillation induces an image current in the two parts of outer electrode, which is detected and multiplied. Finally, the image current is converted to a mass spectrum by fast Fourier transformation (Scigelova and Makarov, 2006; Zubarev and Makarov, 2013; Müller-Tautges, 2014;

Zuth, 2018; Wang, 2018).

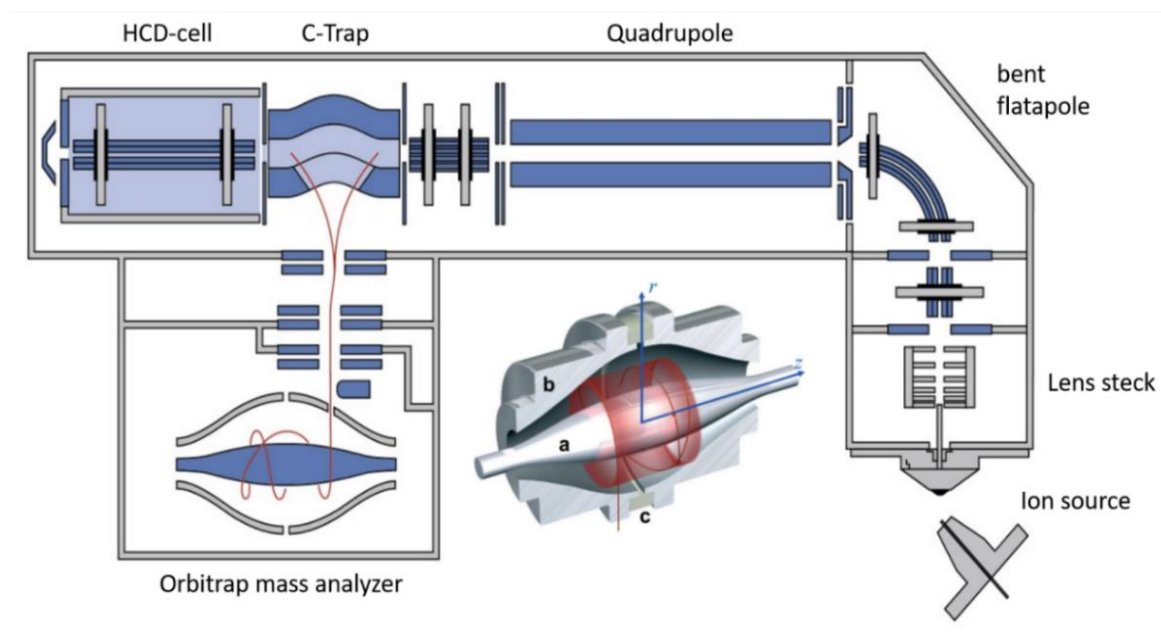


Figure 1.3.5: A schematic of the Q Exactive hybrid quadrupole-orbitrap mass spectrometer, which is composed of the ion source, lens stack, bent flatapole, quadrupole, C-trap, orbitrap mass analyzer and HCD cell. The inset depicts the cross section of Orbitrap consisting of a spindle-shaped central electrode (a), a barrel-shaped outer electrode, composed of two parts (b) and a ceramic ring for segregation (c). The movement of the ions along the z-axis is highlighted with a red orbit (Scigelova and Makarov, 2006; Müller-Tautges, 2014; Zuth, 2018; Wang, 2018).

1.3.4 Data analysis and visualization

UHRMS allows the assignment of molecular formulae to the measured hundreds or thousands of compounds. When determining elemental formulas from the accurate mass measurements, there are several constraints applied to eliminate the compounds not likely to occur in nature, which include the restriction for the number of possible elements present in the molecule (e.g., C, H, O, N, and S), reasonable elemental ratios such as oxygen to carbon (O/C) ratios and hydrogen to carbon (H/C) ratios, nitrogen rule, and double bond equivalent (Nozière et al., 2015). Due to the large amounts and complexity of the UHRMS data, a variety of parameters and visualization tools have been developed to facilitate the interpretation of HRMS data, and are described below.

The double bond equivalent (DBE) reflects the number of double bonds and rings in a molecule,

which can be calculated using equation 1.6 (McLafferty and Turecek, 1993):

$$DBE = 1 + c - 0.5x + 0.5y \quad (1.6)$$

where c is the number of carbon atoms, x is the total number of monovalent atoms (e.g., H, Cl, Br), and y is the total number of trivalent atoms (e.g., N and P) in the molecule. It should be noted that certain heteroatoms may have multiple valence states, e.g., the valence of N is 3 in amines and 5 in alkyl nitrites, thus the calculated values of DBE need to be considered with caution. Moreover, the sulfuroxygen double bonds of the sulfate groups in the molecule are not taken into account in DBE equation (Nizkorodov, 2011; Nozière et al., 2015).

The aromaticity index (AI), proposed by Koch and Dittmar, is a parameter for the identification of aromatic structures in nature organic matter (Koch and Dittmar, 2006). It reflects the C–C double bonds 'density' in a molecule, including the possibility that heteroatoms can form double bonds which not contribute to aromaticity. AI can be calculated from molecular formulae of the compounds containing C, H, O, N, S, and P, expressed as equation 1.7:

$$AI = \frac{DBE_{AI}}{C_{AI}} = \frac{1+C-O-S-0.5H}{C-O-S-N-P} \quad (1.7)$$

where DBE_{AI} is the minimum number of C–C double bonds plus rings in a common molecular structure containing heteroatoms and C_{AI} is the number of carbon reduced by the number of potential double bonds contributed by heteroatoms and if $DBE_{AI} \leq 0$ or $C_{AI} \leq 0$, then $AI = 0$. This approach provides two threshold values for the unequivocal identification of aromatics ($AI > 0.5$) and condensed aromatics ($AI \geq 0.67$). For aromatic molecules with long alkyl chains, their AI value less than 0.5 and they would not be identified as aromatic structures, which results in a lower estimate for aromatic and condensed aromatic compounds in OA by AI approach (Yassine et al., 2014).

The aromaticity equivalent (X_C), introduced by Yassine et al. in 2014, complements the AI classification and improves the identification of aromatic and condensed aromatic structures in OA (Yassine et al., 2014). The X_C of a compound containing C, H, O, N, S, and P can be calculated by equation 1.8:

$$X_C = \frac{3[DBE - (mO + nS)] - 2}{DBE - (mO + nS)} \quad (1.8)$$

If $DBE \leq mO + nS$, then $X_C = 0$, where m and n are the fraction of oxygen and sulfur atoms involved in the π -bond structure of a compound, respectively. i.e., $m = 1$ for aldehyde, ketone, nitroso, and

cyanate chemical classes, $m = 0.5$ for carboxylic acid, ester, and nitro chemical classes, and $m = 0$ for alcohol, ether, peroxide, sulfoxide, sulfones, sulfonic, and sulfonic acid chemical classes; whereas $n = 1$ should be used for thial and thione chemical classes, and $n = 0$ for thiol, sulfide, and disulfide chemical classes. This approach proposed threshold criteria for aromatic compounds ($X_c \geq 2.5000$) and condensed aromatic compounds ($X_c \geq 2.7143$) (Yassine et al., 2014).

The Van Krevelen diagram (VK), constructed by plotting H/C versus O/C elemental ratios, is often utilized to describe the evolution of organic mixtures. VK diagrams can be used to categorize organic aerosols and differentiate their potential sources by the corresponding position. Commonly, the most oxidized compounds lie in the lower right part of the diagram whereas the most reduced/saturated species populate the upper left part of the plot. As illustrated in Figure 1.3.6, aliphatic compounds generally have high H/C ratios (≥ 1.5) and low O/C ratios (≤ 0.5), while aromatic hydrocarbons typically have low H/C ratios (≤ 1.0) and low O/C ratios (≤ 0.5) (Kourtchev et al., 2014; Nozière et al., 2015). However, the complexity of atmospheric aerosol is sometimes not well represented by VK diagrams due to it cannot distinguish formulas with different atom numbers but identical atomic ratios. Thus VK diagrams are frequently plotted as heat maps by adding additional dimensionalities or generated as three-dimensional figures using the N/C ratio or the DBE as a third variable.

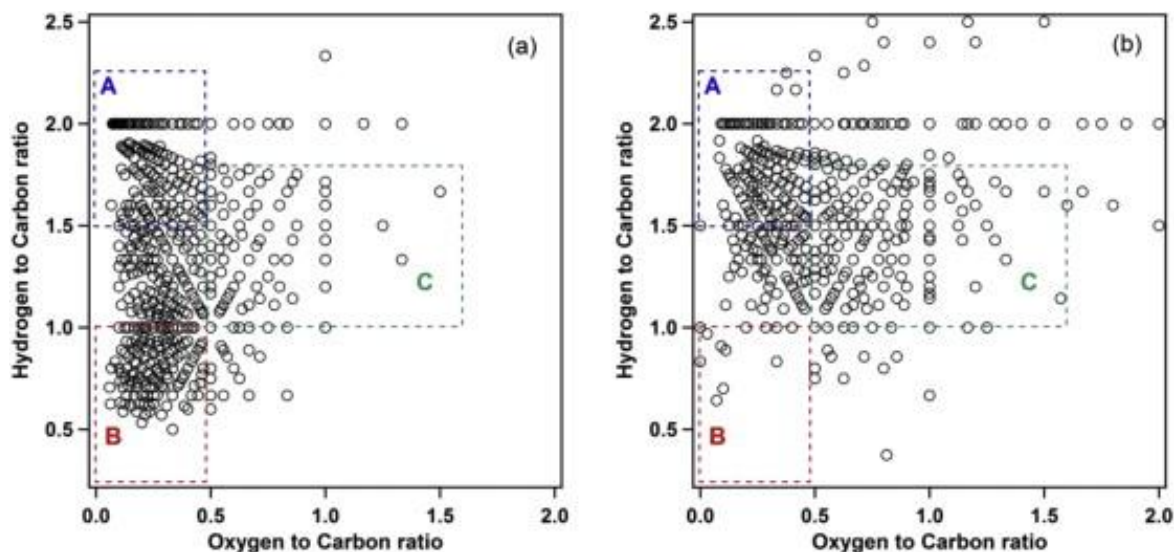


Figure 1.3.6: Van Krevelen (VK) diagrams for all detected ions in (a) urban aerosol samples and (b) remote aerosol samples. Ions in areas 'A', 'B', and 'C' attributed to aliphatic, aromatic, and SOA species, respectively (Kourtchev et al., 2014).

The average O/C ratio is a convenient but not accurately metric for describing the degree of oxidation in organic aerosols since nonoxidative processes such as hydration and dehydration can also affect atomic ratios in a molecule. The carbon oxidation state (OS_C) was suggested by Kroll et al. in 2011 to describe the evolving composition of atmospheric organics undergoing dynamic oxidation processes, which can be calculated from the following equation 1.9:

$$OS_C \approx 2 O/C - H/C \quad (1.9)$$

which is generally used for molecules that contain C, H, and O atoms only (Kroll et al., 2011). OS_C , when coupled with carbon number (n_C), provides a framework for describing the chemical characterization of atmospheric organic aerosol, which can be used to constrain the composition of organic aerosol and facilitate understanding the oxidative evolution of atmospheric organics, as shown in Figure 1.3.7. For instance, hydrocarbon-like organic aerosol (HOA) and biomass burning organic aerosol (BBOA) correspond to primary particulate matter directly emitted into the atmosphere, HOA has OS_C value less than -1 and more than 18 carbon atoms whereas BBOA has OS_C value between -1.5 and 0 with 7–23 carbon atoms. Semivolatile and low-volatility oxidized organic aerosol (SV-OOA and LV-OOA) produced by multistep oxidation reactions have OS_C values between -1 and $+1$ with 18 or less carbon atoms (Kroll et al., 2011; Nozière et al., 2015).

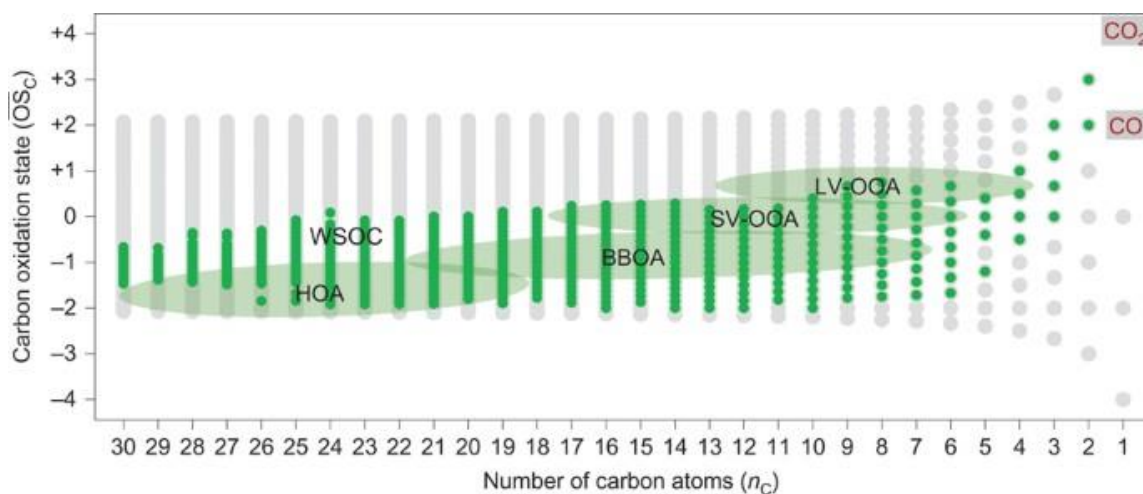


Figure 1.3.7: Carbon oxidation state plot for organic aerosol taken from measurements using three analysis techniques (combustion analysis, HRMS with ESI, and HR-AMS) (Kroll et al., 2011).

Another useful visualization tool is Kendrick Mass (KM) analysis, which is typically used to identify homologous series of compounds differing only by the number of a specific base unit (e.g.

CH₂, CH₂O, etc.). (Kendrick, 1963; Hughey et al., 2001). For example, the Kendrick mass of CH₂ unit is calculated by renormalizing the IUPAC mass (14.01565) of CH₂ to exactly 14.00000 using equation 1.10:

$$KM_{CH_2} = \text{Observed mass} \times \frac{14.00000}{14.01565} \quad (1.10)$$

The Kendrick mass defect (KMD) is defined as the exact Kendrick mass subtracted from the nominal Kendrick mass, calculated using equation 1.11:

$$KMD_{CH_2} = \text{Nominal Mass} - KM_{CH_2} \quad (1.11)$$

As a consequence, compounds with identical KMD can be easily grouped into a homologous series. When the KMD is plotted versus nominal Kendrick mass, homologous series will fall on horizontal lines, as illustrated in Figure 1.3.8 (Hughey et al., 2001; Nizkorodov, 2011; Nozière et al., 2015).

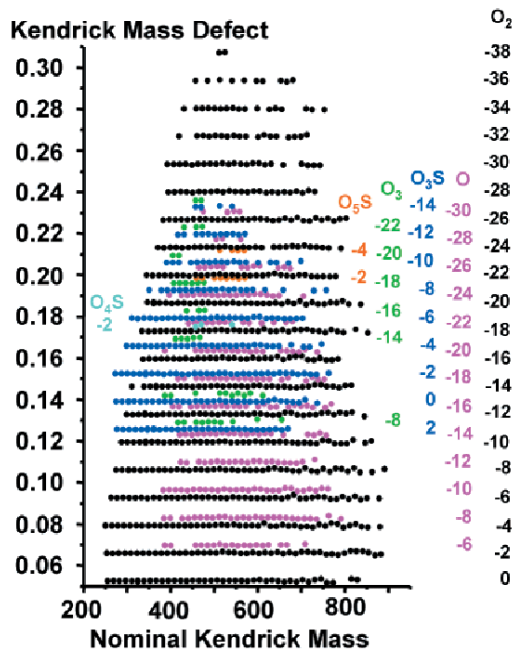


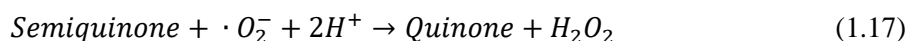
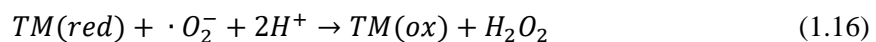
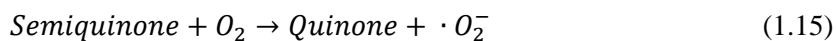
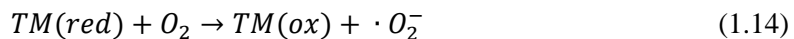
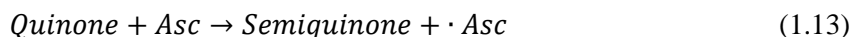
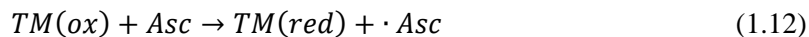
Figure 1.3.8: Kendrick mass defect vs nominal Kendrick mass for odd-mass ¹²C ions. The visual vertical separation of compound classes (e.g., O, O₂ and O₃S) and types (compounds with different number of rings plus double bonds) based on mass defect and the visual horizontal distribution of number of CH₂ groups for a given compound class and type (Hughey et al., 2001).

1.4 Formation of reactive oxygen species by particulate matter

Numerous epidemiological studies show that ambient and indoor air pollution as well as inhalation and deposition of fine particulate matter are correlated with adverse health impacts, including allergic, respiratory, and cardiovascular diseases, lung cancer and increased mortality (Pope et al., 2002; Pöschl, 2005; Pope and Dockery, 2006; Brook et al., 2010; Beelen et al., 2014; Pöschl and Shiraiwa, 2015). One of the most plausible pathophysiological mechanisms to explain the association of PM exposure with adverse health effects is oxidative stress caused by formation of reactive oxygen species (ROS) (Apel and Hirt 2004; Fang et al, 2019). ROS contain hydroxyl radicals ($\bullet\text{OH}$), hydrogen peroxide (H_2O_2), and superoxide ($\bullet\text{O}_2^-$) as well as organic radicals, which can be formed by redox-active components in PM such as transition metals and quinones (Pöschl and Shiraiwa, 2015). Hydroxyl radicals are the most reactive form of ROS, which can cause a variety of oxidative damage to membrane lipids, proteins, and DNA of cells (Valavanidis et al., 2008; Wang et al., 2011). H_2O_2 is relative long lived and generally regarded as having significant indirect biological effects since this small uncharged molecule diffuses across membranes easily (Feierman et al., 1985; LaCagnin et al., 1990). A number of studies have shown that excess ROS can cause oxidative stress leading to cell death and tissue injury in the respiratory tract. Thus, characterizing the formation of ROS is essential to understand how air pollution can cause adverse health effects.

1.4.1 Endogenous formation of ROS

Upon inhalation and deposition in the respiratory tract, redox-active components in PM can induce and involve chemical reactions that endogenously produce ROS in the epithelial lining fluid (ELF). ELF covering the airways contains a range of surfactants and antioxidants such as ascorbate (Asc), uric acid (UA), reduced glutathione (GSH), and α -tocopherol (α -Toc). As shown in Figure 1.4.1, the redox-active species and ROS undergo a multitude of redox reaction cycles. This process starts with the transfer of electrons from antioxidants (e.g. Acs) to transition metals (iron or copper ions) and/or quinones (see equation 1.12 and 1.13). The formed reduced metal ions and/or semiquinones react with O_2 to regenerate the oxidized metal ions and/or quinones and produce $\bullet\text{O}_2^-$ (see equation 1.14 and 1.15). O_2^- radicals are further converted into H_2O_2 (see equation 1.16 and 1.17) and then OH radicals can be formed via Fenton-like reactions of H_2O_2 with iron or copper ions (see equation 1.18) (Kok et al., 2006; Shen et al, 2011; Wang et al., 2011; Lakey et al., 2016; Fang et al., 2019).



where (ox) and (red) represent oxidized and reduced forms of transition metals (TM), respectively.

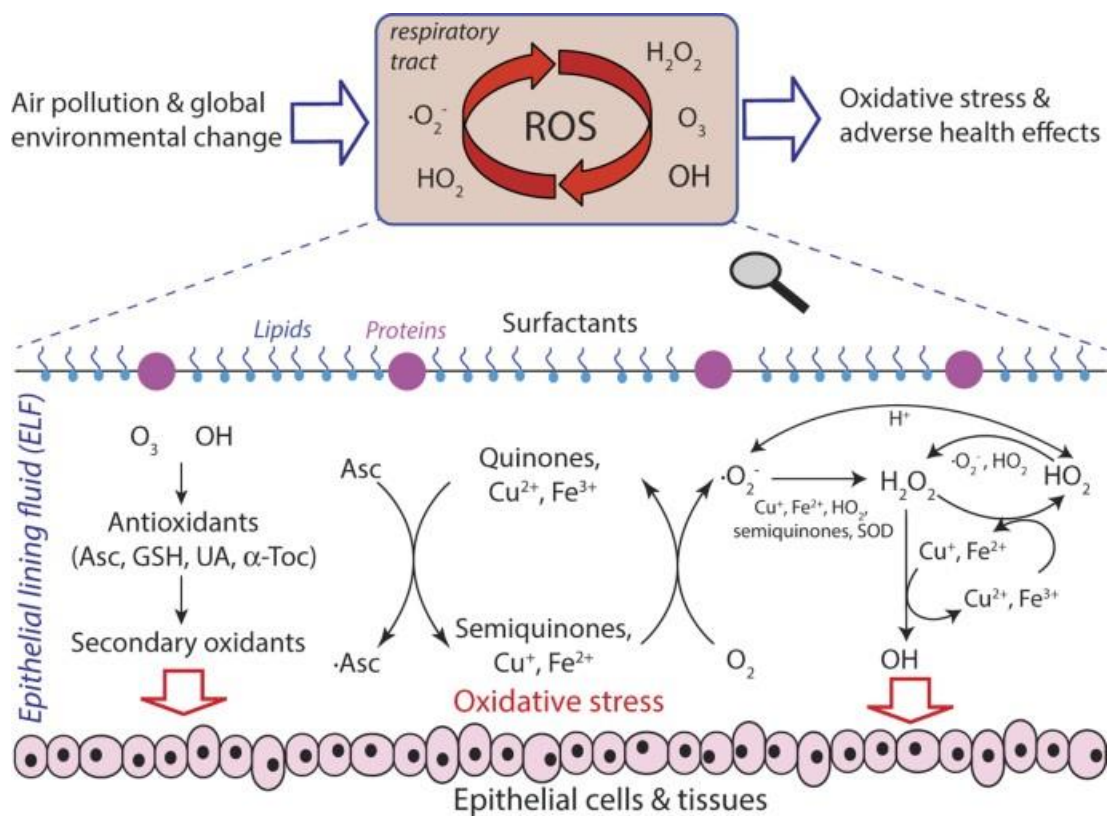


Fig. 1.4.1 Interaction of air pollutions and reactive oxygen species in the epithelial lining fluid of the human respiratory tract (Lakey et al., 2016).

1.4.2 Components in PM related to ROS formation

ROS can directly derived from PM. Laboratory measurements indicates the majority of H_2O_2 associated with ambient particles is generated by the particles themselves in aqueous solutions (Hasson and Paulson 2003; Arellanes et al. 2006). Moreover, ROS can also be produced by redox-active species in PM, including transition metals, environmentally persistent free radicals (EPFRs; e.g. semiquinones), humic-like substances (HULIS), and SOA produced from aromatics such as naphthalene (Wang et al., 2012; Pöschl and Shiraiwa, 2015; Lakey et al., 2016; Fang et al., 2017).

Transition metals play an important role in the formation of ROS. Iron (Fe) and copper (Cu), the most abundant transition metals in particles, are capable of chemically producing ROS via redox reactions (see equations 1.7–1.9). Numerous studies have shown significant correlations between H_2O_2 generation with concentrations of soluble Fe and Cu in PM extracts (Shen et al., 2011; Wang et al., 2012). Furthermore, the Fenton reaction ($\text{Fe}^{2+} + \text{H}_2\text{O}_2$) is one of the most fundamental and widespread reactions in the multiphase chemistry of ROS, which leads to the generation of hydroxyl radicals (Pöschl and Shiraiwa, 2015). The other transition metals like manganese (Mn), nickel (Ni), cobalt (Co), and vanadium (V) can also produce ROS under some conditions. However, these metals may not produce significant levels of ROS due to their low soluble metal concentrations expected from PM (Pöschl and Shiraiwa, 2015).

Quinones are generally originated from engine exhaust or cigarette smoke or can be generated via oxidation of aromatic precursors (Lakey et al., 2016; Fang et al., 2017). Laboratory studies show that 1,4-naphthoquinone, 1,2-naphthoquinone, and phenanthrenequinone are the most reactive quinones associated with ROS generation. Figure 1.4.2 shows redox reaction cycling of quinone-mediated H_2O_2 generation. In the presence of an electron donor, quinones are converted into semiquinone radical anions accompanied by the generation of superoxide radicals and hydrogen peroxide. Superoxide facilitates the regeneration of quinone as well as additional H_2O_2 formation (Wang et al., 2012; Kuang, 2017).

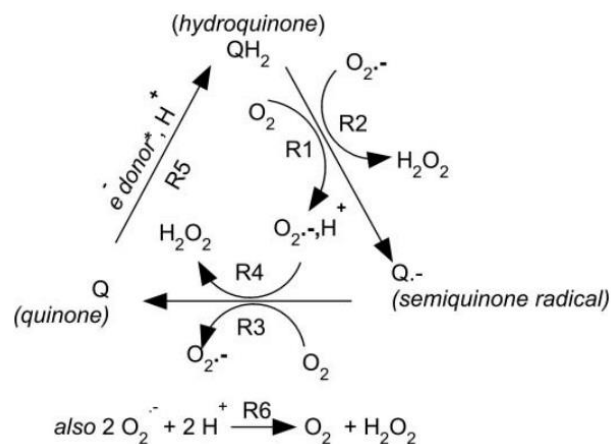


Fig. 1.4.2 Scheme of possible quinone cycling reactions (Wang et al., 2011).

Several studies have found that contributions from transition metals and quinones alone cannot account for all of the observed ROS, indicating there are additional compounds in PM responsible for the production of ROS. Water-soluble humic-Like substances (HULIS) are a mixture of compounds containing polycyclic ring structures with aliphatic side chains and multiple polar functional groups, which derived from biomass burning (Hoffer et al., 2006; Mukai and Ambe 1986; Zappoli et al., 1999) or produced by complex secondary reactions (e.g. heterogeneous and photosensitized reactions) (Decesari et al., 2001; Limbeck et al., 2005). They have recently been recognized to be highly redox-active and play a significant role in driving PM-associated ROS formation (Lin and Yu, 2011; Verma et al., 2015; Ma et al., 2018). The reversible redox sites in the HULIS could serve as an electron transfer intermediate leading to the continuous generation of ROS (Lin and Yu, 2011). In addition, due to HULIS contain organics that chelate transition metals, interactions of which could lead to synergistic or antagonistic effects on ROS formation.

The contribution of SOA to the generation of ROS has got increasing attention. A few studies have shown that SOA derived from both biogenic and anthropogenic precursors can generate a considerable amount of H_2O_2 or radicals in the aqueous phase (Hewitt and Kok, 1991; Hasson et al., 2001; Wang et al., 2011; Kramer et al., 2016; Tong et al., 2018; Tong et al., 2019). The formation of H_2O_2 associated with SOA is likely the decomposition or hydrolysis of organic (hydro)peroxides and related species (Pöschl and Shiraiwa, 2015). Wang et al. suggested SOA formed via ozonolysis and photo-oxidation of α -pinene, β -pinene, and toluene all produced H_2O_2 in the aqueous phase, and α -pinene and β -pinene SOA have higher H_2O_2 generation ability than toluene SOA (Wang et al., 2011). Moreover, isoprene SOA and naphthalene SOA were observed to release substantial amounts of H_2O_2 , OH radicals, and organic radicals upon interaction with

water (Tong et al., 2018). In addition,

1.5 Thesis objectives and outline

Atmospheric aerosol contains thousands of chemical compounds due to various biogenic and anthropogenic sources as well as complex multiphase chemical reactions. In particular, OA often constitutes a substantial fraction of aerosol mass and organic compounds in OA cover a wide range of chemical space with respect to molecular mass, polarity, and functional groups. Furthermore, epidemiological studies have indicated associations of adverse respiratory and cardiovascular health effects with organic fractions of ambient PM. Thus, investigating the chemical characterization of OA is an essential and challenging task, which helps to better understand the chemical composition, sources, and atmospheric processes of OA as well as to identify the health-related organic compounds.

The aim of this work was to characterize the organic compounds in PM_{2.5} collected in different cities and remote regions using the UHPLC-Orbitrap technique and further to provide molecular evidence for the association of ROS formation with organic compounds. Based on the identified elemental compositions, a new parameter 'maximum carbonyl ratio (MCR)' was proposed to improve the classification of organic compounds in OA. This work can be described in three parts as follows:

1. The first part focused on the development of analytical method for OA measurement. PM_{2.5} samples were collected in Beijing (Chinese megacity) and Mainz (a city within the Rhine-Main area, Germany). OA was extracted by a solvent mixture of acetonitrile and water and detected using UHPLC coupled to the UHRMS-Orbitrap with electrospray ionization (ESI). The chemical composition and properties, and related sources of OA in Beijing and Mainz were analyzed and compared.
2. In the second part, we developed a new parameter 'MCR' to interpret the UHRMS data. The MCR expresses the maximum number of carbonyl groups in a molecule and can be calculated based on the elemental composition. By the combination of MCR values and the traditional visualization tool Van Krevelen (VK) diagram, we created the MCR-VK diagram and allocated the typical SOA compounds in the MCR-VK diagram for region division. The approach was tested by using ambient PM_{2.5} samples, which were collected in Hyytiälä (boreal forest region, Finland) and Beijing, respectively, and SOA samples generated from ozonolysis of α -pinene and photo-oxidation of isoprene, respectively. The distributions of OA derived from different samples in the MCR-VK diagram were observed and compared.

3. In the third part, we characterized the chemical composition of organic compounds in ambient PM_{2.5} samples and laboratory-generated SOA samples using the UHPLC-Orbitrap MS method developed in the first part of this work. The PM_{2.5} samples were collected in five urban cities (Mainz, Beijing, Shanghai, Guangzhou, and Xi'an) and a remote region (Hyytiälä), while SOA samples were generated from ozonolysis of α -pinene, β -pinene and limonene, and photo-oxidation of isoprene and naphthalene. Then we proposed the concept 'ratio of relative peak area-weighted fraction of oxidized organic compounds to relative peak area-weighted fraction of unsaturated organic compounds ($R_{\text{OOC/UOC}}$)' base on the classification of organic compounds by their MCR values. Furthermore, we quantified the ROS yield of the samples in water, which was the sum of H₂O₂ yield using a fluorometric probe and radical yield measured by electron paramagnetic resonance. The correlations of $R_{\text{OOC/UOC}}$ of OA with ROS yield were investigated and organic compounds that contributed to the ROS formation were explored.

2 Analytical method development and chemical characterization of OA using ultrahigh resolution mass spectrometry

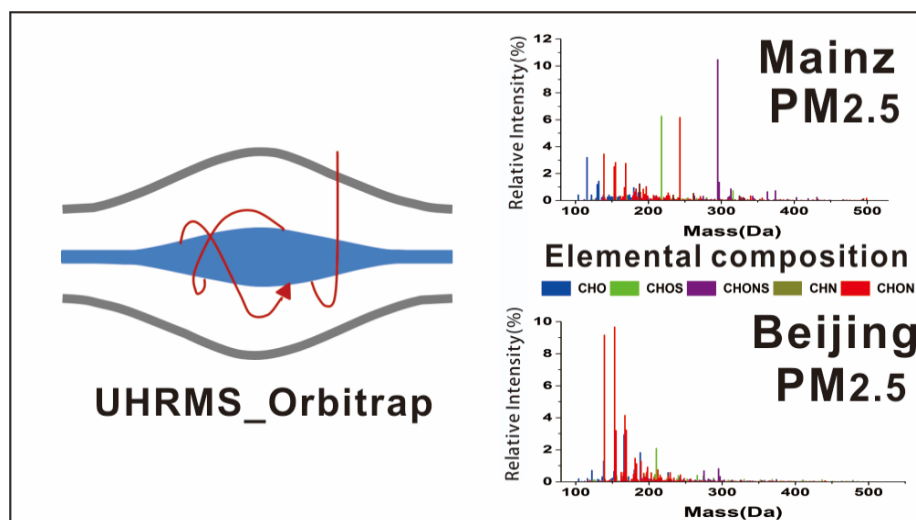
This chapter is a reprint of the article:

Kai Wang, Yun Zhang, Rujin Huang, Junji Cao, and Thorsten Hoffmann

UHPLC- Orbitrap mass spectrometric characterization of organic aerosol from a central European city (Mainz, Germany) and a Chinese megacity (Beijing)

Atmospheric Environment, 2018, 189, pp 22-29,

<https://doi.org/10.1016/j.atmosenv.2018.06.036>



Abstract. Fine urban aerosol particles with aerodynamic equivalent diameter $\leq 2.5 \mu\text{m}$ ($\text{PM}_{2.5}$) were collected in Mainz (a city within the Rhine-Main area, the third largest metropolitan region in Germany) and Beijing (Chinese megacity). A solvent mixture of acetonitrile-water was used to extract the organic aerosol fraction (OA) from the particle samples. The extracts were analyzed by an ultrahigh resolution mass spectrometer (UHRMS) Orbitrap coupled with ultra-high-performance liquid chromatography (UHPLC) both in the negative and positive ion mode. The number of compounds observed in Beijing is a factor of 2–10 higher compared to Mainz. The clear differences on chemical composition of OA in the two cities were observed. The majority of organics in Beijing OA is characterized by lower elemental H/C and O/C ratio but a higher degree of unsaturation and a larger aromaticity equivalent (X_C) compared to Mainz OA, suggesting that aromatics, which are related to direct combustion compounds (e.g., oxidized polycyclic aromatic hydrocarbon (PAH)), play an important role for OA in Beijing. A significant number of organosulfates (OSs) with long-carbon chain and low degree of unsaturation were observed in Beijing OA, indicating that long-chain alkanes emitted by vehicle might be their precursors.

Keywords: Organic aerosol, Orbitrap MS, UHPLC, Megacity, Molecular characterization

2.1 Introduction

Organic aerosol (OA) constitutes a substantial fraction (20–90%) of submicrometer aerosol mass (Jimenez et al., 2009; Kroll et al., 2011) and influences air quality, climate, and human health (Pöschl, 2005; Hallquist et al., 2009). Previous studies have shown that OA contains a variety of organic species, including hydrocarbons, alcohols, aldehydes, carboxylic acids, organosulfates and organonitrates. However, only about 10–30% of OA has been chemically specified so far (Hoffmann et al., 2011). A better understanding of the chemical composition, properties and reactivity of OA are therefore important for assessing the effects of atmospheric aerosols. Since the thousands of compounds in OA covers a very large chemical space with respect to molecular mass, functional group distribution and polarity at trace level concentrations (Lin et al., 2012a; Nozière et al., 2015), characterization of OA is a challenging analytical task.

With the development of mass spectrometric techniques, considerable advances have been made over the past decade in terms of a better understanding of OA. The Aerodyne aerosol mass spectrometer (AMS) has been widely used to measure OA elemental composition and to study the

sources and atmospheric processes (e.g. oxidation state) of OA (Canagaratna et al., 2015; Dall'Osto et al., 2015; Lee et al., 2015). However, the use of 70 eV electron ionization of the AMS leads to a high degree of fragmentation of OA and therefore difficulties in the identification and quantification of individual organics. Several approaches have been developed recently to introduce soft ionization techniques for OA studies, including atmospheric pressure chemical ionization (APCI) and electrospray ionization (ESI) (Hoffmann et al., 2011; Nozière et al., 2015). Especially ultrahigh resolution mass spectrometry (UHRMS) coupled with ESI allows the characterization of complex organic mixtures at the molecular level (Nizkorodov et al., 2011; Lin et al., 2012a; Rincón et al., 2012; Wang and Schrader, 2015). Fourier transform ion cyclotron (FTICR), Orbitrap and high-resolution quadrupole time-of-flight (HR-Q-TOF) are the three major high-resolution mass analyzers (Nozière et al., 2015). Due to the high mass resolving power (≥ 40000) and high mass accuracy (≤ 5 ppm), the UHRMS techniques can detect thousands of individual organic aerosol components and provide their accurate chemical composition for each analysis. A recent review by Nizkorodov et al. (Nizkorodov et al., 2011) shows that UHRMS analysis of secondary OA from smog chamber studies and aerosol samples collected from e.g. biomass burning, forest, rural and urban environment can provide improved understanding of the molecular composition and fundamental chemical transformations of OA. However, UHRMS analysis is instrumentally demanding and UHRMS studies of urban OA are still very scarce. Previous studies focused on the characterization of bulk OA or a group of specific compounds. For example, Lin et al. (Lin et al., 2012a) characterized the element composition of humic-like substances in the Pearl River Delta Region, China. Tao et al. (Tao et al., 2014) reported the analysis of organosulfates (OSs) in OA from Shanghai and Los Angeles. Wang et al. (Wang et al., 2016) studied the OSs in three Chinese cities. Wang et al. investigated the month and diurnal variation of the OA chemical composition in Shanghai. Rincon et al. (Rincón et al., 2012) characterized the chemical composition of OA collected in different seasons at Cambridge, UK. Reemtsma et al. (T. et al., 2006) and Roach et al. (Roach et al., 2010) studied the OA from Riverside, CA and Mexico city, respectively.

Over the past decade, particulate air pollution has become a serious environmental problem in China. Severe and persistent haze pollution occurred frequently in China in recent winters, particularly in megacities and urban complexes (Huang et al., 2014). Very recent studies show that outdoor air pollution, mostly by $PM_{2.5}$, leads to 3.3 million premature deaths per year worldwide, predominantly in Asia (Lelieveld et al., 2015). The yearly mass concentrations of $PM_{2.5}$ often exceed the WHO guideline concentration of $10 \mu g m^{-3}$, even in many European urban areas. Given that about 55–75% of population lives in urban areas in China and European countries, a better

understanding of the chemical composition, sources and atmospheric processes of aerosol in urban areas is important. This is particularly true for the OA fraction as it is much more complex and uncertain than the inorganic aerosol fraction. In this study, PM_{2.5} samples were collected from Beijing (the capital of China with more than 20 million residents) and Mainz (a city within the Rhine-Main area, the third largest metropolitan region in Germany with more than 5.8 million population). However, the two urban regions experience very different natural and anthropogenic influences and it is worthwhile to investigate the similarities and differences in the OA composition in these two cities. Therefore, the organic fraction of the PM_{2.5} samples in Beijing and Mainz were analyzed using UHPLC-Orbitrap MS in both negative and positive polarity and the difference in OA chemical composition is discussed.

2.2 Methodology

2.2.1 Sample collection and preparation

24-h integrated urban PM_{2.5} samples were collected in Beijing (6 samples) and Mainz (3 samples). For the six Beijing samples, three were collected from 7–12 January 2014, during a relatively clean period with PM_{2.5} mass concentrations between 32 and 38 $\mu\text{g m}^{-3}$ (sample ID: BJL (Beijing Low)). The other three samples were collected from 15–23 January 2014, during a severe haze pollution period with high PM_{2.5} mass concentrations of 197–319 $\mu\text{g m}^{-3}$ (sample ID: BJH (Beijing High)). The three Mainz samples were taken from 15–28 January 2015 with relatively low PM_{2.5} concentrations of 20–28 $\mu\text{g m}^{-3}$ (sample ID: MZL (Mainz Low)). The Beijing samples were collected on prebaked quartz-fiber filters (8×10 inch) using a high-volume sampler at a flow rate of 1.05 $\text{m}^3 \text{min}^{-1}$, while the Mainz samples were collected on borosilicate glass fiber coated with fluorocarbon filters (\varnothing 70 mm, Pallflex T60A20, Pall Life Science, USA) using a low-volume sampler at a flow rate of 38.3 L min^{-1} . At each sampling site field blank samples were taken. The filter samples were stored at $-20\text{ }^\circ\text{C}$ until analysis. It should be noted that the PM_{2.5} samples in Mainz and Beijing were collected in two consecutive years. An influence of year-to-year variability due to changing meteorological conditions cannot be excluded, however, both periods were wintertime periods with a similar regional scenario (Chang et al., 2017).

Portions of the filters (1.08–19.23 cm^2 , corresponding to around 600 μg particle mass in each extracted filter) were extracted with 1.5 mL acetonitrile-water (8/2, v/v) in an ultrasonic bath for 30 min. The extraction step was repeated twice with 1 mL of the extraction solution. Then the

combined extracts were filtered with a 0.2 μm Teflon syringe filter to remove insoluble particulate matter. Afterwards the solvent mixture was evaporated to dryness under a gentle stream of nitrogen. The residual was dissolved in 500 μL acetonitrile-water (1/9, v/v) for subsequent analysis.

2.2.2 UHRMS analysis

The analysis of the filter extracts was carried out using an ultrahigh resolution mass spectrometer (Q-Exactive mass spectrometer; Thermo Scientific, Germany) coupled to an UHPLC system (Dionex UltiMate 3000, Thermo Scientific, Germany). A Hypersil Gold column (C18, 50 x 2.0 mm, 1.9 μm particle size, Thermo Scientific, Germany) was used for separation. Eluent A (ultrapure water with 2% acetonitrile and 0.04% formic acid) and eluent B (acetonitrile with 2% ultrapure water) were used in a gradient mode with a flow rate of 500 $\mu\text{L min}^{-1}$. The optimized gradient was as follows: 0–1.5 min 2% B, 1.5–2.5 min from 2% to 20% B, 2.5–5.5 min 20% B, 5.5–6.5 min from 20% to 30% B, 6.5–7.5 min from 30% to 50% B, 7.5–8.5 min from 50% to 98% B, 8.5–11.0 min 98% B, 11.0–11.05 min from 98% to 2% B, 11.05–11.1 min 2% B. Each sample extract was measured in triplicate with an injection volume of 20 μL .

The Q Exactive mass spectrometer was equipped with a heated ESI source at 120 $^{\circ}\text{C}$ in the negative ion mode (ESI $^{-}$) and 150 $^{\circ}\text{C}$ in the positive ion mode (ESI $^{+}$). It was operated with 40 psi sheath gas, 20 psi auxiliary gas, 320 $^{\circ}\text{C}$ capillary temperature and -3.3 kV spray voltage in the ESI $^{-}$ mode and 4.0 kV spray voltage in the ESI $^{+}$ mode. The mass spectrometer was calibrated with standard solution for ESI $^{-}$ and ESI $^{+}$, respectively (See supporting information, SI). Mass spectra of all samples were acquired in both ESI $^{-}$ and ESI $^{+}$ in the mass range between m/z 80 and m/z 500 with a resolving power of 70,000 @ m/z 200. The field blank filters were analyzed to correct for the background spectra. The mass accuracy of the measurements was < 3 ppm.

2.2.3 UHRMS data processing

Data were analyzed by a non-target screening approach using a commercially available software (SIEVE $^{\circledR}$, Thermo Scientific, Germany). This software provides the core functionality of MS data processing: peak detection, background subtraction and molecular formula assignment. The processing steps and settings are described in the following. A threshold intensity value of 1×10^5 arbitrary units in the two-dimensional space of the retention time window from 0–11.05 min and m/z from 80–500 was applied to all measurements. The software automatically searched the

ions with their peak abundance above the threshold intensity value and only ions with peak abundance in the ambient samples 3 times greater than those in the blank samples were retained. After that, the molecular formulas of observed individual peaks were assigned by SIEVE with following constraints: #12C: 1 to 39, #1H: 1 to 72, #16O: 0 to 20, #14N: 0 to 7, #32S: 0 to 4 and #35Cl: 0 to 2 with mass tolerance of ± 2 ppm. In ESI+ mode, 0–1 of Na was also included in the formula calculation because of the high tendency of sodium to form adducts with polar organic molecules. In addition, the isotope signals and ion-adducts (e.g. M–H+ACN) were checked and removed. Furthermore, to eliminate the chemically unreasonable formulas, the identified formulas were constrained by setting H/C, O/C, N/C, S/C and Cl/C ratios in the ranges of 0.3–3, 0–3, 0–1.3, 0–0.8 and 0–0.8, respectively (Kind and Fiehn, 2007; Wozniak et al., 2008; Lin et al., 2012a). The resulting neutral formulas with a non-integer or negative double bond equivalent (DBE) or elemental composition which disobey the nitrogen rule for even electron ions were also removed. It should be noted that only molecular formulas observed in all three samples for each sample ID were considered for further calculation and discussion. The peak abundance of a compound in each sample ID corresponded to the average area of its chromatographic peak in the three filter samples and was blank-corrected. The DBE value was calculated by Eq. (2.1) for elemental composition $C_cH_hO_oN_nS_sCl_x$:

$$DBE = c - \frac{(h+x)}{2} + \frac{n}{2} + 1 \quad (2.1)$$

Additionally, the aromaticity equivalent (X_C) was used to improve the identification and characterization of aromatic and condensed aromatic compounds in OA, which was described in detail by Yassine et al. (Yassine et al., 2014). The X_C value can be calculated by Eq. (2):

$$X_C = \frac{3(DBE - (mN_o + nN_s)) - 2}{DBE - (mN_o + nN_s)} \quad (2.2)$$

where ‘m’ and ‘n’ correspond to a fraction of oxygen and sulfur atoms in π -bond structure of a compound, which varied depending on the compound. If $DBE \leq mN_o + nN_s$ or $X_C \leq 0$, then X_C was defined as zero. Due to the extreme complexity of urban OA, we used $m=n=1$ for the conservative calculation of the X_C , which means every oxygen and sulfur atom was considered as π -bond structure (e.g., ketone and thioketone).

The assigned elemental formulas were classified into six species, including CHO, CHN, CHON, CHOS, CHONS and “other”. CHONS referred to compounds containing carbon, hydrogen, oxygen, nitrogen and sulfur. The other species were defined analogously, while “other” includes CHS, CHNS and chlorine-containing compounds, which represented very low intensity and are not

discussed here.

Since the response of each organic species to the mass spectrometer varies greatly, the average molecular weight (MW), H/C, O/C and DBE values were number-weighted calculated by following equations (2.3–2.6) (Lin et al., 2012a):

$$MW = \sum MW_i / \sum N_i \quad (2.3)$$

$$H/C = \sum H/C_i / \sum N_i \quad (2.4)$$

$$O/C = \sum O/C_i / \sum N_i \quad (2.5)$$

$$DBE = \sum DBE_i / \sum N_i \quad (2.6)$$

where N_i is the number of individual molecular formula i .

2.3 Results and discussion

2.3.1 General characteristics

As shown in Table 2.3.1, 1961–28696 mass peaks were detected in this study and the majority (57%–78%) of these detected peaks could be assigned with unambiguous formulas with mass tolerance less than 2 ppm, reflecting the high mass resolution power and high mass accuracy of the UHRMS technique. 1081–1955 molecular formulas of organic compounds with various numbers of isomers for each formula were detected in Mainz samples, while around 2–10 times more molecular formulas (2597–17596) were observed in Beijing samples, indicating the high complexity of Beijing OA. The number of molecular formulas in this study is much higher compared to other UHRMS studies used direct infusion (Lin et al., 2012a; Lin et al., 2012b; Rincón et al., 2012; Kourtchev et al., 2016) and a previous UHPLC-Orbitrap MS study (Wang et al., 2017). This can be explained because UHPLC not only separates a large number of isomers, it also reduces ion suppression by coelution. In addition, the use of the mixture of ACN/H₂O is more efficient for OA extraction, especially for the less polar compounds (e.g. aromatics), compared to pure water or methanol used in previous studies. Moreover, the high organic carbon concentration (around 200 $\mu\text{g cm}^{-2}$ in BJH) can significantly result in more organic compounds observed in BJH in this study. It should be noted that the number of detected organic compounds is highly depending on the threshold intensity values applied for background subtraction, which always vary in different

studies. 61–92% of molecular formulas in this study contains isomers, indicating that UHPLC technique is very important tool for the characterization of complex ambient OA. And a representative UHPLC chromatogram for the UHPLC performance is shown in Figure S2.3.1 in the Supporting Information (SI).

Table 2.3.1: The number of overall peaks observed in UHRMS, the number of assigned reasonable formulas and the relative abundance of each subgroup depending on their UHPLC chromatographic peaks (%), number-weighted average values of molecular weight, elemental ratios and DBE, and the isomer fraction in each subgroup.

Polarity and subgroup	Number of overall peak ^a	Number of formulas ^b	%	MW (Da)	H/C	O/C	DBE	Isomer fraction (%)
MZL								
total(-)	1961(70%)	1081(100%)	100	243	1.23	0.62	5.38	61
CHO-		347(32%)	23	206	1.05	0.44	6.13	70
CHON-		376(35%)	40	239	1.06	0.56	6.52	57
CHOS-		166(15%)	15	241	1.66	0.78	2.51	51
CHONS-		192(18%)	22	318	1.54	0.91	4.26	61
total(+)	5053(57%)	1955(100%)	100	225	1.34	0.27	5.76	61
CHO+		446(23%)	13	215	1.07	0.33	7.02	64
CHN+		302(15%)	11	177	1.33	0.00	5.93	79
CHON+		1103(56%)	74	236	1.42	0.28	5.34	60
CHONS+		104(6%)	2	292	1.65	0.68	4.29	11
BJL								
total(-)	3950(78%)	2597(100%)	100	241	1.22	0.51	5.85	72
CHO-		937(36%)	24	217	0.98	0.34	7.29	81
CHON-		799(31%)	53	230	0.96	0.50	7.28	68
CHOS-		494(19%)	16	256	1.81	0.63	2.02	70
CHONS-		367(14%)	7	305	1.57	0.81	4.26	57

2 Analytical method development and chemical characterization of urban OA using ultrahigh resolution mass spectrometry

total(+)	13168(72%)	7473(100%)	100	229	1.26	0.19	6.73	80
CHO+		1705(23%)	22	238	1.11	0.24	7.33	80
CHN+		1298(17%)	35	199	1.12	0.00	8.01	92
CHON+		3848(52%)	40	225	1.24	0.19	6.71	82
CHONS+		622(8%)	3	292	2.10	0.42	2.52	41
BJH								
total(-)	6745(72%)	3941(100%)	100	244	1.19	0.45	6.07	78
CHO-		1718(44%)	35	223	0.93	0.34	7.76	89
CHON-		842(21%)	48	221	0.92	0.50	7.24	73
CHOS-		831(21%)	12	280	1.74	0.51	2.26	80
CHONS-		550(14%)	5	292	1.56	0.59	4.74	48
total(+)	28696(75%)	17596(100%)	100	235	1.28	0.21	6.75	89
CHO+		3990(23%)	21	226	1.08	0.22	7.27	91
CHN+		2831(16%)	39	210	1.14	0.00	8.16	96
CHON+		8400(48%)	36	229	1.20	0.21	7.15	90
CHONS+		2375(13%)	4	302	2.04	0.44	2.74	71

^aValues in the parentheses are the percentage of peaks that can be assigned with unambiguous formulas.

^bValues in the parentheses are the percentage of different subgroups among the assigned reasonable formulas.

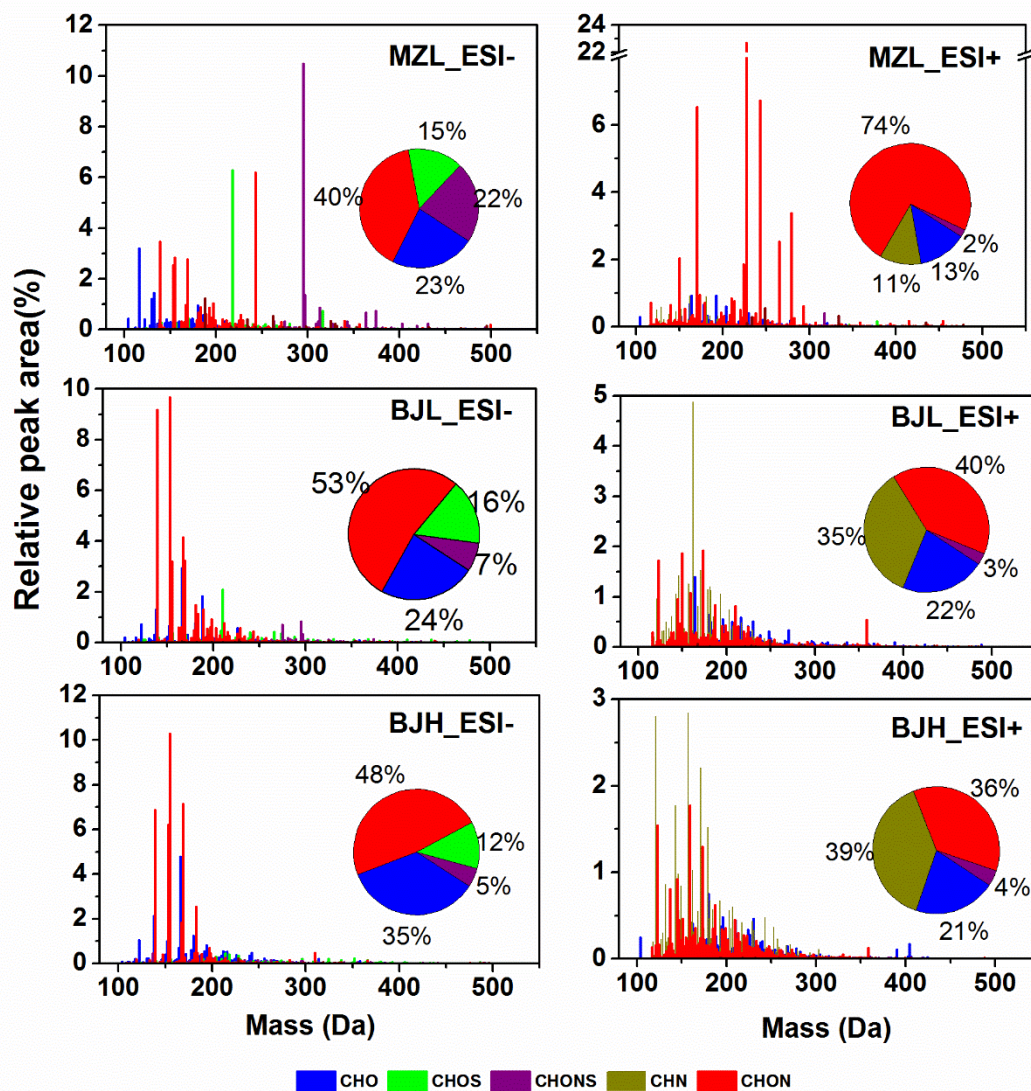


Figure 2.3.1: Mass spectra of detected organic compounds in ESI- and ESI+. The pie charts are proportional to the peak areas of an organic compound subgroup in each sample.

Mass spectra of observed organic compounds were reconstructed in both ESI- and ESI+ (see Figure 2.3.1). It should be noted that different organic species have different signal response in the mass spectrometer, so uncertainties exist when comparing the peak areas of organics in different subgroups. In this work, all species are assumed to have the same signal response when we compare peak areas of organics among different samples. A significant difference between ESI- and ESI+ is observed in terms of both the number and abundance of the detected compounds (Table 2.3.1 and Figure 2.3.1). Except CHOS compounds, all other subgroups have much more formulas in ESI+ mode compared to ESI- mode, indicating the less ionization suppression for these compounds

in ESI+. However, according to the peak abundance showed in Figure 2.3.1, the abundance fractions of CHO, CHOS and CHONS compounds in ESI- mode are higher than that in ESI+ mode, while CHN compounds have higher abundance fraction in ESI+ and the fractions for CHON compounds vary depending on different samples. This is due to the different mechanisms between negative and positive ionization mode in the electrospray, where ESI- is especially sensitive to deprotonatable compounds (e.g. organic acids) and ESI+ is prone to protonatable compounds (e.g. organic basic compounds). In both Mainz and Beijing samples, CHON compounds show the highest total peak abundance of the detected compounds, which is consistent with other urban OA studies (Lin et al., 2012a; Rincón et al., 2012; Wang et al., 2017), indicating the importance of CHON compounds to the urban atmosphere.

Table 2.3.1 shows that the number-weighted averaged molecular weight of the total detected compounds is similar between Mainz and Beijing samples (241–244 Da in ESI- and 225–229 in ESI+). However, the number-weighted averaged H/C and O/C ratios of total compounds in Beijing samples are significantly lower compared to Mainz samples and the number-weighted averaged DBE in Beijing samples is higher than that in Mainz samples. This observation suggests that organics in Beijing OA are more condensed and unsaturated compared to Mainz OA and aromatics (e.g. oxidized PAH) have an important impact on the Beijing atmosphere.

2.3.2 CHO compounds

In this study, CHO compounds account for 23–35% of the peak abundance among the organic compounds detected in ESI-, while the fraction decreases to 13–22% in ESI+ mode (see Table 2.3.1), indicating CHO compound in this study are more sensitive in ESI- mode. This is consistent with a previous study from Lin et al. (Lin et al., 2012a), which shows that most CHO compounds in OA contain carboxylic groups and are prone to deprotonate in ESI- mode. To further characterize the CHO compounds, Van Krevelen (VK) and carbon oxidation state (OS_c) diagrams are produced. The VK diagram is often utilized to describe the compositional characteristics of complex organic mixtures. It provides a broad overview on their average composition and can be used to qualitatively classify different composition domains (Hockaday et al., 2009; Lin et al., 2012a; Rincón et al., 2012). The VK diagram for CHO compounds observed in ESI- is shown in Figure 2.3.2, while the VK diagram for CHO compounds observed in ESI+ is showed in Figure S2.3.2. According to the H/C and O/C ratios, organic compounds can be divided into two different classes: aliphatic compounds with high H/C ratio (≥ 1.5) and low O/C ratios (≤ 0.5) (area A in Figure 2.3.2) and low-oxygen-containing aromatic hydrocarbons with low H/C ratio (≤ 1.0) and low O/C ratio

(≤ 0.5) (area B in Figure 2.3.2) (Kourtchev et al., 2014). As can be seen in Figure 2.3.2 (and Figure S2.3.2), the majority of CHO compounds are located in the region A and B, which agrees well with previous urban OA studies (Rincón et al., 2012; Kourtchev et al., 2014). However, much more CHO compounds detected in Beijing samples were plotted in the region B, indicating that Beijing OA contains more low-oxygen-containing aromatic hydrocarbons. The number weighted averaged H/C and O/C ratios of CHO compounds detected in ESI- are 1.05 and 0.44, respectively, in Mainz samples, while lower H/C and O/C ratios (0.98 and 0.34 in BJL; 0.93 and 0.34 in BJH) are observed in Beijing samples. This result is also consistent with previous studies, for example, the H/C and O/C ratios are lower in the samples from the Pearl River Delta region in Southern China compared to those from Cambridge in the UK (Lin et al., 2012a; Rincón et al., 2012). The low H/C and O/C ratios indicate the unsaturated characteristics of CHO in urban aerosol samples from China. This is further confirmed by the aromaticity equivalent (X_C), which is a parameter determining the presence of aromatics ($X_C \geq 2.5$) and condensed aromatics ($X_C \geq 2.7$) (Yassine et al., 2014). As shown in the pie chart of Figure 2.3.2, the fractions of aromatics and condensed aromatics are about 2 times and 1.7 times higher, respectively, in Beijing than in Mainz. The large difference in chemical characteristics of CHO compounds in Beijing and Mainz is likely associated with the different emission sources and/or atmospheric processes.

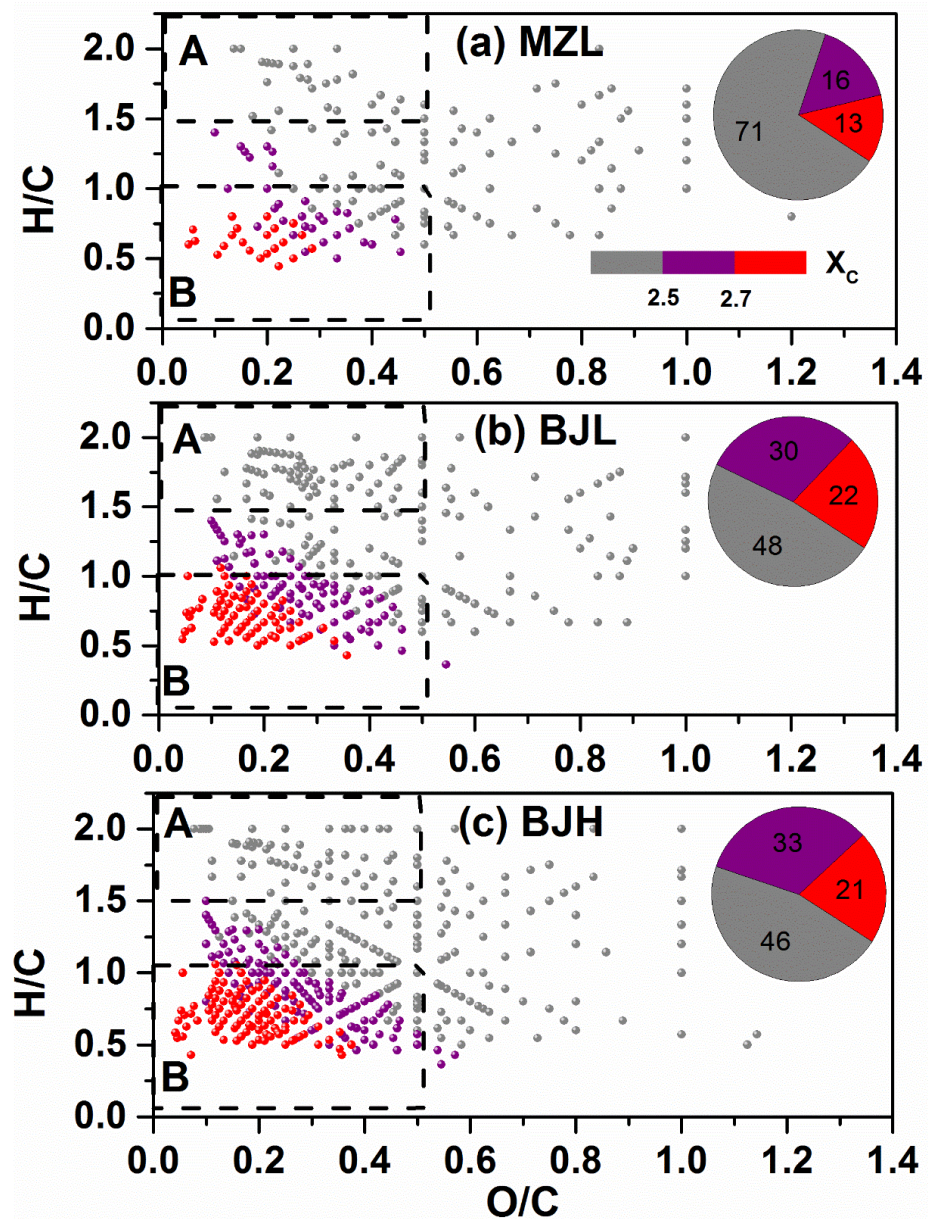


Figure 2.3.2: The Van Krevelen diagram for CHO compounds detected in ESI- mode. Areas ‘A’ and ‘B’ refer to aliphatic compounds and low-oxygen-containing aromatic hydrocarbons in organic aerosol, respectively. The colour bar denotes the aromaticity equivalent (gray with $X_C < 2.50$, purple with $2.50 \leq X_C < 2.70$ and red with $X_C \geq 2.70$). The pie chat shows the percentage of the number of each color-coded compound in each sample.

The carbon oxidation state (OS_C), introduced by Kroll et al. (Kroll et al., 2011) is another parameter used to describe the composition of a complex mixture of organics experiencing dynamic oxidation processes. OS_C can be calculated for each molecular formula of CHO compounds

identified in the mass spectra following Eq. (2.7).

$$OS_C \approx 2 O/C - H/C \quad (2.7)$$

Figure 2.3.3 shows the overlaid OS_C as a function of carbon number for samples from Beijing and Mainz. Consistent with previous studies (Kourtchev et al., 2015; Kourtchev et al., 2016; Wang et al., 2017), the majority of molecules in the CHO subgroup have OS_C between -1.5 and $+1$ with number of carbon atoms up to 30. The molecules with OS_C between -1 and -2 with 18 or more carbon atoms are suggested to be associated with hydrocarbon-like organic aerosol (HOA). The molecules with OS_C between -1.25 and -0.25 with 7–23 carbon atoms are associated with biomass burning organic aerosol (BBOA) directly emitted into the atmosphere. The molecules with OS_C between -0.5 and $+0.25$ with 5–18 carbon atoms are associated with semi-volatile oxygenated organic aerosol (SV-OOA), while the molecules with OS_C between $+0.25$ and $+1.0$ with 4–13 carbon atoms are associated with low-volatility oxygenated organic aerosol (LV-OOA) as defined by Kroll et al. (Kroll et al., 2011). As shown in Figure 2.3.3, a large majority of CHO molecules are attributed to SV-OOA for both Beijing and Mainz samples, indicating the importance of atmospheric oxidation and aging in OA production. Significantly more BBOA associated molecules are obtained in Beijing compared to Mainz, reflecting the enhanced biomass burning activities in Beijing and surrounding areas (Zhang et al., 2008; Cheng et al., 2013; Huang et al., 2014; Elser et al., 2016). It should be noted that coal combustion is also an important OA source (Zhang et al., 2013; Huang et al., 2014; Elser et al., 2016; Zhang et al., 2016), which is not discussed here due to the lack of source characterization with UHRMS study.

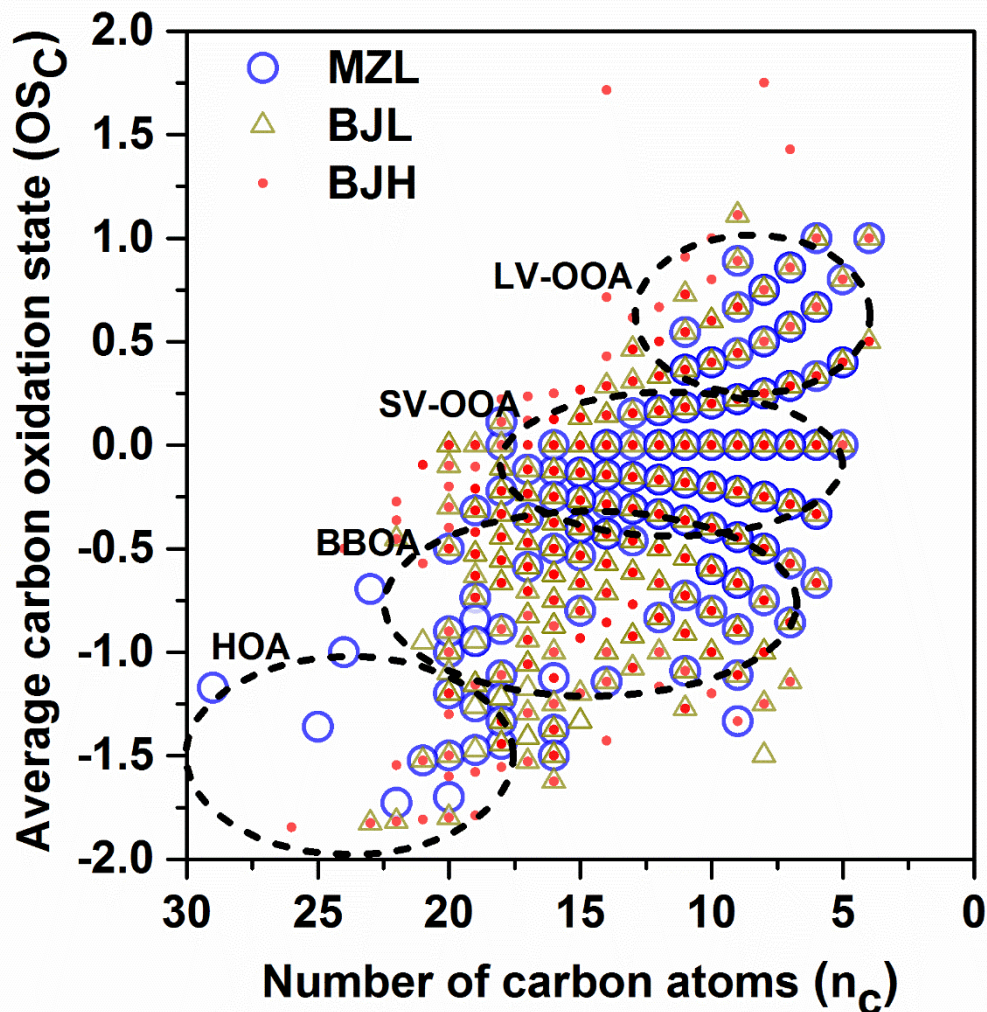


Figure 2.3.3: Carbon oxidation state plots for CHO compounds detected in ESI⁻ mode. The black dash ovals area marked as HOA, BBOA, SV-OOA and LV-OOA correspond to hydrocarbon-like organic aerosol, biomass burning organic aerosol, semivolatile and low-volatility organic aerosol.

2.3.3 CHON compounds

A large amount of organic nitrogen compounds has been observed in fog water, continental precipitation as well as aerosol samples (Altieri et al., 2009; Mazzoleni et al., 2010; Lin et al., 2012a; Jiang et al., 2016). In this study, 376–842 of CHON⁻ compounds (CHON compounds detected in ESI⁻) and 1103–8400 of CHON⁺ compounds (CHON compounds detected in ESI⁺) were determined. The peak area of CHON⁻ accounts for 40% in Mainz samples and it increases to 74%

for CHON⁺. On the contrary, the peak area fractions of CHON⁻ in Beijing samples (53% in BJL and 48% in BJH) are higher compared to that for CHON⁺ (40% in BJL and 36% in BJH). This observation indicates that most CHON compounds in Mainz samples contain amino functional groups, which are prone to be protonated in ESI⁺ mode, while CHON compounds in Beijing samples contain more nitro groups, which are preferentially to be deprotonated in ESI⁻ mode.

The CHON compounds are further classified into different subgroups based on the O/N ratios. Figure 2.3.4 shows the relative contribution of each subgroup to the sum of CHON peak intensities observed in ESI⁺ and ESI⁻ mode. Compounds in the subgroups with O/N < 3 are preferentially detected in ESI⁺ mode, again likely due to the presence of reduced nitrogen containing functional groups (e.g. amines). Interestingly, in ESI⁺ mode, a large fraction (~40%) of CHON⁺ compounds have O/N ratio of 2 for samples from Mainz, while compounds with O/N ratio of 1 dominate (~55%) for samples from Beijing regardless of the pollution level. This is an indication that CHON⁺ compounds in Beijing OA contain more reduced nitrogen atoms, which could be produced from a minor pyrolytic and oxidative processing (e.g. smoldering burning) of N-heterocycle compounds (e.g. imidazole) (Lin et al., 2012a). The number-weighted averaged DBE for CHON⁺ compounds is 5.34 in Mainz samples, while higher averaged DBEs (6.71 in BJL and 7.15 in BJH) are observed in Beijing samples, indicating CHON⁺ compounds in Beijing OA are more unsaturated. This is further confirmed by the VK diagram in Figure S2.3.3, which shows that much more CHON⁺ compounds in Beijing samples are suggested to be low-oxygen-containing aromatic hydrocarbons in area B. And, the pie chart in Figure S2.3.3 shows that the fractions of aromatics and condensed aromatics in Beijing samples are about 1.25 times and 6 times higher, respectively, compared to Mainz samples. It indicates that reduced nitrogen-containing aromatic precursors have more influence on CHON⁺ compounds in Beijing than in Mainz. Another interesting subgroup of CHON compounds are those compounds with O/N ≥ 3, which are preferentially observed in ESI⁻ mode, likely associated with the nitrooxy (-ONO₂) or oxygenated nitrooxy group (O/N ≥ 4). The majority of CHON⁻ compounds has O/N ratio of 3 or 4, indicating that besides the nitrooxy group most CHON⁻ compounds contain additionally not more than one oxidized group. This observation is confirmed by the modified VK diagram for CHON⁻ compounds in Figure S2.3.4 (in which the VK diagram was constructed by plotting the H/C ratio versus the (O-3N)/C ratio instead of O/C ratio), showing a large number of CHON⁻ compounds are observed with low (O-3N)/C ratio between 0 and 0.2. However, compared to the CHON⁻ compounds in MZL and BJL samples dominating with O/N ratio of 3, the CHON⁻ compounds in BJH samples are dominated with O/N ratio of 4, suggesting CHON⁻ compounds undergo relatively higher oxidized process in polluted air. Consistent with the CHON⁺ compounds, the number-weighted averaged DBE (see Table 2.3.1)

and the fraction of aromatics of CHON- compounds (see Figure S2.3.4) in Beijing samples are higher than those in Mainz samples, indicating that nitrogen containing aromatics are more important precursors in Beijing OA, which agrees well with Wang et al.'s study (Wang et al., 2017) showing many nitroxy-aromatic compounds (e.g., nitrophenol) with high abundance observed in the OA of Shanghai. It should be noted that only a small fraction of CHON compounds is observed in both ESI+ and ESI- modes (see overlapped bar in Figure 2.3.4). Actually this fraction of CHNO compounds could consist of amino acids, which contain both acidic (-COOH) and basic (-NH₂) functional groups and which have been identified in biomass burning and fossil fuel combustion emissions (Mace, 2003;Barbaro et al., 2011).

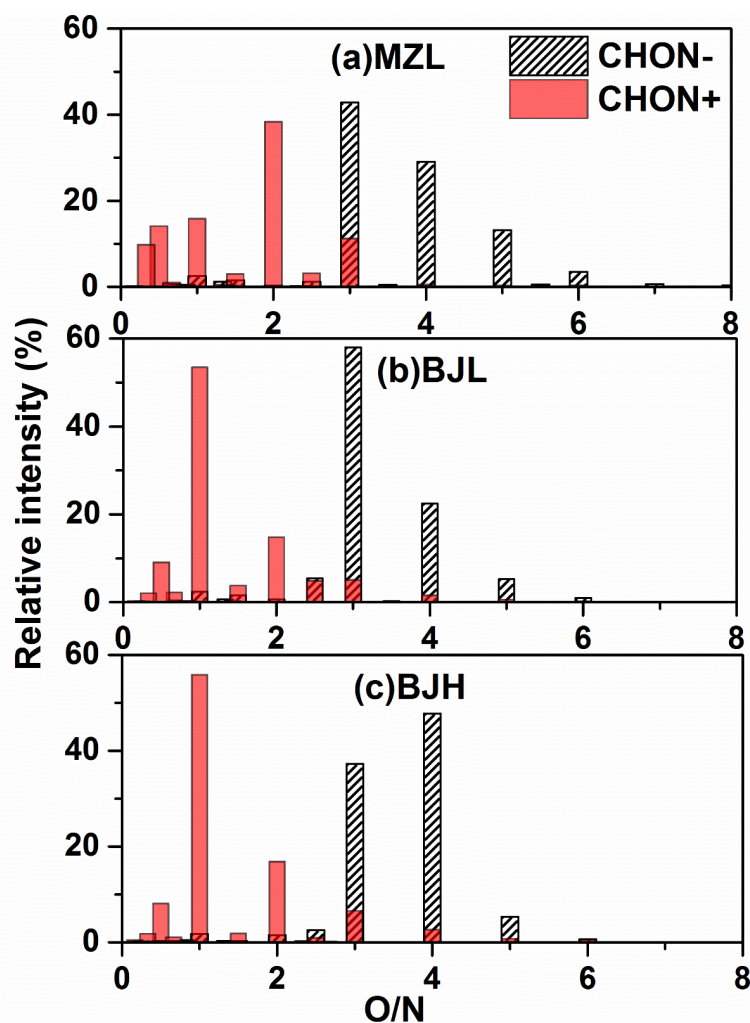


Figure 2.3.4: Classification of CHON compounds into different subgroups according to O/N ratios in their molecules. The y-axis indicates the relative contribution of each subgroup to the sum of CHON compounds peak intensities observed in the ESI- and ESI+ modes, respectively.

2.3.4 CHN compounds

The CHN compounds can be detected only in ESI, which are very likely associated with nitrile and amine species (Lin et al., 2012a). The number-weighted averaged molecular weight of CHN compounds is the smallest in all subgroups. However, the number-weighted averaged DBE (5.93–8.16) of CHN compounds is the highest, indicating that this group of molecules is highly unsaturated. CHN compounds accounts for around 11% of the total peak abundance in Mainz sample, while it is more than three times higher in Beijing samples (35% in BJJ and 39% in BJJ), suggesting that CHN compounds have more important impact on Beijing OA compared to Mainz OA.

Figure 2.3.5 shows the Kendrick mass defect (KMD) diagram for the CHN compounds observed in Mainz and Beijing samples. The KMD diagram is commonly used to investigate the relationship among a large set of molecular formulas in the UHRMS study (Kendrick, 1963; Hughey et al., 2001; Lin et al., 2012a; Rincón et al., 2012). Here, we set the molar mass of CH₂ to exactly 14 u as the reference mass for calculating the Kendrick mass (KM) following Eq. (2.8) and the KMD is defined as the difference between the nominal mass and the KM as shown in Eq. (2.9).

$$KM(CH_2) = mass \times [mass\ CH_2] / mass\ CH_2 \quad (2.8)$$

$$KMD(CH_2) = [mass] - KM(CH_2) \quad (2.9)$$

where brackets refer to the nominal mass obtained by rounding the mass to the nearest integer. When the KMD of a compound is plotted vs. its neutral molecular weight, homologous series of compounds differing only by CH₂ fall on horizontal lines and are clearly distinguishable. As can be seen in Figure 2.3.5, the majority of CHN compounds belong to members of several different homologous series. However, compared to the homologous series of CHN compounds in Mainz samples, the homologous series in Beijing samples often have a higher number of members with larger molecular weights. This could be explained by more primary biological aerosol particles with long chain aromatic amines or N-heterocycle compounds in Beijing atmosphere (Rincón et al., 2012; Jiang et al., 2014). The X_C values suggest that most CHN compounds are condensed aromatics (X_C ≥ 2.7) and aromatics (X_C ≥ 2.5). To facilitate the imagination of possible chemical species within Figure 2.3.5, the elemental composition, the DBE and a potential chemical structure for the first compound of three homologous series are also illustrated in the figure, representing a condensed aromatic species, an aromatic compound and a non-aromatic species. In previous MS/MS studies of CHN compounds (Simoneit et al., 2003; Laskin et al., 2009; Lin et al., 2012a),

these nitrogen containing aromatic compounds are suggested to be alkaloids with one or two nitrogen atoms embedded into five-membered (e.g., pyrazole, imidazole, and their derivatives) or six-membered rings (e.g., pyridazine and their derivatives), which are likely formed during biomass burning from dialkanoic acids and ammonia. It is worth noting that a significant number of CHN compounds with 12–23 DBE and 15–29 carbon atoms (those above the dash line in Figure 2.3.5) are exclusively present in Beijing samples. These compounds are assigned to polycyclic aromatic N-heterocycle hydrocarbons (PANH) with four or more aromatic rings, which are strong mutagens and potential human carcinogens. This result is consistent with a previous study in which several PANH with 4–8 aromatic rings were observed in ambient organic aerosol from Beijing (Jiang et al., 2014).

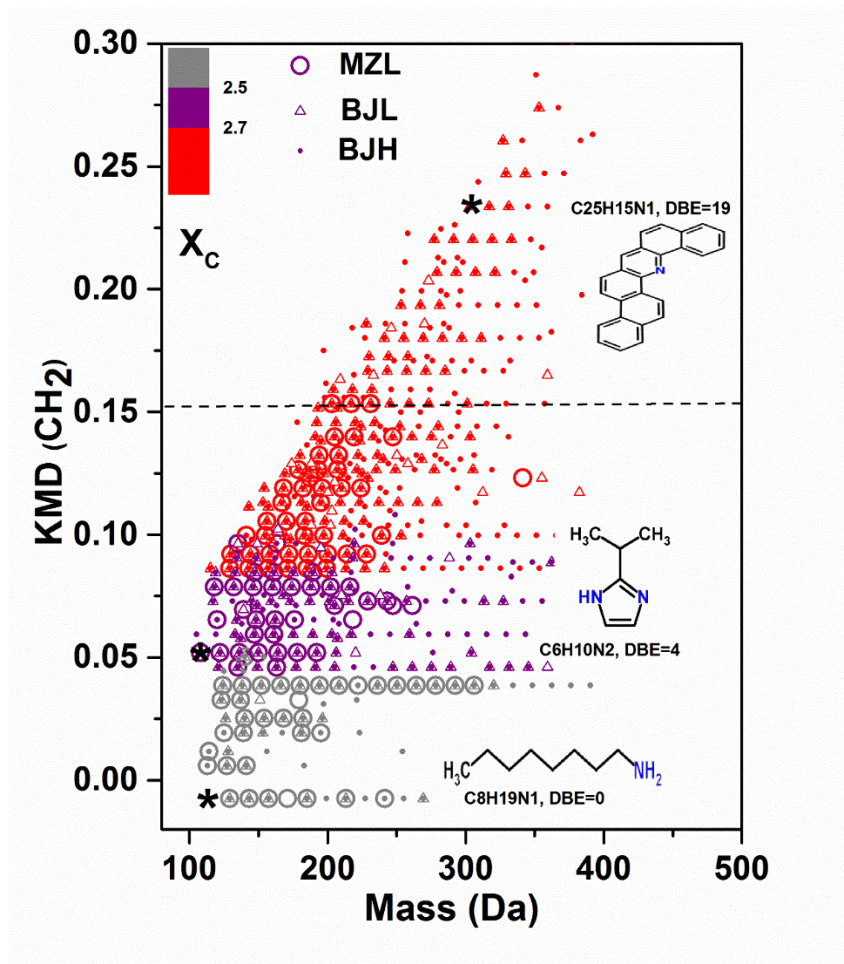


Figure 2.3.5: Kendrick mass defect diagram of CHN compounds detected in ESI+ mode. The colour bar denotes the aromaticity equivalent (gray with $X_C < 2.50$, purple with $2.50 \leq X_C < 2.70$ and red with $X_C \geq 2.70$). The element composition, DBE and a potential chemical structure for the first compound (the black asterisk) of three homologous series are illustrated in the figure.

2.3.5 Sulfur compounds (CHOS and CHONS subgroups)

A large number of S-containing organic compounds have been observed in urban and rural OA (Tao et al., 2014; Jiang et al., 2016; Wang et al., 2016; Wang et al., 2017). In this study, 166–831 CHOS formulas were determined in ESI- mode. 86–93% of CHOS formulas are assigned to possess a molecular composition with O/S ratio ≥ 4 , suggesting they represent organosulfates (OSs), which is consistent with previous studies (Tao et al., 2014; Wang et al., 2016). The number-weighted average molecular weight of CHOS compounds in Beijing samples (250 Da in BJL and 280 Da in BJH) is larger than that (241 Da) in Mainz samples. In contrast, the number-weighted average DBE in Beijing samples (2.02 in BJL and 2.26 in BJH) is lower than that (2.51) in Mainz samples. Moreover, the DBE vs. carbon number diagram in Figure S2.3.5 shows that more CHOS compounds with low DBE and high carbon numbers were observed in Beijing samples, indicating that CHOS compounds with longer carbon chain and lower degree of unsaturation make an important contribution to Beijing OSs. This result is similar to a previous study (Tao et al., 2014), which revealed that the OSs in Shanghai have longer aliphatic carbon chains and lower degree of unsaturation than the OSs in Los Angeles. As observed in smog chamber studies (Riva et al., 2016), the OSs with high molecular weight and low degree of unsaturation can be formed from long-chain alkanes (e.g. dodecane) emitted from combustion sources. Besides the CHOS compounds, the other S-containing organics are assigned to be CHONS compounds, which are also prone to be measured in ESI- mode. The CHONS compounds account for around 22% of the total peak abundance in ESI- mode in the Mainz samples, while the fraction decreases to 5–7% in the samples from Beijing. The compound with the formula $C_{10}H_{17}O_7NS$, which has been identified as an α -pinene-derived nitrooxy-OSs, shows the highest concentration in Mainz (see Figure 2.3.1), while its concentration is much smaller in Beijing, indicating the important role of monoterpene precursor on CHONS compounds in Mainz OA. In Mainz and BJL samples, 61–65% of detected CHONS- formulas have the $O/(4S+3N)$ ratio ≥ 1 , allowing their assignment to nitrooxy-OSs with both $-OSO_3H$ and $-ONO_2$ groups. However, in BJH samples, only 29% of the CHONS- formulas are suggested to be nitrooxy-Oss. To further understand the chemical properties of these CHONS compounds, MS/MS analysis should be performed in the future.

2.4 Conclusion and implication

In this study, we applied the UHPLC-Orbitrap MS for the analysis of the organic fraction of $PM_{2.5}$ samples from one European city Mainz and one Chinese city Beijing. Roughly 18000 organic

compounds were identified based on unambiguous elemental composition in the urban OA, while the number of organics in Beijing samples are around 2–10 times more than Mainz samples. The information of these organic compounds can enrich the database of the molecular composition of OA in urban regions. 61–92% of the detected organics have more than one isomer, indicating that the UHPLC separation is important for the OA characterization and suggested to be applied prior to the mass spectrometer for the identification or quantification of individual organic substances in the OA in future studies.

The chemical characteristics of OA in Mainz and Beijing shows clear differences. The organic species of CHO, CHON and CHN in Beijing OA have lower elemental H/C and O/C (except CHN) but higher DBE and Xc compared to Mainz OA, demonstrating that organics in Beijing OA are highly unsaturated. The Van Krevelen and KMD diagrams show that much more mono/poly aromatics were observed in Beijing OA, suggesting that they are combustion related compounds. The majority of CHOS compounds are suggested to be OSs, while OSs in the two cities have different molecular characteristics showing that many OS with low DBE and high carbon numbers were only detected in Beijing OA. Most CHONS compounds were observed in low concentrations in PM_{2.5} (MZL and BJL). These elemental compositions can be assigned to represent mostly nitrooxy-OS. Only 29% of CHONS compounds collected during high PM_{2.5} episodes (BJH) are suggested to be nitrooxy-OSs, point out the large differences in the chemical composition of CHONS compounds in the heavily and in the less polluted atmosphere. In future studies more detailed MS studies (e.g. MS/MS analysis) should be performed for a better understanding the molecular structures, sources or formation pathways of these compounds. As shown in this study, biogenic and anthropogenic precursors have a different influence on the Beijing OA and Mainz OA. Therefore, dedicated smog chamber experiments with mixtures of biogenic (e.g. α -pinene) and anthropogenic (e.g. naphthalene) precursors might be conducted to better understand their influence on OA formation in urban regions.

Supporting Information

The description of the calibration standard solution for mass spectrometer, five supporting figures (Figure S2.3.1–S2.3.5).

Acknowledgements

This study was supported by the National Natural Science Foundation of China (NSFC, Grant No. 41403110, No. 41673134, and No. 91644219) and the German Research Foundation (Deutsche Forschungsgemeinschaft, DFG) under Grant No. INST 247/664-1 FUGG. K. Wang acknowledges the scholarship from Chinese Scholarship Council (CSC) and Max Plank Graduate Center with Johannes Gutenberg University of Mainz (MPGC). We also thank Berthold Friederich (Institute of

Atmospheric Physics, Johannes Gutenberg University of Mainz) for his assistance in sample collection in Mainz.

2.5 Additional information and results

This following results and information are not part of the actual manuscript, however are supporting the results discussed above.

2.5.1 Difference of chemical composition between ACN/H₂O and H₂O extraction method

In previous studies, pure water (H₂O) were always used for the OA sample extraction with the following steps: Portions of OA filter samples were extracted using 2.5 mL pure water in an ultrasonic bath for 30 min two times, respectively. The extracts were filtered with a 0.2 μm Teflon syringe filter and acidified to pH = 2 using HCl before performing a solid phase extraction (SPE) step. The filter extracts were then loaded on a SPE cartridge (Oasis HLB, 30 μm, 60 mg per cartridge, Waters Corporation, Milford, MA) with the aim to remove inorganic ions, low molecular weight organic molecules and sugars. The loaded cartridge was subsequently rinsed two times with 1 mL pure water and then eluted with 1.5 mL of methanol containing 2% (w/w) ammonia. Immediately after eluting from the SPE column the extract was evaporated to dryness under a gentle stream of nitrogen. The residues were dissolved in 500 μL acetonitrile and water (1/9, v/v) for LC-MS analysis.

Previous studies have shown the effect of the solvent on the characterization of OA (Bateman et al., 2008; Heaton et al., 2009; Tao et al., 2014). However, it is still not clear to what extent the extraction solvent affects the characterization of OA from different sources and mass loadings. Therefore, the PM_{2.5} samples from Beijing and Mainz, representing high and low mass loading and different pollution sources, were extracted with ACN/H₂O (A/W) and H₂O (W), respectively. Figure 2.5.1 shows the number of individually assigned molecular formulas in Mainz and Beijing samples. As can be seen in the figure the number of organic compounds observed in the Beijing samples are 2–10 times higher than in the Mainz samples. However, large solvent-dependent differences are observed for ESI⁺ and ESI⁻. While the number of compounds extracted with ACN/H₂O (A/W⁻) is similar to those extracted with pure H₂O (W⁻) for ESI⁻ analysis, much more organic compounds are observed with ESI⁺ analysis when ACN/H₂O (A/W⁺) is used for extraction

compared to pure H₂O (W+). A plausible explanation for this observation is that most of organics detected in the ESI- contain carboxylic acid functional groups, which enhance the water solubility of the compounds. A more detailed analysis compares the overlapping percentage of number and intensity of compounds observed in ESI+ and ESI- using the two extraction methods (see Table 2.5.1). For example, in ESI- mode 72% of compounds obtained in the H₂O extracts are also observed in ACN/H₂O extracts, while only 56% of compounds observed in the ACN/H₂O extracts are obtained in H₂O extracts. Meanwhile, 90% of the total peak intensity from the H₂O extracts matches the peak intensity from the ACN/H₂O extracts, while only 75% of the total peak intensity from the ACN/H₂O extracts matched assigned peaks in the H₂O extracts. It is clear that a majority of organics observed in the H₂O extracts can also be measured in the ACN/H₂O extracts, in particular for those organics of high concentrations. More important, ACN/H₂O can extract more organic compounds which are not found in the H₂O extracts. In summary, the results demonstrate that ACN/H₂O is superior to H₂O for the extraction of organics in OA.

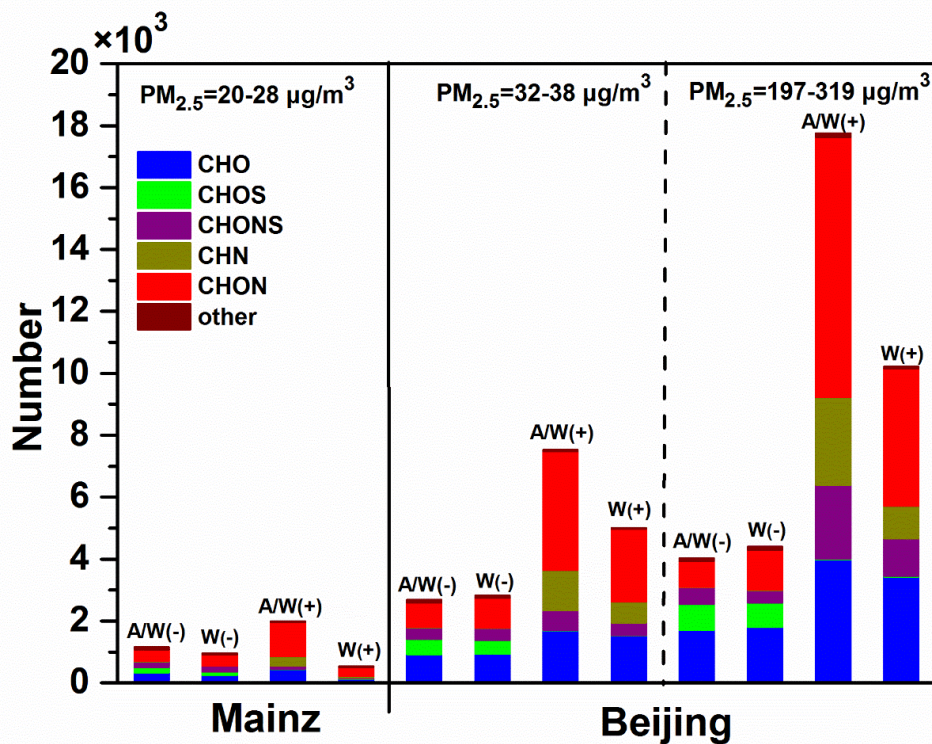


Figure 2.5.1: The number of individually assigned molecular formulas observed in ACN/H₂O and H₂O methods in Mainz and Beijing samples. Each subgroup is marked by the different colors.

Table 2.5.1: The overlapping percentage of number and intensity of compounds extracted in the two extraction methods

Sample ID	Method	Number of the overlapped molecular formulas (%)		Intensity of the overlapped formulas (%)	
		ESI-	ESI+	ESI-	ESI+
MZL	ACN-H ₂ O	56	20	75	32
	H ₂ O	72	60	90	65
BJL	ACN-H ₂ O	70	46	92	78
	H ₂ O	70	68	95	92
BJH	ACN-H ₂ O	59	43	91	80
	H ₂ O	60	70	95	94

3 The maximum carbonyl ratio as a metric for the structural classification of OA

This chapter is a reprint of the article:

Yun Zhang, Kai Wang, Haijie Tong, Ru-Jin Huang, Thorsten Hoffmann

The maximum carbonyl ratio (MCR) as a new index for the structural classification of secondary organic aerosol components

Rapid Communications in Mass Spectrometry, 2021, 35, e9113,

<https://doi.org/10.1002/rcm.9113>

Abstract. Organic aerosols (OA) account for a large fraction of atmospheric fine particulate matter and thus are affecting climate and public health. Elucidation of the chemical composition of OA is the key for addressing the role of ambient fine particles at the atmosphere-biosphere interface and mass spectrometry is the main method to achieve this goal. High resolution mass spectrometry (HRMS) is on its way to become one of the most prominent techniques, also for the analysis of atmospheric aerosols. The combination of high mass resolution and accurate mass determination allows the elemental composition of numerous compounds to be easily elucidated. Here a new parameter for the improved classification of OA is introduced – the maximum carbonyl ratio (MCR) – which is directly derived from the molecular composition and is particularly suitable for the identification and characterization of secondary organic aerosols (SOA). The concept is exemplified by the analysis of ambient OA samples from two measurement sites (Hyytiälä, Finland; Beijing, China) and of laboratory-generated SOA based on ultrahigh performance liquid chromatography (UHPLC) coupled to Orbitrap MS. To interpret the results, MCR-Van Krevelen (VK) diagrams are generated for the different OA samples and the individual compounds are categorized into specific areas of the diagrams. The results show that the MCR index is a valuable parameter for representing atmospheric SOA components in composition and structure-dependent visualization tools such as VK diagrams. Therefore, the MCR index is suggested as a tool for a better characterization of the sources and the processing of atmospheric OA components based on HRMS data. Since the MCR contains information on the concentration of highly electrophilic organic compounds in particulate matter (PM) as well as on the concentration of organic (hydro)peroxides, the MCR could be a promising metric for identifying health-related particulate matter parameters by HRMS.

3.1 Introduction

Organic aerosols (OA) account for a large fraction (20–90%) of submicron particulate mass in the atmosphere with consequences for climate and public health (Pöschl, 2005; Jimenez et al., 2009; Hallquist et al., 2009; Kroll et al., 2011; Pöschl and Shiraiwa, 2015). Atmospheric OA, including primary organic aerosol particles emitted directly from sources and secondary organic aerosol (SOA) formed by oxidation of precursors in the atmosphere, originate from a wide variety of biogenic (e.g., terrestrial vegetation) and anthropogenic (e.g., biomass burning and fossil fuel combustion) sources (Seinfeld and Pandis, 2016). Due to their diverse sources, various formation

pathways and complex multiphase aging processes, the OA fraction is composed of thousands of different compounds, which contain various functional groups including hydroxyl, hydroperoxide, carbonyl and carboxyl groups but also sulfur and nitrogen containing functional groups (organic nitrates and sulfates). The vast number of individual compounds not only results in a wide range of physical, chemical and toxicological properties and complicates the OA characterization, this complexity in combination with sophisticated mass spectrometric instrumentation also offers the possibility to decipher OA sources, formation pathways and their fate in the atmosphere (Lin et al., 2012; Kourtchev et al., 2016; Glasius et al., 2016; Wang et al., 2018; Glasius et al., 2018; Daellenbach et al., 2019; Yee et al., 2020). Thus, it is essential to develop highly efficient analytical techniques to gather detailed, compound-specific chemical information.

In the last decade, analytical methods based on high-resolution mass spectrometry (HRMS), such as Fourier transform ion cyclotron (FTICR) and Orbitrap MS, in combination with soft ionization techniques, including atmospheric pressure chemical ionization (APCI) and electrospray ionization (ESI) have been successfully applied to OA research (Lin et al., 2012; Nozière et al., 2015; Kourtchev et al., 2016; Glasius et al., 2016; Song et al., 2018; Laskin, et al., 2018; Wang et al., 2018; Glasius et al., 2018). HRMS benefits from two outstanding features, high mass spectrometric resolution ($> 40,000$) and high mass accuracy (< 5 ppm). As a consequence, HRMS allows the assignment of unique elemental compositions and enables the calculation of the molecular formulae for the analytes of interest even in highly complex samples, often hundreds or thousands of compounds. However, accompanying the complexity and size of the datasets, new needs and challenges arise concerning the interpretation and visualization of the HRMS results. Consequently, visualization tools like Van Krevelen (VK) diagrams (Kim et al., 2003; Sleighter et al., 2007; Hockaday et al., 2009), Kendrick mass defect (KMD) analysis (Kendrick et al., 1963; Hughey et al., 2001) and carbon oxidation state (OSc) plots (Kroll et al., 2011; Wang et al., 2018) were developed. Most often VK diagrams are applied, which place every assigned unique chemical formula on a 2D scatterplot of H/C ratio versus O/C ratio, to sort and group the organic compounds identified by the HR mass spectra.

One obvious chemical feature which directly results from the elemental composition of the analytes is their degree of unsaturation (DU) or double bond equivalents (DBE). The DBE represents the sum of the number of double bonds and rings in a molecule and is a well established and helpful tool in mass spectrometry (Barrow et al., 2009; Yassine et al., 2014). However, a limitation of this metric is that the DBE cannot distinguish C-C double bonds from C-O/C-S double bonds when divalent atoms (e.g., O and S) are present in the molecules. By definition of the DBE the divalent oxygen does not influence the DBE value, although obviously oxygen can also

contribute to double bonds of organic molecules. Therefore, aiming towards a better structural characterization of complex organic mixtures, the aromaticity index (AI) (Koch and Dittmar, 2016) and aromaticity equivalent (Xc) (Yassine et al., 2014) have been introduced in recent years. The advantage of AI and Xc over the simple use of DBE is that they also consider heteroatoms (O, S, N) as contributors to the degree of unsaturation and that they define threshold values to quantify the aromaticity of the organic molecules. As a consequence, parameters such as AI or Xc are beneficial for the characterization of aromatic/condensed aromatic compounds. However, for the characterization of chemical structures of typical ambient SOA compounds, AI or Xc are less appropriate. First of all, the majority of typical SOA components rarely contain aromatic structures, since the main gaseous SOA precursors are non-aromatic compounds (Hallquist et al., 2009). Moreover, even when aromatic VOCs serve as SOA precursors, which can be expected in mostly anthropogenically influenced areas, their aromaticity is frequently lost during the initial oxidation steps, i.e., due to the dominant OH addition to the aromatic ring followed by rapid further oxidation steps (Ziemann and Atkinson, 2012). Actually, also other structural elements influencing the DBE of SOA precursor molecules, such as C-C multiple bonds or carbon ring structures, are prone to be lost in the process of SOA formation. This is especially true for C-C double bonds, which represent the main chemical feature of biogenic VOCs (e.g., isoprene, monoterpenes, sesquiterpenes), which in turn are the most important SOA precursors on the global scale. The double bonds are preferentially attacked by atmospheric oxidants (OH, ozone, nitrate radicals), hence tend to disappear prior to the gas-to-particle conversion of the products. Less obvious but with the same tendency behave cyclic compounds, for which ring-opening pathways yield especially low-volatile oxidation products that finally make a notable contribution to the particle phase. Therefore, in the process of SOA formation most structural elements (C=C and rings) which usually contribute to a carbon related degree of unsaturation in organic matter disappear and are replaced by unsaturation connected with the introduced oxygen containing functionalities.

In principle, SOA components contain oxygen atoms in the form of hydroxyl (OH), hydroperoxide (OOH) or peroxide (-OO-), carbonyl (C=O), carboxyl (COOH) and epoxide groups (Nozière et al., 2015). Obviously, the carbonyl group, in the form of an aldehyde, ketone or carboxyl group as well as the epoxide group can contribute to the degree of unsaturation. In contrast, in the absence of unsaturation of a specific SOA compound (oxygen is always present in SOA) alcohol or peroxide functionalities must be present. In the context of SOA chemistry especially the latter functionality has created pronounced scientific interest, since highly oxidized multifunctional organic compounds (HOMs) are supposed to be multifunctional hydroperoxides formed via autooxidation (Bianchi et al., 2019). Due to their low vapour pressure, HOMs are able to contribute

to the formation of new particles in the atmosphere and thus, via their function as cloud condensation nuclei, ultimately have a major impact on the atmospheric radiation balance (Carslaw et al., 2017). However, peroxide functionalities may also play an important role in health-related effects of SOA, since organic (hydro)peroxides are thought to contribute to the formation of reactive oxygen species (ROS) by transporting oxidants on/in particles into the respiratory system (Verma et al., 2015; Tong et al., 2018).

It is noteworthy to point out that the degree of unsaturation as discussed above results in distinct chemical properties. For example, both carbonyls and epoxides possess a high electrophilic reactivity. The polarized double bond in carbonyls and even more pronounced the 3-membered ring in epoxides induce a high reactivity towards nucleophilic addition reactions. This reactivity enables the formation of covalent bonds between the electrophile (carbonyl/epoxide carbon) and a nucleophilic partner molecule (alcohols, other carbonyls, amines). On the one hand, this reactivity is directly relevant for atmospheric heterogeneous/multiphase chemistry and the formation of higher molecular weight compounds in SOA. In other words, higher concentrations of carbonyls/epoxides cause a higher potential for condensed phase chemistry and the formation of oligomers by homogeneous aging (Rudich et al., 2007). In contrast, low carbonyl/epoxide content together with the presence of high molecular weight compounds could indicate that condensed phase chemistry already happened (homogeneously aged SOA). On the other hand, and probably diagnostically more valuable, represents the high electrophilic reactivity of the oxygen-related degree of unsaturation a chemical feature that determines the biochemical behavior towards bioactive sites. The majority of biological macromolecules (nucleic acids, proteins) are nucleophilic. For example, in proteins, accessible thiol and primary amino groups constitute strongly nucleophilic centers. Chemical modification of these nucleophilic sites often alters or decreases protein function, resulting in cytotoxicity (Zimniak, 2011). Therefore, a measure of the presence of carbonyls/epoxides in aerosol particles might assist in the prediction of electrophilic stress induced by airborne particle-bound chemicals. Otherwise, oxygen-rich organics in SOA with no or a low contribution of carbonyls/epoxides functionalities suggests that the oxygen is present as peroxides, in this case potentially increasing oxidative stress and causing disruptions in normal mechanisms of cellular signaling leading to many pathophysiological conditions. Since the awareness of health effects of particulate matter is increasing, knowledge about the potential carbonyl/epoxide contribution or its absence could help to understand physiological impacts of atmospheric particulate matter (Schwöbel et al., 2011).

For the above-mentioned reasons, we suggest a new metric – the maximum carbonyl ratio (MCR) –, which describes the maximal contribution of carbonyl/epoxide functionalities in

individual molecules composing organic aerosols, that can be directly derived from HRMS datasets. It should be clearly noted here that the proposed MCR is meant as a metric for the interpretation of mass spectrometry data sets in which hundreds to thousands of compounds are identified. Similar to other metrics that have been successfully used in the interpretation of HRMS data (e.g., DBE, AI), a calculated MCR value of a single molecular formula is not unequivocal evidence of the presence of carbonyl functionalities. Applied to a variety of compounds, however, the presented metric can be useful to visualize and interpret results on the chemical composition of complex, oxygen-rich multifunctional mixtures such as atmospheric SOA. Actually, based on the discussion above the suggested metric should be named ‘maximum carbonyl/epoxide ratio’. However, it is generally assumed that the contribution of epoxides to SOA is low (Atkinson et al., 1991; Ji et al., 2017) and therefore most of the degree of unsaturation introduced by oxygen functionalities in connection with SOA formation can be expected to result from carbonyl groups. Consequently, from now on just the expressions ‘carbonyls’ or ‘carbonyl ratio’ are used for convenience instead of ‘carbonyl/epoxide’ when we refer to the degree of unsaturation by oxygen functionalities. Nevertheless, atmospheric chemical interest in epoxy chemistry has recently increased considerably, especially in connection with isoprene chemistry and the formation of organosulfates (Paulot et al., 2009; Shrivastava et al., 2019). But also the very high electrophilicity of epoxides and thus their high toxic potency, means that the contribution of epoxides to the MCR value should not be ignored. The purpose of this paper is to introduce MCR as a new metric for the analysis of HRMS data and to present it in combination with Van Krevelen diagrams as a visualization tool (MCR-VK diagrams) to achieve a better categorization of complex ambient OA samples. The validation and applicability of the MCR-VK diagram are tested by applying the concept to selected samples of ambient organic aerosols and a few samples from laboratory-generated SOA.

3.2 Material and methods

3.2.1 Laboratory SOA generation and collection

SOA was formed from the ozonolysis and photooxidation of selected volatile organic compounds (VOC) in a 7 L quartz flow tube (Tong et al., 2016). Ozonolysis was performed by mixing α -pinene in the flow tube with ozone. The concentrations of the SOA precursor were adjusted in the range between 400 and 700 ppb and the O₃ concentration between 980 and 1100 ppb. Isoprene SOA was generated in a 33 L smog chamber through gas phase photo-oxidation of

the SOA precursor. The isoprene concentration was adjusted in the range between 300 and 500 ppb and the concentration of OH radicals during the experiments was estimated to be $\sim 5.2 \times 10^{11} \text{ cm}^{-3}$. A Scanning Mobility Particle Sizer (SMPS, GRIMM Aerosol Technik GmbH & Co. KG) was used to measure the number and size distribution of the formed SOA particles. SOA was collected on 47 mm Omnipore Teflon filters (100 nm pore size, Merck Chemicals GmbH).

3.2.2 Ambient PM sampling

The 24-hour integrated PM samples were collected at the SMEAR II station in Hyytiälä, a boreal forest monitoring station in Finland, and at a central urban site in Beijing (China). A three-stage Dekati PM₁₀ impactor (Pallflex Tissuquartz 2500QAT-UP) was used for the boreal forest samples collected from 17-19 July 2017. The sampling flow rate through the sampler was set to 35 L min⁻¹. The fine particle mode (< 2.5 μm) were collected on Teflon filters (PALL, 47 mm diameter). The samples from Beijing were collected from January 7 to 9, 2014 on prebaked quartz fiber filters (8×10 inches) using a large volume sampler (Tisch, Cleveland, OH, USA) at a flow rate of 1050 L min⁻¹. All filters were stored in glass vials at -20 °C or -80 °C until analysis.

3.2.3 Sample preparation and UHRMS analysis

The analysis of the filter samples was carried out at the Johannes Gutenberg University in Mainz. Parts of the filters were extracted twice with 1.5 mL methanol in an ultrasonic bath for 30 min. After insoluble particles had been removed by a 0.2 μm Teflon filter, the extracts were evaporated to dryness under a gentle nitrogen stream. Finally, the extracts were dissolved with a variable volume of an acetonitrile-water mixture (1/9, v/v) to adjust the particle mass concentration between 150 and 400 μg/mL.

The filter extract solution was then analyzed by an ultrahigh performance liquid chromatography (UHPLC) system (Dionex UltiMate 3000, Thermo Scientific, Germany) coupled to a Q Exactive Hybride-Quadrupole-Orbitrap mass spectrometer (Thermo Scientific, Germany) (HPLC-Orbitrap MS). The detailed description of the UHPLC-Orbitrap MS method can be found in a previous study (Wang et al., 2018). In brief, analytes were separated using a Hypersil Gold column (C18, 50 x 2.0 mm, 1.9 μm particle size, Thermo Scientific, Germany) with the mobile phase consisting of (A) ultrapure water with 2% acetonitrile and 0.04% formic acid and (B) acetonitrile with 2% ultrapure water. The gradient elution was performed by the A/B mixture at a

total flow rate of 500 $\mu\text{L}/\text{min}$ as follows: 0–1.5 min 2% B, 1.5–2.5 min from 2% to 20% B, 2.5–5.5 min 20% B, 5.5–6.5 min from 20% to 30% B, 6.5–7.5 min from 30% to 50% B, 7.5–8.5 min from 50% to 98% B, 8.5–11.0 min 98% B, 11.0–11.05 min from 98% to 2% B, 11.05–11.1 min 2% B. The Q Exactive Orbitrap MS was equipped with a heated ESI source at 120 $^{\circ}\text{C}$, using a spray voltage of -3.3 Kv for the negative ion mode. The mass resolution power was 70000 at m/z 200 and the mass scanning range was set to m/z 80–500.

3.2.4 Data processing

The data obtained from UHPLC-Orbitrap MS were analyzed by an open-source software for mass spectrometry data processing with the main focus on LC-MS data (MZmine 2.37). The detailed processing steps and parameters in the software are shown in the supporting information (Table S3.2.1). The output of MZmine data includes m/z ratios, formulas, retention times and peak areas of detected organic compounds. Molecular formulas were expressed as $\text{C}_c\text{H}_h\text{O}_o\text{N}_n\text{S}_s$, where c , h , o , n , and s correspond to the numbers of carbon, hydrogen, oxygen, nitrogen and sulfur atoms in the molecular formula. To remove chemically unreasonable formulae, identified assignments were constraint by setting H/C, O/C, N/C and S/C ratios in the ranges of 0.3–3, 0–3, 0–1.3 and 0–0.8, respectively (Wang et al., 2018).

3.3 Results and discussion

3.3.1 Definition of maximum carbonyl ratio (MCR)

It is recognized that the structural characteristics of organic molecules in aerosols are essential for the evaluation of their behaviour and their environmental interactions, i.e., chemical reactivity, vapour pressure, interaction with water or biological activity. A central metric, which can be directly calculated from the elemental composition, is the number of double bonds in a molecule (double-bond equivalent (DBE) also named degree of unsaturation). The DBE is calculated assuming that all atoms obey the octet rule (except for hydrogen) and that the degree of unsaturation is caused by covalent bonds between carbons. For $\text{C}_c\text{H}_h\text{O}_o\text{N}_n\text{S}_s$ compounds the DBE can than be expressed as equation 3.1:

$$DBE = 1 + C - 0.5H + 0.5N \quad (3.1)$$

Based on this definition, the DBE describes the number of C-C multiple bonds plus rings in a molecule and is a well-established metric to assess the degree of unsaturation of molecules obtained by mass spectrometry. By its definition the DBE is thus independent of the number of O and S atoms, which results in a potential overestimation of the number of C-C double/triple bonds in O/S-containing molecules. Therefore, the aromaticity index (AI) (Koch and Dittmar, 2016) and the aromaticity equivalent (Xc) (Yassine et al., 2014) for $C_C H_H O_O N_N S_S$ compounds were introduced, which also consider the influence of O and S on the degree of unsaturation:

$$AI = \frac{DBE_{AI}}{C_{AI}} = \frac{1+C-O-S-0.5H}{C-O-S-N} \quad (3.2)$$

$$X_C = \frac{3[DBE - (mO + nS)] - 2}{DBE - (mO + nS)} \quad (3.3)$$

where m and n are the fraction of oxygen atoms and sulfur atoms involved in π -bond structure of the compound, respectively.

The AI reflects the C-C double bond density in a molecule including the possibility that heteroatoms can also form double bonds, the Xc further refines this concept by making it independent from the degree of alkylation. In principle, both indices are minimum criteria for the presence of aromatics and condensed aromatics in the sample material by correcting the DBE assuming contributions from heteroatom π -bond structures, such as C=O or S=O containing functionalities. Both parameters are successfully used for the characterization of natural organic matter (NOM) or mineral oils and have been proved to represent a step towards structural identification of complex organic mixtures. The concept presented here follows a similar approach, but now by estimating a maximum criterion for the presence of carbonyl functionalities. This is done first for pure CHO compounds, often the largest group of organic compounds in atmospheric aerosol particles. A simple distinction of the cases is the basis for the MCR definition. When the number of oxygen atoms O in a $C_C H_H O_O$ compound is larger or equals the DBE of this compound ($O \geq DBE$), then the MCR is calculated as:

$$MCR = \frac{DBE}{O} \quad (3.4)$$

or in other words, it is assumed that in case unsaturation is observed, all oxygen atoms contribute to it (i.e., the molecule's unsaturation is only contributed by oxygen atoms by forming the carbonyl group and all oxygen atoms are part of a C=O functionality). For example, for $C_2H_2O_2$ (DBE = 2) MCR is 1 (e.g. glyoxal), for $C_2H_4O_2$ (DBE = 1) MCR is 0.5 (e.g. glycolaldehyde) and for $C_2H_6O_2$

(DBE = 0) MCR is zero (e.g. glycol). If the number of oxygen atoms in the molecule is smaller than its DBE value ($O < \text{DBE}$), then MCR is considered to equal one (i.e., all oxygen atoms contribute to the DBE), again the maximum criteria for the presence of carbonyl functionalities. In this case all of oxygen atoms are assumed in the form of carbonyl group (e.g., aldehydes or ketones). Thus, MCR is a metric to predict the possible maximum of carbonyl groups in the molecules.

3.3.2 MCR-VK diagram

Motivated by the capabilities of HRMS in combination with soft ionization techniques to observe protonated or deprotonated molecular ions and directly assign thousands of elemental compositions, a useful concept was recently introduced which is named the “compositional space of molecules” (Herkorn et al., 2007). It represents the isomer-filtered complement of the entire space of molecular structures based on a given elemental composition, e.g. $C_cH_HO_o$. The compositional space is defined by the laws of chemical binding and is typically restricted to a certain mass range. This concept was also used here to relate the variety of observed organic aerosol components to all possible CHO compounds within the framework of VK diagrams. Consequently, an artificial dataset was constructed which comprise all theoretical $C_cH_HO_o$ molecular formulae for CHO compounds with up to 15 carbon atoms. To further explore the resulting chemical space the MCR values of all individual compound were calculated as described above.

In Figure 3.3.1, the dots represent the C,H,O-compositional space of molecules within the molecular H/C range between 0–2.5 and O/C range between 0 and 1.2. The different gray scale colours relate to defined MCR ranges based on the theoretically possible functionalities of the underlying chemical components. The white dots represent all compounds in the MCR range between 0 and 0.2 and include compounds without any carbonyl functionality (MCR = 0), i.e., completely saturated compounds, up to compounds in which 20% of the oxygen atoms can be present in a carbonyl functionality. Aiming on a practicable categorization system we introduce three threshold lines (A, B, C; see Figure 3.3.1). Compounds between line A and line B possess MCR values in the range 0.2–0.5, compounds between line B and line C have MCR values in the range 0.5–0.9, and compounds below line C values in the range 0.9–1.0. This means that, for example, compounds located above line A either contain no carbonyl functionalities or a maximum of 20% of the oxygen atoms can be carbonyl oxygen (C=O), the majority (80–100%) of the oxygens within these compounds has to be single-bounded hydroxyl (R-OH), hydroperoxy (R-OOH), ether (R-O-R) or peroxy oxygen (R-OOR). In contrast, in compounds appearing below line C in the VK diagram, 90 % of the unsaturation can be present in the form of carbonylic oxygen. As in the case

of AI and Xc, one cannot read a certain chemical functionality from the position of a dot (e.g., number of carbonyl O or number of aromatic rings), the MCR parameter is simply a limit value consideration to better structure the VK diagram in a region that is not covered by AI or Xc.

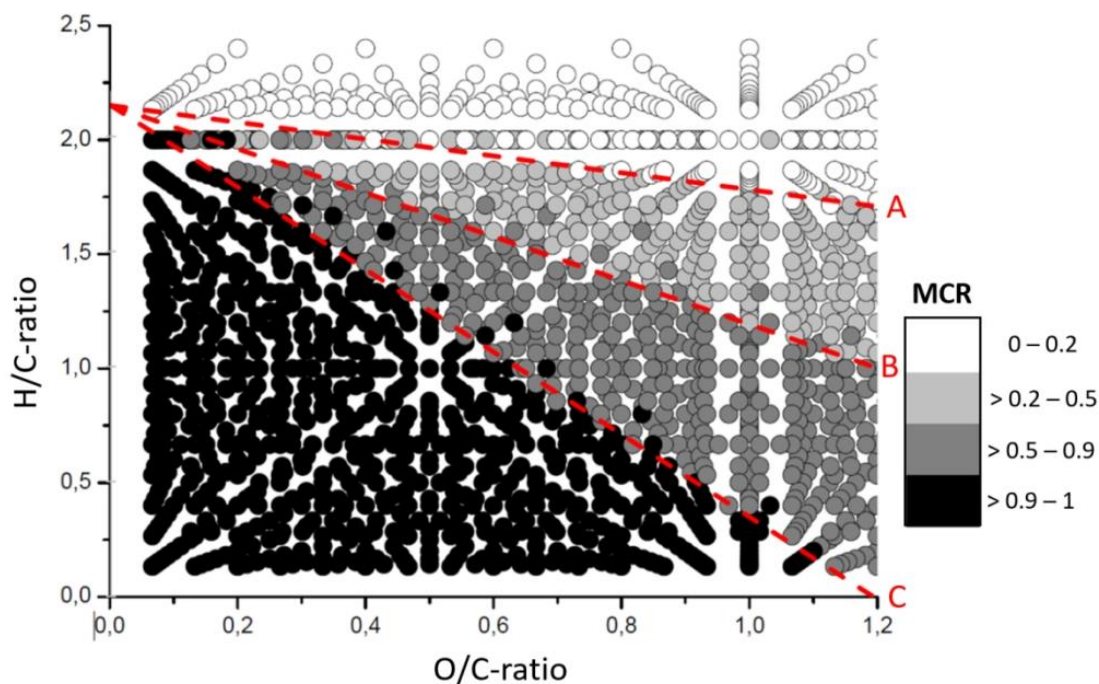


Figure 3.3.1: The MCR-VK diagram of all possible CHO subgroups with up to 15 carbon numbers. The different colors indicate the value of maximum carbonyl ratio (MCR). The dashed lines (A, B and C) represent different boundaries for a practicable categorization of SOA CHO compounds.

To get an idea about potential candidates contributing to the different areas in the MCR-VK diagram, lines A, B and C shown in Figure 3.3.1 are also depicted in Figure 3.3.2, where selected typical SOA precursors and SOA compounds are shown (Ramdahl, 1989; Myoseon, 1997; Matthew and Fraser, 2000; Edney et al., 2005; Kenneth et al., 2005; Henze and Seinfeld, 2006; Jaoui et al., 2007; Sakulyanontvittaya et al., 2008; Fu et al., 2009; Kautzman et al., 2010; Surratt et al., 2010; Ding et al., 2011; Borrás and Tortajada-Genaro, 2012; Ehn et al., 2012; Ehn et al., 2014; Kristensen et al., 2014; Nguyen et al., 2014; Yu et al., 2014; Shen et al., 2015; Zhang et al., 2015; González et al., 2016; Kurten et al., 2016; Utieyin, 2016; Tu et al., 2016; Al-Naiema and Stone, 2017; Martinsson et al., 2017; Pecha, 2017; Yee et al., 2018; Zhu et al., 2018). The molecular formulas, structures, DBE values, MCR values and suggested precursors of the selected marker molecules are listed in Table S3.3.1 in the supporting information. SOA compounds formed from gas phase chemistry are colored in blue, compounds which are known to be formed from condensed

phase chemistry are represented in purple, while a selection of marker compounds related to combustion processes are yellow-colored and a selection of SOA precursors are colored in grey. The biogenic SOA markers generated from gas phase chemistry are further divided based on their origin from isoprene (light blue), monoterpene (MT, blue) or sesquiterpene (SQT, dark blue) oxidation. The shape of the data points indicates whether the specific marker is mainly biogenic (circles), anthropogenic (triangle) or from mixed sources (square).

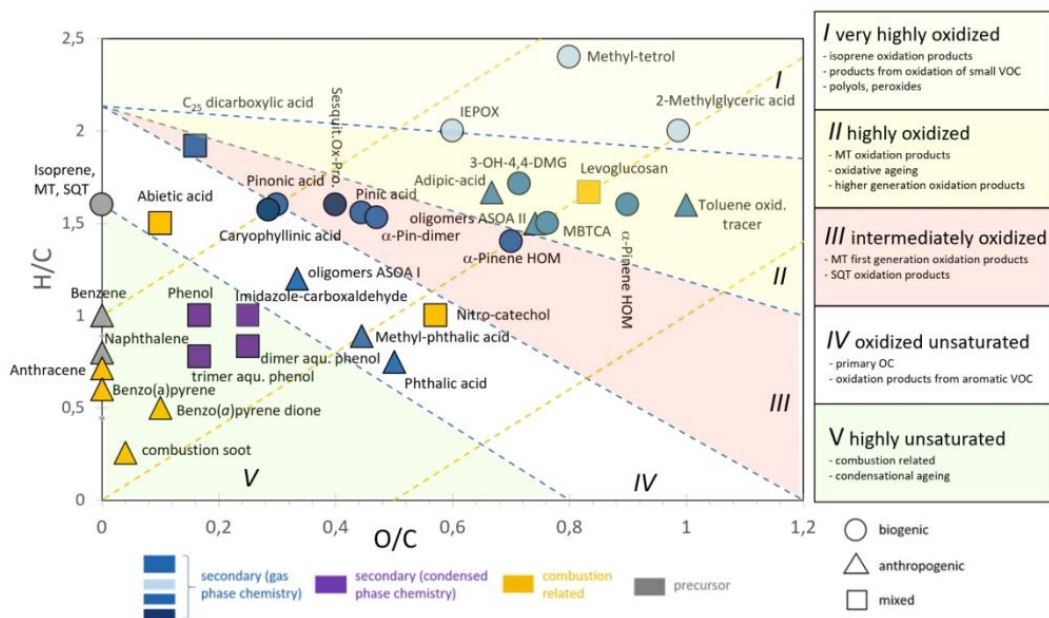


Figure 3.3.2: MCR-VK diagram of well-known organic marker compounds, which are defined as different colors and shapes according to their source and functionality. MCR-VK diagram was divided into five areas: I for very highly oxidized organic compounds (VHOOCs), II for highly oxidized organic compounds (HOOCs), III for intermediately oxidized organic compounds (IOOCs), IV for oxidized unsaturated organic compounds (OUOCs) and V for highly unsaturated organic compounds (HUOCs).

Although definitely the data points scatter within the MCR-VK diagram, a certain structure is visible. Most of the typical SOA compounds are located in the areas I, II and III, defined by the MCR as explained above. For example, isoprene particle phase oxidation products show up in area I, which generally includes products from the oxidation of smaller VOCs. Several MT and SQT first generation products (e.g. pinic acid) are located in area III, while higher generation oxidation products, such as 3-methyl-1,2,3-butanetricarboxylic acid (MBTCA) or highly oxygenated organic molecules (HOMs), which are formed by multiple oxidation steps, are preferentially located in area II (Yasmeen et al., 2012; Wang et al., 2017; Wang et al., 2018). These observations can be

explained by the well-known gas/particle partitioning behaviour of the products: Smaller VOC precursors, such as the C₅ hydrocarbon isoprene, have to undergo multiple oxidation steps and the introduction of more oxygen-containing functionalities before the vapour pressure of the products enables them to partition into the particle phase. Several of the atmospheric gas phase oxidation mechanisms not only introduce oxygen (shifting the molecules to the right along the x-axis in the VK diagram) and use up unsaturation of C-C double bonds or cyclic structures, but also introduce hydrogen (reaction with HO₂, hydrolysis), shifting the products up in the VK diagram. However, when the SOA precursors are larger VOCs, exemplified here by MT or SQT derived SOA, the products will partition into the particle phase much earlier, i.e., not necessarily have to undergo multiple oxidation steps before they enter the particle phase. Nevertheless, a certain degree of chemical aging still proceeds, shifting these products from area III into area II. To name the described areas more specifically, we characterize them as very highly oxidized organic compounds (VHOOCs) (area I), highly oxidized organic compounds (HOOCs) (area II) and intermediately oxidized organic compounds (IOOCs) (area III). In addition, according to the degree of unsaturation and oxygen content, the MCR-VK diagram in Figure 3.3.2 is further differentiated into the areas IV and V. Within area IV, named oxidized unsaturated organic compounds (OUOCs), primarily released aromatic OA components and oxidation products from aromatic VOCs are located, compounds which still contain aromatic ring structures. Finally, in area V condensed aromatic structures are showing up, including polycyclic aromatic hydrocarbons (PAHs) or oxygen containing PAHs, defined here as highly unsaturated organic compounds (HUOCs). In this region most of the oxygen atoms are suggested to be present in the form of carbonyl oxygen. These combustion-related compounds are able to explain the observed very low H/C ratios. Another group of compounds which might contribute to area V are products from aqueous phase chemistry for example of phenolic compounds or glyoxal heterogeneous chemistry (Sun et al., 2011; Yu et al., 2014). However, there is no doubt that the MCR value loses meaningfulness in regions IV and V, but here the use of the aromatic indices AI and X_c already introduced above helps to further categorise the CHO compounds localised in these areas (see Figure 3.3.3).

3.3.3 MCR-VK diagram application on aerosol samples

To test the usefulness or limitations of the proposed MCR concept and MCR-VK diagrams in the analysis of complex atmospheric aerosol samples we analysed the chemical composition of SOA samples from both laboratory experiments and field measurements. The chemical composition of the samples was measured by UHPLC combined with ESI Orbitrap MS as described

above.

The MCR-VK diagrams from samples of laboratory α -pinene and isoprene SOA, as well as of field samples from Hyytiälä and Beijing are shown in Figure 3.3.3. It should be noted that in Figure 3.3.3 only compounds consisting of carbon, hydrogen and oxygen atoms (CHO compounds) are presented. The size of the dots in Figure 3.3.3 are logarithmically scaled by the fourth root of peak area of the respective CHO compounds and the colours are selected based on the X_c value (with $0 \leq X_c < 2.5$ (grey), $2.5 \leq X_c < 2.7143$ (purple) and $X_c \geq 2.7143$ (red), background colors of areas of I–V are the same as in Figure 3.3.2).

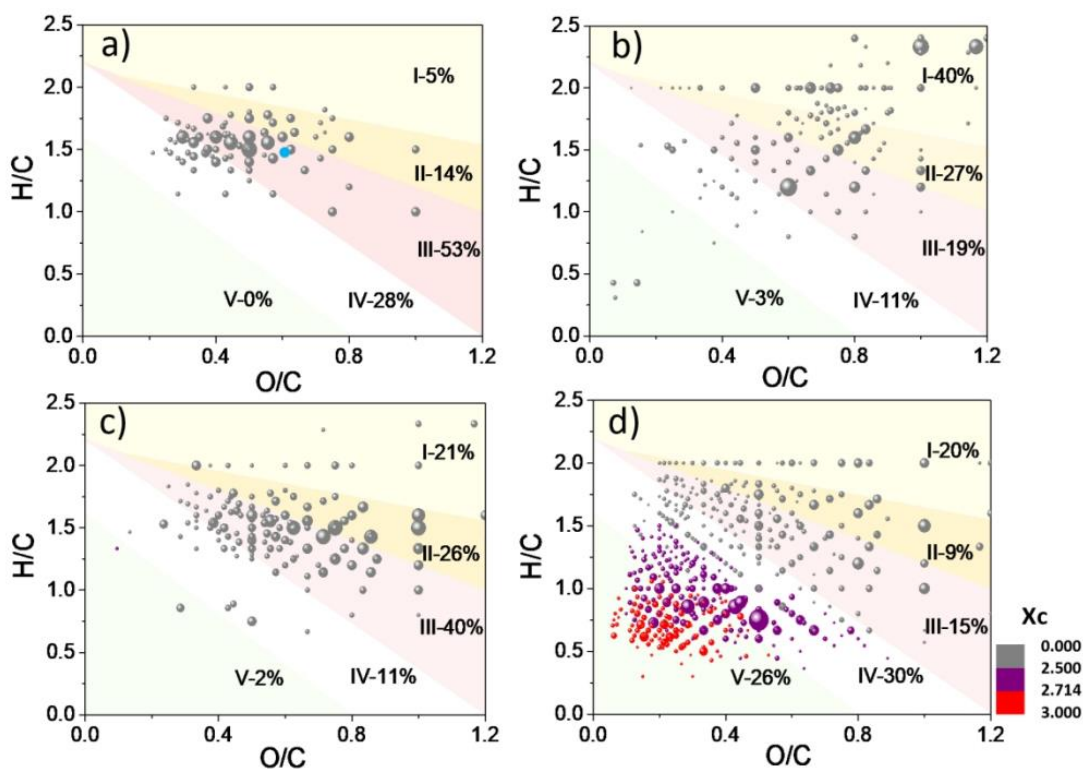


Figure 3.3.3: MCR-VK diagrams of α -pinene ozonolysis SOA (a), isoprene photo-oxidation SOA (b), Hyytiälä OA (c) and Beijing OA (d). The size of the bubbles indicates the fourth root of the intensity of each compound and the colors correspond to the X_c value. The blue dot in (a) shows the results of Claflin et al. 2018, who studied functional group composition of SOA formed from ozonolysis of α -pinene under similar experimental conditions.

Figure 3.3.3a shows particle phase α -pinene SOA composition depicted in the MCR-VK diagram. The largest fraction (53%) of α -pinene SOA components is located in area III, while only a few compounds show up in area I. This observation indicates that most SOA products from ozone-oxidation of α -pinene are carbonyl oxygen-containing compounds with MCR value of 0.5–0.9 and

only a few of them are pure hydroxyl or peroxide oxygen containing compounds with MCR values between 0–0.2. Since these laboratory flow tube experiments allowed only a low level of further oxidation processes, the aerosol consists mainly of first-generation oxidation products of the monoterpene. The blue dot in Figure 3.3.3a is taken from a study by Clafin et al. (2018) in which a combination of derivatization and spectrophotometric methods were used to quantify peroxide, carbonyl, carboxyl, ester, and hydroxyl groups to examine the α -pinene/ozone SOA composition, actually under similar experimental conditions. Although completely different analytical methods were used and, of course, only one data point is available on the total composition, the results of the Clafin et al. study are not only roughly in the centre of the data shown here (they report average O/C and H/C ratios), but the [carbonyl-O] to [total-O] ratio of 0.56 calculated by Clafin et al. also fits well with the MCR concept as presented here (Clafin et al., 2018). Figure 3.3.3b shows MCR-VK diagram of SOA products from isoprene reacted with OH radicals. As can be seen in the figure, the distribution of products generated from α -pinene and isoprene to areas of I-V are quite different. Isoprene SOA products span over a considerably larger region of the MCR-VK diagram than the α -pinene SOA products. Most isoprene SOA products (40%) show up in area I, clearly demonstrating that these compounds are VHOOCs with a very low MCR value (0–0.2) and that the majority of oxygen functionalities are presented in the form of non-carbonyl groups (e.g., OH and OOH). This observation agrees well with the fact that a large amount of diols, tetrols and hydroperoxides were identified in isoprene-derived SOA in previous studies (Carlton et al., 2009). Figure 3.3.3c and 3.3.3d show MCR-VK diagrams for ambient aerosol samples. Figure 3.3.3c, which shows the results of the LC-MS analysis of aerosol field samples from Hyytiälä, indicates a similar aerosol composition as in the case of α -pinene SOA (Figure 3.3.3a). The largest fraction (40%) of the compounds are located in area III, followed by areas of II (26%), I (21%), IV (11%) and V (2%). The observed similarity can be explained by the fact that at this measurement site monoterpenes are the primary source of SOA and α -pinene is one of the most important individual monoterpene released at this site. Also previous studies have shown that the photo-oxidation and ozonolysis of biogenic VOCs contribute to the major fraction of aerosol components in Hyytiälä (Cavalli et al., 2006; Lee et al., 2006; Kourchev et al., 2013). However, compared to the laboratory α -pinene SOA shown in Figure 3.3.3a, significantly more particle phase products in areas of I and II were observed, indicating that the particles in the ambient atmosphere experienced more intensive oxidation processes and oxidative ageing compared to laboratory α -pinene SOA. Finally, Figure 3.3.3d shows the application of MCR-VK diagram on the Beijing aerosol samples, certainly a location with very different atmospheric conditions compared to the boreal forest station. The majority of Beijing particle phase compounds are located in the highly unsaturated and less

oxidized region of the MCR-VK diagram, i.e., areas of IV (30%) and V (26%). As already discussed above, the indication of the presence of are OUOCs (IV) and HUOCs (V), which mostly contain aromatic structures with low degree of oxidation, are probably related to combustion processes (Wang et al., 2018). The numeric comparison yield, 20%, 9% and 15% of Beijing aerosol products are located in areas of I (VHOOCs), II (HOOCs) and III (IOOCs), respectively, indicating that also in Beijing samples a significant contribution from oxidative processing of SOA components and probably SOA generated by biomass burning (Ding et al., 2016; Ding et al., 2016).

3.4 Conclusion and implication

The maximum carbonyl ratio (MCR) is a metric that can be used to estimate the contribution of carbonyl groups in a molecule. According to the MCR value, the maximum number of carbonyl groups in molecules can be quantified. Furthermore, an updated visualization tool, the MCR-VK diagram, is developed by the combination of the MCR value and a traditional VK diagram. By locating selected typical SOA compounds within the MCR-VK diagram, five areas were defined referring to very highly oxidized organic compounds (area I, VHOOCs), highly oxidized organic compounds (area II, HOOCs), intermediately oxidized organic compounds (area III, IOOCs), oxidized unsaturated organic compounds (area IV, OUOCs) and highly unsaturated organic compounds (area V, HUOCs), to better understand the structural information of SOA compounds in terms of the carbonyl functional group. The MCR-VK diagram approach was tested and validated using laboratory-generated SOA from ozonolysis of α -pinene, photo-oxidation of isoprene and ambient aerosol samples collected in Hyytiälä (boreal forest) and Beijing (megacity). Distinct distributions in the MCR-VK diagram were observed in the various aerosol samples and the comparison between them can improve the characterization of organic aerosol samples, especially an improved understanding of SOA sources and formation pathways. In summary, the use of the MCR concept or the application of MCR-VK diagrams should help to better understand the sources and the processing of atmospheric OA components based on HRMS data. As discussed above, the MCR might also prove useful for the evaluation of health-related effects of organic aerosols, since the MCR contains information about the presence of electrophilic particle-bound multifunctional organics (larger MCR values) or the presence of highly oxidized non-carbonyl organics (low MCR values), such as (hydro)peroxides, inducing oxidative stress in the respiratory system. Although oxidative and electrophilic stress are linked, the biological pathways causing the adverse health effects of particulate air pollution are poorly understood and there is no conclusive evidence as to which particle properties are causing their toxicity. Chemical components in the particle phase are

likely a key factor, but are difficult to accurately define. The suggested MCR value, easily extracted from HRMS data, might be a valuable tool to identify health-relevant particle parameters, components and sources, information which is crucial for improved and efficient air pollution mitigation strategies. In future work, the combination of MCR or MCR-VK diagrams and other metrics such as AI, Xc and OSc could be further used to better understand the composition, origin, history and effects of complex organic aerosols.

Supporting Information

The detailed description of the data processing (Table S3.2.1) and the information of selected SOA markers (Table S3.3.1).

Acknowledgements

This work was funded by the Deutsche Forschungsgemeinschaft (DFG, HO 1748/19-1 and HO 1748/20-1), the German Federal Ministry of Education and Research (BMBF contract 01LK1602D), the Max Planck Society and the National Natural Science Foundation of China (NSFC) (Grant No. 41925015). Y. Zhang and K. Wang acknowledge the scholarship from the Chinese Scholarship Council (CSC). K. Wang acknowledges the scholarship from the Max Planck Graduate Center with Johannes Gutenberg University of Mainz (MPGC). The authors acknowledge stimulating exchange with U. Pöschl.

4 Molecular evidence for the association of reactive oxygen species yield with oxidized organic compounds

This chapter is a reprint of the manuscript:

Yun Zhang, Steven Lelieveld, Alexander Filippi, Fangxia Shen, Ru-jin Huang, Helmi-Marja Keskinen, Tuukka Petäjä, Ulrich Pöschl, Kai Wang, Thorsten Hoffmann, Haijie Tong

Molecular Evidence for the Association of Reactive Oxygen
Species Yield with Oxidized Organic Compounds

In preparation for Atmospheric Chemistry and Physics

Abstract. The health effects of atmospheric fine particulate matter with aerodynamic diameter $\leq 2.5 \mu\text{m}$ ($\text{PM}_{2.5}$) are closely correlated with redox-active components. However, the health-related organic components and relationship between the redox activities and chemical characteristics of $\text{PM}_{2.5}$ are largely unknown. In this study, the molecular composition of organic aerosols was analyzed by ultra-high resolution mass spectrometry (UHRMS) Orbitrap coupled with ultra-high performance liquid chromatography (UHPLC) in the negative electrospray ionization mode. After the assignment of molecular formulas for the detected compounds, the compounds were categorized into oxidized organic compounds (OOC) and unsaturated organic compounds (UOC) based on the value of maximum carbonyl ratio (MCR) of individual compound. Afterwards, the parameter defined as the ‘ratio of relative peak area-weighted fraction of OOC to relative peak area-weighted fraction of UOC ($R_{\text{OOC/UOC}}$)’ was proposed. The yield of reactive oxygen species (ROS) generated by ambient $\text{PM}_{2.5}$ and laboratory-generated secondary organic aerosol (SOA) samples were quantified to characterize the redox activities of aerosols, which referred to the sum of H_2O_2 yield and radical yield measured by a fluorometric probe and electron paramagnetic resonance, respectively. We found that the $R_{\text{OOC/UOC}}$ of both urban $\text{PM}_{2.5}$ samples and laboratory-generated SOA samples had significant positive correlations with ROS yield (mainly contributed to H_2O_2 yield). It indicates that organic components, particularly oxidized organic compounds, might make important contribution to the ROS formation. Our study highlights the important contribution of organic aerosols to the formation of reactive species and the relationship between the chemical characteristics of organic aerosols and the ROS formation. The $R_{\text{OOC/UOC}}$ can be utilized as a valuable parameter to identify health-related organic components, furthermore, the curve-fitting equations with good performance offer the possibility to predict of the ROS yield of $\text{PM}_{2.5}$.

4.1 Introduction

Exposure to atmospheric particulate has been associated with adverse health outcomes including respiratory illnesses and cardiovascular diseases (Fuzzi et al., 2015; Pöschl and Shiraiwa, 2015). One proposed mechanism is particulate matter (PM) exposure leading to increased production of reactive oxygen species (ROS) in biological system and target cells, which causes oxidative stress and cell damage (Pöschl and Shiraiwa, 2015; Lakey et al., 2016; Arangio et al., 2016). ROS are a class of reactive oxygen-bearing compounds, including hydrogen peroxide

(H₂O₂), hydroxyl radicals (•OH), superoxide radicals (•O₂⁻) and organic radicals (Lakey et al., 2016). Previous studies have shown that ROS can be generated by different redox-active components in PM, such as transition metals, quinones and secondary organic aerosol (SOA) (Chung et al., 2006; Wang et al., 2010; Shen et al., 2011; Wang et al., 2012; Badali et al., 2015; Lakey et al., 2016; Arangio et al., 2016; Tong et al., 2016; Hems et al., 2017; Tong et al., 2018; Bates et al., 2019; Chowdhury et al., 2019; Lin and Yu, 2020). In particular, the impacts of the redox-active organic components on the oxidative potential of PM and the association with ROS formation have been receiving increasing attention. Tong et al. (2018) reported that the SOA generated by isoprene, β-pinene and naphthalene was able to produce a substantial amount of H₂O₂ upon interaction with water, furthermore, the organic hydroperoxides in the biogenic SOA were suggested to be the important precursors of ROS formation. Recently, we found that highly oxygenated molecules (HOMs) are closely associated with the radical formation by PM in water (Tong et al., 2018). These studies mainly investigated the ROS yield of the bulk SOA or the correlation of ROS yield with a class of specific compounds (e.g. peroxides). However, it is difficult to target the chemical components related to the adverse health effects in complex aerosol samples due to our limited understanding of detailed chemical composition of organic aerosols (Hoffmann et al., 2011; Wang et al., 2018).

Identification of organic compounds in atmospheric aerosols is always a challenging task due to the high complexity of organic aerosols (Nozière et al., 2015). Recent years, analytical methods based on ultrahigh resolution mass spectrometry (UHRMS), e.g., Orbitrap MS and Fourier transform ion cyclotron (FTICR), coupled with soft ionization techniques including atmospheric pressure chemical ionization (APCI) and electrospray ionization (ESI) have been successfully applied to characterize the chemical composition of organic aerosols at a molecular level (Lin et al., 2012; Vogel et al., 2016; Song et al., 2018; Zuth et al., 2018; Wang et al., 2019). Based on the UHRMS technique, thousands of unambiguous molecular formulas have been assigned to the organic compounds in aerosol samples. Moreover, several metrics (e.g., double bond equivalent (DBE) and aromaticity equivalent) have been used to interpret these assigned molecular formulas to further understand the chemical properties of organic aerosols, such as the degrees of unsaturation and aromaticity (Koch and Dittmar, 2006; Yassine et al., 2014). Very recently, we proposed a new metric named maximum carbonyl ratio (MCR), which is used to improve the characterization of organic aerosol samples. Furthermore, in the combination with the composition dependent visualization tool Van Krevelen diagram, the MCR was suggested as a tool for better characterizing the sources and processing the components of atmospheric OA based on UHRMS data. The MCR might also be useful for the identification of health-relevant organic components

in PM, since the MCR containing information on the highly electrophilic organic compounds related to electrophilic stress as well as organic (hydro)peroxides linked to oxidative stress.

In this study, we investigated the relationship between the ROS yield and molecular composition of atmospheric aerosols. Particulate aerosol samples were collected at several cities, a forest site and a laboratory chamber facility. The molecular composition of particulate aerosol samples was characterized by an Ultra High-Performance Liquid Chromatograph coupled to an Electrospray Ionization source of an Orbitrap Mass Spectrometer (UHPLC/ESI-Orbitrap-MS). The identified organic compounds were classified into oxidized organic compounds (OOC) and unsaturated organic compounds (UOC) according to the MCR value of individual compound. We introduced a new index defined as ‘the ratio of relative peak area-weighted fraction of OOC to relative peak area-weighted fraction of UOC ($R_{OOC/UOC}$)’ and calculated the values of $R_{OOC/UOC}$ for different samples. Moreover, the H_2O_2 yield and radical yield of particulate aerosol samples were quantified using a fluorometric probe and electron paramagnetic resonance spectrometry in combination with a spin-trapping technique, respectively. Finally, the correlation of ROS yield with the chemical characteristics of aerosols was studied, giving simple equations for fitting the ROS yield based on the molecular composition of aerosols and the abundance of individual molecules. The results of this study will help to provide a new insight into the link between the chemical composition of PM and ROS formation as well as improve the assessment of the toxicity of PM.

4.2 Material and methods

4.2.1 Ambient particle sampling

Ambient fine PM samples were collected at a boreal forest site (Hyytiälä, Finland), an European city (Mainz, Germany) and four Chinese megacities (i.e., Beijing, Xi’an, Shanghai and Guangzhou). The Hyytiälä $PM_{2.5}$ samples were collected at Station for Measuring Forest Ecosystem-Atmosphere Relations station (SMEAR II) (61.51°N, 24.17°E) during 5–14 June 2017 using a Dekati impactor with 47 mm diameter Teflon filters (PALL, Teflon) at an air flow rate of 35 L min^{-1} . The Mainz $PM_{1.8}$ (particulate matter with aerodynamic equivalent diameter $\leq 1.8 \mu m$) samples were collected on 47 mm diameter Teflon filters (100 nm pore size, Merck Chemicals GmbH) with a micro-orifice uniform deposition impactor (MOUDI, 110-R, MSP Corporation) at the air flow rate of 30 L min^{-1} on the roof of Max Planck Institute for Chemistry (49.99°N, 8.23°E) during 22–30 August 2017. The Beijing $PM_{2.5}$ samples were collected from 26 February to 10 March 2019 on 47mm diameter Teflon filters (Whatman®) at the campus of Beihang University

(40.15°N, 116.27°E) using a low-volume sampler at a flow rate of 15 L min⁻¹. The Xi'an PM_{2.5} samples were collected on 90 mm diameter Teflon filters (100 nm pore size, Omnipore JVWP09025, Millipore) during 5–9 November 2018 using a low-pressure cascade impactor at a flow rate of 50 L min⁻¹ at the campus of Xi'an Jiaotong University (34.25°N, 108.98°E). The PM_{2.5} samples of Shanghai (31.30°N, 121.50°E) and Guangzhou (12.12°N, 113.36°E) were collected on prebaked quartz-fiber filters (20.3×25.4 cm, Whatman®) in the period of 5–27 of January 2014 using a high-volume air sampler at a flow rate of 1050 L min⁻¹. Information about the detailed location of sampling sites and samples can be found in Table S4.2.1.

4.2.2 Laboratory SOA formation

Laboratory SOA experiments were performed in a 7 L quartz flow tube and a 19 L potential aerosol mass (PAM) chamber, respectively. The particulate SOA were generated from the gas phase ozonolysis of α -pinene, β -pinene and limonene, respectively, with the O₃ concentration of ~1000 ppb in the flow tube. The isoprene- and naphthalene- SOA were generated from the gas phase photooxidation of isoprene and naphthalene, respectively, with the concentration of OH· radical of $\sim 5.0 \times 10^{11}$ cm⁻³ in the PAM chamber. The concentration of precursors was estimated to be 1–2 ppm for α -pinene, β -pinene and limonene and 0.5–1 ppm for isoprene and naphthalene. SOA samples were collected on 47 mm diameter Teflon filters (JVWP04700, Omnipore membrane filter) and extracted immediately after sampling. More information about the SOA formation and collection processes can be found in our previous study (Tong et al., 2019).

4.2.3 UHRMS measurements and Data processing

The procedure of filter extraction was presented in detail in our previous studies (Wang et al., 2018; Wang et al., 2019; Wang et al., 2019; Tong et al., 2019). In brief, a portion of filter (corresponding to approximate 600 μ g particle mass in each extracted filter) was extracted twice with 1.5 ml of methanol in an ultrasonic bath for 30 min. The combined extracts were filtered with a 0.2 μ m polytetrafluoroethylene (PTFE) membrane syringe filter to remove insoluble particulate matter, and then the extracts were evaporated to dryness under a gentle stream of nitrogen. Afterwards, the extracts were dissolved in 1.0 mL of acetonitrile/ultrapure water (ACN/H₂O) mixture (1/9, v/v) for subsequent analysis.

The chemical measurement of organic compounds was carried out based on ultrahigh

resolution mass spectrometry (UHRMS) using an Orbitrap mass spectrometer (Q-Exactive, Thermo Scientific, Germany) coupled to an UHPLC system (Dionex UltiMate 3000, Thermo Scientific, Germany). A Hypersil Gold column (C18, 50 × 2.0 mm, 1.9 μm particle size, Thermo Scientific, Germany) was used for separation of analytes. The mobile phase was applied on a gradient mode at a flow rate of 0.5 mL min⁻¹, consisting of eluent A (ultrapure H₂O with 2% ACN and 0.04% formic acid) and eluent B (ACN with 2% ultrapure H₂O). The Orbitrap was equipped with a heated electrospray ionization source (HESI) and operated in the negative ion mode (ESI⁻) with a -3.3 kV spray voltage. A mass resolving power of 70,000 @ *m/z* 200 and a scanning range of 50–500 *m/z* were applied. Detailed information of optimized gradient of mobile phase and MS approach can be found in our previous studies (Wang et al., 2018; Wang et al., 2019; Wang et al., 2019; Tong et al., 2019).

The obtained chromatograms and mass spectra were proceeded by a non-target screening approach using an open-source software (MZmine 2.37). The detailed processing steps and parameters applied in the software are shown in Table S2. The software automatically searched the ions with absolute peak abundance above 1 × 10⁵ and calculated all mathematically possible molecular formulas for ion signals with a mass tolerance of ± 2 ppm. The molecular formulas were presented as C_cH_hO_oN_nS_s, where c, h, o, n and s are the number of carbon, hydrogen, oxygen, nitrogen and sulfur atoms, respectively, which were in the range of 1–39, 1–72, 0–20, 0–7 and 0–4. To eliminate chemically unreasonable molecular formulas, ratios of H/C, O/C, N/C and S/C were further constrained in the range of 0.3–3, 0–3, 0–1.3 and 0–0.8, respectively (Tong et al., 2019).

4.2.4 Quantification of H₂O₂ yield

One fourth of each ambient PM filter or a whole SOA-loaded filter was extracted with 1.0 mL of ultra-pure water by stirring with a vortex shaker for 15 minutes. Afterwards, the extracts were centrifuged at 9000 rpm using a centrifuge (Eppendorf Minispin) for 3 minutes. Finally, the concentration of H₂O₂ in the supernatants was quantified using a fluorometric Hydrogen Peroxide Assay Kit (MAK165, Sigma). The detailed procedure of H₂O₂ measurement has been presented in our previous study (Tong et al., 2018). Briefly, 50 μL of supernatant and 50 μL of detection reagent containing horseradish peroxidase and Amplex Red substrate were mixed in a 96-well plate. The fluorescence was detected using a microplate reader (Synergy™ NEO, BioTek; excitation at 540 nm and emission at 590 nm) after 30 minutes of incubation. The concentration of H₂O₂ in extracts was determined using a H₂O₂ calibration curve obtained using standard H₂O₂ solutions and was

corrected by blank measurements.

4.2.5 Measurement of radical yield by EPR

The procedure of radical yield measurement was presented in our previous studies (Tong et al., 2018; Tong et al., 2019). In brief, one fourth of each ambient PM filter or a whole SOA-loaded filter was extracted with 10 mM 5-tert-Butoxycarbonyl-5-methyl-1-pyrroline N-oxide (BMPO, high purity, Enzo Life Sciences GmbH), which was used as the spin-trapping agent by vortex shaking (Heidolph Reax 1) for 15 minutes. A continuous-wave electron paramagnetic resonance (CW-EPR) X-band spectrometer (EMXplus-10/12; Bruker Corporation) was applied for identification and quantification of radicals. The operating parameters of EPR is briefly displayed as following: a modulation frequency of 100 KHz, a modulation amplitude of 1 G, a microwave power of 2.1 mW (20 dB), a receiver gain of 40 dB, a scan number of 50 and a sweep width of 100 G. The spin-counting method named Xenon embedded in the Bruker software was used to quantify the radicals.

4.3 Results and discussion

4.3.1 MCR-VK diagram

UHRMS technique has been increasingly applied to elucidate the unambiguous the molecular formulas of organic compounds in atmospheric aerosols. However, the interpretation of molecular structures based on the assigned molecular formulas by UHRMS technique is limited. The metrics of double bond equivalent (DBE), aromaticity index (AI) and aromaticity equivalent (Xc) have been successfully introduced to indicate the double bonds and aromatic rings in molecular structures of organic compounds (Koch and Dittmar, 2006; Yassine et al., 2014). We proposed a new metric named maximum carbonyl ratio (MCR), which describes the potentially maximal contribution of carbonyl functionalities in the molecular structures of organic compounds detected by HRMS technique. For a given molecular formula of $C_cH_hO_oN_nS_s$, the MCR can be calculated by equation 4.1:

$$\text{MCR} = \frac{\text{DBE}}{o}, \text{ for } o \geq \text{DBE} \quad (4.1)$$

where o was the number of oxygen atoms in the compound. MCR is considered to equal one if $o <$

DBE.

An updated visualization tool, the MCR-VK diagram, is developed by the combination of the MCR value and the traditional VK diagram. In this study, as shown in Figure 4.3.1a, MCR-VK diagram is divided to two regions by the black dash line, which represents the MCR value of 0.9. Compounds located in the blue area in Figure 4.3.1a are classified as oxidized organic compounds (OOC) with the MCR values less than 0.9, while compounds in the gray area are classified as unsaturated organic compounds (UOC) with the value of $MCR \geq 0.9$. OOC include several types of compounds, such as very highly oxidized organic compounds (e.g., peroxides and isoprene epoxydiols), highly oxidized organic compounds (e.g. 3-methyl-1, 2, 3-butanetricarboxylic acid (MBTCA)) and intermediately oxidized organic compounds (e.g., pinic acid and pinonic acid) (Yasmeen et al., 2012; Müller et al., 2012; Nguyen et al., 2014; Wang et al., 2018) as shown in Figure S4.3.1a. Highly oxidized multifunctional molecules (HOMs) (Mutzel et al., 2015; Wang et al., 2017), which undergo different oxidation and aging processes, can also be assigned to OOC. UOC mainly include oxidized unsaturated organic compounds (e.g., primary organic compounds and oxidation products from aromatic volatile organic compounds) and highly unsaturated organic compounds (e.g., combustion related compounds and compounds from condensational ageing) (see Figure S4.3.1a).

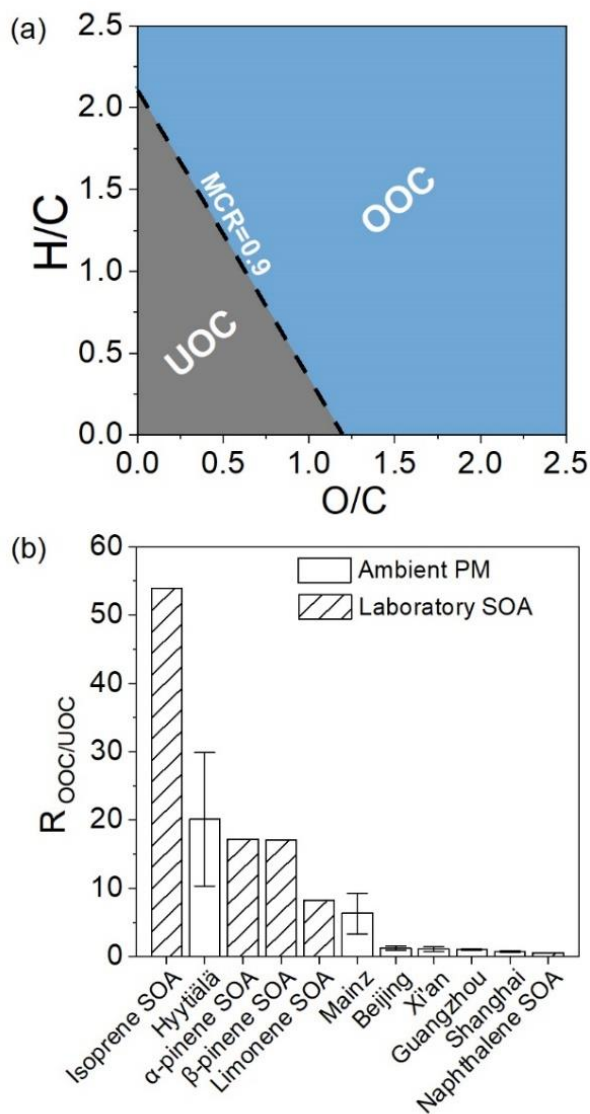


Figure 4.3.1: (a) MCR-VK diagram applied to classify the organic compounds in particulate organic aerosols. The black dash line represents the boundary ($MCR = 0.9$) between the oxidized organic compounds (OOC, $MCR < 0.9$) located in the blue region and the unsaturated organic compounds (UOC, $MCR \geq 0.9$) in the gray region. (b) Ratio of relative peak area-weighted fraction of OOC to relative peak area-weighted fraction of UOC ($R_{OOC/UOC}$) of the ambient fine PM samples (blank pattern) and laboratory-generated SOA samples (slash pattern). The error bars represent the standard deviations of $R_{OOC/UOC}$ of the samples collected at each location or each laboratory experiment.

4.3.2 Contribution of OOC and UOC to ambient and laboratory particulate aerosol samples

Based on the compound classification by MCR-VK diagram, a new parameter was defined as 'ratio of relative peak area-weighted fraction of OOC to relative peak area-weighted fraction of UOC ($R_{\text{OOC/UOC}}$)' in this study, which reflected the relative contribution of OOC and UOC to the particulate organic aerosol. Figure 4.3.1b displays the $R_{\text{OOC/UOC}}$ of the ambient fine PM and laboratory-generated SOA samples, which were averaged from all samples collected at each location or laboratory experiment. It shows that the $R_{\text{OOC/UOC}}$ of isoprene SOA is highest with the value of 54, followed by Hyytiälä $\text{PM}_{2.5}$ (20), α/β -pinene SOA (17), limonene SOA (8), urban fine PM (i.e., Mainz (6), Beijing (1.3), Xi'an (1.2), Guangzhou (1.1) and Shanghai (0.75)) and naphthalene SOA (0.57). The extremely high value (54) of $R_{\text{OOC/UOC}}$ of isoprene SOA indicates the major contribution of OOC to the organic compounds in isoprene SOA. It can be explained by that the oxygen atoms in the molecular structures of typical products generated from photooxidation of isoprene (e.g., 2-methyl-tetrols) (Wang et al., 2018) are in the form of OH functional group, which are assigned to OOC with the low value of MCR. The $R_{\text{OOC/UOC}}$ of α/β -pinene SOA with the value of 17 is also very high and OOC in α -pinene SOA and β -pinene SOA account for 95% and 94%, respectively (See Figure S4.3.1b). It agrees well with our recent study showing that the typical products formed through the ozonolysis of α -pinene and β -pinene, e.g., pinonic acid, pinic acid and MBTCA from α -pinene oxidation and nopinone and pinic acid from β -pinene oxidation (Yasmeen et al., 2012; Müller et al., 2012; Zhang et al., 2015), were located in the blue area of MCR-VK diagram. Interestingly, the $R_{\text{OOC/UOC}}$ (20) of $\text{PM}_{2.5}$ samples collected at a remote forest site of Hyytiälä is comparable to that of α/β -pinene SOA, which can probably be explained by that α/β -pinene make important contribution to the formation of SOA at Hyytiälä location (Cavalli et al., 2006; Kourtschev et al., 2013).

On the contrary, the $R_{\text{OOC/UOC}}$ (0.57) of naphthalene SOA is significantly lower compared to the $R_{\text{OOC/UOC}}$ (54) of the SOA generated from biogenic precursors. Such low value of $R_{\text{OOC/UOC}}$ of naphthalene SOA indicates that the products formed through the photooxidation of naphthalene are dominated by UOC with relative fraction value of 64% (see Figure S4.3.1b). Previous studies showed that compounds located at the lower left corner of the VK diagram with H/C ratio ≤ 1.0 and O/C ratio ≤ 0.5 were suggested to be low-oxygen-containing aromatic hydrocarbons (Kourtschev et al., 2014; Wang et al., 2018). Since the majority of UOC are also located at the lower left corner of the MCR-VK diagram, these UOC are likely to be aromatic compounds. This observation is consistent with a previous study by Kautzman et al. (2010) showing that the SOA

generated from the photooxidation of naphthalene under low-NO_x conditions were dominated by ring-retaining compounds (e.g. 1,4-benzoquinone) and ring-opening species (e.g. phthalaldehyde). It can be explained by that the photo-oxidation process is not able to break the two benzene rings in the structure of naphthalene, resulting in one benzene ring remaining in the structure of the products.

In urban fine PM, the relative peak area-weighted fractions of UOC span a wide range from ~15% to ~57% (see Figure S4.3.1b), indicating the complex chemical composition of urban organic aerosol due to various kinds of precursors and formation processes in urban regions. The $R_{\text{OOC/UOC}}$ of ambient PM_{2.5} samples collected at Beijing, Xi'an, Guangzhou and Shanghai are 1.3, 1.2, 1.1 and 0.75, respectively, which are close to the $R_{\text{OOC/UOC}}$ (0.57) of naphthalene SOA but highly different from the $R_{\text{OOC/UOC}}$ (8–54) of SOA generated from the biogenic precursors. It indicates that a large amount of aromatic compounds were probably generated in these Chinese urban regions. This observation agrees well with our previous studies showing that the majority of compounds in the Chinese cities of Beijing, Shanghai, Guangzhou and Changchun were considered to mono- and poly-aromatics (Wang et al., 2019). However, the $R_{\text{OOC/UOC}}$ (6) of Mainz fine PM samples is much higher than that of the Chinese megacities, indicating the less aromatic compounds in Mainz fine PM samples, which is again consistent with our previous study (Wang et al., 2018).

Interestingly, the $R_{\text{OOC/UOC}}$ (20) of the Hyytiälä PM_{2.5} is in the range of the $R_{\text{OOC/UOC}}$ (8–54) of biogenic SOA and much higher than the $R_{\text{OOC/UOC}}$ (0.57) of anthropogenic SOA, while all the $R_{\text{OOC/UOC}}$ (0.75–6) of urban samples are lower than the $R_{\text{OOC/UOC}}$ of biogenic SOA and close to that of anthropogenic SOA. It implies that the SOA in urban areas is affected by a large degree of anthropogenic sources compared to remote forest regions.

4.3.3 Yield and formation potential of ROS by ambient fine PM

Chemical characteristic of organic aerosols is likely a key factor linked to health effect, however, it is difficult to identify a set of chemical reactions or redox-active components responsible for reactive species formation due to the complexity of organic aerosols. Since the MCR might release the health-related information, as introduced in our recent study, the MCR index together with the $R_{\text{OOC/UOC}}$ parameter are promising to identify the health-related organic compound in the complex aerosol samples.

Figure 4.3.2a and 4.3.2b display the volume-normalized (pmol m^{-3}) and mass-normalized ($\text{pmol } \mu\text{g}^{-1}$) ROS yield, i.e., the sum of H₂O₂ yield and radical yield, by ambient fine PM as a function of the concentration of PM. Beijing PM_{2.5} exhibited the highest formation potential of

ROS with 263 pmol m^{-3} , whereas the Hyytiälä $\text{PM}_{2.5}$ samples with concentration of $5 \text{ } \mu\text{g m}^{-3}$ generated only 13 pmol m^{-3} ROS. Figure 4.3.2a shows that the volume-normalized ROS yield generated by the ambient fine PM has a positive linear correlation ($R^2 = 0.81$) with the mass concentration of PM, indicating that the potential of ROS formation by ambient fine PM increases with the increase of pollution levels. This positive correlation is not surprising, since this ROS yield is volume-normalized and higher PM concentration refers to more PM mass in each volume of air, generating more ROS. It is very interesting that the linear coefficient of R^2 between the volume-normalized ROS yield and PM concentration has a high value of 0.8, meaning that we could estimate the volume-normalized ROS yield of ambient fine PM samples simply based on the PM concentration. Moreover, since the ROS yield presented in Figure 4.3.2a and 4.3.2b is the sum of H_2O_2 yield and radical yield, we also presented the volume-normalized H_2O_2 yield and radical volume-normalized yield as a function of the concentration of PM in Figure S4.3.4, again showing positive linear correlations with $R^2 = 0.79$ and $R^2 = 0.91$, respectively.

In comparison to the volume-normalized ROS yields, the mass-normalized yield of ROS is independent of filter loading, which can better reflect the redox potential associated with redox-active species (e.g., peroxides and transition metals) in PM. As shown in Figure 4.3.2b, no obvious correlation was observed between the mass-normalized ROS yield and the concentration of PM. Figure S4.3.4c shows that the mass-normalized H_2O_2 yield had no obvious correlation with the concentration of PM. While the mass-specific radical yield of ambient fine PM exhibits a good negative linear correlation with PM concentration (see Figure S4.3.4d), which agrees well with our previous study (Tong et al., 2019).

The correlation of $R_{\text{OOC/UOC}}$ of ambient fine PM samples with the concentration of PM is displayed in Figure 4.3.2c. It shows that the $R_{\text{OOC/UOC}}$ of organic aerosols is negatively correlated with the PM concentration, indicating that PM in clean areas exhibits higher $R_{\text{OOC/UOC}}$ value, whereas PM is associated with low $R_{\text{OOC/UOC}}$ in polluted regions. Interestingly, the $R_{\text{OOC/UOC}}$ of ambient fine PM decreases with the increasing concentration of PM, showing a similar trend with mass-specific ROS yields by urban fine PM samples (see Figure 4.3.2b), particularly for urban fine PM (i.e., Mainz, Beijing, Xi'an, Guangzhou, and Shanghai). Thus, the relationship between chemical characteristics of organic aerosols based on $R_{\text{OOC/UOC}}$ parameter and ROS generated by ambient fine PM as well as laboratory-generated SOA samples was further explored.

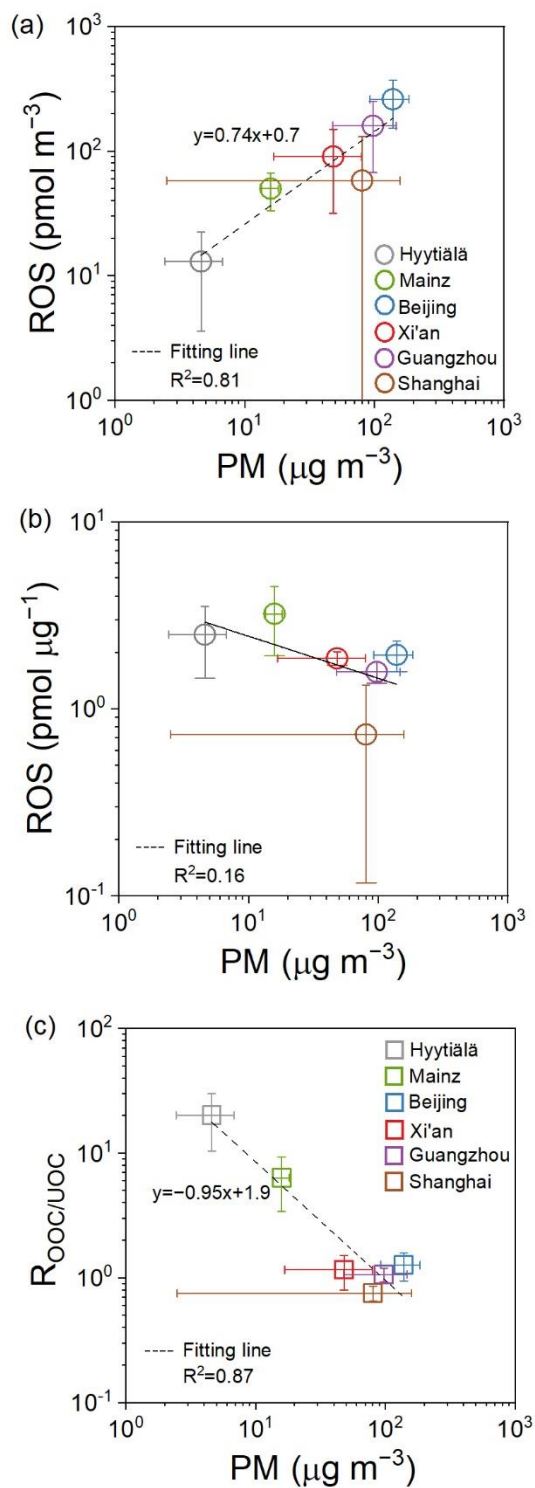


Figure 4.3.2: Correlation of volume-normalized ROS yields (a), mass-specific ROS yields (b) and $R_{OOC/UOC}$ (c) with the concentration of ambient fine PM. The error bars represent standard deviations.

4.3.4 Correlation between $R_{\text{OOC/UOC}}$ and ROS yield

To get insights into the relationship between chemical characteristics of organic aerosols and ROS generation, the correlations of particle mass normalized H_2O_2 yield, radical yield, and the sum of them, with the $R_{\text{OOC/UOC}}$ of organic compounds in ambient fine PM and laboratory-generated SOA samples were shown in Figure 4.3.3.

As shown in Figure 4.3.3a, a significant positive exponential correlation ($y = 3.2 - 7.6\exp(-1.5x)$, $R^2 = 0.94$) was observed between the ROS yield and the $R_{\text{OOC/UOC}}$ of urban fine PM samples (i.e., Mainz, Beijing, Xi'an, Guangzhou, and Shanghai). It indicates that ROS yield is closely associated with organic components, moreover, the ROS generated by organic aerosols in water increase exponentially with $R_{\text{OOC/UOC}}$ value of fine PM. It should be noted that the dot of Hyytiälä $\text{PM}_{2.5}$ (the gray dot) was not fit the exponential curve, which may be explained by the large different chemical characteristics between the Hyytiälä $\text{PM}_{2.5}$ samples and urban fine PM samples.

Figure 4.3.3b shows that H_2O_2 yield is positive exponential correlated ($y = 3.0 - 8.0\exp(-1.6x)$, $R^2 = 0.98$) with the $R_{\text{OOC/UOC}}$ of ambient samples, which is highly similar to the correlation shown in Figure 4.3.3a, implying that the relatively stable H_2O_2 may make an important contribution to the ROS formation by ambient fine PM. Furthermore, Figure S4.3.5 indicates H_2O_2 yield accounts for the majority fraction (77%–99%) of the total ROS yield by ambient fine PM and laboratory-generated SOA samples.

The good correlations of H_2O_2 yield with the $R_{\text{OOC/UOC}}$ of urban fine PM (see Figure 4.3.3b) as well as relative fraction of OOC in urban fine PM (see Figure S4.3.6b) indicate that the organic components, especially OOC, in urban aerosols make significant contribution to the H_2O_2 generation. This observation agrees well with the previous studies showing that decomposition or hydrolysis of hydroperoxides and organic peroxides (assigned to OOC) is likely an important pathway of H_2O_2 formation in the water (Wang et al., 2011; Badali et al., 2015; Tong et al., 2018).

Another interesting observation is that the data dot of ROS yield of Hyytiälä $\text{PM}_{2.5}$ (the gray dot in Figure 4.3.3a), as well as the ROS yield of Hyytiälä $\text{PM}_{2.5}$ (the gray dot in Figure 4.3.3b) of Hyytiälä $\text{PM}_{2.5}$, are beyond the exponential curve fitted by the urban fine PM samples. It implies that the curve equations of urban aerosols are not suitable to apply for the forest aerosols samples of Hyytiälä. This observation reflects that the sources and mechanisms of H_2O_2 formation may be different between the urban aerosols and remote forest aerosols due to their large difference in term of chemical composition. For example, some quinones (assigned to UOC) and several transition metals (e.g., Fe, Cu, and Mn) commonly found in urban fine PM samples can also contribute to H_2O_2 yield. On the contrary, remote fine PM samples contain a rare number of metals and quinones

but a large amount of biogenic precursor-generated particles.

Figure 4.3.33c shows that the radical yield of Hyytiälä PM_{2.5} samples with extremely high R_{OOc/UOC} value is much higher compared to urban fine PM samples with lower R_{OOc/UOC} value. It can be explained by our previous study showing that HOMs (assigned to OOC) may play an important role in radical formation in water and a higher relative fraction of HOMs in Hyytiälä PM_{2.5} was observed compared to that in the urban fine PM.

In contrast to ambient fine PM, laboratory-generated SOA samples exhibited much higher ROS yields as shown in Figure 4.3.3d. Among laboratory-generated SOA, isoprene SOA had the highest ROS yield of 5.9 pmol μg⁻¹, followed by α-pinene SOA (4.5 pmol μg⁻¹), β-pinene SOA (3.4 pmol μg⁻¹) and limonene SOA (3.4 pmol μg⁻¹), whereas naphthalene SOA had the lowest ROS yield of 1.8 pmol μg⁻¹. The positive linear correlation ($y = 47.8 + 5.8x$, $R^2 = 0.95$) of R_{OOc/UOC} of laboratory SOA with ROS yield could confirm the significant effect of organic aerosols, especially OOC, on ROS formation. It agrees well with the finding of Tong et al. (2018) showing that a positive correlation was observed between the total peroxide concentration and ROS yield generated by isoprene SOA, β-pinene SOA and naphthalene SOA, indicating that organic (hydro)peroxides (assigned to OOC) may play an important role in ROS formation.

As shown in Figure 4.3.3e, similar with ambient samples, the increasing trend of H₂O₂ yield of SOA generated from different precursors is consistent with that of ROS yield (see Figure 4.3.3d). This observation may mainly be due to that H₂O₂ is the most abundance ROS species accounting for 95%–99% (see Figure S4.3.5b). It clearly shows that higher H₂O₂ yield by biogenic SOA (i.e., α/β-pinene SOA, limonene SOA, and isoprene SOA) was observed than that by naphthalene SOA. The positive linear correlation ($y = 46.1 + 5.7x$, $R^2 = 0.94$) between the H₂O₂ yield generated by laboratory-generated SOA samples and the R_{OOc/UOC} values implies that SOA samples with high R_{OOc/UOC} can generate more H₂O₂. Furthermore, OOC likely make significant contribution to H₂O₂ generation. Previous studies reported that H₂O₂ generated in water by organic aerosols is likely due to decomposition or hydrolysis of a certain type of organic compounds, e.g., hydroxyhydroperoxides (products from ozonolysis of α- and β-pinene) and peroxy acids (RC(O)OOH, formed from ozonolysis of α-pinene) (Hasson et al., 2001; Venkatachari and Hopke, 2008; Wang et al., 2011; Badali et al., 2015).

No obvious correlation is found between the radical yield and the R_{OOc/UOC} values for these laboratory-generated SOA samples as shown in Figure 4.3.3f. Tong et al. (2018) found that the radical production rates of SOA in water was related with the abundance of total peroxides in SOA, however, naphthalene SOA can generate more •O₂⁻, which is most likely generated by redox reactions of semiquinones contained in naphthalene SOA.

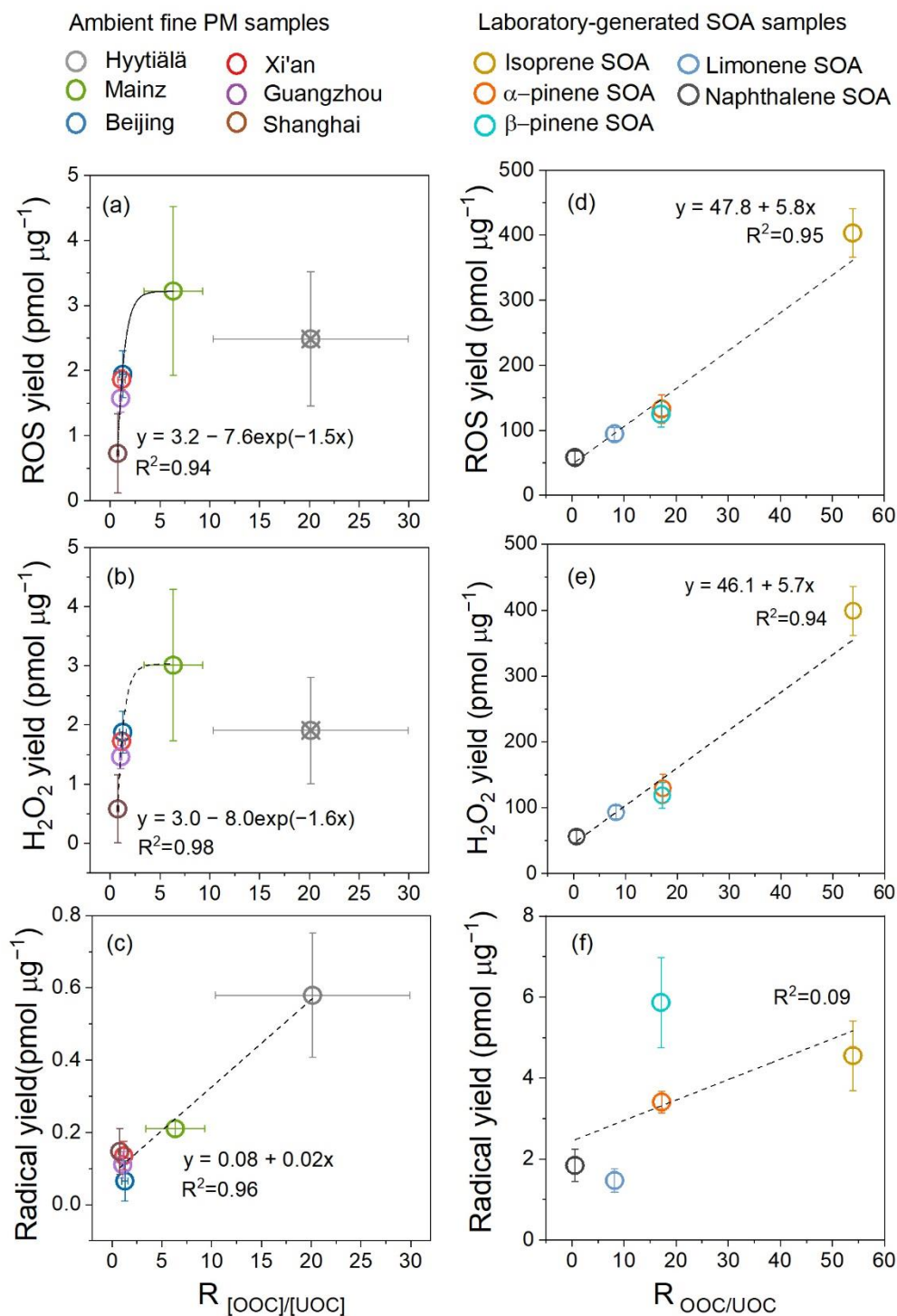


Figure 4.3.3: Correlation of mass-specific ROS yields (a), H₂O₂ yields (b) and radical yields (c) with $R_{\text{OOC}/\text{UOC}}$ of ambient fine PM samples and correlation of mass-specific ROS yields (d), H₂O₂ yields (e) and radical yields (f) with $R_{\text{OOC}/\text{UOC}}$ of laboratory-generated SOA samples, respectively. The error bars represent standard deviations.

4.4 Conclusion and implication

Particulate aerosol samples were collected at six cities (Mainz, Beijing, Shanghai, Guangzhou, and Xi'an), a forest site (Hyytiälä), as well as laboratory flow tube and chamber facilities. The organic compounds identified by UHRMS were classified into oxidized organic compounds (OOC) and unsaturated organic compounds (UOC) according to the MCR value of individual compound. Moreover, the H_2O_2 yield and radical yield of particulate aerosol samples were quantified using a fluorometric probe and electron paramagnetic resonance spectrometry, respectively. A new index defined as 'the ratio of relative peak area-weighted fraction of OOC to relative peak area-weighted fraction of UOC ($R_{\text{OOC/UOC}}$)' based on the MAC metric was introduced to investigate the relationship between the ROS yield and molecular composition of atmospheric aerosol.

We found that the positive correlations between the ROS yield and the $R_{\text{OOC/UOC}}$ were observed in both ambient urban fine PM and laboratory-generated SOA, indicating that the ROS generation is closely associated with organic components in the particulate aerosol samples, particularly with the oxidized organic compounds. The results of this study will help to provide more evidence for the link between the organic compounds in PM and ROS formation, furthermore, the proposed $R_{\text{OOC/UOC}}$ is suggested to infer the health-related organic species in PM. In the future, by investigating the relationship between the chemical composition and ROS formation of more different locations and generated from different types of precursors, the equations could be improved and be used to predict the ROS yield by the concentration of PM and further better assess the toxicity of PM.

Supporting Information

The detailed information of ambient PM sampling (Table S4.2.1), molecular formulas of organic compounds detected in ambient PM and laboratory-generated SOA (Table S4.3.1–S4.3.5), and seven figures (Figure S4.2.1, S4.3.1–S4.3.6)

Acknowledgements

This work was funded by the Deutsche Forschungsgemeinschaft (DFG, HO 1748/19-1, HO 1748/20-1), the German Federal Ministry of Education and Research (BMBF contract 01LK1602D), and the Max Planck Society and the National Natural Science Foundation of China (NSFC) (Grant No. 41925015). Y. Zhang acknowledges the scholarship from the Chinese Scholarship Council (CSC). The authors acknowledge stimulating exchange with U. Pöschl.

5 Conclusions and Outlook

The application of ultrahigh resolution mass spectrometry (UHRMS) in the field of atmospheric aerosol research, that was, the chemical composition characterization of organic aerosols (OA) at a molecular level was demonstrated within this thesis. A rapid and simple sample pre-treatment method using a solvent mixture of acetonitrile and water was developed to extract the organic compounds, which was proved to be efficient for both polar compounds like organic acids and non-polar compounds such as polycyclic aromatic hydrocarbons. Ultrahigh performance liquid chromatography (UHPLC) technique was applied prior to UHRMS coupled with electrospray ionization source, which was able to achieve the separation of the isomer compounds and reduction of the ion suppression. Based on the mass spectra data obtained by UHRMS, non-target screening methods were developed with a commercial software 'SIEVE' and an open-source software 'MZmine', respectively. The identified thousands of organic compounds were classified into CHO, CHON, CHOS, CHONS, and CHN (only in positive mode) according to their elemental composition. Various typical metrics including double bond equivalent, carbon oxidation state, and aromaticity equivalent and several visualization tools, i.e., Van Krevelen diagram and Kendrick mass defect diagram, were applied to interpret the UHRMS data and describe the chemical properties and possible sources of OA.

A new metric – the maximum carbonyl ratio (MCR) – was suggested in this work, which described the maximal contribution of carbonyl/epoxide functionalities in individual compounds in OA, that can be directly derived from the molecular composition. MCR was presented in combination with Van Krevelen diagrams as an updated visualization tool (MCR-VK diagram) aiming to better categorize complex organic compounds in ambient aerosol samples. By locating selected typical SOA compounds, MCR-VK diagram was divided into five regions corresponding to very highly oxidized organic compounds, highly oxidized organic compounds, intermediately oxidized organic compounds, oxidized unsaturated organic compounds, and highly unsaturated organic compounds, respectively. The approach was applied to the ambient OA samples and laboratory-generated SOA samples based on the UHRMS data. By observing and comparing the distributions of organic compounds in the MCR-VK diagram, the understanding of chemical properties, sources, and formation pathways of OA was improved.

Investigating the sources, formation processes, and amount of ROS is an effective pathway to evaluate the redox activity and toxicity of OA. Chemical components in OA are likely a key factor but are difficult to be identified accurately. The suggested metric of MCR, easily extracted from

UHRMS data, might be a valuable tool to identify health-relevant particle parameters and components. The ROS yield, which refers to the sum of H₂O₂ yield and radical yield in this thesis, produced by ambient PM_{2.5} samples and laboratory-generated SOA samples in water was quantified. The yield of H₂O₂ was measured using a fluorometric probe, while the yield of radicals was detected by electron paramagnetic resonance. The total intensity of oxidized organic compounds (i.e., very highly oxidized organic compounds, highly oxidized organic compounds, intermediately oxidized organic compounds) in ambient urban PM_{2.5} samples and laboratory-generated SOA both showed significant positive correlations with the ROS yield, indicating oxidized organic compounds, e.g. (hydro)peroxides, might make an important contribution to the ROS formation.

The UHRMS technique presented in this thesis is allowed to give the molecular formula information of thousands of organic compounds from complex OA matrix. However, due to such high numbers of organic compounds, it is difficult to elucidate the molecular structures of these organic compounds. In the future, more detailed tandem MS (MSⁿ) studies should be performed for a better understanding of the molecular structures. Meanwhile, the interpretation method for UHRMS data should be further developed, like combining the information of molecular formulas and retention times in UHPLC to predict the volatilities of different compounds. Moreover, the proposed MCR metric might be utilized as a valuable parameter to identify health-related organic components, providing new insights into the ROS formation. In future work, the combination between MCR or MCR-VK diagram and other metrics, such as carbon oxidation states, can be further explored to analyze the chemical structures in the complex aerosol components.

6 References

- Al-Naiema, I. M., and Stone, E. A.: Evaluation of anthropogenic secondary organic aerosol tracers from aromatic hydrocarbons, *Atmos. Chem. Phys.*, 17, 3, 2053-2065, 2017.
- Altieri, K. E., Turpin, B. J., and Seitzinger, S. P.: Composition of dissolved organic nitrogen in continental precipitation investigated by ultra-high resolution FT-ICR mass spectrometry, *Environ. Sci. Technol.*, 43, 6, 2009.
- Apel, K., and Hirt, H.: Reactive oxygen species: metabolism, oxidative stress, and signal transduction. *Annu. Rev. Plant Biol.* 55:373-399, 2004.
- Arangio, A. M., Tong, H., Socorro, J., Pöschl, U., and Shiraiwa, M.: Quantification of environmentally persistent free radicals and reactive oxygen species in atmospheric aerosol particles, *Atmos. Chem. Phys.*, 16, 20, 13105-13119, 2016.
- Arellanes, C., Paulson, S. E., Fine, P. M., and Sioutas C.: Exceeding of Henry's law by hydrogen peroxide associated with urban aerosols, *Env. Sci. Tech.*, 40:4859-4866, 2006.
- Atkinson, R.: Gas-phase tropospheric chemistry of organic compounds: A review, *Atmos. Environ.*, 24A, 1-41, 1991.
- Atkinson, R., and Arey, J.: Atmospheric degradation of volatile organic compounds, *Chem. Rev.*, 103, 12, 4605-4638, 2003.
- Badali, K. M., Zhou, S., Aljawhary, D., Antiñolo, M., Chen, W. J., Lok, A., Mungall, E., Wong, J. P. S., Zhao, R., Abbatt, and J. P. D.: Formation of hydroxyl radicals from photolysis of secondary organic aerosol material, *Atmos. Chem. Phys.* 15, 14, 7831-7840, 2015.
- Bates, J. T., Fang, T., Verma, V., Zeng, L., Weber, R. J., Tolbert, P. E., Abrams, J. Y., Sarnat, S. E., Klein, M., Mulholland, J. A., and Russell, A. G.: Review of acellular assays of ambient particulate matter oxidative potential: Methods and relationships with composition, sources, and health effects, *Environ. Sci. Technol.*, 53, 8, 4003-4019, 2019.
- Barrow, M. P., Headley, J. V., Peru, K. M., and Derrick, P. J.: Data visualization for the characterization of naphthenic acids within petroleum samples, *Energy & Fuels*, 23, 5, 2592-2599, 2009.
- Beelen, R., Raaschou-Nielsen, O., Stafoggia, M., Andersen, Z. J., Weinmayr, G., Hoffmann, B., Wolf, K., Samoli, E., Fischer, P., Nieuwenhuijsen, M., Vineis, P., Xun, W. W., et al.: Effects of long-term exposure to air pollution on natural-cause mortality: an analysis of 22 European cohorts within the multicentre ESCAPE project, *THE LANCET*, 383, 9919, 785-795, 2014.
- Bianchi, F., Kurten, T., Riva, M., et al.: Highly oxygenated organic molecules (HOM) from gas-phase autoxidation involving peroxy radicals: A key contributor to atmospheric aerosol, *Chem. Rev.*, 119, 3472-3509, doi:10.1021/acs.chemrev.8b00395, 2019.
- Brook, R. D., Rajagopalan, S., Pope, C. A., et al.: An update to the scientific statement from the American Heart Association, *Circulation*, 121, 2331-2378, doi.org/10.1161/CIR.0b013e3181d8e1, 2010.

- Borrás, E., and Tortajada-Genaro, L. A.: Secondary organic aerosol formation from the photo-oxidation of benzene, *Atmos. Environ.*, 47, 154-163, 2012.
- Brüggemann, M., Vogel, A., and Hoffmann, T.: Analysis of organic aerosols using a micro-orifice volatilization impactor (MOVI) coupled to an atmospheric-pressure chemical ionization mass spectrometer (APCI-MS), *European Journal of Mass Spectrometry*, 20, 1, 31-41, doi: 10.1255/ejms.1260, 2014.
- Brüggemann, M.: Development, characterization, and application of flowing atmospheric-pressure afterglow ionization for mass spectrometric analysis of ambient organic aerosols, Ph. D. thesis, Max Planck Graduate Center, University of Mainz, Germany, 2015.
- Brüggemann, M., Poulain, L., Held, A., Stelzer, T., Zuth, C., Richters, S., Mutzel, A., van Pinxteren, D., Iinuma, Y., Katkevica, S., Rabe, R., Herrmann, H., and Hoffmann, T.: Real-time detection of highly oxidized organosulfates and BSOA marker compounds during the F-BEACH 2014 field study, *Atmos. Chem. Phys.*, 17, 1453-1469, 2017.
- Canagaratna, M.R., Jayne, J.T., Jimenez, J.L., Allan, J.D., Alfarra, M.R., Zhang, Q., Onasch, T.B., Drewnick, F., Coe, H., Middlebrook, A., Delia, A., Williams, L.R., Trimborn, A.M., Northway, M.J., DeCarlo, P.F., Kolb, C.E., Davidovits, P., and Worsnop, D.R.: Chemical and microphysical characterization of ambient aerosols with the aerodyne aerosol mass spectrometer, *Mass spectrom. rev.*, 26, 185-222, 2007.
- Carlton, A. G., Wiedinmyer, C., and Kroll, J. H.: A review of secondary organic aerosol (SOA) formation from isoprene, *Atmos. Chem. Phys.*, 9, 14, 4987-5005, 2009.
- Carslaw, K. S., Gordon, H., Hamilton, D. S., et al.: Aerosols in the pre-industrial atmosphere, *Curr. Clim. Change Rep.*, 3, 1-15, doi:10.1007/s40641-017-0061-2, 2017.
- Cavalli, M. C. F., Decesari, S., Emblico, L., et al.: Size-segregated aerosol chemical composition at a boreal site in southern Finland, during the QUEST project, *Atmos. Chem. Phys.*, 6, 993-1002, 2006.
- Cech, N. B., and Enke, C. G.: Practical implications of some recent studies in electrospray ionization fundamentals, *Mass spectrom. rev.*, 20, 362-387, 10.1002/mas.10008, 2001.
- Chang, Y., Deng, C., Cao, F., Cao, C., Zou, Z., Liu, S., Lee, X., Li, J., Zhang, G., and Zhang, Y.: Assessment of carbonaceous aerosols in Shanghai, China – Part 1: long-term evolution, seasonal variations, and meteorological effects, *Atmos. Chem. Phys.*, 17, 9945-9964, 10.5194/acp-17-9945-2017, 2017.
- Chen, Q., Wang, M., Wang, Y., Zhang, L., Li, Y., and Han, Y.: Oxidative potential of water-soluble matter associated with chromophoric substances in PM_{2.5} over Xi'an, China, *Environ. Sci. Technol.*, 53, 15, 8574-8584, 2019.
- Cheng, Y., Engling, G., He, K. B., Duan, F. K., Ma, Y. L., Du, Z. Y., Liu, J. M., Zheng, M., and Weber, R. J.: Biomass burning contribution to Beijing aerosol, *Atmos. Chem. Phys.*, 13, 7765-7781, 10.5194/acp-13-7765-2013, 2013.
- Chowdhury, P. H., He, Q., Carmieli, R., Li, C., Rudich, Y., and Pardo, M.: Connecting the oxidative potential of secondary organic aerosols with reactive oxygen species in exposed lung cells, *Environ. Sci. Technol.*, 53, 23, 13949-13958, 2019.

- Chung, M. Y., Lazaro, R. A., Lim, D., Jackson, J., Lyon, J., Rendulic, D., and Hasson, A. S.: Aerosol-borne quinones and reactive oxygen species generation by particulate matter extracts, *Environ. Sci. Technol.*, 40, 16, 4880-6, 2006.
- Claflin, M. S., Krechmer, J. E., Hu, W. W., et al.: Functional group composition of secondary organic aerosol formed from ozonolysis of alpha-pinene under high VOC and autoxidation conditions, *ACS Earth Space Chem.*, 2, 11, 1196-1210, doi:10.1021/acsearthspacechem.8b00117, 2018.
- Daellenbach, K. R., Kourtchev, I., Vogel, A. L., et al.: Impact of anthropogenic and biogenic sources on the seasonal variation in the molecular composition of urban organic aerosols: a field and laboratory study using ultra-high-resolution mass spectrometry, *Atmos. Chem. Phys.*, 19, 9, 5973-5991, doi: 10.5194/acp-19-5973-2019, 2019.
- Dall'Osto, M., Paglione, M., Decesari, S., Facchini, M. C., O'Dowd, C., Plass-Duellmer, C., and Harrison, R. M.: On the origin of AMS "cooking organic aerosol" at a rural site, *Environ. Sci. Technol.*, 49, 13964-13972, 10.1021/acs.est.5b02922, 2015.
- Decesari, S., Facchini, M. C., Matta, E., Lettini, F., Mircea, M., Fuzzi, S., Tagliavini, E., and Putaud J. P.: Chemical features and seasonal variation of fine aerosol water-soluble organic compounds in the Po Valley, Italy, *Atmos. Environ.*, 35, 3691-3699, 2001.
- Ding, X., Wang X. M., and Zheng, M.: The influence of temperature and aerosol acidity on biogenic secondary organic aerosol tracers: Observations at a rural site in the central Pearl River Delta region, South China, *Atmos. Environ.*, 45, 6, 1303-1311, 2011.
- Ding, X., Zhang, Y. Q., He, Q. F., et al.: Spatial and seasonal variations of secondary organic aerosol from terpenoids over China, *J. Geophys. Res. Atmos.*, 121, 24, 14, 661-614, 678, 2016.
- Ding, X., He, Q. F., Shen, R. Q., et al.: Spatial and seasonal variations of isoprene secondary organic aerosol in China: Significant impact of biomass burning during winter, *Sci. Rep.*, 6, 20411, 2016.
- Donahue, N.M., Robinson, A.L., Stanier, C.O., and Pandis, S.N.: Coupled partitioning, dilution, and chemical aging of semivolatile organics, *Environ. Sci. Technol.*, 40, 2635-2643, 2006.
- Edney, E. O., Kleindienst, T. E., Jaoui, M., et al.: Formation of 2-methyl tetrols and 2-methylglyceric acid in secondary organic aerosol from laboratory irradiated isoprene/NOX/SO2/air mixtures and their detection in ambient PM2.5 samples collected in the eastern United States, *Atmos. Environ.*, 39, 29, 5281-5289, 2005.
- Ehn, M., Kleist, E., Junninen, H., et al.: Gas phase formation of extremely oxidized pinene reaction products in chamber and ambient air, *Atmos. Chem. Phys.*, 12, 11, 5113-5127, 2012.
- Ehn, M., Thornton, J. A., Kleist, E., Sipilä, M., Junninen, H., Pullinen, I., Springer, M., Rubach, F., Tillmann, R., Lee, B., Lopez-Hilfiker, F., et al.: A large source of low-volatility secondary organic aerosol, *Nature*, 506, 479-479, 2014.
- Elser, M., Huang, R.-J., Wolf, R., Slowik, J. G., Wang, Q., Canonaco, F., Li, G., Bozzetti, C., Daellenbach, K. R., Huang, Y., Zhang, R., Li, Z., Cao, J., Baltensperger, U., El-Haddad, I., and Prévôt, A. S. H.: New insights into PM2.5 chemical composition and sources in two major cities in China during extreme haze events using aerosol mass spectrometry, *Atmos. Chem. Phys.*, 16, 3207-3225, 10.5194/acp-16-3207-2016, 2016.

- Fang, T., Zeng, L., Gao, D., Verma, V., Stefaniak, A. B., Rodney J., and Weber, R. J.: Ambient size distributions and lung deposition of aerosol dithiothreitol-measured oxidative potential: contrast between soluble and insoluble particles, *Environ. Sci. Technol.*, 51, 12, 6802–6811, 2017.
- Fang, T., Lakey, P. S. J., Weber, R. J., and Shiraiwa, M.: Oxidative potential of particulate matter and generation of reactive oxygen species in epithelial lining fluid, *Environ. Sci. Technol.*, 53, 12784–12792, 2019.
- Farmer, D. K., and Jimenez, J. L.: Real-time atmospheric chemistry field instrumentation, *Anal.Chem.*, 82, 10.1021/ac1010603, 2010.
- Feierman, D. E., Winston, G. W., and Cederbaum, A. I.: Ethanol oxidation by hydroxyl radicals: role of iron chelates, superoxide, and hydrogen peroxide, *Alcoholism: Clinical and Experimental Research*, 9, 2, 95-102, 1985.
- Fu, P., Chen, J., and Barrie, L. A.: Isoprene, monoterpene, and sesquiterpene oxidation products in the high arctic aerosols during late winter to early summer, *Environ. Sci. Technol.*, 43, 4022-4028, 2009.
- Fu, X., Wang, S., Chang, X., Cai, S., Xing, J., and Hao, J.: Modeling analysis of secondary inorganic aerosols over China: pollution characteristics, and meteorological and dust impacts, *Sci. Rep.*, 6, 35992, 10.1038/srep35992, 2016.
- Fuzzi, S., Baltensperger, U., Carslaw, K., Decesari, S., Denier van der Gon, H., Facchini, M. C., Fowler, D., Koren, I., Langford, B., Lohmann, U., Nemitz, E., Pandis, S., Riipinen, I., Rudich, Y., Schaap, M., Slowik, J. G., Spracklen, D. V., Vignati, E., Wild, M., Williams, M., and Gilardoni, S.: Particulate matter, air quality and climate: lessons learned and future needs. *Atmos. Chem. Phys.*, 15, 14, 8217-8299, 2015.
- George, J., Lim, J. S., Jang, S. J., Cun, Y., Ozretić, L., Kong, G., Leenders, F., Lu, X., Fernández-Cuesta, L., Bosco, G., Müller, C., Dahmen, I., Jahchan, N. S., Park, K., Yang, D., Karnezis, A. N., Vaka, D., Torres, A., Wang, M. S., Korbel, J. O., Menon, R., Chun, S., Kim, D., et al.: Comprehensive genomic profiles of small cell lung cancer, *Nature*, 524, 47-53, 2015.
- Glasius, M., Hansen, A. M. K., Claeys, M., et al.: Composition and sources of carbonaceous aerosols in Northern Europe during winter, *Atmos. Environ.*, 173, 127-141, doi:10.1016/j.atmosenv.2017.11.005, 2018.
- Glasius, M., Bering, M. S., Yee, L. D., et al.: Organosulfates in aerosols downwind of an urban region in central Amazon, *Environ. Sci. Proc. Imp.*, 20, 11, 1546-1558. doi:10.1039/c8em00413g, 2018.
- González, P. L., Corral, A. P., Aregahegn, K. Z., et al.: Heterogeneous photochemistry of imidazole-2-carboxaldehyde: HO₂ radical formation and aerosol growth, *Atmos. Chem. Phys.*, 16, 18, 11823-11836, 2016.
- Hallquist, M., Wenger, J. C., Baltensperger, U., Rudich, Y., Simpson, D., Claeys, M., Dommen, J., Donahue, N. M., George, C., Goldstein, A. H., Hamilton, J. F., Herrmann, H., Hoffmann, T., et al.: The formation, properties and impact of secondary organic aerosol: current and emerging issues, *Atmos. Chem. Phys.*, 9, 5155-5236, <https://doi.org/10.5194/acp-9-5155-2009>, 2009.

- Hasson, A. S., Orzechowska, G. E., and Paulson, S. E.: Production of stabilized Criegee intermediates and peroxides in the gas phase ozonolysis of alkenes: 1. Ethene, trans-2-butene, and 2,3-dimethyl-2-butene, *J. Geophys. Res.*, 106, 34143-34153, 2001.
- Hasson, A. S., and Paulson, S. E.: An investigation of the relationship between gas-phase and aerosol borne hydroperoxides in urban air, *J Aerosol Sci.*, 34, 4, 459-468, 2003.
- Heald, C. L., Jacob, D. J., Park, R. J., Russell, L. M., Huebert, B. J., Seinfeld, J. H., Liao, H., and Weber, R. J.: A large organic aerosol source in the free troposphere missing from current models, *Atmos. Sci.*, 32, L18809, 2005.
- Hems, R. F., Hsieh, J. S., Slodki, M. A., Zhou, S., and Abbatt, J. P. D.: Suppression of OH generation from the photo-Fenton reaction in the presence of α -pinene secondary organic aerosol material, *Environ. Sci. Technol. Lett.*, 4, 10, 439-443, 2017.
- Henze, D. K., and Seinfeld, J. H.: Global secondary organic aerosol from isoprene oxidation, *Geophys. Res. Lett.*, 33, 9, 2006.
- Hertkorn, N., Ruecker, C., Meringer, M., et al.: High-precision frequency measurements: indispensable tools at the core of the molecular-level analysis of complex systems, *Anal. Bioanal. Chem.*, 389, 5, 1311-1327, 2007.
- Hewitt, C. N., and Kok, G.: Formation and occurrence of organic hydroperoxides in the troposphere: laboratory and field observations, *J. Atmos. Chem.*, 12, 181-194, 1991.
- Ho, C. S., Lam, C. W. K., Chan, M. H. M., Cheung, R. C. K., Law, L. K., Suen, M. W. M., and Tai, H. L.: Electrospray ionisation mass spectrometry: principles and clinical application, *Clin. Biochem. Rev.*, 24, 10, 2003.
- Hockaday, W. C., Purcell, J. M., Marshall, A. G., Baldock, J. A., and Hatcher, P. G.: Electrospray and photoionization mass spectrometry for the characterization of organic matter in natural waters: a qualitative assessment, *Limnol. Oceanogr.: Methods*, 7, 81-95, 2009.
- Hoffer, A., Gelencsér, A., Guyon, P., Kiss, G., Schmid, O., Frank, G., Artaxo, P., and Andreae M.: Optical properties of humic-like substances (HULIS) in biomass-burning aerosols, *Atmosph. Chem. Phys.*, 6, 3563-3570, 2006.
- Hoffmann, T., Huang, R. J., and Kalberer, M.: Atmospheric analytical chemistry, *Anal. Chem.*, 83, 4649-4664, 10.1021/ac2010718, 2011.
- Huang, R. J., Zhang, Y., Bozzetti, C., Ho, K. F., Cao, J. J., Han, Y., Daellenbach, K. R., Slowik, J. G., Platt, S. M., Canonaco, F., Zotter, P., Wolf, R., Pieber, S. M., Bruns, E. A., Crippa, M., Ciarelli, G., Piazzalunga, A., Schwikowski, M., Abbaszade, G., Schnelle-Kreis, J., Zimmermann, R., An, Z., Szidat, S., Baltensperger, U., El Haddad, I., and Prevot, A. S.: High secondary aerosol contribution to particulate pollution during haze events in China, *Nature*, 514, 218-222, 10.1038/nature13774, 2014.
- Hughey, C. A., Hendrickson, C. L., Rodgers, R. P., and Marshall, A. G.: Kendrick mass defect spectrum: A compact visual analysis for ultrahigh-resolution broadband mass spectra, *Anal. Chem.*, 73, 4676-4681, 2001.

- Jaoui, M., Lewandowski, M., Kleindienst, T. E., Offenberg, J. H., and Edney, E. O.: β -caryophyllinic acid: An atmospheric tracer for β -caryophyllene secondary organic aerosol, *Geophys. Res. Lett.*, 34, 5, 2007.
- Ji, Y., Zhao, J., Terazono, H., et al.: Reassessing the atmospheric oxidation mechanism of toluene, *PNAS*, 114, 8169–8174, doi:10.1073/pnas.1705463114, 2017.
- Jimenez, J. L., Canagaratna, M. R., Donahue, N. M., Prevot, A. S. H., Zhang, Q., Kroll, J. H., DeCarlo, P. F., Allan, J. D., Coe, H., Ng, N. L., Aiken, A. C., Docherty, K. S., Ulbrich, I. M., et al.: Evolution of organic aerosols in the atmosphere, *Science*, 326, 1525-1529, 10.1126/science.1180353, 2009.
- Jiang, B., Liang, Y., Xu, C., Zhang, J., Hu, M., and Shi, Q.: Polycyclic aromatic hydrocarbons (PAHs) in ambient aerosols from Beijing: characterization of low volatile PAHs by positive-ion atmospheric pressure photoionization (APPI) coupled with Fourier transform ion cyclotron resonance, *Environ. Sci. Technol.*, 48, 4716-4723, 10.1021/es405295p, 2014.
- Jiang, B., Kuang, B. Y., Liang, Y., Zhang, J., Huang, X. H. H., Xu, C., Yu, J. Z., and Shi, Q.: Molecular composition of urban organic aerosols on clear and hazy days in Beijing: a comparative study using FT-ICR MS, *Environ. Chem.*, 13, 888, 10.1071/en15230, 2016.
- Kautzman, K. E., Surratt, J. D., Chan, M. N., Chan, A. W., Hersey, S. P., Chhabra, P. S., Dalleska, N. F., Wennberg, P. O., Flagan, R. C., and Seinfeld, J. H.: Chemical composition of gas- and aerosol-phase products from photooxidation of naphthalene, *J. Phys. Chem. A*, 114, 913-934, 10.1021/jp908530s, 2010.
- Kendrick, E.: A mass scale based on $\text{CH}_2=14.0000$ for high resolution mass spectrometry of organic compounds, *Anal. Chem.*, 35, 2146-2154, 1963.
- Kenneth, S., Docherty, W. W., Yong, B. L., and Paul, J. Z.: Contributions of organic peroxides to secondary aerosol formed from reactions of monoterpenes with O_3 , *Environ. Sci. Technol.*, 39, 4049-4059, 2005.
- Kim, S., Kramer, R. W., and Hatcher, P. G.: Graphical method for analysis of ultrahigh-resolution broadband mass spectra of natural organic matter, the Van Krevelen diagram, *Anal. Chem.*, 75, 20, 5336-5344, 2003.
- Koch, B. P., and Dittmar, T.: From mass to structure: an aromaticity index for high-resolution mass data of natural organic matter, *Rapid Commun. Mass Spectrom.*, 20, 926-932, <https://doi.org/10.1002/rcm.2386>, 2006.
- Kok, T. M.C.M, Driese, H. A. L., Hogervorst, J. G. F., and Briede, J. J.: Toxicological assessment of ambient and traffic-related particulate matter: A review of recent studies, *ScienceDirect*, 613, 103-122, 2006.
- Kourtchev, I., Fuller, S., Aalto, J., Ruuskanen, T. M., McLeod, M. W., Maenhaut, W., Jones, R., Kulmala, M., and Kalberer, M.: Molecular composition of boreal forest aerosol from Hyytiälä, Finland, using ultrahigh resolution mass spectrometry, *Environ. Sci. Technol.*, 47, 9, 4069-4079, 2013
- Kourtchev, I., O'Connor, I. P., Giorio, C., Fuller, S. J., Kristensen, K., Maenhaut, W., Wenger, J. C., Sodeau, J. R., Glasius, M., and Kalberer, M.: Effects of anthropogenic emissions on the molecular composition of urban organic aerosols: An ultrahigh resolution mass spectrometry study, *Atmo. Environ.*, 89, 525-532, 10.1016/j.atmosenv.2014.02.051, 2014.

- Kourtchev, I., Doussin, J. F., Giorio, C., Mahon, B., Wilson, E. M., Maurin, N., Pangui, E., Venables, D. S., Wenger, J. C., and Kalberer, M.: Molecular composition of fresh and aged secondary organic aerosol from a mixture of biogenic volatile compounds: a high-resolution mass spectrometry study, *Atmos. Chem. Phys.*, 15, 5683-5695, 10.5194/acp-15-5683-2015, 2015.
- Kourtchev, I., Godoi, R. H. M., Connors, S., Levine, J. G., Archibald, A. T., Godoi, A. F. L., Paralovo, S. L., Barbosa, C. G. G., Souza, R. A. F., Manzi, A. O., Seco, R., Sjostedt, S., Park, J.-H., Guenther, A., Kim, S., Smith, J., Martin, S. T., and Kalberer, M.: Molecular composition of organic aerosols in central Amazonia: an ultra-high-resolution mass spectrometry study, *Atmos. Chem. Phys.*, 16, 11899-11913, <https://doi.org/10.5194/acp-16-11899-2016>, 2016.
- Kramer, A. J., Rattanavaraha, W., Zhang, Z., Gold, A., Surratt, J. D., and Lin, Y. H.: Assessing the oxidative potential of isoprene-derived epoxides and secondary organic aerosol, *Atmos. Environ.*, 130, 211-218, 2016.
- Kristensen, K., Cui, T., Zhang, H., Gold, A., Glasius, M., and Surratt, J. D.: Dimers in α -pinene secondary organic aerosol: effect of hydroxyl radical, ozone, relative humidity and aerosol acidity, *Atmos. Chem. Phys.*, 14, 8, 4201-4218, 2014.
- Kroll, J. H., Donahue, N. M., Jimenez, J. L., Kessler, S. H., Canagaratna, M. R., Wilson, K. R., Altieri, K. E., Mazzoleni, L. R., Wozniak, A. S., Bluhm, H., Mysak, E. R., Smith, J. D., Kolb, C. E., and Worsnop, D. R.: Carbon oxidation state as a metric for describing the chemistry of atmospheric organic aerosol, *Nat. Chem.*, 3, 133-139, 10.1038/nchem.948, 2011.
- Kuang, X. B.: Formation of reactive oxygen species by ambient particulate matter: probing causative agents, Ph. D. thesis, University of California, Los Angeles, 2017.
- Kurten, T., Tiusanen, K., Roldin, P., et al.: alpha-Pinene autoxidation products may not have extremely low saturation vapor pressures despite high O:C ratios, *J. Phys. Chem. A*, 120, 16, 2569-2582, 2016.
- LaCagnin, L. B., Bowman, L., Ma, J. Y. C., and Miles, P. R.: Metabolic changes in alveolar 14 type II cells after exposure to hydrogen peroxide, *Am J Physiol*, 259, L57-L65, 1990.
- Lakey, P. S., Berkemeier, T., Tong, H., Arangio, A. M., Lucas, K., Poschl, U., and Shiraiwa, M.: Chemical exposure-response relationship between air pollutants and reactive oxygen species in the human respiratory tract, *Sci. Rep.*, 6, 32916, 2016.
- Laskin, A., Smith, J. S., and Laskin, J.: Molecular characterization of nitrogen-containing organic compounds in biomass burning aerosols using high-resolution mass spectrometry, *Environ. Sci. Technol.*, 43, 3764-3771, 2009.
- Laskin, J., Laskin, A., Roach, P. J., Slysz, G. W., Anderson, G. A., Nizkorodov, S. A., Bones, D. L., and Nguyen, L. Q.: High-resolution desorption electrospray ionization mass spectrometry for chemical characterization of organic aerosols, *Anal. Chem.*, 82, 2048-2058, 10.1021/ac902801f, 2010.
- Laskin, A., Laskin, J., and Nizkorodov, S. A.: Chemistry of atmospheric brown carbon, *Chem. Rev.*, 115, 4335-4382, 10.1021/cr5006167, 2015.
- Laskin, J., Laskin, A., and Nizkorodov, S. A.: Mass spectrometry analysis in atmospheric chemistry, *Anal. Chem.*, 90, 166-189, 10.1021/acs.analchem.7b04249, 2018.

- Lee, A., Goldstein, A. H., Kroll, J. H., Ng, N. L., Varutbangkul, V., Flagan, R. C., and Seinfeld, J. H.: Gas-phase products and secondary aerosol yields from the photooxidation of 16 different terpenes, *J. Geophys. Res.*, 111, 10.1029/2006jd007050, 2006.
- Lee, T., Choi, J., Lee, G., Ahn, J., Park, J. S., Atwood, S. A., Schurman, M., Choi, Y., Chung, Y., and Collett, J. L.: Characterization of aerosol composition, concentrations, and sources at Baengnyeong Island, Korea using an aerosol mass spectrometer, *Atmos. Environ.*, 120, 297-306, 10.1016/j.atmosenv.2015.08.038, 2015.
- Lelieveld, J., Evans, J. S., Fnais, M., Giannadaki, D., and Pozzer, A.: The contribution of outdoor air pollution sources to premature mortality on a global scale, *Nature*, 525, 367-371, 10.1038/nature15371, 2015.
- Limbeck, A., Handler, M., Neuberger, B., Klatzer, B., and Puxbaum H.: Carbon-specific analysis of humic-like substances in atmospheric aerosol and precipitation samples, *Anal. Chem.*, 77, 7288-7293, 2005.
- Lin, M., and Yu, J. Z.: Assessment of interactions between transition metals and atmospheric organics: ascorbic acid depletion and hydroxyl radical formation in organic-metal mixtures, *Environ. Sci. Technol.*, 54, 3, 1431-1442, 2020.
- Lin, P., and Yu, J. Z.: Generation of reactive oxygen species mediated by humic-like substances in atmospheric aerosols, *Environ. Sci. Technol.*, 45:10362-10368, 2011.
- Lin, P., Rincon, A. G., Kalberer, M., and Yu, J. Z.: Elemental composition of HULIS in the Pearl River Delta Region, China: results inferred from positive and negative electrospray high resolution mass spectrometric data, *Environ. Sci. Technol.*, 46, 7454-7462, 10.1021/es300285d, 2012a.
- Lin, P., Yu, J. Z., Engling, G., and Kalberer, M.: Organosulfates in humic-like substance fraction isolated from aerosols at seven locations in East Asia: a study by ultra-high-resolution mass spectrometry, *Environ. Sci. Technol.*, 46, 13118-13127, 10.1021/es303570v, 2012b.
- Lin, P., Laskin, J., Nizkorodov, S. A., and Laskin, A.: Revealing brown carbon chromophores produced in reactions of methylglyoxal with ammonium sulfate, *Environ. Sci. Technol.*, 49, 14257-14266, 10.1021/acs.est.5b03608, 2015.
- Ma, Y., Cheng, Y., Qiu, X., Cao, G., Fang, Y., Wang, J., Zhu, T., Yu, J., and Hu, D.: Sources and oxidative potential of water-soluble humic-like substances (HULISWS) in fine particulate matter (PM_{2.5}) in Beijing, *Atmos. Chem. Phys.*, 18, 5607-5617, 2018.
- Makarov A.: Electrostatic axially harmonic Orbital trapping: a high-performance technique of mass analysis, *Anal. Chem.*, 72, 6, 1156-1162, <https://doi.org/10.1021/ac991131p>, 2000.
- Martinsson, J., Monteil, G., Sporre, M. K., Kaldal Hansen, A. M., Kristensson, A., Eriksson Stenström, K., Swietlicki, E., and Glasius, M.: Exploring sources of biogenic secondary organic aerosol compounds using chemical analysis and the FLEXPART model, *Atmos. Chem. Phys.*, 17, 11025-11040, <https://doi.org/10.5194/acp-17-11025-2017>, 2017.
- Matthew, P., and Fraser, K. L.: Using levoglucosan as a molecular marker for the long-range transport of biomass combustion aerosols, *Environ. Sci. Technol.*, 34, 4560-4564, 2000.

- Mazzoleni, L. R., Ehrmann, B. M., Sheng, X. H., Marshall, A. G., and Collett, J. L.: Water-soluble atmospheric organic matter in fog exact masses and chemical formula identification by ultrahigh-resolution fourier transform ion cyclotron resonance mass spectrometry, *Environ. Sci. Technol.*, 44, 8, 2010.
- McLafferty, F. W., and Turecek, F.: Interpretation of mass spectra, Fourth edition, University Science Books, Mill Valley, California, 1993.
- Mentel, T. F., Springer, M., Ehn, M., Kleist, E., Pullinen, I., Kurtén, T., Rissanen, M., Wahner, A., and Wildt, J.: Formation of highly oxidized multifunctional compounds: autoxidation of peroxy radicals formed in the ozonolysis of alkenes – deduced from structure–product relationships, *Atmos. Chem. Phys.*, 15, 6745-6765, 10.5194/acp-15-6745-2015, 2015.
- Mukai, H., and Ambe, Y.: Characterization of a humic acid-like brown substance in airborne particulate matter and tentative identification of its origin, *Atmos. Environ.*, 20, 813-819, 1986.
- Müller, L., Reinnig, M. C., Naumann, K. H., Saathoff, H., Mentel, T. F., Donahue, N. M., and Hoffmann, T.: Formation of 3-methyl-1,2,3-butanetricarboxylic acid via gas phase oxidation of pinonic acid – a mass spectrometric study of SOA aging, *Atmos. Chem. Phys.*, 12, 3, 1483-1496, 2012.
- Müller-Tautges, C.: Development and application of mass-spectrometric methods for the quantification and characterization of organic compounds in ice cores, Ph. D. thesis, University of Mainz, Germany, 2014.
- Mutzel, A., Poulain, L., Berndt, T., Iinuma, Y., Rodigast, M., Boge, O., Richters, S., Spindler, G., Sipila, M., Jokinen, T., Kulmala, M., and Herrmann, H.: Highly oxidized multifunctional organic compounds observed in tropospheric particles: A field and laboratory study, *Environ. Sci. Technol.*, 49, 13, 7754-61, 2015.
- Myoseon, Jang SRM.: Products of benz[a]anthracene photodegradation in the presence of known organic constituents of atmospheric aerosols, *Environ. Sci. Technol.*, 31, 1046-1053, 1997.
- Nguyen, Q. T., Christensen, M. K., Cozzi, F., Zare, A., Hansen, A. M. K., Kristensen, K., Tulinius, T. E., Madsen, H. H., Christensen, J. H., Brandt, J., Massling, A., Noejaard, J. K., and Glasius, M.: Understanding the anthropogenic influence on formation of biogenic secondary organic aerosols in Denmark via analysis of organosulfates and related oxidation products, *Atmos. Chem. Phys.*, 14, 8961-8981, 8921 pp., <https://doi.org/10.5194/acp-14-8961-2014>, 2014.
- Nizkorodov, S. A., Laskin, J., and Laskin, A.: Molecular chemistry of organic aerosols through the application of high resolution mass spectrometry, *Phys. Chem. Chem. Phys.*, 13, 3612-3629, 10.1039/c0cp02032j, 2011.
- Nozière, B., Kalberer, M., Claeys, M., Allan, J., D'Anna, B., Decesari, S., Finessi, E., Glasius, M., Grgic, I., Hamilton, J. F., Hoffmann, T., Iinuma, Y., Jaoui, M., Kahnt, A., Kampf, C. J., Kourtchev, I., Maenhaut, W., Marsden, N., Saarikoski, S., Schnelle-Kreis, J., Surratt, J. D., Szidat, S., Szmigielski, R., and Wisthaler, A.: The molecular identification of organic compounds in the atmosphere: state of the art and challenges, *Chem. Rev.*, 115, 3919-3983, 10.1021/cr5003485, 2015.

- Odum, J. R., Hoffmann, T., Bowman, F., Collins, D., Flagan, R. C., and Seinfeld, J. H.: Gas/particle partitioning and secondary organic aerosol yields, *Environ. Sci. Technol.*, 30, 8, 2580–2585, 1996.
- Pankow, J. F.: An absorption model of gas/particle partitioning of organic compounds in the atmosphere, *Atmos. Environ.*, 28, 185–188, 1994a.
- Pankow, J. F.: An absorption model of the gas/aerosol partitioning involved in the formation of secondary organic aerosol, *Atmos. Environ.*, 28, 189–193, 1994b.
- Pathak, R. K., Presto, A. A., Lane, T. E., Stanier, C. O., Donahue, N. M., and Pandis, S. N.: Ozonolysis of α -pinene: parameterization of secondary organic aerosol mass fraction, *Atmos. Chem. Phys.*, 7, 3811–3821, doi:10.5194/acp-7-3811-2007, 2007.
- Paulot, F., Crounse, J. D., Kjaergaard, H. G., et al.: Unexpected epoxide formation in the gas-phase photooxidation of isoprene, *Science*, 325, 730–733, doi:10.1126/science.1172910, 2009.
- Pecha, M. B.: Understanding and controlling lignocellulosic pyrolysis for the production of renewable fuel and chemical precursors. PhD thesis, Washington State University. USA. 2017.
- Pope, C. A., Burnett, R. T., Thun, M. J., Calle, E. E., Krewski, D., PhD; Ito, K., and Thurston, G. D.: Lung cancer, cardiopulmonary mortality, and long-term exposure to fine particulate air pollution, *JAMA Network*, 287, 9, 1132–1141, doi:10.1001/jama.287.9.1132, 2002.
- Pope, C. A., and Dockery, D. W.: Health effects of fine particulate air pollution: lines that connect, *Journal of the Air & Waste Management Association*, <https://doi.org/10.1080/10473289.2006.10464485>, 2006
- Pöschl, U.: Atmospheric aerosols: composition, transformation, climate and health effects, *Angew. Chem. Int. Ed.*, 44, 7520–7540, 10.1002/anie.200501122, 2005.
- Pöschl, U., and Shiraiwa, M.: Multiphase chemistry at the atmosphere-biosphere interface influencing climate and public health in the anthropocene, *Chem. Rev.*, 115, 4440–4475, 10.1021/cr500487s, 2015.
- Pratt, K. A., and Prather, K. A.: Mass spectrometry of atmospheric aerosols--recent developments and applications. Part II: On-line mass spectrometry techniques, *Mass Spectrom. Rev.*, 31, 17–48, 10.1002/mas.20330, 2012.
- Pratt, K.A., and Prather, K.A.: Mass spectrometry of atmospheric aerosols--recent developments and applications. Part I. Off-line mass spectrometry techniques, *Mass spectrom. rev.*, 31, 1–16, 2012a.
- Pratt, K.A., and Prather, K.A.: Mass spectrometry of atmospheric aerosols--recent developments and applications. Part II. On-line mass spectrometry techniques, *Mass spectrom. rev.*, 31, 17–48, 2012b.
- Presto, A. A. and Donahue, N. M.: Investigation of alpha-pinene plus ozone secondary organic aerosol formation at low total aerosol mass, *Environ. Sci. Technol.*, 40, 3536–3543, 2006.
- Ramdahl, T.: Retene—a molecular marker of wood combustion in ambient air, *Nature*, 306, 8, 1983.

- Rincón, A. G., Calvo, A. I., Dietzel, M., and Kalberer, M.: Seasonal differences of urban organic aerosol composition - an ultra-high resolution mass spectrometry study, *Environ. Chem.*, 9, 298, 10.1071/en12016, 2012.
- Roach, P. J., Laskin, J., and Laskin, A.: Molecular Characterization of Organic Aerosols Using Nanospray-Desorption/Electrospray Ionization-Mass spectrometry, *Anal. Chem.*, 82, 7979-7986, 10.1029/2007jd008683, 2010.
- Rudich, Y., Donahue, N. M., and Mentel, T. F.: Aging of organic aerosol: bridging the gap between laboratory and field studies, *Annu. Rev. Phys. Chem.*, 58, 321-352, 2007.
- Sakulyanontvittaya, T., Helmig, D., Milford, J., and Wiedinmyer, C.: Secondary organic aerosol from sesquiterpene and monoterpene emissions in the United States, *Environ. Sci Technol.*, 42, 8784-8790, 2008.
- Scigelova, M., and Makarov, A.: Orbitrap mass analyzer--overview and applications in proteomics, *Proteomics*, 6 Suppl 2, 16-21, 10.1002/pmic.200600528, 2006.
- Schwöbel, J. A. H., Koleva, Y. K., Enoch, S. J., et al.: Measurement and estimation of electrophilic reactivity for predictive toxicology, *Chem. Rev.*, 111, 2562-2596, doi:10.1021/cr100098n, 2011.
- Seinfeld, J. H., and Pankow, J. F.: Organic atmospheric particulate material, *Annual review of physical chemistry*, 54, 121-140, 10.1146/annurev.physchem.54.011002.103756, 2003.
- Seinfeld, J. H., and Pandis, S. N.: *Atmospheric chemistry and physics: From air pollution to climate change*, 2nd., J. Wiley, Hoboken, N.J, xxviii., 1203, 2006.
- Shen, H., Barakat, A. I., and Anastasio, C.: Generation of hydrogen peroxide from San Joaquin Valley particles in a cell-free solution, *Atmos. Chem. Phys.*, 11, 2, 753-765, 2011.
- Shen, R. Q., Ding, X., He, Q. F., Cong, Z. Y., Yu, Q. Q., and Wang, X. M.: Seasonal variation of secondary organic aerosol tracers in Central Tibetan Plateau, *Atmos. Chem. Phys.*, 15, 15, 8781-8793, 2015.
- Shrivastava, M., Andreae, M. O., Artaxo, P., et al.: Urban pollution greatly enhances formation of natural aerosols over the Amazon rainforest, *Nature Comm.*, 10, 1046, doi: 10.1038/s41467-019-08909-4, 2019.
- Simoneit, B. R. T., Rushdi, A. I., Bin Abas, M. R., and Didyk, B. M.: Alky Amides and Nitriles as Novel Traces for Biomass Burning, *Environ. Sci. Technol.*, 37, 16-21, 2003.
- Sleighter, R. L., and Hatcher, P. G.: The application of electrospray ionization coupled to ultrahigh resolution mass spectrometry for the molecular characterization of natural organic matter, *J. Mass Spectrom.*, 42, 5, 559-574, 2007.
- Song, J., Li, M., Jiang, B., Wei, S., Fan, X., and Peng, P.: Molecular characterization of water-soluble humic like substances in smoke particles emitted from combustion of biomass materials and coal using ultrahigh-resolution electrospray ionization fourier transform ion cyclotron resonance mass spectrometry, *Environ. Sci. Technol.*, 52, 2575-2585, 10.1021/acs.est.7b06126, 2018.
- Stock, N. L.: Introducing graduate students to high-resolution mass spectrometry (HRMS) using a hands-on approach, *J. Chem. Educ.*, 94, 1978-1982, 10.1021/acs.jchemed.7b00569, 2017.

- Sun, Y. L., Zhang, Q., Anastasio, C., and Sun, J.: Insights into secondary organic aerosol formed via aqueous-phase reactions of phenolic compounds based on high resolution mass spectrometry, *Atmos. Chem. Phys.*, 10, 10, 4809-4822, 2010.
- Surratt, J. D., Gómez-González, Y., Chan, A. W., Vermeylen, R., Shahgholi, M., Kleindienst, T. E., Edney, E. O., Offenberg, J. H., Lewandowski, M., Jaoui, M., Maenhaut, W., Claeys, M., Flagan, R. C., and Seinfeld, J. H.: Organosulfate formation in biogenic secondary organic aerosol, *J. Phys. Chem. A*, 112, 34, 2008.
- Surratt, J. D., Chan, A. W., Eddingsaas, N. C., et al.: Reactive intermediates revealed in secondary organic aerosol formation from isoprene, *PNAS*, 107, 15, 6640-6645, 2010.
- T., R., THESe, A., Venkatachari, P., Xia, X. Y., Hopke, P. K., Springer, A., and Linscheid, M.: Identification of fulvic acids and sulfated and nitrated analogues in atmospheric aerosol by electrospray ionization fourier transform ion cyclotron resonance mass spectrometry, *Anal. Chem.*, 78, 8299-8304, 2006.
- Tao, S., Lu, X., Levac, N., Bateman, A. P., Nguyen, T. B., Bones, D. L., Nizkorodov, S. A., Laskin, J., Laskin, A., and Yang, X.: Molecular characterization of organosulfates in organic aerosols from Shanghai and Los Angeles urban areas by nanospray-desorption electrospray ionization high-resolution mass spectrometry, *Environ. Sci. Technol.*, 48, 10993-11001, 10.1021/es5024674, 2014.
- Tong, H., Arangio, A. M., Lakey, P. S. J., et al.: Hydroxyl radicals from secondary organic aerosol decomposition in water, *Atmos. Chem. Physics.*, 16, 3, 1761-1771, 2016.
- Tong, H., Lakey, P. S. J., Arangio, A. M., Socorro, J., Shen, F., Lucas, K., Brune, W. H., Poschl, U., and Shiraiwa, M.: Reactive oxygen species formed by secondary organic aerosols in water and surrogate lung fluid, *Environ. Sci. Technol.*, 52, (20), 11642-11651, 2018.
- Tong H. J., Zhang. Y., Filippi A., Wang T., Li C. P., Liu F. B., Leppla D., Kourtchev I., Wang K., Keskinen H. K., Levula J. T., Arangio A. M., et al.: Radical formation by fine particulate matter associated with highly oxygenated molecules, *Environ. Sci. Technol.*, 53, 21, 12506-12518, 2019.
- Tu, P., Hall, W. A. t., and Johnston, M. V.: Characterization of highly oxidized molecules in fresh and aged biogenic secondary organic aerosol, *Anal. Chem.*, 88, 4495-4501, 10.1021/acs.analchem.6b00378, 2016.
- Utieyin, O. O.: Advanced oxidation process using ozone/heterogeneous catalysis for the degradation of phenolic compounds (chlorophenols) in aqueous system, PhD thesis, Cape Peninsula University of Technology, South Africa, 2016.
- Valavanidis, A., Fiotakis, K., Bakeas, E., and Vlahogianni, T.: Electron paramagnetic resonance study of the generation of reactive oxygen species catalysed by transition metals and quinoid redox cycling by inhalable ambient particulate matter, *Redox Report*, 10, 37-51, 2005.
- Venkatachari, P., and Hopke, P. K.: Characterization of products formed in the reaction of ozone with alpha-pinene: case for organic peroxides. *J Environ. Monitor., JEM*, 10, 8, 966-74, 2008.
- Verma, V., Wang, Y., El-Afifi, R., Fang, T., Rowland, J., Russell, A. G., and Weber, R. J.: Fractionating ambient humic-like substances (HULIS) for their reactive oxygen species activity – Assessing the importance of quinones and atmospheric aging, *Atmos. Environ.*,

- 120, 351-359, 2015.
- Vogel, A. L., Äijälä, M., Brüggemann, M., Ehn, M., Junninen, H., Petäjä, T., Worsnop, D. R., Kulmala, M., Williams, J., and Hoffmann, T.: Online atmospheric pressure chemical ionization ion trap mass spectrometry (APCI-IT-MSn) for measuring organic acids in concentrated bulk aerosol – a laboratory and field study, *Atmos. Meas. Tech.* 6(2):431–443. doi: 10.5194/amt-6-431-2013, 2013.
- Vogel, A.: Complementary mass spectrometric techniques for the characterization of the organic fraction in atmospheric aerosols, Ph. D. thesis, Max Planck Graduate Center, University of Mainz, Germany, 2014.
- Vogel, A. L., Schneider, J., Müller-Tautges, C., Klimach, T., and Hoffmann, T.: Aerosol chemistry resolved by mass spectrometry: Insights into particle growth after ambient new particle formation, *Environ. Sci. Technol.*, 50, 20, 10814-10822, 2016.
- Wang, Y., Arellanes, C., Curtis, D. B., and Paulson, S. E.: Probing the source of hydrogen peroxide associated with coarse mode aerosol particles in southern California, *Environ. Sci. Technol.*, 44, 11, 4070-5, 2010.
- Wang, Y., Kim, H., and Paulson, S. E.: Hydrogen peroxide generation from α - and β -pinene and toluene secondary organic aerosols, *Atmos. Environ.*, 45, (18), 3149-3156, 2011.
- Wang, Y., Arellanes, C., and Paulson, S. E.: Hydrogen peroxide associated with ambient fine-mode, diesel, and biodiesel aerosol particles in Southern California, *Aerosol Sci. and Technol.*, 46, 4, 394-402, 2012.
- Wang, K.: Chemical characterization of organic aerosol from Chinese cities using high resolution mass spectrometry, Ph. D. thesis, Max Planck Graduate Center, University of Mainz, Germany, 2018.
- Wang, K., Zhang, Y., Huang, R.-J., Cao, J., and Hoffmann, T.: UHPLC-Orbitrap mass spectrometric characterization of organic aerosol from a central European city (Mainz, Germany) and a Chinese megacity (Beijing), *Atmos. Environ.*, 189, 22-29, 10.1016/j.atmosenv.2018.06.036, 2018.
- Wang, K., Zhang, Y., Huang, R. J., Wang, M., Ni, H. Y., Kampf, C., Cheng, Y. F., Bilde, M., Glasius, M., and Hoffmann T.: Molecular characterization and source identification of atmospheric particulate organosulfates using ultrahigh resolution mass spectrometry, *Environ. Sci. Technol.*, 53, 11, 6192-6202, 2019.
- Wang K., Huang, R. J., Brüggemann M., Zhang, Y., Yang L., Ni H. Y., Guo J., Han J. J., Bilde M., Glasius M., and Hoffmann T.: Urban organic aerosol composition in Eastern China differs from North to South: Molecular insight from a liquid chromatography-Orbitrap mass spectrometry study, *Atmos. Chem. Phys. Discuss.*, doi.org/10.5194/acp-2019-908, 2020.
- Wang, S., Riva, M., Yan, C., Ehn, M., and Wang, L.: Primary formation of highly oxidized multifunctional products in the OH-initiated oxidation of isoprene. A combined theoretical and experimental study, *Environ. Sci. Technol.*, 52, 21, 12255-12264, doi: 10.1021/acs.est.8b02783, 2018.
- Wang, S., Ye, J., Soong, R., Wu, B., Yu, L., Simpson, A. J., and Chan, A. W. H.: Relationship between chemical composition and oxidative potential of secondary organic aerosol from polycyclic aromatic hydrocarbons, *Atmos. Chem. Phys.*, 18, 6, 3987-4003, 2018.

- Wang, S., Wu, R., Berndt, T., Ehn, M., and Wang, L.: Formation of highly oxidized radicals and multifunctional products from the atmospheric oxidation of alkylbenzenes, *Environ. Sci. Technol.*, 51, 15, 8442-8449, 2017.
- Wang, X., and Schrader, W.: Selective analysis of sulfur-containing species in a heavy crude oil by deuterium labeling reactions and ultrahigh resolution mass spectrometry, *Int. J. Mol. Sci.*, 16, 30133-30143, 10.3390/ijms161226205, 2015.
- Wang, X. K., Rossignol, S., Ma, Y., Yao, L., Wang, M. Y., Chen, J. M., George, C., and Wang, L.: Molecular characterization of atmospheric particulate organosulfates in three megacities at the middle and lower reaches of the Yangtze River, *Atmos. Chem. Phys.*, 16, 2285-2298, <https://doi.org/10.5194/acp-16-2285-2016>, 2016.
- Wang, X. K., Hayeck, N., Brüggemann, M., Yao, L., Chen, H. F., Zhang, C., Emmelin, C., Chen, J. M., George, C., and Wang, L.: Chemical characterization of organic aerosol in: A study by ultrahigh-performance liquid chromatography coupled with orbitrap mass spectrometry, *J. Geophys. Res.-Atmos.*, doi.org/10.1002/2017JD026930, 2017.
- Yee, L. D., Isaacman-VanWertz, G., Wernis, R. A., et al.: Observations of sesquiterpenes and their oxidation products in central Amazonia during the wet and dry seasons, *Atmos. Chem. Phys.*, 18(14), 10433-10457, [doi: 10.5194/acp-18-10433-2018](https://doi.org/10.5194/acp-18-10433-2018), 2018.
- Yee, L. D., Isaacman-VanWertz, G., Wernis, R. A., et al.: Natural and anthropogenically influenced isoprene oxidation in southeastern United States and central Amazon, *Environ. Sci. Technol.*, 54, 10, 5980-5991, [doi: 10.1021/acs.est.0c00805](https://doi.org/10.1021/acs.est.0c00805), 2020.
- Yassine, M. M., Harir, M., Dabek-Zlotorzynska, E., and Schmitt-Kopplin, P.: Structural characterization of organic aerosol using Fourier transform ion cyclotron resonance mass spectrometry: aromaticity equivalent approach, *Rapid Commun. Mass Sp.*, 28, 2445-2454, [10.1002/rcm.7038](https://doi.org/10.1002/rcm.7038), 2014.
- Yasmeen, F., Vermeylen, R., Maurin, N., Perraudin, E., Doussin, J. F., and Claeys, M.: Characterisation of tracers for aging of α -pinene secondary organic aerosol using liquid chromatography/negative ion electrospray ionisation mass spectrometry, *Environ. Chem.*, 9, 3, 236, 2012.
- Yu, L., Smith, J., Laskin, A., Anastasio, C., Laskin, J., and Zhang, Q.: Chemical characterization of SOA formed from aqueous-phase reactions of phenols with the triplet excited state of carbonyl and hydroxyl radical, *Atmos. Chem. Phys.*, 14, 24, 13801-13816, 2014.
- Zappoli, S., Andracchio, A., Fuzzi, S., Facchini, M., Gelencser, A., Kiss, G., Krivacsy, Z., Molnar, A., Meszaros, E., and Hansson H. C.: Inorganic, organic and macromolecular components of fine aerosol in different areas of Europe in relation to their water solubility, *Atmos. Environ.*, 33, 2733-2743, 1999.
- Zhang, J. K., Cheng, M. T., Ji, D. S., Liu, Z. R., Hu, B., Sun, Y., and Wang, Y. S.: Characterization of submicron particles during biomass burning and coal combustion periods in Beijing, China, *Sci Total Environ*, 562, 812-821, [10.1016/j.scitotenv.2016.04.015](https://doi.org/10.1016/j.scitotenv.2016.04.015), 2016.
- Zhang, R., Jing, J., Tao, J., Hsu, S. C., Wang, G., Cao, J., Lee, C. S. L., Zhu, L., Chen, Z., Zhao, Y., and Shen, Z.: Chemical characterization and source apportionment of PM_{2.5} in Beijing: seasonal perspective, *Atmos. Chem. Phys.*, 13, 7053-7074, [10.5194/acp-13-7053-2013](https://doi.org/10.5194/acp-13-7053-2013), 2013.

- Zhang, R. C. M., Huang, D. D., Dalleska, N. F., et al.: Formation and evolution of molecular products in α -pinene secondary organic aerosol, *PNAS*, 112, 46 2015.
- Zhang, T., Claeys, M., Cachier, H., Dong, S., Wang, W., Maenhaut, W., and Liu, X.: Identification and estimation of the biomass burning contribution to Beijing aerosol using levoglucosan as a molecular marker, *Atmos. Environ.*, 42, 7013-7021, 10.1016/j.atmosenv.2008.04.050, 2008.
- Zhang, X., McVay, R. C., Huang, D. D., Dalleska, N. F., Aumont, B., Flagan, R. C., and Seinfeld, J. H.: Formation and evolution of molecular products in α -pinene secondary organic aerosol, *PNAS*, 112, 14168–14173, 2015.
- Ziemann, P. J., and Atkinson, R.: Kinetics, products, and mechanisms of secondary organic aerosol formation, *Chem. Soc. Rev.*, 41, 6582–6605, doi:10.1039/c2cs35122f, 2012.
- Zimniak, P.: Relationship of electrophilic stress to aging, *Free Radic. Biol. Med.*, 51, 1087–1105, doi:10.1016/j.freeradbiomed.2011.05.039, 2011.
- Zhu, W., Luo, L., Cheng, Z., Yan, N., Lou, S., and Ma, Y.: Characteristics and contributions of biogenic secondary organic aerosol tracers to PM 2.5 in Shanghai, China, *Atmos. Pollut. Res.*, 9, 2, 179-188, 2018.
- Zubarev, R. A., and Makarov, A.: Orbitrap Mass Spectrometry, *Anal. Chem.*, 85, 5288-5296, 10.1021/ac4001223, 2013.
- Zuth, C.: Organic trace analysis using high resolution mass spectrometry for the characterization of ancient, present and simulated atmospheric systems, Ph. D. thesis, University of Mainz, Germany, 2018.
- Zuth, C., Vogel, A. L., Ockenfeld, S., Huesmann, R., and Hoffmann, T.: Ultrahigh-resolution mass spectrometry in real time: atmospheric pressure chemical ionization Orbitrap mass spectrometry of atmospheric organic aerosol, *Anal. Chem.*, 90, 15, 8816–8823, 2018.

6 References

7 Appendix

A. Supplementary material to chapter 2

B. Supplementary material to chapter 3

C. Supplementary material to chapter 4

D. List of related publications and presentations

E. Acknowledgements

F. Curriculum vitae

A. Supplementary material to chapter 2

“UHPLC-Orbitrap mass spectrometric characterization of organic aerosol from a central European city (Mainz, Germany) and a Chinese megacity (Beijing)”

This supplementary material contains one appendice and five figures (S2.3.1–S2.3.5).

The description of calibration standard solution for mass spectrometer

Calibration standard solution were purchased from Sigama-Aldrich, Germany. For positive mode: caffeine (molecular weight 194 Da), MRFA (L-methionyl-arginyl-phenylalanyl-alanine, molecular weight 523 Da), Ultramark 1621 (a mixture of perfluorinated phosphazenes, molecular weight in the range of 1021–1921 Da) and n-butylamine (molecular weight 73 Da). For negative mode: sodium dodecyl sulfate (molecular weight 288 Da), sodium taurocholate hydrate (molecular weight 537 Da) and Ultramark 1621.

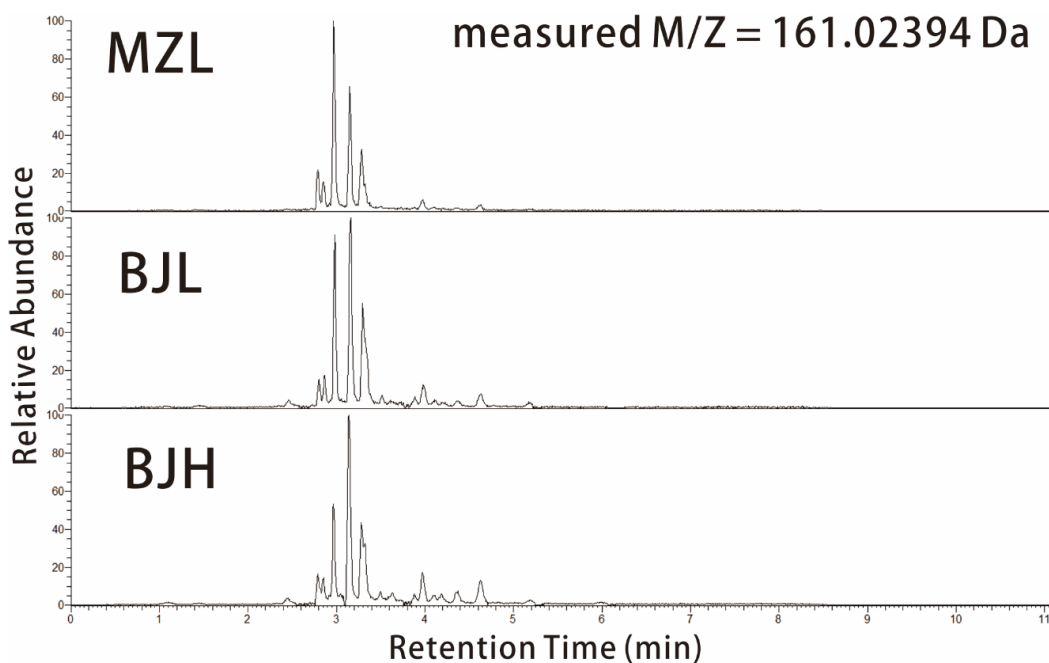


Figure S2.3.1: The UHPLC chromatograms of tentatively determined M/Z 161.02394 Da in Mainz and Beijing samples.

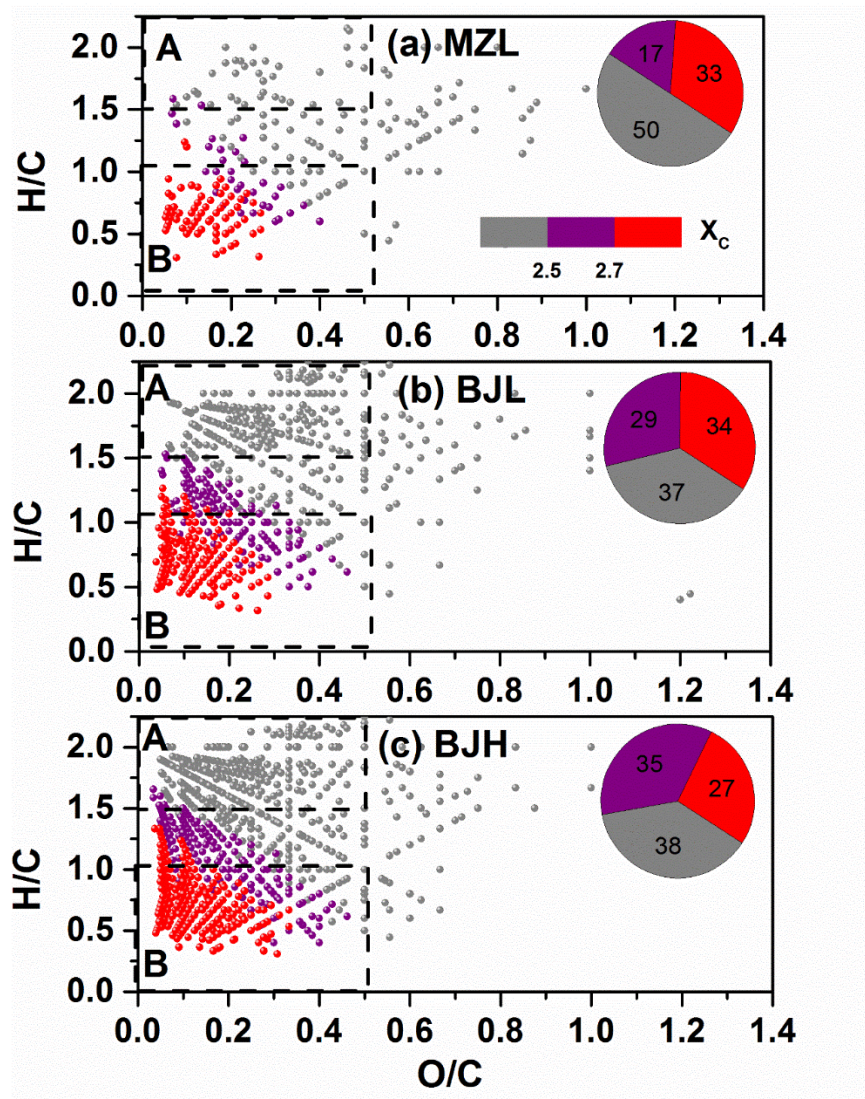


Figure S2.3.2: The Van Krevelen diagram for CHO compounds detected in ESI+ mode. Areas 'A' and 'B' refer to aliphatic compounds and oxidised aromatic hydrocarbons in organic aerosol, respectively. The colour bar denotes the aromaticity equivalent (gray ball with $X_c < 2.50$, purple ball with $2.50 \leq X_c < 2.70$ and red ball with $X_c \geq 2.70$). The pie chat shows the percentage of the number of each color-coded compound in each sample.

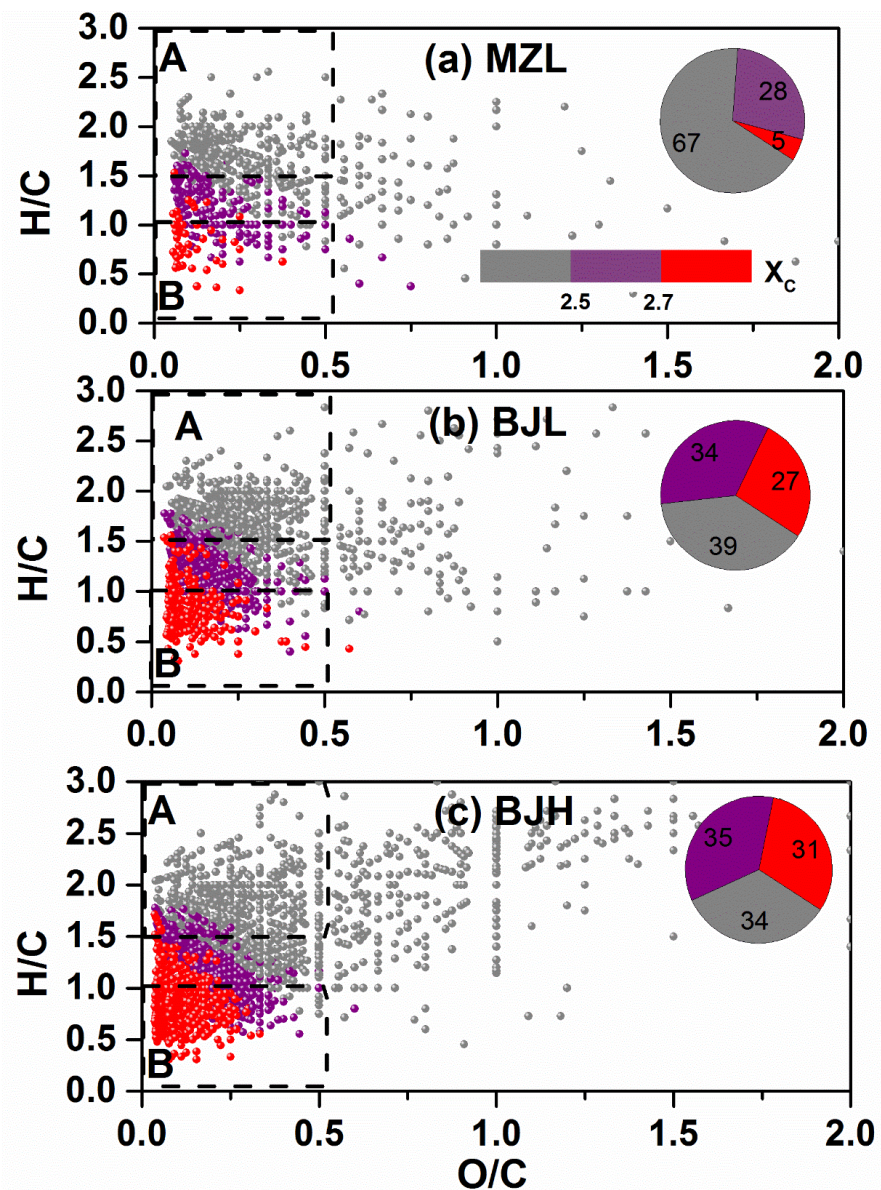


Figure S2.3.3: The Van Krevelen diagram of CHON compounds detected in ESI+ mode. Areas 'A' and 'B' refer to aliphatic compounds and oxidised aromatic hydrocarbons in organic aerosol, respectively. The colour bar denotes the aromaticity equivalent (gray ball with $X_C < 2.50$, purple ball with $2.50 \leq X_C < 2.70$ and red ball with $X_C \geq 2.70$). The pie chat shows the percentage of the number of each color-coded compound in each sample.

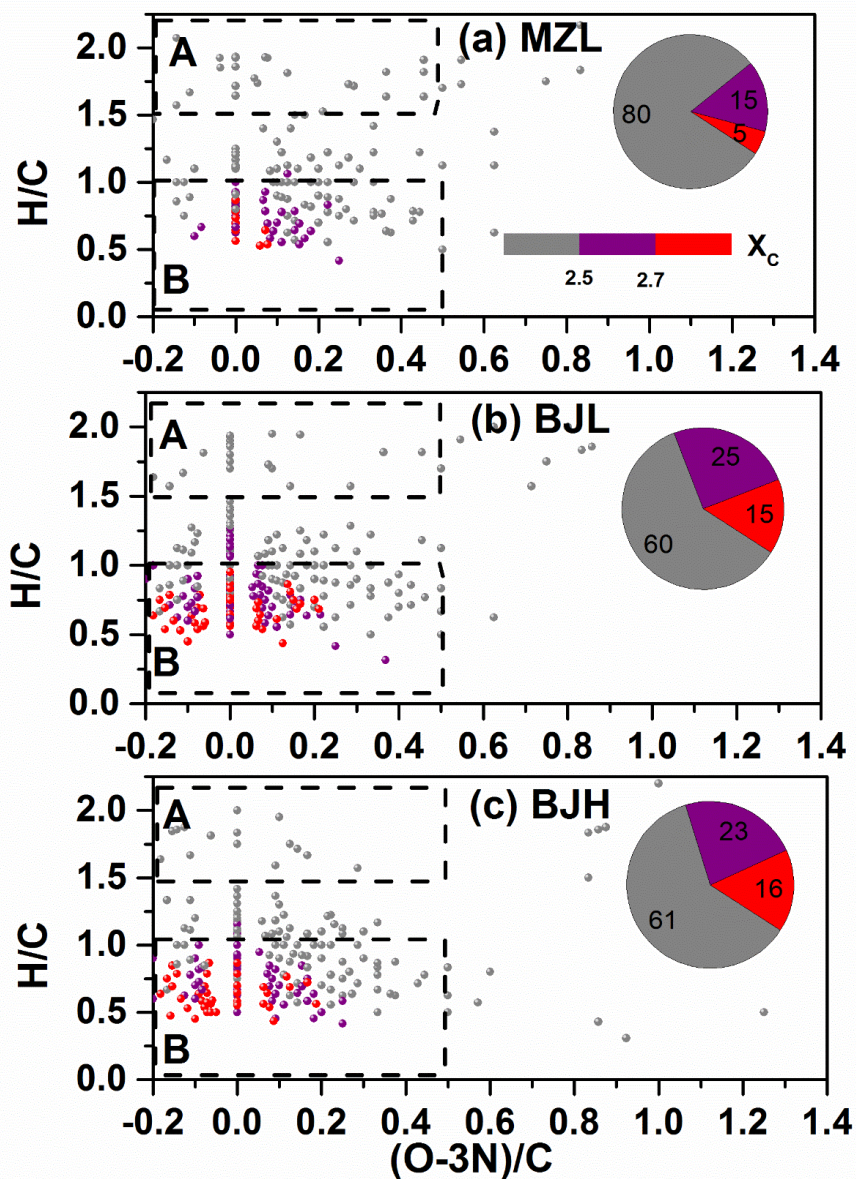


Figure S2.3.4: The Van Krevelen diagram constructed by plotting the H/C ratio against the (O-3N)/C ratio for CHON compounds detected in ESI- mode. Areas 'A' and 'B' refer to aliphatic compounds and oxidised aromatic hydrocarbons in organic aerosol, respectively. The colour bar denotes the aromaticity equivalent (gray ball with $X_c < 2.50$, purple ball with $2.50 \leq X_c < 2.70$ and red ball with $X_c \geq 2.70$). The pie chart shows the percentage of the number of each color-coded compound in each sample.

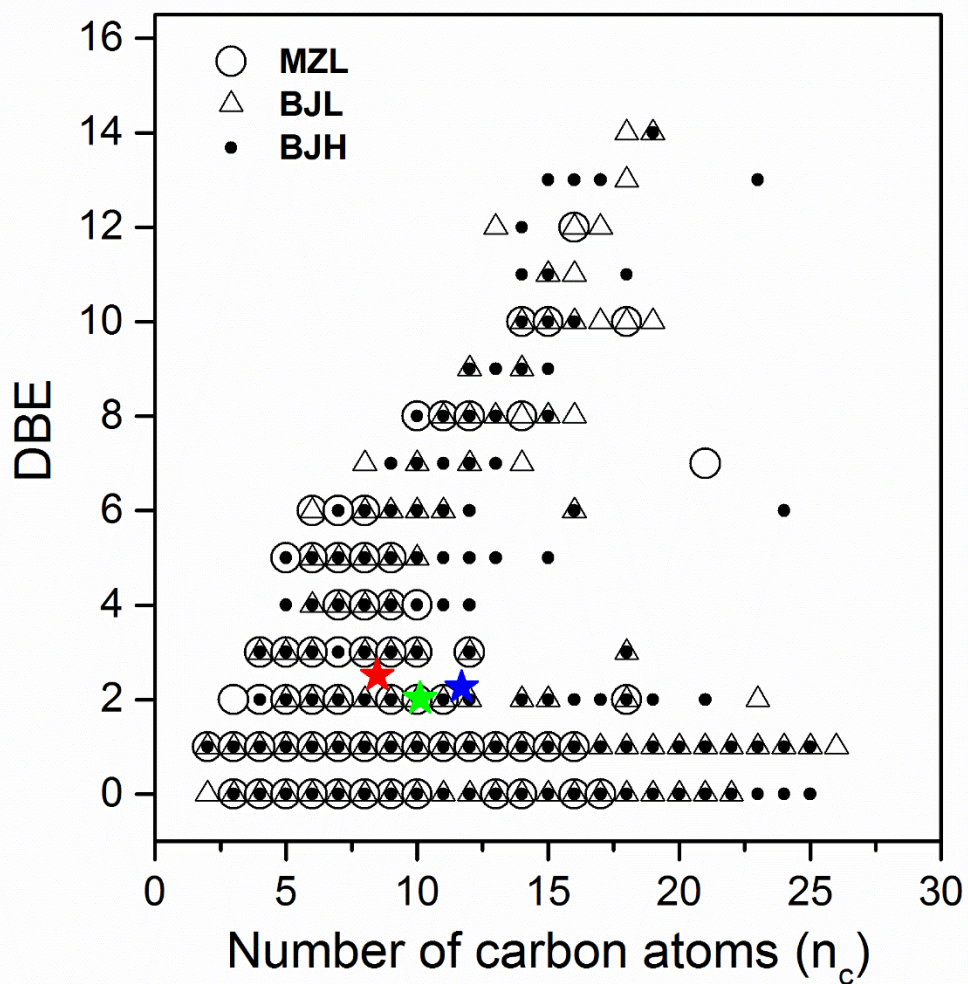


Figure S2.3.5: The DBE vs. carbon number diagram of CHOS compounds observed in MZL (circles), BJJ (triangles) and BJH (dots). The stars in the figure indicate the averaged DBE and carbon number of CHOS compounds in MZL (red star), BJJ (green star) and BJH (blue star).

B. Supplementary material to chapter 3

“The maximum carbonyl ratio as a metric for the structural classification of OA”

This supplementary material contains two tables (S3.2.1 and S3.3.1).

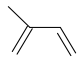
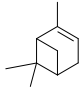
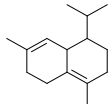
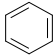
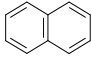
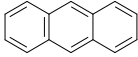
Table S3.2.1: Parameters and settings for the non-target data analysis workflow in Mzmine 2.37

1) Import data		
Raw data methods	Raw data import	
2) Peak detection		
Raw data methods	Peak detection	Mass detection
Parameters	Raw data files	All raw data files
	Scans_set filters	All
	Mass detector	Wavelet transform
		Noise level = 1000
	Mass list name	masses
3) FTMS shoulder peaks filter		
Raw data methods	Peak detection	FTMS shoulder peak filter
Parameters	Raw data files	All raw data files
	Mass list	masses
	Mass resolution	70000
	Peak model function	Gaussian
	Suffix	filtered
	Remove original peak list	Off
4) ADAP chromatogram builder		
Raw data methods	Peak detection	ADAP chromatogram builder
Parameters	Raw data files	All raw data files
	Scans_set filters	
		MS level: 1
		Polarity: Any
		Spectrum type: Any
	Mass list	masses
	Min group size in # of scans	6
	Group intensity threshold	1000
	Min highest intensity	10000
	m/z tolerance	$4.0E-4$ m/z or 2.0 ppm
	Suffix	chromatograms
5) Smoothing		
Peak list methods	Smoothing	
Parameters	Peak lists	Those created by previous batch step

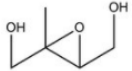
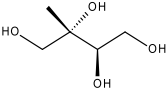
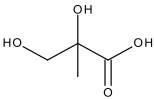
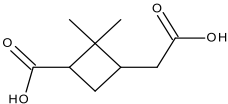
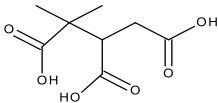
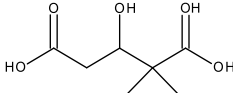
	Filename suffix	smoothed
	Filter width	5
	Remove original peak list	Off
6) Chromatogram deconvolution		
Peak list methods	Chromatogram deconvolution	
	Peak lists	Those created by previous batch step
	Suffix	deconvoluted
	Algorithm	Wavelets (ADAP)
		S/N threshold = 10
		S/N estimator = Intensity window SN
		Min feature height = 10000
		coefficient/area threshold = 110
		Peak duration range = 0.03–1.00
		RT wavelet range = 0.01–0.2
	<i>m/z</i> center calculation	MEDIAN
	<i>m/z</i> range for MS ² scan pairing	Off
	RT range for MS ² scan pairing	Off
	Remove original peak list	Off
7) Remove isotope chromatograms		
Peak list methods	isotopes	Isotopic peaks grouper
	Peak lists	Those created by previous batch step
	Name suffix	deisotoped
	<i>m/z</i> tolerance	4.0E–4 <i>m/z</i> or 2.0 ppm
	RT tolerance	0.1 absolute (min)
	Monotonic shaoe	Off
	Maximum charge	1
	Representative isotope	Most intense
	Remove original peak list	Off
8) Finds and removes adduct signals from peak list		
Peak list methods	Identification	Adduct search
	Peak lists	Those created by previous batch step
	RT tolerance	0.1 absolute (min)
	Adducts	[M+CH ₂ O ₂] 46.0055 <i>m/z</i>
		[M+ACN] 41.0266 <i>m/z</i>
	<i>m/z</i> tolerance	4.0E–4 <i>m/z</i> or 2.0 ppm
	Max relative adduct peak height	50%
9) Finds and removes ion complexes from peak list		
Peak list methods	Identification	Complex search
	Peak lists	Those created by previous batch step
	Ionization method	[M–H] [–]
	RT tolerance	0.1 absolute (min)
	<i>m/z</i> tolerance	4.0E–4 <i>m/z</i> or 2.0 ppm
	Max complex peak height	50%

10) Sort peak lists (Join aligner, finds signals from same molecules in different samples, joins peak lists of different samples into one table)		
Peak list methods	Alignment	Join aligner
	Peak lists	Those created by previous batch step
	Peak list name	Aligned peak list
	m/z tolerance	4.0E-4 m/z or 2.0 ppm
	Weight for m/z	5
	Retention time tolerance	0.2 absolute (min)
	Weight for RT	4
	Require same charge state	Off
	Require same ID	Off
	Compare isotope patten	On
		Isotope m/z tolerance = 0.001 m/z or 5.0 ppm
		Minimum absolute intensity = 1000
		Minimum score = 85%
11) Formula prediction		
Peak list methods	Identification	Formula prediction
	Charge	1
	ionization type	[M-H] ⁻
	Peak lists	Those created by previous batch step
	m/z tolerance	4.0E-4 m/z or 2.0 ppm
	max best formulas per peak	1
	Elements	
		C = 1-39
		H = 1-72
		O = 0-20
		N = 0-7
		S = 0-4
	Element count heuristics	On
		H/C ratio: yes
		NOPS/C ratio: yes
		Multiple element counts: yes
	RDBE restritions	On
		RDBE range=0-30
		RDBE must be an integer: yes
	Isotope pattern filter	On
		Isotope m/z tolerance: 0.001 m/z or 5.0 ppm
		Minimum absolute intensity: 500
		Minimum score = 75%
	MS/MS filter	Off
12) Export data		
Peak list methods	Export	Export to CSV file

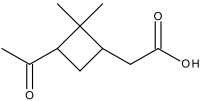
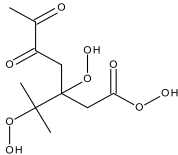
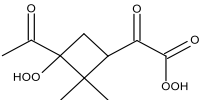
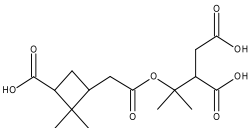
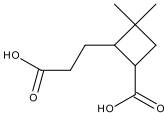
Table S3.3.1: Molecular formula, possible structure, DBE value, MCR value and suggested precursor of typical marke

Marker	Molecular formula	Structure (or possible structure)	DBE	MCR	Precursor
Isoprene	C_5H_8		2	1.00	
MT (monoterpene)	$C_{10}H_{16}$		3	1.00	
SQT (sesquiterpene)	$C_{15}H_{24}$		4	1.00	
Benzene	C_6H_6		4	1.00	
Naphtalene	$C_{10}H_8$		7	1.00	
Anthracene	$C_{14}H_{10}$		10	1.00	

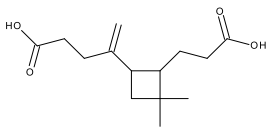
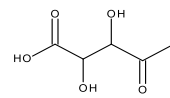
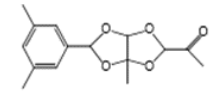
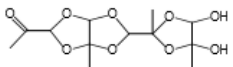
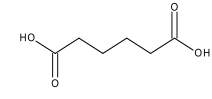
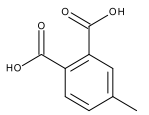
7 Appendix

IEPOX	$C_5H_{10}O_3$		1	0.33	isoprene
2-methyl-tetrols	$C_5H_{12}O_4$		0	0.00	isoprene
2-methylglyceric acid	$C_4H_8O_4$		1	0.25	isoprene
Pinic acid	$C_9H_{14}O_4$		3	0.75	monoterpenes
MBTCA	$C_8H_{12}O_6$		3	0.50	monoterpenes
3-OH-4,4-DMG [Jaoui et al., 2008, doi: 10.1029/2007JD009426]	$C_7H_{12}O_5$		2	0.40	monoterpenes

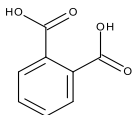

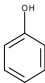
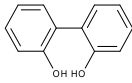
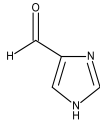
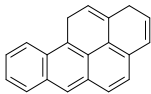
7 Appendix

Pinonic acid	$C_{10}H_{16}O_3$		3	1.00	monoterpenes
α -Pinene HOM	$C_{10}H_{16}O_9$		3	0.33	monoterpenes
α -pinene HOM	$C_{10}H_{14}O_7$		4	0.57	monoterpenes
α -pinene dimer [Beck et al., 2016, doi: 10.1016/j.atmosenv.2015.0 9.012]	$C_{17}H_{26}O_8$		5	0.63	monoterpenes
sesquiterpene oxidation product [van Eijck et al., 2013, doi: 10.1016/j.atmosenv.2013.0 7.060]	$C_{10}H_{16}O_4$		3	0.75	sesquiterpenes

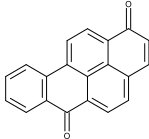
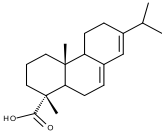
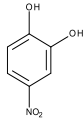
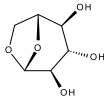
7 Appendix

<p>β-caryophyllinic acid</p> <p>[van Eijck et al., 2013, doi: 10.1016/j.atmosenv.2013.07.060]</p>	$C_{14}H_{22}O_4$		4	1.00	sesquiterpenes
<p>Tolene oxidation tracer</p> <p>[Jaoui et al., 2008, doi: 10.1029/2007JD009426]</p>	$C_5H_8O_5$		2	0.40	toluene
<p>Oligomers aqSOA I</p> <p>[Kalberer et al., 2004, doi: 10.1126/science.1092185]</p>	$C_{15}H_{18}O_5$		7	1.00	phenolic
<p>Oligomers aqSOA I</p> <p>[Kalberer et al., 2004, doi: 10.1126/science.1092185]</p>	$C_{12}H_{18}O_9$		4	0.44	cellulose
<p>Adipic acid</p>	$C_6H_{10}O_4$		2	0.50	cyclohexene
<p>Methylphthalic acid</p>	$C_9H_8O_4$		6	1.00	benzene

7 Appendix

Phthalic acid	$C_8H_6O_4$		6	1.00	benzene
C25-dicarboxylic acid	$C_{25}H_{48}O_4$		2	0.50	fatty acids
Phenol	C_6H_6O		4	1.00	
dimer aqueous phenol [Yu, et al., 2016, doi: 10.5194/acp-16-4511- 2016]	$C_{12}H_{10}O_2$		8	1.00	
Imidazole-carboxaldehyde [Kampf et al., 2016, doi: 10.1039/c6cp03029g]	$C_4H_4ON_2$		4	1.00	
Benzo(a)pyrene	$C_{20}H_{12}$		15	1.00	BB

7 Appendix

Benzo(a)pyrene-dione	$C_{20}H_{10}O_2$		16	1.00	BB
combustion soot			1.07	1.00	BB
Abietic acid	$C_{20}H_{30}O_2$		6	1.00	BB
Nitro-catechol	$C_6H_5O_4N$		5	1.00	BB, phenolic
Levoglucosan	$C_6H_{10}O_5$		2	0.40	BB, cellulose

C. Supplementary material to chapter 4

“Molecular evidence for the association of reactive oxygen species yield with oxidized organic compounds”

This supplementary material contains six figures (Figure S4.2.1, S4.3.1–S4.3.6) and twelve tables (Table S4.2.1, S4.3.1–S4.3.11).

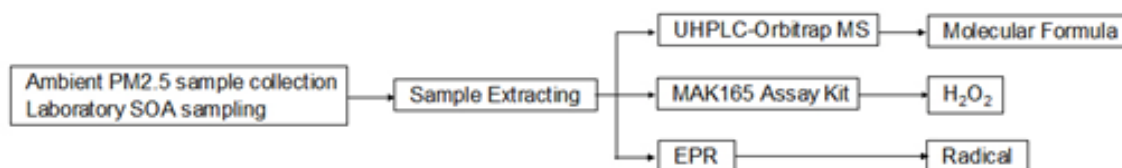


Figure S4.2.1: Schematic outline of the experimental approach: collection of ambient fine particulate matter (PM) samples and sampling of secondary organic aerosols (SOA), samples extraction and application of different experimental techniques to measure organic components, H₂O₂ yield and radical yield.

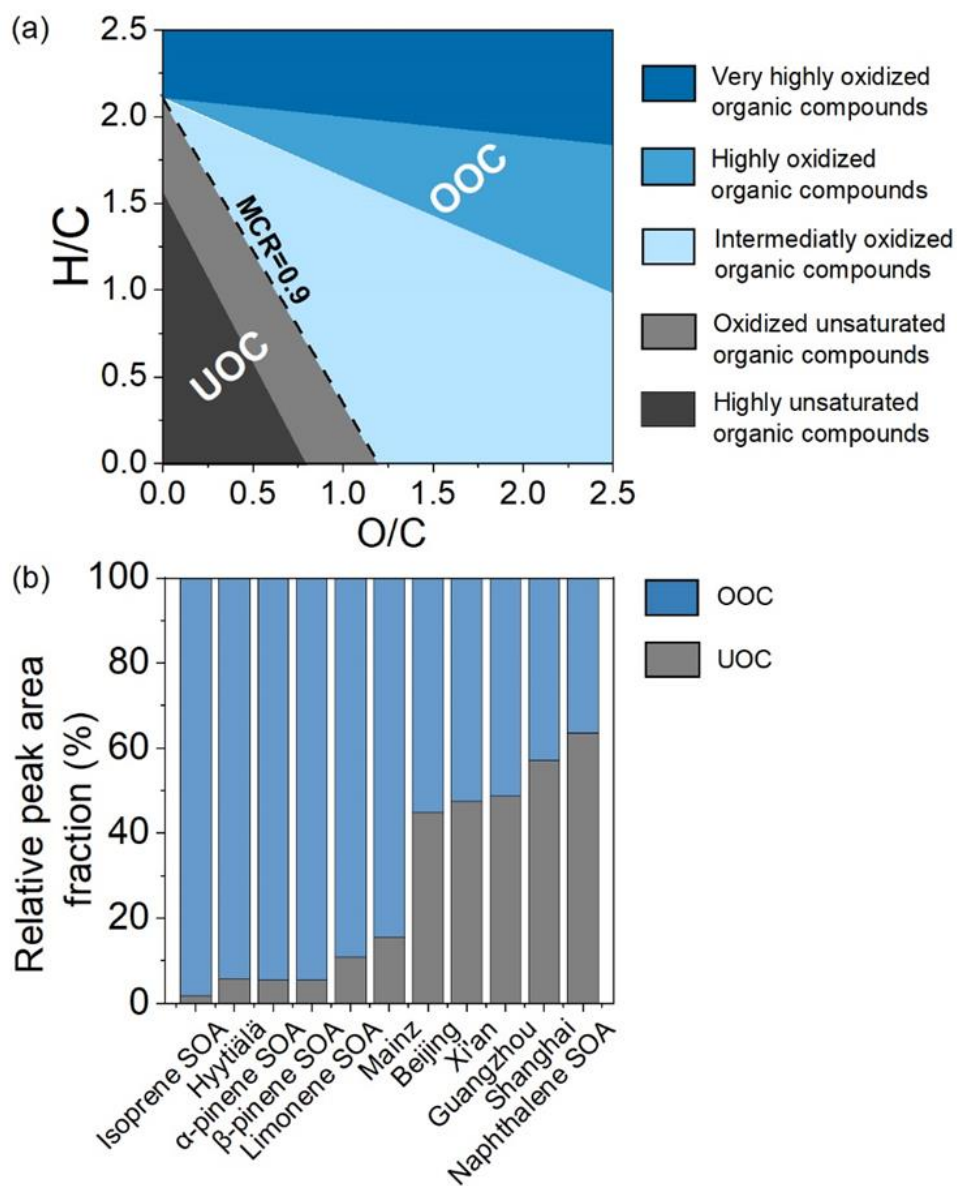


Figure S4.3.1: (a) Maximum carbonyl ratio (MCR)-Van Krevelen (VK) diagram. Oxidized organic compounds (OOC) include very highly oxidized organic compounds (dark blue), highly oxidized organic compounds (blue) and intermediately oxidized organic compounds (light blue), while unsaturated organic compounds (UOC) include oxidized unsaturated organic compounds (gray) and highly unsaturated organic compounds (dark gray). (b) Relative peak area-weighted fractions of OOC (blue) and UOC (gray) in the ambient $\text{PM}_{2.5}$ and laboratory SOA samples. The error bars represent the standard deviations of the relative peak area-weighted fractions of OOC and UOC in the samples collected at each location.

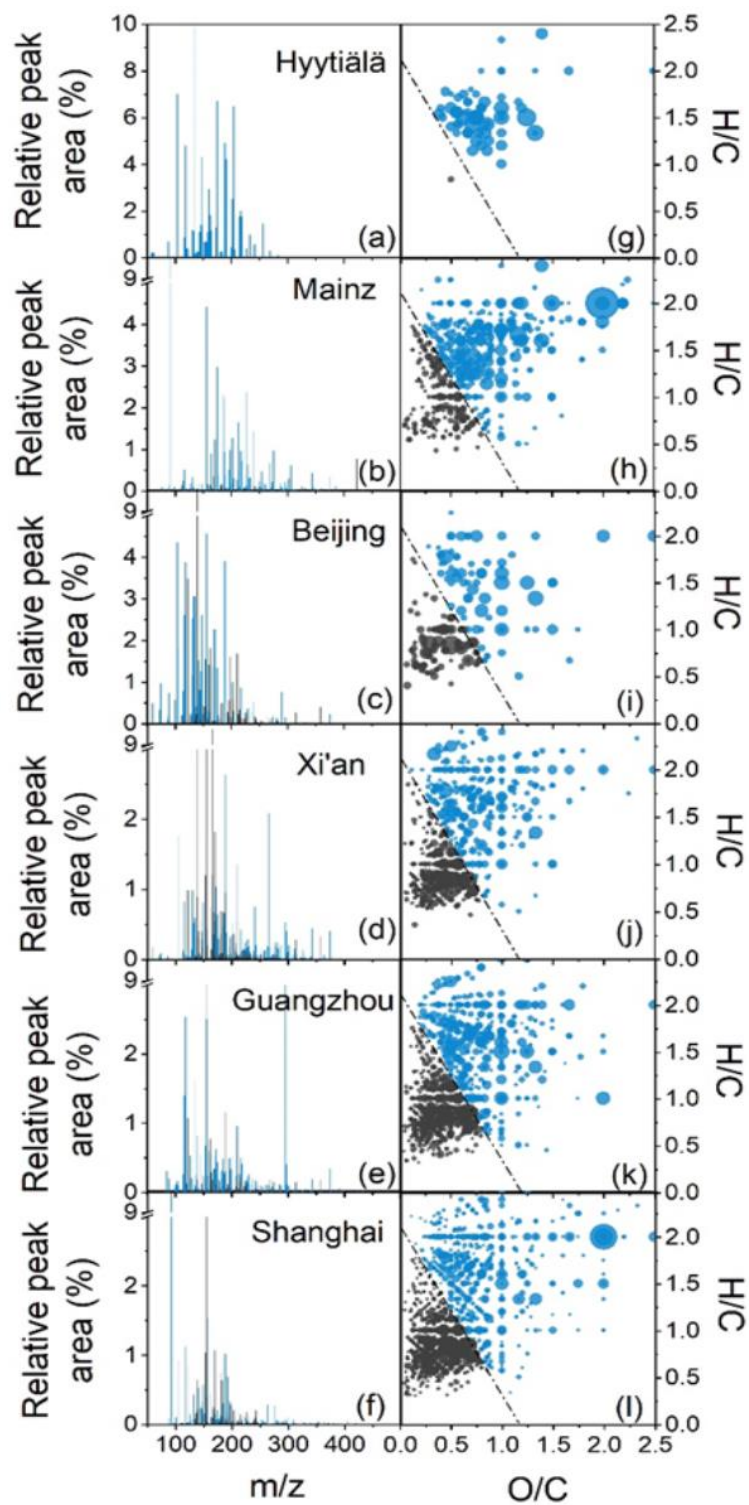


Figure S4.3.2: Mass spectra (a-f) and MCR-VK diagrams (g-l) of OOC (blue) and UOC (gray) in ambient fine PM samples collected from different locations. The size of symbols in MCR-VK diagrams is proportional to the fourth root of the abundance of each compound.

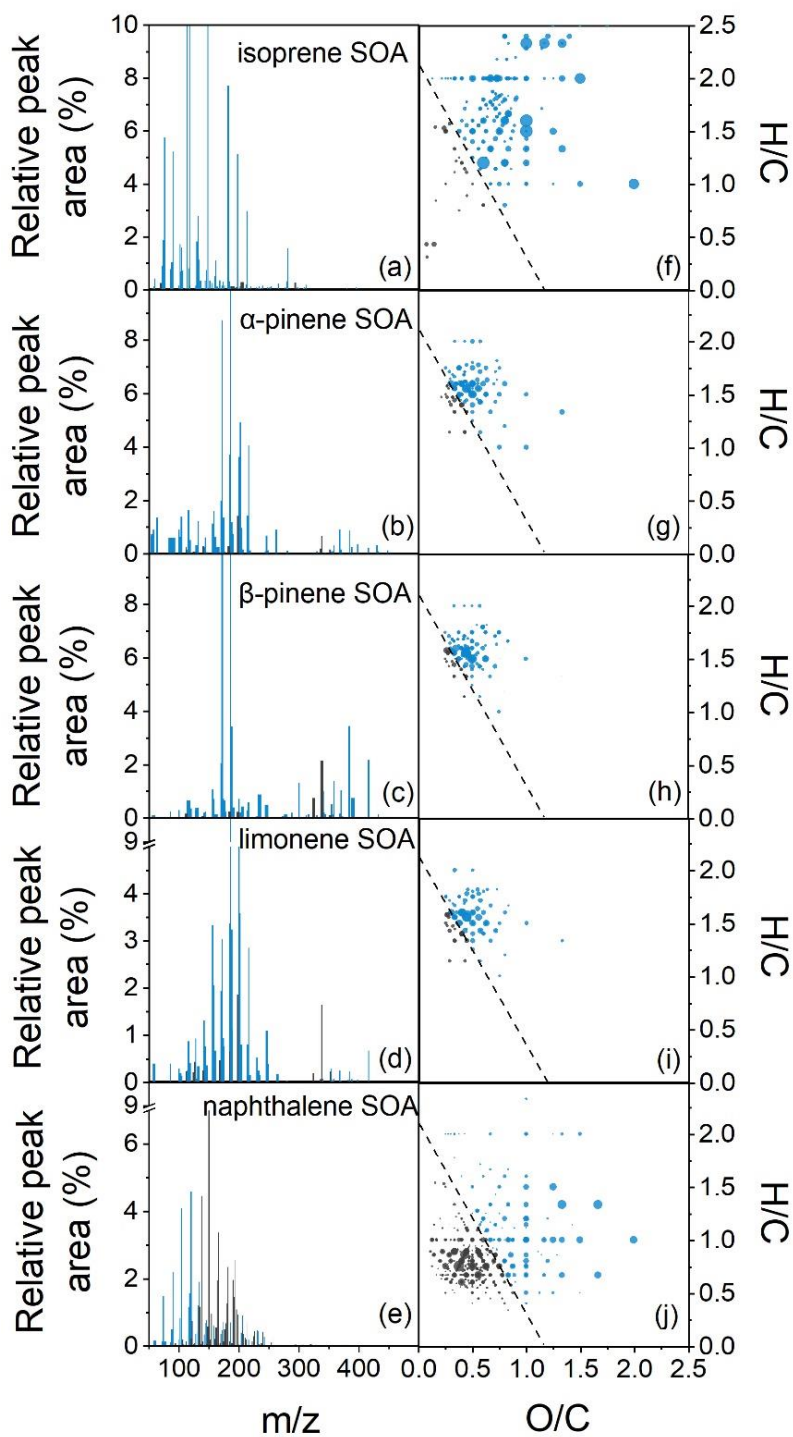


Figure S4.3.3: Mass spectra (a–f) and MCR-VK diagrams (g–l) of OOC (blue) and UOC (gray) in ambient fine PM samples collected from different locations. The size of symbols in MCR-VK diagrams is proportional to the fourth root of the abundance of each compound.

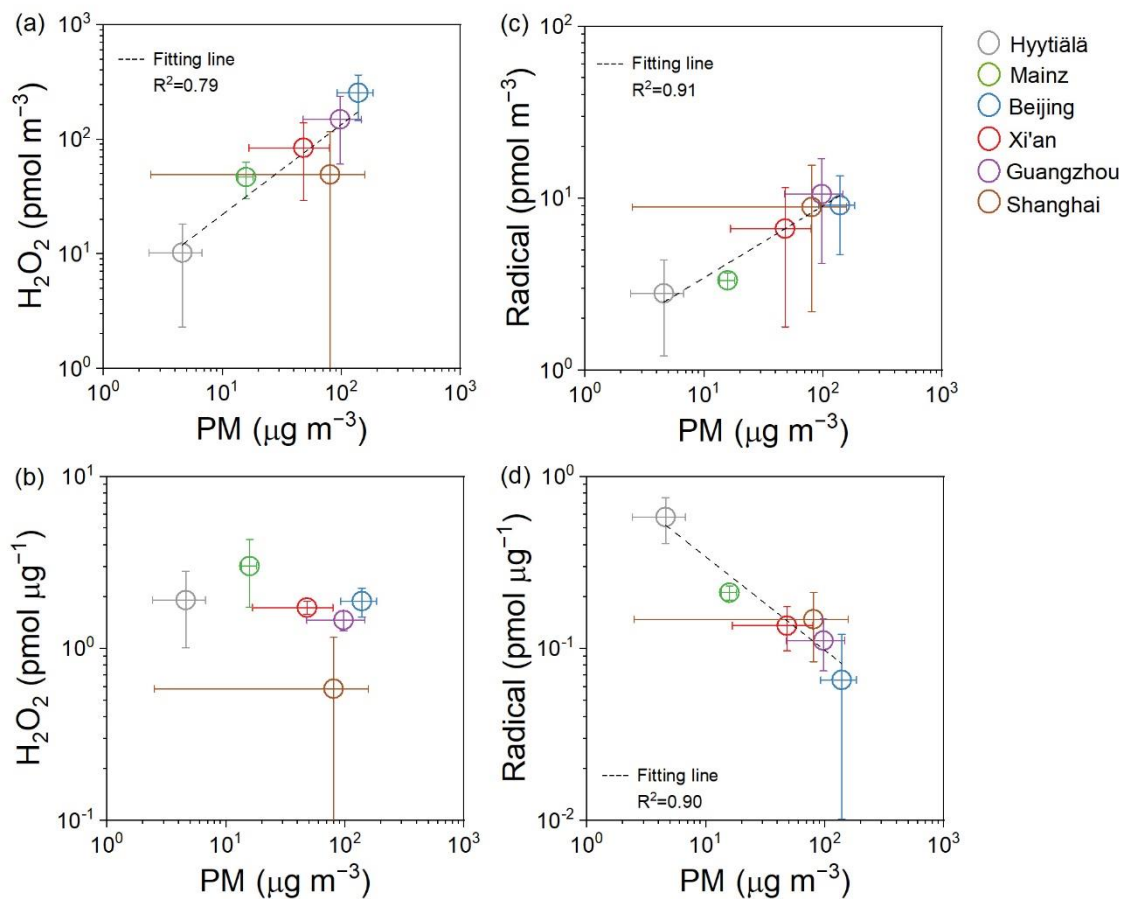


Figure S4.3.4: Correlation of volume-normalized H₂O₂ yield (a), volume-specific radical yield (b), mass-specific H₂O₂ yield (c) and mass-specific radical yield (d) with the concentration of ambient fine PM samples. The error bars at x-axis represent the standard deviations of the concentration of fine PM samples collected at each location, and the error bars at y-axis represent the standard deviations of H₂O₂ yield (a, b) and radical yield (c, d), respectively.

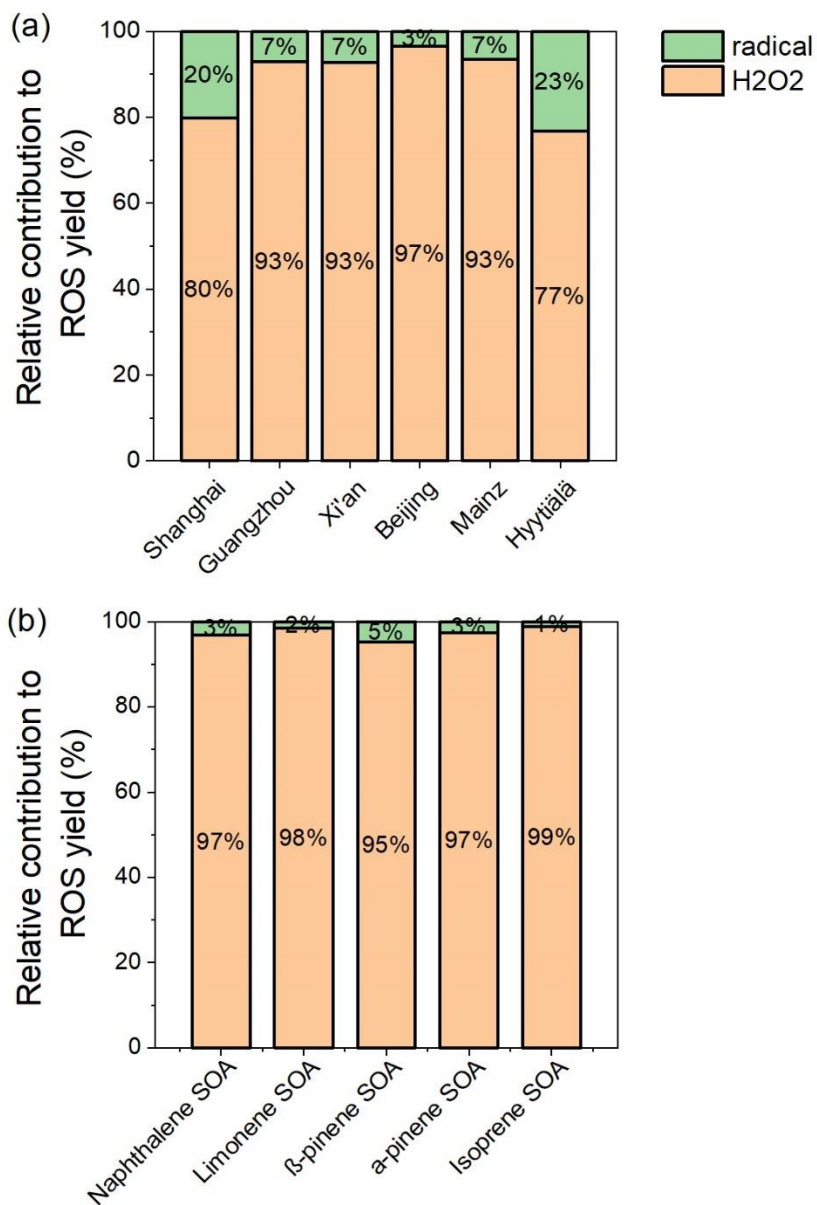


Figure S4.3.5: Relative fraction of H₂O₂ (concentration of H₂O₂ to the sum of H₂O₂ and radicals, orange color) and relative fraction of radical (concentration of radical to the sum of H₂O₂ and radicals, green color) generated by ambient PM_{2.5} samples from each site (a) or SOA samples from each laboratory experiment (b). The error bars represent the standard deviations of the relative fraction of H₂O₂ and radical.

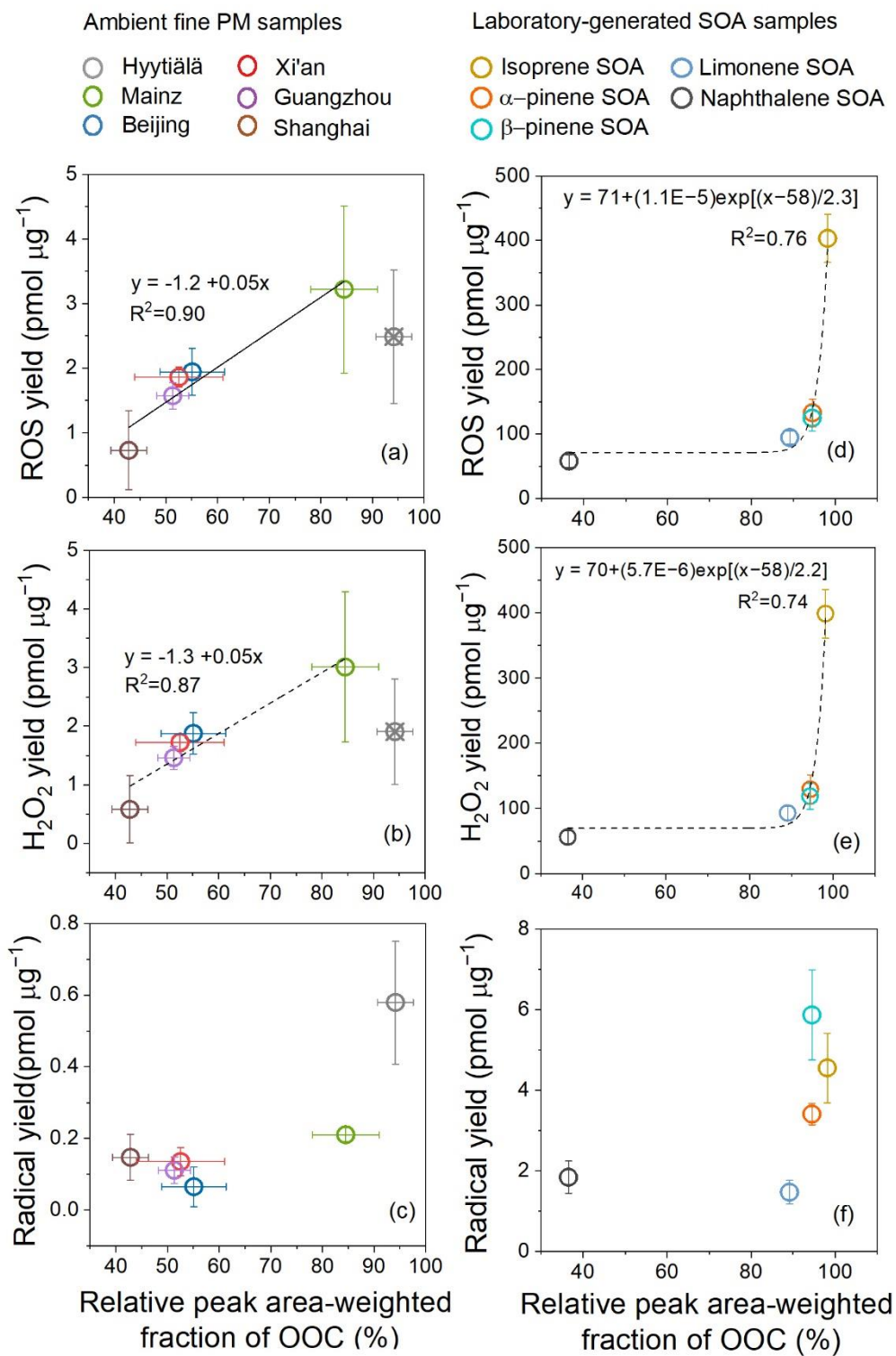


Figure S4.3.6: Correlation of mass-specific ROS yield (a, d), H_2O_2 yield (b, e) radical yield (c, f) with the relative peak area-weighted fraction of OOC of ambient fine PM samples (a, b, c) and laboratory SOA samples (d, e, f), respectively.

Table S4.2.1: Ambient particle sampling information

Site	Location	Air flow rate L ⁻¹ min ⁻¹	Volume of air/m ³	Particle size	Sampler	Sampling time
Hyytiälä	61.85°N, 24.29°E	35	293	PM _{2.5}	Dekati PM ₁₀ impactor (Dekati Ltd., Tampere, Finland)	02–05/06/2017
			252	PM _{2.5}		21–26/06/2017
			100	PM _{2.5}		26–28/06/2017
			99	PM _{2.5}		28–30/06/2017
Mainz	49.99°N, 8.23°E	29	80	PM _{1.8}	MOUDI (122R, MSP corporation, USA)	22–24/08/2017
			80	PM _{1.8}		26–28/08/2017
			80	PM _{1.8}		28–30/08/2017
			80	PM _{1.8}		25–27/09/2017
Beijing	116.27°E, 40.15°N	15	22	PM _{2.5}	Homemade PM _{2.5} sampler	26–27/02/2019
			22	PM _{2.5}		27–28/02/2019
			22	PM _{2.5}		28–29/02/2019
			22	PM _{2.5}		01–02/03/2019
			22	PM _{2.5}		02–03/03/2019
			21	PM _{2.5}		03–04/03/2019
			22	PM _{2.5}		04–05/03/2019
			22	PM _{2.5}		08–09/03/2019
			22	PM _{2.5}		09–10/03/2019
			22	PM _{2.5}		10–11/03/2019
Shanghai	121.43°E, 34.50°N	1050	1612	PM _{2.5}	Homemade PM _{2.5} sampler	01–02/01/2014
			1585	PM _{2.5}		19–20/01/2014
			1620	PM _{2.5}		20–21/01/2014
			1628	PM _{2.5}		24–25/01/2014
			1614	PM _{2.5}		26–27/01/2014
			1612	PM _{2.5}		27–28/01/2014
Guangzhou	113.27°E, 23.13°N	1050	1690	PM _{2.5}	Homemade PM _{2.5} sampler	05–06/01/2014
			1599	PM _{2.5}		06–07/01/2014
			1596	PM _{2.5}		11–12/01/2014
			1601	PM _{2.5}		08–09/01/2014
			1616	PM _{2.5}		12–13/01/2014
			1646	PM _{2.5}		13–14/01/2014
Xi'an	108.95°E, 34.27°N	50	72	PM _{2.5}	Tisch TE-20-800, USA	05–06/11/2018
			72	PM _{2.5}		06–07/11/2018
			72	PM _{2.5}		07–08/11/2018
			72	PM _{2.5}		08–09/11/2018
			60	PM _{2.5}		09–10/11/2018

Table S4.3.1 Molecular formulas of organic compounds detected in Hyytiälä OA in ESI⁻ mode.

Formula [M]	Neutral mass (Da)	RT (min)	MCR	H/C	O/C
C4H6O5	134.0215	0.41	0.40	1.50	1.25
C8H12O6	204.0634	2.29	0.50	1.50	0.75
C5H12O7S	216.0304	0.37	0.00	2.40	1.40
C3H4O4	104.0110	0.41	0.50	1.33	1.33
C7H10O5	174.0528	0.77	0.60	1.43	0.71
C8H12O5	188.0685	1.27	0.60	1.50	0.63
C7H10O6	190.0477	0.55	0.50	1.43	0.86
C9H14O5	202.0841	2.76	0.60	1.56	0.56
C10H16O5	216.0998	2.98	0.60	1.60	0.50
C9H12O6	216.0634	2.40	0.67	1.33	0.67
C9H12O6	216.0634	1.53	0.67	1.33	0.67
C8H12O6	204.0634	1.52	0.50	1.50	0.75
C8H12O6	204.0634	0.61	0.50	1.50	0.75
C6H8O5	160.0372	0.47	0.60	1.33	0.83
C13H20O5	256.1311	4.97	0.80	1.54	0.38
C7H10O4	158.0579	1.65	0.75	1.43	0.57
C5H8O4	132.0423	0.47	0.50	1.60	0.80
C7H8O5	172.0372	0.74	0.80	1.14	0.71
C8H10O6	202.0477	0.79	0.67	1.25	0.75
C9H14O5	202.0841	1.49	0.60	1.56	0.56
C5H6O5	146.0215	0.39	0.60	1.20	1.00
C12H18O5	242.1154	3.87	0.80	1.50	0.42
C7H8O6	188.0321	0.48	0.67	1.14	0.86
C5H8O6	164.0321	0.38	0.33	1.60	1.20
C10H14O5	214.0841	2.60	0.80	1.40	0.50
C3H6O5S	153.9936	0.40	0.20	2.00	1.67
C6H8O4	144.0423	0.69	0.75	1.33	0.67
C9H12O7	232.0583	0.82	0.57	1.33	0.78
C7H10O6	190.0477	0.96	0.50	1.43	0.86
C8H14O5	190.0841	1.23	0.40	1.75	0.63
C9H12O5	200.0685	2.35	0.80	1.33	0.56
C9H14O6	218.0790	1.26	0.50	1.56	0.67
C9H12O6	216.0634	0.67	0.67	1.33	0.67
C8H10O7	218.0427	0.48	0.57	1.25	0.88
C7H12O7S	240.0304	0.49	0.29	1.71	1.00
C10H16O4	200.1049	4.23	0.75	1.60	0.40
C6H14O6	182.0790	0.34	0.00	2.33	1.00
C10H18O7S	282.0773	0.75	0.29	1.80	0.70
C2H4O5S	139.9779	0.37	0.20	2.00	2.50
C8H14O6	206.0790	0.57	0.33	1.75	0.75
C2H4O2	60.0211	0.42	0.50	2.00	1.00
C6H10O7S	226.0147	0.49	0.29	1.67	1.17
C3H6O4S	137.9987	0.38	0.25	2.00	1.33
C8H14O4	174.0892	1.36	0.50	1.75	0.50
C7H10O4	158.0579	1.19	0.75	1.43	0.57
C2H4N2O5	136.0120	0.35	0.40	2.00	2.50
C8H12O8S	268.0253	0.55	0.38	1.50	1.00
C3H4N2O4	132.0171	0.37	0.75	1.33	1.33
C4H6O4	118.0266	0.54	0.50	1.50	1.00
C5H8O5	148.0372	0.46	0.40	1.60	1.00
C9H16O4	188.1049	3.71	0.50	1.78	0.44
C6H10O5	162.0528	0.57	0.40	1.67	0.83
C5H8O4	132.0423	0.78	0.50	1.60	0.80
C3H4O3	88.0160	0.38	0.67	1.33	1.00
C5H6O4	130.0266	0.59	0.75	1.20	0.80
C4H4O4	116.0110	0.46	0.75	1.00	1.00
C6H10O4	146.0579	1.66	0.50	1.67	0.67
C6H10O4	146.0579	0.62	0.50	1.67	0.67
C4H8O4	120.0423	0.44	0.25	2.00	1.00
C7H12O4	160.0736	0.86	0.50	1.71	0.57
C5H8O4	132.0423	1.08	0.50	1.60	0.80
C5H10O4	134.0579	0.47	0.25	2.00	0.80
C6H5NO3	139.0269	3.73	1.00	0.83	0.50

Table S4.3.2 Molecular formulas of organic compounds detected in Mainz OA in ESI⁻ mode.

Formula [M]	Neutral mass (Da)	RT (min)	MCR	H/C	O/C
C2H4O4	92.0110	0.15	0.25	2.00	2.00
C2H4O6S	155.9729	0.36	0.17	2.00	3.00
C8H10O5	186.0528	3.02	0.80	1.25	0.63
C5H8O7S	211.9991	0.45	0.29	1.60	1.40
C7H10O5	174.0528	0.76	0.60	1.43	0.71
C4H8O6S	184.0042	0.44	0.17	2.00	1.50
C6H10O7S	226.0147	0.50	0.29	1.67	1.17
C5H4N2O3	140.0222	2.36	1.00	0.80	0.60
C3H6O6S	169.9885	0.40	0.17	2.00	2.00
C5H12O7S	216.0304	0.38	0.00	2.40	1.40
C8H12O5	188.0685	0.85	0.60	1.50	0.63
C9H16O4	188.1049	3.71	0.50	1.78	0.44
C10H16O6	232.0947	3.04	0.50	1.60	0.60
C5H8O6	164.0321	0.37	0.33	1.60	1.20
C5H10O6S	198.0198	0.56	0.17	2.00	1.20
C5H10N2O11S	306.0005	2.58	0.18	2.00	2.20
C5H6O5	146.0215	0.38	0.60	1.20	1.00
C7H12O7S	240.0304	0.63	0.29	1.71	1.00
C7H8O6	188.0321	0.48	0.67	1.14	0.86
C8H11NO7	233.0536	3.02	0.57	1.38	0.88
C4H4O6S	179.9729	0.46	0.50	1.00	1.50
C6H12O7S	228.0304	0.48	0.14	2.00	1.17
C5H8O6S	196.0042	0.46	0.33	1.60	1.20
C8H10O6	202.0477	0.78	0.67	1.25	0.75
C5H10N2O11S	306.0005	2.33	0.18	2.00	2.20
C6H12O6S	212.0355	0.94	0.17	2.00	1.00
C8H11NO8	249.0485	2.88	0.50	1.38	1.00
C7H12O7S	240.0304	0.91	0.29	1.71	1.00
C9H12O7	232.0583	0.81	0.57	1.33	0.78
C7H10O6	190.0477	0.93	0.50	1.43	0.86
C5H8O4	132.0423	0.47	0.50	1.60	0.80
C7H7NO4	169.0375	3.80	1.00	1.00	0.57
C9H12O6	216.0634	1.52	0.67	1.33	0.67
C6H10O2	114.0681	2.73	1.00	1.67	0.33
C5H9NO10S	274.9947	0.58	0.20	1.80	2.00
C10H17NO10S	343.0573	2.65	0.30	1.70	1.00
C6H6O6	174.0164	0.40	0.67	1.00	1.00
C7H12O5	176.0685	2.35	0.40	1.71	0.71
C8H10O7	218.0427	0.48	0.57	1.25	0.88
C8H12O8S	268.0253	0.60	0.38	1.50	1.00
C7H10O8S	254.0096	0.49	0.38	1.43	1.14
C8H11NO8	249.0485	2.49	0.50	1.38	1.00
C6H10O6S	210.0198	0.58	0.33	1.67	1.00
C10H14O6	230.0790	2.23	0.67	1.40	0.60
C7H8O7	204.0270	0.43	0.57	1.14	1.00
C7H12O6S	224.0355	0.85	0.33	1.71	0.86
C10H15NO9S	325.0468	3.00	0.44	1.50	0.90
C5H10N2O11S	306.0005	3.07	0.18	2.00	2.20
C4H6O6S	181.9885	0.44	0.33	1.50	1.50
C9H16O7S	268.0617	2.15	0.29	1.78	0.78
C5H8O3	116.0473	0.50	0.67	1.60	0.60
C3H4O8S	199.9627	0.36	0.25	1.33	2.67
C13H24N2O4	272.1736	2.30	0.75	1.85	0.31
C7H10O2	126.0681	1.23	1.00	1.43	0.29
C11H16O6	244.0947	2.68	0.67	1.45	0.55
C8H14O7S	254.0460	1.06	0.29	1.75	0.88
C22H30O8	422.1941	6.90	1.00	1.36	0.36
C11H19N3O12	385.0969	8.22	0.33	1.73	1.09
C8H10O5	186.0528	2.28	0.80	1.25	0.63
C7H5NO5	183.0168	2.95	1.00	0.71	0.71
C10H17NO10S	343.0573	2.88	0.30	1.70	1.00
C13H20O3	224.1412	8.13	1.00	1.54	0.23
C4H4O5	132.0059	0.39	0.60	1.00	1.25
C8H14O3	158.0943	2.80	0.67	1.75	0.38

7 Appendix

C5H8O2	100.0524	0.70	1.00	1.60	0.40
C6H10O	98.0732	3.02	1.00	1.67	0.17
C10H18N2O11S	374.0631	4.40	0.27	1.80	1.10
C10H16O7S	280.0617	1.06	0.43	1.60	0.70
C10H16O7S	280.0617	2.53	0.43	1.60	0.70
C8H12N2O10	296.0492	3.02	0.40	1.50	1.25
C5H6O3	114.0317	0.46	1.00	1.20	0.60
C6H10O3	130.0630	0.75	0.67	1.67	0.50
C7H7NO4	169.0375	4.60	1.00	1.00	0.57
C5H10O5S	182.0249	0.56	0.20	2.00	1.00
C10H7NO3	189.0426	7.73	1.00	0.70	0.30
C9H6O5	194.0215	2.59	1.00	0.67	0.56
C10H17NO8S	311.0675	3.79	0.38	1.70	0.80
C2H3NO3	89.0113	0.38	0.67	1.50	1.50
C5H10N2O11S	306.0005	1.70	0.18	2.00	2.20
C2H2O3	74.0004	0.37	0.67	1.00	1.50
C8H13NO11S	331.0209	1.05	0.27	1.63	1.38
C8H14O10S	302.0308	0.58	0.20	1.75	1.25
C6H6O7	190.0114	0.38	0.57	1.00	1.17
C6H8O3	128.0473	0.49	1.00	1.33	0.50
C6H12O9S	260.0202	0.56	0.11	2.00	1.50
C8H6N2O2	162.0429	6.01	1.00	0.75	0.25
C8H10O6	202.0477	1.48	0.67	1.25	0.75
C7H12O2	128.0837	1.74	1.00	1.71	0.29
C6H6N2O3	154.0378	2.84	1.00	1.00	0.50
C10H10O4	194.0579	3.76	1.00	1.00	0.40
C5H7NO5	161.0324	0.37	0.60	1.40	1.00
C5H9NO9S	258.9998	0.71	0.22	1.80	1.80
C5H9NO9S	258.9998	1.07	0.22	1.80	1.80
C8H9NO4	183.0532	3.34	1.00	1.13	0.50
C6H12O4	148.0736	0.54	0.25	2.00	0.67
C14H10O4	242.0579	5.00	1.00	0.71	0.29
C10H18N2O11S	374.0631	3.88	0.27	1.80	1.10
C7H4N2O7	228.0019	4.13	1.00	0.57	1.00
C8H9NO5	199.0481	3.52	1.00	1.13	0.63
C7H9NO7	219.0379	2.78	0.57	1.29	1.00
C7H10O4	158.0579	2.74	0.75	1.43	0.57
C4H6O5S	165.9936	0.40	0.40	1.50	1.25
C8H7NO3	165.0426	5.03	1.00	0.88	0.38
C8H14O7S	254.0460	0.74	0.29	1.75	0.88
C11H17NO8	291.0954	2.95	0.50	1.55	0.73
C9H6O5	194.0215	0.84	1.00	0.67	0.56
C10H18N2O11S	374.0631	3.23	0.27	1.80	1.10
C8H14O7S	254.0460	2.29	0.29	1.75	0.88
C2H4O3	76.0160	0.73	0.33	2.00	1.50
C9H6O6	210.0164	1.15	1.00	0.67	0.67
C8H7NO4	181.0375	3.86	1.00	0.88	0.50
C11H18N2O11	354.0911	8.07	0.36	1.64	1.00
C5H3NO4S	172.9783	0.60	1.00	0.60	0.80
C7H10O2	126.0681	2.88	1.00	1.43	0.29
C10H16O8S	296.0566	0.76	0.38	1.60	0.80
C3H3N3O3	129.0174	0.39	1.00	1.00	1.00
C10H15NO9	293.0747	3.26	0.44	1.50	0.90
C8H14O9S	286.0359	1.23	0.22	1.75	1.13
C9H16O7S	268.0617	0.87	0.29	1.78	0.78
C8H14O6S	238.0511	1.55	0.33	1.75	0.75
C7H14O6S	226.0511	2.17	0.17	2.00	0.86
C10H16O6	232.0947	0.87	0.50	1.60	0.60
C8H10O7	218.0427	1.04	0.57	1.25	0.88
C9H6O6	210.0164	1.90	1.00	0.67	0.67
C8H6O5	182.0215	2.80	1.00	0.75	0.63
C8H14O10S	302.0308	2.28	0.20	1.75	1.25
C6H8O2	112.0524	1.14	1.00	1.33	0.33
C6H8O4	144.0423	1.29	0.75	1.33	0.67
C7H7NO3	153.0426	5.16	1.00	1.00	0.43
C11H21NO9	311.1216	2.48	0.22	1.91	0.82
C8H9NO3	167.0582	7.55	1.00	1.13	0.38
C7H4N2O3S	195.9943	3.15	1.00	0.57	0.43
C5H3NO5	157.0011	0.75	1.00	0.60	1.00
C8H7NO5	197.0324	3.35	1.00	0.88	0.63

7 Appendix

C7H12O9S	272.0202	0.76	0.22	1.71	1.29
C8H9NO5	199.0481	2.47	1.00	1.13	0.63
C7H8O4	156.0423	2.57	1.00	1.14	0.57
C10H10O4	194.0579	3.14	1.00	1.00	0.40
C6H6O4	142.0266	0.46	1.00	1.00	0.67
C4H9NO9S	246.9998	0.53	0.11	2.25	2.25
C4H3NO2S	128.9884	0.60	1.00	0.75	0.50
C9H15NO8S	297.0518	3.28	0.38	1.67	0.89
C5H5NO3	127.0269	1.05	1.00	1.00	0.60
C13H20O6	272.1260	3.12	0.67	1.54	0.46
C5H10O5S	182.0249	0.96	0.20	2.00	1.00
C4H6O8	182.0063	0.47	0.25	1.50	2.00
C6H11NO9S	273.0155	2.69	0.22	1.83	1.50
C12H14O5	238.0841	3.40	1.00	1.17	0.42
C5H4O4	128.0110	0.43	1.00	0.80	0.80
C7H5NO6	199.0117	3.47	1.00	0.71	0.86
C8H6O5	182.0215	1.09	1.00	0.75	0.63
C7H10O3	142.0630	0.77	1.00	1.43	0.43
C6H3N3O7	228.9971	4.12	1.00	0.50	1.17
C7H6O6	186.0164	0.46	0.83	0.86	0.86
C8H7NO5	197.0324	4.71	1.00	0.88	0.63
C7H6N2O6	214.0226	3.52	1.00	0.86	0.86
C11H18N2O10	338.0961	7.47	0.40	1.64	0.91
C8H13NO8	251.0641	1.23	0.38	1.63	1.00
C7H8O8S	251.9940	0.58	0.50	1.14	1.14
C12H15NO3	221.1052	7.05	1.00	1.25	0.25
C20H14N2O5	330.0827	6.73	1.00	0.70	0.05
C13H18O5	254.1154	7.40	1.00	1.38	0.38
C8H6N2O5	210.0277	7.33	1.00	0.75	0.63
C10H12O7	244.0583	0.67	0.71	1.20	0.70
C10H20O5S2	284.0752	3.54	0.20	2.00	0.50
C11H19NO9	309.1060	3.89	0.33	1.73	0.82
C8H18O4S	210.0926	6.47	0.00	2.25	0.50
C14H22O4	254.1518	6.69	1.00	1.57	0.29
C8H10O4	170.0579	1.09	1.00	1.25	0.50
C4H8O4	120.0423	0.95	0.25	2.00	1.00
C9H16O4	188.1049	2.58	0.50	1.78	0.44
C5H7NO9S	256.9842	1.77	0.33	1.40	1.80
C7H11NO10S	301.0104	1.08	0.30	1.57	1.43
C7H10O3	142.0630	2.33	1.00	1.43	0.43
C4H8O2	88.0524	0.49	0.50	2.00	0.50
C13H18O7	286.1053	2.78	0.71	1.38	0.54
C7H6O4	154.0266	1.31	1.00	0.86	0.57
C12H16O7	272.0896	2.69	0.71	1.33	0.58
C14H24O4	256.1675	3.92	0.75	1.71	0.29
C12H18O5	242.1154	3.87	0.80	1.50	0.42
C8H11NO8	249.0485	0.82	0.50	1.38	1.00
C6H6O3	126.0317	0.47	1.00	1.00	0.50
C10H14O2	166.0994	7.20	1.00	1.40	0.20
C7H4N2O4	180.0171	3.50	1.00	0.57	0.57
C6H8O3	128.0473	2.33	1.00	1.33	0.50
C14H6N4O5	310.0338	1.22	1.00	0.43	0.36
C10H12N2O6	256.0695	8.03	1.00	1.20	0.60
C9H16O5	204.0998	0.88	0.40	1.78	0.56
C12H9NO3	215.0582	8.10	1.00	0.75	0.25
C8H8O3	152.0473	2.64	1.00	1.00	0.38
C9H13NO8	263.0641	3.10	0.50	1.44	0.89
C7H8O5	172.0372	2.79	0.80	1.14	0.71
C9H10O6	214.0477	0.71	0.83	1.11	0.67
C8H8O6	200.0321	0.55	0.83	1.00	0.75
C6H4O5	156.0059	0.72	1.00	0.67	0.83
C8H18O3S	194.0977	5.21	0.00	2.25	0.38
C8H13NO6	219.0743	3.02	0.50	1.63	0.75
C12H7NO4	229.0375	7.99	1.00	0.58	0.33
C7H13NO9S	287.0311	2.78	0.22	1.86	1.29
C6H6O3S	158.0038	0.76	1.00	1.00	0.50
C5H4O3	112.0160	0.42	1.00	0.80	0.60
C5H6O2	98.0368	0.47	1.00	1.20	0.40
C6H10O5S	194.0249	0.54	0.40	1.67	0.83
C6H12O3	132.0786	1.26	0.33	2.00	0.50

7 Appendix

C8H5NO5	195.0168	3.14	1.00	0.63	0.63
C9H13NO7	247.0692	3.28	0.57	1.44	0.78
C6H8O2	112.0524	0.56	1.00	1.33	0.33
C12H16O8	288.0845	2.68	0.63	1.33	0.67
C14H22O7	302.1366	3.06	0.57	1.57	0.50
C6H12O6S	212.0355	1.57	0.17	2.00	1.00
C7H9NO4	171.0532	0.49	1.00	1.29	0.57
C6H11NO10S	289.0104	0.70	0.20	1.83	1.67
C13H18O6	270.1103	2.88	0.83	1.38	0.46
C11H19NO9	309.1060	5.63	0.33	1.73	0.82
C5H12O5S	184.0405	0.54	0.00	2.40	1.00
C8H14O8S	270.0409	1.20	0.25	1.75	1.00
C7H5NO6	199.0117	2.68	1.00	0.71	0.86
C11H10O5	222.0528	2.90	1.00	0.91	0.45
C9H15NO6	233.0899	3.23	0.50	1.67	0.67
C8H13NO8	251.0641	0.85	0.38	1.63	1.00
C9H7NO6	225.0273	3.20	1.00	0.78	0.67
C13H20O5	256.1311	4.64	0.80	1.54	0.38
C6H5NO3	139.0269	0.49	1.00	0.83	0.50
C7H8O3	140.0473	0.52	1.00	1.14	0.43
C9H14O8S	282.0409	1.91	0.38	1.56	0.89
C6H10O5	162.0528	2.43	0.40	1.67	0.83
C10H17NO7S	295.0726	4.71	0.43	1.70	0.70
C8H6O2	134.0368	1.80	1.00	0.75	0.25
C8H12N2O11	312.0441	3.49	0.36	1.50	1.38
C5H4O5	144.0059	0.39	0.80	0.80	1.00
C4H4O2	84.0211	0.39	1.00	1.00	0.50
C5H8O	84.0575	0.75	1.00	1.60	0.20
C5H9NO8S	243.0049	2.59	0.25	1.80	1.60
C8H8O6	200.0321	2.60	0.83	1.00	0.75
C8H13NO9	267.0590	1.07	0.33	1.63	1.13
C7H9NO9	251.0277	0.66	0.44	1.29	1.29
C12H9NO4	231.0532	7.42	1.00	0.75	0.33
C9H4O5	192.0059	2.82	1.00	0.44	0.56
C3H2N2O3	114.0065	0.42	1.00	0.67	1.00
C16H12OS	252.0609	2.23	1.00	0.75	0.06
C12H21NO9	323.1216	3.34	0.33	1.75	0.75
C10H17NO7S	295.0726	7.04	0.43	1.70	0.70
C8H8N2O6	228.0382	4.05	1.00	1.00	0.75
C11H19N3O15	433.0816	8.09	0.27	1.73	1.36
C7H5NO5	183.0168	1.27	1.00	0.71	0.71
C20H13N3O3S	375.0678	8.23	1.00	0.65	0.15
C8H9NO4	183.0532	7.00	1.00	1.13	0.50
C11H6N4OS	242.0262	0.63	1.00	0.55	0.09
C7H5NOS	151.0092	3.93	1.00	0.71	0.14
C9H15NO8S	297.0518	2.92	0.38	1.67	0.89
C13H22O4	242.1518	6.74	0.75	1.69	0.31
C10H14O6S	262.0511	3.01	0.67	1.40	0.60
C15H22O6	298.1416	3.14	0.83	1.47	0.40
C4H6O	70.0419	0.44	1.00	1.50	0.25
C8H16O9S	288.0515	1.22	0.11	2.00	1.13
C10H12O7	244.0583	2.46	0.71	1.20	0.70
C5H5NO4	143.0219	1.25	1.00	1.00	0.80
C16H26O6	314.1729	7.21	0.67	1.63	0.38
C8H15NO9S	301.0468	2.34	0.22	1.88	1.13
C5H5NO3	127.0269	0.38	1.00	1.00	0.60
C4H3NO3	113.0113	0.54	1.00	0.75	0.75
C8H16N2O5S2	284.0501	1.45	0.40	2.00	0.63
C9H16O4	188.1049	1.46	0.50	1.78	0.44
C6H11NO9S	273.0155	0.99	0.22	1.83	1.50
C8H13NO10S	315.0260	2.69	0.30	1.63	1.25
C9H15NO7	249.0849	2.91	0.43	1.67	0.78
C6H7NO5	173.0324	0.75	0.80	1.17	0.83
C9H8O5	196.0372	2.76	1.00	0.89	0.56
C7H6O4	154.0266	2.59	1.00	0.86	0.57
C7H7NO2	137.0477	2.36	1.00	1.00	0.29
C15H22O9	346.1264	2.92	0.56	1.47	0.60
C6H4N2O5	184.0120	4.48	1.00	0.67	0.83
C10H14O8S	294.0409	0.87	0.50	1.40	0.80
C7H9NO8	235.0328	1.05	0.50	1.29	1.14

7 Appendix

C8H6O3	150.0317	0.84	1.00	0.75	0.38
C8H14O2	142.0994	3.17	1.00	1.75	0.25
C7H11NO8	237.0485	1.54	0.38	1.57	1.14
C10H13NO4	211.0845	7.68	1.00	1.30	0.40
C10H18N2O11S	374.0631	5.00	0.27	1.80	1.10
C9H9NO6	227.0430	3.37	1.00	1.00	0.67
C11H9NO3	203.0582	8.07	1.00	0.82	0.27
C7H4N2O3	164.0222	3.98	1.00	0.57	0.43
C9H10O2	150.0681	3.76	1.00	1.11	0.22
C10H6N2O5	234.0277	7.62	1.00	0.60	0.50
C5H11N3O11	289.0394	2.67	0.18	2.20	2.20
C8H6O3	150.0317	1.16	1.00	0.75	0.38
C10H6O5	206.0215	3.17	1.00	0.60	0.50
C5H10N2O8	226.0437	2.91	0.25	2.00	1.60
C10H18N2O8	294.1063	6.73	0.38	1.80	0.80
C8H11NO5	201.0637	0.93	0.80	1.38	0.63
C13H8O2	196.0524	7.53	1.00	0.62	0.15
C7H5NO4	167.0219	3.77	1.00	0.71	0.57
C11H15NO2	193.1103	7.18	1.00	1.36	0.18
C12H16O5	240.0998	5.50	1.00	1.33	0.42
C9H11NO3	181.0739	7.95	1.00	1.22	0.33
C7H8O3	140.0473	2.53	1.00	1.14	0.43
C5H10O2	102.0681	0.62	0.50	2.00	0.40
C8H9NO5	199.0481	5.36	1.00	1.13	0.63
C10H17N3O11	355.0863	7.47	0.36	1.70	1.10
C3H2N2O4	130.0015	0.59	1.00	0.67	1.33
C12H20O8S	324.0879	2.75	0.38	1.67	0.67
C8H12O2	140.0837	1.16	1.00	1.50	0.25
C16H19NO3	273.1365	7.39	1.00	1.19	0.19
C8H10O5	186.0528	8.26	0.80	1.25	0.63
C9H12O7S	264.0304	1.74	0.57	1.33	0.78
C11H6N4O5S	242.0262	0.91	1.00	0.55	0.09
C8H8N4O5S	272.0215	1.86	1.00	1.00	0.63
C8H8O6	200.0321	0.93	0.83	1.00	0.75
C9H16O6S	252.0668	4.10	0.33	1.78	0.67
C12H12O5	236.0685	3.15	1.00	1.00	0.42
C7H6N2O3	166.0378	3.45	1.00	0.86	0.43
C8H7NO3	165.0426	2.13	1.00	0.88	0.38
C5H8O	84.0575	0.54	1.00	1.60	0.20
C7H9NO9S	282.9998	0.99	0.44	1.29	1.29
C13H18O5	254.1154	3.11	1.00	1.38	0.38
C6H11NO8S	257.0205	2.08	0.25	1.83	1.33
C6H10O9S	258.0046	0.96	0.22	1.67	1.50
C10H17NO7S	295.0726	6.32	0.43	1.70	0.70
C10H18O6S	266.0824	2.61	0.33	1.80	0.60
C6H13NO8	227.0641	0.70	0.13	2.17	1.33
C10H20O4	204.1362	2.84	0.25	2.00	0.40
C16H29NO8	363.1893	8.19	0.38	1.81	0.50
C9H6O5	194.0215	1.25	1.00	0.67	0.56
C8H8O5S	216.0092	1.01	1.00	1.00	0.63
C8H6O5	182.0215	2.51	1.00	0.75	0.63
C10H17NO7S	295.0726	6.62	0.43	1.70	0.70
C10H9NO4	207.0532	4.84	1.00	0.90	0.40
C11H8O6	236.0321	2.98	1.00	0.73	0.55
C9H11NO4	197.0688	6.59	1.00	1.22	0.44
C7H14N2O8S	286.0471	1.26	0.25	2.00	1.14
C8H10O3	154.0630	2.68	1.00	1.25	0.38
C5H9N3O13S	350.9856	6.68	0.23	1.80	2.60
C15H20O10	360.1056	2.79	0.60	1.33	0.67
C8H8N4O5S	272.0215	1.28	1.00	1.00	0.63
C4H7NO8S	228.9892	1.09	0.25	1.75	2.00
C6H9NO3	143.0582	0.64	1.00	1.50	0.50
C9H8N4O3S2	284.0038	2.29	1.00	0.89	0.33
C5H9NO7S	227.0100	3.14	0.29	1.80	1.40
C10H9NO4	207.0532	4.52	1.00	0.90	0.40
C11H20N2O11	356.1067	3.75	0.27	1.82	1.00
C8H8N2O6	228.0382	3.76	1.00	1.00	0.75
C5H8O2	100.0524	2.37	1.00	1.60	0.40
C15H24O6	300.1573	7.11	0.67	1.60	0.40
C6H12O4	148.0736	1.28	0.25	2.00	0.67

7 Appendix

C12H15NO4	237.1001	5.60	1.00	1.25	0.33
C9H10O3	166.0630	3.07	1.00	1.11	0.33
C8H7NO3	165.0426	3.18	1.00	0.88	0.38
C4H5N3O2	127.0382	1.08	1.00	1.25	0.50
C10H11NO6	241.0586	3.52	1.00	1.10	0.60
C10H18O6	234.1103	0.66	0.33	1.80	0.60
C10H19NO7	265.1162	3.16	0.29	1.90	0.70
C7H11NO6	205.0586	2.84	0.50	1.57	0.86
C14H26O4	258.1831	4.33	0.50	1.86	0.29
C9H16O3	172.1099	2.75	0.67	1.78	0.33
C10H17N3O10	339.0914	8.22	0.40	1.70	1.00
C10H16N2O10S	356.0526	7.39	0.40	1.60	1.00
C8H16O4	176.1049	2.39	0.25	2.00	0.50
C13H8O2	196.0524	7.16	1.00	0.62	0.15
C7H11NO10S	301.0104	1.84	0.30	1.57	1.43
C10H14O7S	278.0460	2.56	0.57	1.40	0.70
C9H7NO5	209.0324	3.96	1.00	0.78	0.56
C8H13NO7	235.0692	2.72	0.43	1.63	0.88
C7H11NO7	221.0536	3.13	0.43	1.57	1.00
C17H24O10	388.1369	3.05	0.60	1.41	0.59
C7H9NO5	187.0481	2.79	0.80	1.29	0.71
C13H16O6	268.0947	2.98	1.00	1.23	0.46
C5H7NO9S	256.9842	0.76	0.33	1.40	1.80
C6H5NO2	123.0320	1.57	1.00	0.83	0.33
C15H13NO2S	271.0667	4.11	1.00	0.87	0.13
C15H25NO7	331.1631	7.70	0.57	1.67	0.47
C8H9NO4	183.0532	4.14	1.00	1.13	0.50
C19H22O4	314.1518	7.71	1.00	1.16	0.21
C8H18O4S	210.0926	7.18	0.00	2.25	0.50
C6H5NO5	171.0168	1.05	1.00	0.83	0.83
C9H7NO6	225.0273	3.68	1.00	0.78	0.67
C6H12N2O5S	224.0467	7.57	0.40	2.00	0.83
C9H13NO10S	327.0260	3.16	0.40	1.44	1.11
C3H6O	58.0419	0.54	1.00	2.00	0.33
C13H9NO3	227.0582	8.23	1.00	0.69	0.23
C5H8O	84.0575	2.79	1.00	1.60	0.20
C10H17NO7	263.1005	4.19	0.43	1.70	0.70
C9H16O4S	220.0769	2.01	0.50	1.78	0.44
C16H19NO3	273.1365	7.72	1.00	1.19	0.19
C8H8N2O4	196.0484	3.18	1.00	1.00	0.50
C18H14O8	358.0689	7.45	1.00	0.78	0.44
C13H9NO2S	243.0354	1.64	1.00	0.69	0.15
C4H4O3	100.0160	2.78	1.00	1.00	0.75
C11H22O7	266.1366	0.76	0.14	2.00	0.64
C12H18O4	226.1205	3.07	1.00	1.50	0.33
C9H13NO10S	327.0260	2.78	0.40	1.44	1.11
C7H7NO5	185.0324	2.59	1.00	1.00	0.71
C16H20O10	372.1056	2.77	0.70	1.25	0.63
C4H4N2O4	144.0171	0.95	1.00	1.00	1.00
C9H8O4	180.0423	1.36	1.00	0.89	0.44
C9H15NO7	249.0849	4.78	0.43	1.67	0.78
C6H9NO7	207.0379	2.63	0.43	1.50	1.17
C11H14N2O4	238.0954	7.57	1.00	1.27	0.36
C12H16O4	224.1049	3.08	1.00	1.33	0.33
C9H9NO7S	275.0100	3.34	0.86	1.00	0.78
C8H6O5	182.0215	1.90	1.00	0.75	0.63
C17H24O8	356.1471	3.13	0.75	1.41	0.47
C3H6O2	74.0368	3.02	0.50	2.00	0.67
C8H14O	126.1045	2.55	1.00	1.75	0.13
C6H7NO	109.0528	0.72	1.00	1.17	0.17
C8H15NO8S	285.0518	3.33	0.25	1.88	1.00
C10H16N2O10	324.0805	7.68	0.40	1.60	1.00
C8H8O4	168.0423	3.12	1.00	1.00	0.50
C9H9NO4	195.0532	6.23	1.00	1.00	0.44
C8H13NO4	187.0845	0.91	0.75	1.63	0.50
C9H6O3	162.0317	3.16	1.00	0.67	0.33
C9H6O3	162.0317	2.87	1.00	0.67	0.33
C14H9NO3	239.0582	8.21	1.00	0.64	0.21
C8H15NO10S	317.0417	2.72	0.20	1.88	1.25
C8H16O3	160.1099	1.10	0.33	2.00	0.38

7 Appendix

C16H20O11	388.1006	2.78	0.64	1.25	0.69
C19H32O5	340.2250	7.85	0.80	1.68	0.26
C13H10N4O5	270.0575	2.15	1.00	0.77	0.08
C15H10N4O2S2	342.0245	1.22	1.00	0.67	0.13
C10H19NO11S	361.0679	2.82	0.18	1.90	1.10
C9H17NO7	251.1005	3.07	0.29	1.89	0.78
C13H6O10	321.9961	0.83	1.00	0.46	0.77
C14H10O4S2	306.0020	0.88	1.00	0.71	0.29
C10H17NO9S	327.0624	4.34	0.33	1.70	0.90
C11H7NO5	233.0324	7.26	1.00	0.64	0.45
C16H10N4O4S2	386.0143	1.23	1.00	0.63	0.25
C7H5NO6	199.0117	0.97	1.00	0.71	0.86
C8H9NO3	167.0582	2.80	1.00	1.13	0.38
C7H6O5	170.0215	1.46	1.00	0.86	0.71
C8H8O4S	200.0143	1.00	1.00	1.00	0.50
C8H7NO6	213.0273	3.26	1.00	0.88	0.75
C17H29NO9	391.1842	7.50	0.44	1.71	0.53
C8H16O3	160.1099	1.48	0.33	2.00	0.38
C8H9NO4	183.0532	4.70	1.00	1.13	0.50
C5H9NO3	131.0582	0.89	0.67	1.80	0.60
C5H8O6S	196.0042	1.05	0.33	1.60	1.20
C6H7NO3	141.0426	2.47	1.00	1.17	0.50
C9H10O5S	230.0249	2.53	1.00	1.11	0.56
C7H10O6S	222.0198	1.08	0.50	1.43	0.86
C12H20O7S	308.0930	2.82	0.43	1.67	0.58
C10H17NO7	263.1005	5.48	0.43	1.70	0.70
C7H5NO6	199.0117	1.57	1.00	0.71	0.86
C12H8N4O5	256.0419	1.06	1.00	0.67	0.08
C9H7NO3	177.0426	2.76	1.00	0.78	0.33
C7H6O4	154.0266	1.06	1.00	0.86	0.57
C16H19NO3	273.1365	8.21	1.00	1.19	0.19
C15H24O8S	364.1192	3.06	0.50	1.60	0.53
C14H10O5	258.0528	3.66	1.00	0.71	0.36
C8H7NO4	181.0375	1.48	1.00	0.88	0.50
C11H20O7S	296.0930	2.52	0.29	1.82	0.64
C8H12O5	188.0685	8.07	0.60	1.50	0.63
C18H34O5	330.2406	7.45	0.40	1.89	0.28
C9H17NO8	267.0954	2.70	0.25	1.89	0.89
C12H12O4	220.0736	3.20	1.00	1.00	0.33
C8H6N2O7	242.0175	6.55	1.00	0.75	0.88
C11H17NO10S	355.0573	3.02	0.40	1.55	0.91
C12H16O10	320.0743	2.59	0.50	1.33	0.83
C16H26O6	314.1729	3.39	0.67	1.63	0.38
C11H19NO7	277.1162	7.00	0.43	1.73	0.64
C20H14N2O5	330.0827	4.28	1.00	0.70	0.05
C14H9NO5	271.0481	7.51	1.00	0.64	0.36
C11H14N2O4	238.0954	7.91	1.00	1.27	0.36
C10H14O6	230.0790	8.23	0.67	1.40	0.60
C19H28O7	368.1835	7.18	0.86	1.47	0.37
C10H12O3	180.0786	7.88	1.00	1.20	0.30
C9H9NO3	179.0582	2.96	1.00	1.00	0.33
C13H17NO3	235.1208	7.58	1.00	1.31	0.23
C20H14N2O5	330.0827	5.50	1.00	0.70	0.05
C2H4O5S	139.9779	2.68	0.20	2.00	2.50
C13H10O3S2	278.0071	1.64	1.00	0.77	0.23
C16H17NO4	287.1158	3.82	1.00	1.06	0.25
C10H13NO5	227.0794	3.99	1.00	1.30	0.50
C3H6O5S	153.9936	2.59	0.20	2.00	1.67
C6H6N2O2	138.0429	0.94	1.00	1.00	0.33
C10H18N2O10	326.0961	3.89	0.30	1.80	1.00
C17H26O7	342.1679	7.97	0.71	1.53	0.41
C16H29NO7	347.1944	7.95	0.43	1.81	0.44
C6H6N2O3	154.0378	2.14	1.00	1.00	0.50
C14H18O5	266.1154	3.30	1.00	1.29	0.36
C14H8O4	240.0423	3.96	1.00	0.57	0.29
C9H8O2	148.0524	2.38	1.00	0.89	0.22
C10H16N2O9	308.0856	7.51	0.44	1.60	0.90
C8H8O4S	200.0143	2.70	1.00	1.00	0.50
C5H4O8S2	255.9348	2.05	0.50	0.80	1.60
C15H22O3	250.1569	8.28	1.00	1.47	0.20

7 Appendix

C4H7NO3	117.0426	0.88	0.67	1.75	0.75
C7H12O	112.0888	2.69	1.00	1.71	0.14
C11H13NO5	239.0794	8.09	1.00	1.18	0.45
C14H20O5	268.1311	7.66	1.00	1.43	0.36
C7H12O	112.0888	1.33	1.00	1.71	0.14
C27H22O3	394.1569	8.39	1.00	0.81	0.11
C8H12O	124.0888	2.83	1.00	1.50	0.13
C11H19NO7	277.1162	3.89	0.43	1.73	0.64
C9H17NO9S	315.0624	6.32	0.22	1.89	1.00
C8H6N2O5	210.0277	3.41	1.00	0.75	0.63
C11H19N3O12	385.0969	7.68	0.33	1.73	1.09
C7H11NO4	173.0688	1.73	0.75	1.57	0.57
C13H8O3	212.0473	7.50	1.00	0.62	0.23
C11H19NO9S	341.0781	3.51	0.33	1.73	0.82
C13H23NO10S	385.1043	4.78	0.30	1.77	0.77
C13H18O4	238.1205	3.17	1.00	1.38	0.31
C12H21NO7	291.1318	7.49	0.43	1.75	0.58
C12H18O4	226.1205	5.85	1.00	1.50	0.33
C10H16N2O9	308.0856	7.86	0.44	1.60	0.90
C14H30O3S	278.1916	8.39	0.00	2.14	0.21
C5H7NO9S	256.9842	2.22	0.33	1.40	1.80
C9H15NO4	201.1001	1.52	0.75	1.67	0.44
C8H4N2O10S	319.9587	8.61	0.80	0.50	1.25
C10H13NO4	211.0845	6.62	1.00	1.30	0.40
C8H5NO7	227.0066	2.28	1.00	0.63	0.88
C13H20O3	224.1412	7.65	1.00	1.54	0.23
C16H24O2	248.1776	8.55	1.00	1.50	0.13
C20H14N2OS	330.0827	7.31	1.00	0.70	0.05
C6H11NO3	145.0739	1.45	0.67	1.83	0.50
C17H24O7	340.1522	8.11	0.86	1.41	0.41
C16H26N2O10	406.1587	8.39	0.50	1.63	0.63

Table S4.3.3 Molecular formulas of organic compounds detected in Beijing OA in ESI⁻ mode.

Formula [M]	Neutral mass (Da)	RT (min)	MCR	H/C	O/C
C6H5NO3	139.0269	3.72	1.00	0.83	0.50
C2H4O6S	155.9729	0.36	0.17	2.00	3.00
C4H6O5	134.0215	0.38	0.40	1.50	1.25
C3H6O6S	169.9885	0.38	0.17	2.00	2.00
C7H6O2	122.0368	2.70	1.00	0.86	0.29
C5H6O5	146.0215	0.38	0.60	1.20	1.00
C5H6O4	130.0266	0.40	0.75	1.20	0.80
C5H4N2O3	140.0222	2.36	1.00	0.80	0.60
C4H2O11S2	289.9039	0.34	0.36	0.50	2.75
C8H7NO3	165.0426	5.04	1.00	0.88	0.38
C13H8O2	196.0524	7.53	1.00	0.62	0.15
C7H6N2O5	198.0277	7.39	1.00	0.86	0.71
C7H7NO3	153.0426	5.95	1.00	1.00	0.43
C4H8O3	104.0473	0.10	0.33	2.00	0.75
C5H6O3	114.0317	0.40	1.00	1.20	0.60
C7H7NO3	153.0426	5.15	1.00	1.00	0.43
C5H8O3	116.0473	0.09	0.67	1.60	0.60
C6H6N2O3	154.0378	2.83	1.00	1.00	0.50
C5H8O4	132.0423	0.41	0.50	1.60	0.80
C2H4O2	60.0211	0.40	0.50	2.00	1.00
C8H8O3	152.0473	2.64	1.00	1.00	0.38
C9H6O6	210.0164	1.15	1.00	0.67	0.67
C8H6N2O2	162.0429	6.01	1.00	0.75	0.25
C18H14O8	358.0689	7.45	1.00	0.78	0.44
C4H6O6S	181.9885	0.39	0.33	1.50	1.50
C9H8O2	148.0524	3.08	1.00	0.89	0.22
C4H10O5S	170.0249	0.40	0.00	2.50	1.25
C5H4O4	128.0110	0.39	1.00	0.80	0.80
C5H10O3	118.0630	0.14	0.33	2.00	0.60
C15H6OS	234.0139	2.69	1.00	0.40	0.07

7 Appendix

C8H9NO4	183.0532	7.00	1.00	1.13	0.50
C2H3NO3	89.0113	0.39	0.67	1.50	1.50
C13H8O2	196.0524	7.16	1.00	0.62	0.15
C17H14O6	314.0790	7.97	1.00	0.82	0.35
C2H2O3	74.0004	0.36	0.67	1.00	1.50
C7H6O4	154.0266	1.30	1.00	0.86	0.57
C3H4O2	72.0211	0.40	1.00	1.33	0.67
C7H6O5S	201.9936	0.64	1.00	0.86	0.71
C12H6O4	214.0266	5.48	1.00	0.50	0.33
C9H16O5	204.0998	2.77	0.40	1.78	0.56
C4H4O5	132.0059	0.37	0.60	1.00	1.25
C6H12O3	132.0786	0.15	0.33	2.00	0.50
C7H6O4	154.0266	2.59	1.00	0.86	0.57
C3H3N3O3	129.0174	0.38	1.00	1.00	1.00
C14H8O3	224.0473	7.57	1.00	0.57	0.21
C8H6O6	198.0164	3.13	1.00	0.75	0.75
C9H7NO4	193.0375	3.46	1.00	0.78	0.44
C4H6O2	86.0368	0.40	1.00	1.50	0.50
C7H12O7S	240.0304	0.58	0.29	1.71	1.00
C4H4O3	100.0160	0.41	1.00	1.00	0.75
C3H8O4S	140.0143	0.51	0.00	2.67	1.33
C8H9NO7S	263.0100	3.60	0.71	1.13	0.88
C5H5NO3	127.0269	1.03	1.00	1.00	0.60
C7H5NO2	135.0320	2.66	1.00	0.71	0.29
C6H6O4	142.0266	0.40	1.00	1.00	0.67
C6H3N3O7	228.9971	4.09	1.00	0.50	1.17
C8H8O3	152.0473	1.72	1.00	1.00	0.38
C13H7NO4	241.0375	7.83	1.00	0.54	0.31
C5H4O3	112.0160	0.39	1.00	0.80	0.60
C3H3NO4	117.0062	0.40	0.75	1.00	1.33
C8H6O2	134.0368	1.77	1.00	0.75	0.25
C13H11NO3	229.0739	8.11	1.00	0.85	0.23
C7H5NO6	199.0117	3.46	1.00	0.71	0.86
C8H5NO6	211.0117	3.03	1.00	0.63	0.75
C9H6O3	162.0317	3.16	1.00	0.67	0.33
C9H16O5	204.0998	2.57	0.40	1.78	0.56
C7H12O6S	224.0355	0.81	0.33	1.71	0.86
C4H5NO2	99.0320	0.11	1.00	1.25	0.50
C8H8N2O5	212.0433	7.91	1.00	1.00	0.63
C8H9NO5	199.0481	2.47	1.00	1.13	0.63
C6H8O2	112.0524	1.00	1.00	1.33	0.33
C6H6N2O2	138.0429	0.40	1.00	1.00	0.33
C6H5NO2	123.0320	0.40	1.00	0.83	0.33
C10H16O7S	280.0617	1.03	0.43	1.60	0.70
C5H5NO3	127.0269	0.39	1.00	1.00	0.60
C12H8O4	216.0423	4.03	1.00	0.67	0.33
C10H17NO7S	295.0726	4.68	0.43	1.70	0.70
C8H9NO4	183.0532	6.44	1.00	1.13	0.50
C6H9NO4	159.0532	0.40	0.75	1.50	0.67
C15H9NO3S	283.0303	3.79	1.00	0.60	0.20
C9H7NO	145.0528	2.26	1.00	0.78	0.11
C7H5NO6	199.0117	2.68	1.00	0.71	0.86
C14H10O4S	274.0300	7.11	1.00	0.71	0.29
C5H4N2O3	140.0222	0.41	1.00	0.80	0.60
C13H8O3	212.0473	7.03	1.00	0.62	0.23
C9H7NO3	177.0426	3.21	1.00	0.78	0.33
C16H10O	218.0732	8.36	1.00	0.63	0.06
C5H5NO4	143.0219	0.39	1.00	1.00	0.80
C4H4N2O2	112.0273	0.39	1.00	1.00	0.50
C7H5NO	119.0371	3.12	1.00	0.71	0.14
C9H6O7	226.0114	2.91	1.00	0.67	0.78
C7H7NO2	137.0477	2.36	1.00	1.00	0.29
C8H18O4S	210.0926	7.17	0.00	2.25	0.50
C13H8O3	212.0473	7.51	1.00	0.62	0.23
C10H10O2	162.0681	3.39	1.00	1.00	0.20
C5H3N3O2	137.0225	3.17	1.00	0.60	0.40
C6H4N2O5	184.0120	6.20	1.00	0.67	0.83
C6H4O4	140.0110	0.39	1.00	0.67	0.67
C5H8O2	100.0524	0.67	1.00	1.60	0.40
C6H7NO	109.0528	0.49	1.00	1.17	0.17

7 Appendix

C9H7NO4	193.0375	2.35	1.00	0.78	0.44
C10H18N2O11S	374.0631	4.38	0.27	1.80	1.10
C8H6O	118.0419	3.17	1.00	0.75	0.13
C14H8O5	256.0372	7.07	1.00	0.57	0.36
C15H10O2	222.0681	7.22	1.00	0.67	0.13
C9H9NO3	179.0582	7.43	1.00	1.00	0.33
C9H6O7	226.0114	1.07	1.00	0.67	0.78
C6H11NO3	145.0739	0.64	0.67	1.83	0.50
C4H3N3O4	157.0124	3.21	1.00	0.75	1.00
C9H7NO4	193.0375	1.35	1.00	0.78	0.44
C3H2O5	117.9902	0.38	0.60	0.67	1.67
C4H8O2	88.0524	0.43	0.50	2.00	0.50
C9H7NO	145.0528	3.47	1.00	0.78	0.11
C7H6N2O3	166.0378	3.45	1.00	0.86	0.43
C7H8N2O3	168.0535	3.72	1.00	1.14	0.43
C11H8O3	188.0473	7.77	1.00	0.73	0.27
C6H5N3O4	183.0280	4.90	1.00	0.83	0.67
C11H18O6	246.1103	4.35	0.50	1.64	0.55
C13H8O3	212.0473	6.52	1.00	0.62	0.23
C12H5NO6	259.0117	3.94	1.00	0.42	0.50
C15H8O4	252.0423	7.61	1.00	0.53	0.27
C6H10N2O3	158.0691	1.06	1.00	1.67	0.50
C11H8O3	188.0473	7.26	1.00	0.73	0.27
C7H9NO	123.0684	0.69	1.00	1.29	0.14
C9H9NO4	195.0532	6.23	1.00	1.00	0.44
C6H4N2O5	184.0120	4.47	1.00	0.67	0.83
C10H6O6	222.0164	1.35	1.00	0.60	0.60
C14H13NO3	243.0895	8.27	1.00	0.93	0.21
C8H6N2O6	226.0226	3.01	1.00	0.75	0.75
C15H8O4	252.0423	5.25	1.00	0.53	0.27
C13H10O4	230.0579	5.35	1.00	0.77	0.31
C8H9NO4	183.0532	4.14	1.00	1.13	0.50
C14H8O3	224.0473	6.88	1.00	0.57	0.21
C14H8O5	256.0372	6.45	1.00	0.57	0.36
C13H8O2	196.0524	4.95	1.00	0.62	0.15
C10H17NO4	215.1158	3.62	0.75	1.70	0.40
C18H34O5	330.2406	7.45	0.40	1.89	0.28
C12H8N2O6	276.0382	7.94	1.00	0.67	0.50
C15H12O2	224.0837	8.10	1.00	0.80	0.13
C7H12O	112.0888	3.12	1.00	1.71	0.14
C4H4N4O7S	251.9801	0.82	0.71	1.00	1.75
C8H5NO6	211.0117	2.57	1.00	0.63	0.75
C9H16O4	188.1049	3.72	0.50	1.78	0.44
C3H4O4	104.0110	0.39	0.50	1.33	1.33
C5H8O5	148.0372	0.40	0.40	1.60	1.00
C4H6O4	118.0266	0.53	0.50	1.50	1.00
C4H4O4	116.0110	0.40	0.75	1.00	1.00
C2H4O5S	139.9779	0.36	0.20	2.00	2.50
C6H8O5	160.0372	0.40	0.60	1.33	0.83
C5H8O4	132.0423	0.76	0.50	1.60	0.80
C9H14O5	202.0841	2.68	0.60	1.56	0.56
C10H18O4	202.1205	5.19	0.50	1.80	0.40
C3H6O4S	137.9987	0.37	0.25	2.00	1.33
C10H16O5	216.0998	2.95	0.60	1.60	0.50
C7H10O5	174.0528	0.93	0.60	1.43	0.71
C6H8O4	144.0423	0.67	0.75	1.33	0.67
C8H12O5	188.0685	1.83	0.60	1.50	0.63
C10H12N4OS2	268.0453	3.72	1.00	1.20	0.10
C7H12O3	144.0786	1.10	0.67	1.71	0.43
C8H12O6	204.0634	2.27	0.50	1.50	0.75
C16H22O4	278.1518	8.48	1.00	1.38	0.25
C3H6O2	74.0368	0.42	0.50	2.00	0.67
C6H12O4	148.0736	0.54	0.25	2.00	0.67
C8H15NO3	173.1052	2.59	0.67	1.88	0.38
C8H14O	126.1045	3.71	1.00	1.75	0.13
C10H18O4	202.1205	2.89	0.50	1.80	0.40
C3H5NO3	103.0269	0.39	0.67	1.67	1.00
C13H20O6	272.1260	3.11	0.67	1.54	0.46
C7H6N4OS2	225.9983	1.64	1.00	0.86	0.14

Table S4.3.4 Molecular formulas of organic compounds detected in Shanghai OA in ESI⁻ mode.

Formula [M]	Neutral mass (Da)	RT (min)	MCR	H/C	O/C
C2H4O4	92.0110	0.18	0.25	2.00	2.00
C2H4O4	92.0110	0.41	0.25	2.00	2.00
C6H8O7	192.0270	0.38	0.43	1.33	1.17
C10H7NO3	189.0426	7.73	1.00	0.70	0.30
C7H7NO4	169.0375	3.82	1.00	1.00	0.57
C7H7NO4	169.0375	4.66	1.00	1.00	0.57
C7H6O3	138.0317	2.34	1.00	0.86	0.43
C6H5N3O4	183.0280	4.91	1.00	0.83	0.67
C8H5NO2	147.0320	3.26	1.00	0.63	0.25
C13H8O2	196.0524	7.52	1.00	0.62	0.15
C18H14O8	358.0689	7.43	1.00	0.78	0.44
C10H6O5	206.0215	3.14	1.00	0.60	0.50
C8H6O5S	213.9936	1.59	1.00	0.75	0.63
C8H5NO3	163.0269	2.66	1.00	0.63	0.38
C3H8O5S	156.0092	0.36	0.00	2.67	1.67
C4H6O7S	197.9834	0.35	0.29	1.50	1.75
C9H6O5	194.0215	0.83	1.00	0.67	0.56
C10H17NO7S	295.0726	4.68	0.43	1.70	0.70
C9H8O2	148.0524	3.09	1.00	0.89	0.22
C8H7NO5	197.0324	4.69	1.00	0.88	0.63
C7H6O3	138.0317	2.77	1.00	0.86	0.43
C13H8O2	196.0524	7.18	1.00	0.62	0.15
C8H6N2O2	162.0429	6.07	1.00	0.75	0.25
C8H6O5	182.0215	2.46	1.00	0.75	0.63
C8H8O3	152.0473	2.64	1.00	1.00	0.38
C5H4N2O3	140.0222	2.40	1.00	0.80	0.60
C12H9NO3	215.0582	7.86	1.00	0.75	0.25
C4H10O5S	170.0249	0.38	0.00	2.50	1.25
C11H9NO3	203.0582	7.97	1.00	0.82	0.27
C14H10O4	242.0579	5.04	1.00	0.71	0.29
C7H6O5S	201.9936	0.63	1.00	0.86	0.71
C9H6O5	194.0215	2.60	1.00	0.67	0.56
C8H12O4	172.0736	2.47	0.75	1.50	0.50
C3H4N2O2S	131.9993	0.33	1.00	1.33	0.67
C8H6O5	182.0215	1.07	1.00	0.75	0.63
C8H9NO7S	263.0100	3.59	0.71	1.13	0.88
C7H6O4	154.0266	2.60	1.00	0.86	0.57
C12H8O4	216.0423	4.04	1.00	0.67	0.33
C9H8O4	180.0423	2.75	1.00	0.89	0.44
C5H5NO4S	174.9939	0.36	1.00	1.00	0.80
C9H5NO4	191.0219	2.64	1.00	0.56	0.44
C9H9NO7S	275.0100	4.20	0.86	1.00	0.78
C5H8O6	164.0321	0.36	0.33	1.60	1.20
C8H9NO4	183.0532	7.04	1.00	1.13	0.50
C10H8O5	208.0372	2.55	1.00	0.80	0.50
C10H8O4	192.0423	3.10	1.00	0.80	0.40
C9H6O5	194.0215	2.79	1.00	0.67	0.56
C13H31N3O11	405.1959	8.00	0.00	2.38	0.85
C12H7NO4	229.0375	8.00	1.00	0.58	0.33
C9H6O6	210.0164	1.98	1.00	0.67	0.67
C8H6O5	182.0215	1.93	1.00	0.75	0.63
C8H8O2	136.0524	3.04	1.00	1.00	0.25
C6H6N2O3	154.0378	2.84	1.00	1.00	0.50
C8H16O6S	240.0668	2.86	0.17	2.00	0.75
C10H8O5	208.0372	2.81	1.00	0.80	0.50
C8H9NO4	183.0532	5.67	1.00	1.13	0.50
C4H10O4S	154.0300	0.93	0.00	2.50	1.00
C7H4N2O4	180.0171	3.51	1.00	0.57	0.57
C8H6O4	166.0266	1.34	1.00	0.75	0.50
C10H8O4	192.0423	6.98	1.00	0.80	0.40
C6H6O6	174.0164	0.37	0.67	1.00	1.00
C8H6O6S	229.9885	2.52	1.00	0.75	0.75
C6H8O4	144.0423	0.70	0.75	1.33	0.67
C8H6O3	150.0317	0.82	1.00	0.75	0.38

7 Appendix

C14H14N2O5S2	354.0344	2.65	1.00	1.00	0.36
C12H9NO4	231.0532	7.43	1.00	0.75	0.33
C8H5NO3	163.0269	2.99	1.00	0.63	0.38
C8H7NO5	197.0324	4.29	1.00	0.88	0.63
C9H8O3	164.0473	2.48	1.00	0.89	0.33
C5H10O5S	182.0249	0.51	0.20	2.00	1.00
C8H8O3	152.0473	5.33	1.00	1.00	0.38
C10H10O4	194.0579	3.67	1.00	1.00	0.40
C6H14O6S	214.0511	0.38	0.00	2.33	1.00
C9H5NO4	191.0219	2.05	1.00	0.56	0.44
C5H5NO5S	190.9888	0.38	0.80	1.00	1.00
C3H3NO2	85.0164	0.09	1.00	1.00	0.67
C10H10O3	178.0630	3.80	1.00	1.00	0.30
C9H6O3	162.0317	3.14	1.00	0.67	0.33
C10H20O5S	252.1031	7.00	0.20	2.00	0.50
C12H9NO4	231.0532	7.80	1.00	0.75	0.33
C16H10O	218.0732	8.36	1.00	0.63	0.06
C11H8O3	188.0473	7.77	1.00	0.73	0.27
C6H6O5	158.0215	0.38	0.80	1.00	0.83
C5H6O3	114.0317	0.38	1.00	1.20	0.60
C9H15NO8S	297.0518	3.26	0.38	1.67	0.89
C13H7NO4	241.0375	7.83	1.00	0.54	0.31
C5H7NO6S	208.9994	0.38	0.50	1.40	1.20
C14H10O3	226.0630	7.20	1.00	0.71	0.21
C9H6O4	178.0266	2.95	1.00	0.67	0.44
C3H7NO5S	169.0045	0.36	0.20	2.33	1.67
C10H17NO7S	295.0726	6.60	0.43	1.70	0.70
C12H11NO3	217.0739	8.21	1.00	0.92	0.25
C14H8O4	240.0423	7.25	1.00	0.57	0.29
C12H14O5	238.0841	3.41	1.00	1.17	0.42
C7H10O6	190.0477	0.39	0.50	1.43	0.86
C9H7NO5S	241.0045	2.11	1.00	0.78	0.56
C8H16O4S	208.0769	4.84	0.25	2.00	0.50
C6H5NO3	139.0269	3.24	1.00	0.83	0.50
C6H12O5S	196.0405	0.84	0.20	2.00	0.83
C8H7NO3	165.0426	5.07	1.00	0.88	0.38
C7H6N2O3	166.0378	3.45	1.00	0.86	0.43
C4H8O3	104.0473	0.61	0.33	2.00	0.75
C9H11NO4	197.0688	7.36	1.00	1.22	0.44
C10H17NO7S	295.0726	6.30	0.43	1.70	0.70
C5H8O5S	180.0092	0.39	0.40	1.60	1.00
C6H5NO3	139.0269	0.38	1.00	0.83	0.50
C4H9NO7S	215.0100	1.49	0.14	2.25	1.75
C6H8O4	144.0423	1.34	0.75	1.33	0.67
C7H5NO6	199.0117	2.66	1.00	0.71	0.86
C9H16O5S	236.0718	2.65	0.40	1.78	0.56
C8H9NO4	183.0532	3.50	1.00	1.13	0.50
C8H9NO5	199.0481	4.24	1.00	1.13	0.63
C8H16O5S	224.0718	2.76	0.20	2.00	0.63
C14H10O4	242.0579	6.91	1.00	0.71	0.29
C11H12N2O3S2	284.0289	3.85	1.00	1.09	0.27
C6H5NO5	171.0168	2.31	1.00	0.83	0.83
C8H8O3	152.0473	6.22	1.00	1.00	0.38
C13H8O4	228.0423	7.87	1.00	0.62	0.31
C9H9NO6S	259.0151	0.59	1.00	1.00	0.67
C9H9NO3	179.0582	3.33	1.00	1.00	0.33
C6H10O4	146.0579	2.48	0.50	1.67	0.67
C8H8O3	152.0473	4.37	1.00	1.00	0.38
C11H8O3	188.0473	7.28	1.00	0.73	0.27
C7H8O6	188.0321	0.38	0.67	1.14	0.86
C6H14O4S	182.0613	3.50	0.00	2.33	0.67
C8H8O	120.0575	3.06	1.00	1.00	0.13
C2H6O3S	110.0038	0.35	0.00	3.00	1.50
C10H18O5S	250.0875	3.08	0.40	1.80	0.50
C15H10O2	222.0681	7.23	1.00	0.67	0.13
C6H6O3S	158.0038	0.74	1.00	1.00	0.50
C7H6N2O6	214.0226	3.53	1.00	0.86	0.86
C4H6O6S	181.9885	0.38	0.33	1.50	1.50
C12H8O4	216.0423	4.44	1.00	0.67	0.33
C7H10O4	158.0579	2.75	0.75	1.43	0.57

7 Appendix

C7H4N2O3	164.0222	4.00	1.00	0.57	0.43
C8H14N2O6S	266.0573	7.38	0.50	1.75	0.75
C7H6O4	154.0266	1.30	1.00	0.86	0.57
C13H8O3	212.0473	7.01	1.00	0.62	0.23
C9H8O4	180.0423	4.12	1.00	0.89	0.44
C6H10O4	146.0579	0.59	0.50	1.67	0.67
C8H9NO4	183.0532	6.49	1.00	1.13	0.50
C7H4N2O7	228.0019	4.06	1.00	0.57	1.00
C14H8O5	256.0372	7.07	1.00	0.57	0.36
C9H6O7	226.0114	2.87	1.00	0.67	0.78
C7H16O4S	196.0769	5.12	0.00	2.29	0.57
C2H3NO3S	120.9834	0.35	0.67	1.50	1.50
C10H10O5S	242.0249	2.98	1.00	1.00	0.50
C6H5NO3	139.0269	2.94	1.00	0.83	0.50
C8H6O2	134.0368	1.83	1.00	0.75	0.25
C13H8O3	212.0473	7.49	1.00	0.62	0.23
C8H5NO4	179.0219	5.38	1.00	0.63	0.50
C3H4O3	88.0160	0.06	0.67	1.33	1.00
C9H17NO8S	299.0675	3.37	0.25	1.89	0.89
C11H10O5	222.0528	2.90	1.00	0.91	0.45
C15H22O8	330.1315	3.07	0.63	1.47	0.53
C7H5NO6	199.0117	3.42	1.00	0.71	0.86
C9H7NO4	193.0375	7.16	1.00	0.78	0.44
C4H10N4O10S	306.0118	3.84	0.20	2.50	2.50
C10H20O5S2	284.0752	7.78	0.20	2.00	0.50
C4H6O3	102.0317	0.38	0.67	1.50	0.75
C10H8O4	192.0423	3.28	1.00	0.80	0.40
C7H5NO2	135.0320	2.68	1.00	0.71	0.29
C6H14O4S	182.0613	3.03	0.00	2.33	0.67
C9H10O3	166.0630	7.30	1.00	1.11	0.33
C9H7NO3	177.0426	3.27	1.00	0.78	0.33
C9H9NO6	227.0430	3.36	1.00	1.00	0.67
C16H16N2O5S2	380.0501	7.43	1.00	1.00	0.31
C13H9NO3	227.0582	8.23	1.00	0.69	0.23
C10H8O6	224.0321	2.46	1.00	0.80	0.60
C10H8O3	176.0473	3.23	1.00	0.80	0.30
C7H12N2O3	172.0848	2.49	1.00	1.71	0.43
C12H5NO6	259.0117	3.86	1.00	0.42	0.50
C7H6O2	122.0368	0.83	1.00	0.86	0.29
C5H6O5S	177.9936	0.45	0.60	1.20	1.00
C12H10O5S	266.0249	3.33	1.00	0.83	0.42
C8H8O5S	216.0092	1.81	1.00	1.00	0.63
C9H6O3	162.0317	2.96	1.00	0.67	0.33
C9H9NO3	179.0582	7.45	1.00	1.00	0.33
C14H8O4	240.0423	7.45	1.00	0.57	0.29
C9H7NO	145.0528	2.25	1.00	0.78	0.11
C6H12O6S	212.0355	1.00	0.17	2.00	1.00
C5H5NO3	127.0269	1.03	1.00	1.00	0.60
C9H5NO5	207.0168	3.93	1.00	0.56	0.56
C13H9NO4	243.0532	7.74	1.00	0.69	0.31
C9H6O7	226.0114	1.07	1.00	0.67	0.78
C5H8O3	116.0473	0.40	0.67	1.60	0.60
C11H4O6	232.0008	3.17	1.00	0.36	0.55
C7H5NO4	167.0219	0.35	1.00	0.71	0.57
C8H7NO5	197.0324	3.26	1.00	0.88	0.63
C10H8O6	224.0321	3.09	1.00	0.80	0.60
C10H9NO4	207.0532	2.82	1.00	0.90	0.40
C11H6O5	218.0215	3.04	1.00	0.55	0.45
C7H14O5S	210.0562	1.94	0.20	2.00	0.71
C9H5NO5	207.0168	2.50	1.00	0.56	0.56
C9H16O6S	252.0668	2.61	0.33	1.78	0.67
C7H12O4	160.0736	0.91	0.50	1.71	0.57
C8H6O	118.0419	3.14	1.00	0.75	0.13
C15H8O4	252.0423	5.28	1.00	0.53	0.27
C11H12O6S	272.0355	2.49	1.00	1.09	0.55
C10H7NO7S	284.9943	1.03	1.00	0.70	0.70
C13H10O3	214.0630	8.03	1.00	0.77	0.23
C2H4O4S	123.9830	0.70	0.25	2.00	2.00
C15H10O4	254.0579	7.89	1.00	0.67	0.27
C10H10O6S	258.0198	1.75	1.00	1.00	0.60

7 Appendix

C8H15NO8S	285.0518	2.98	0.25	1.88	1.00
C8H9NO4	183.0532	5.95	1.00	1.13	0.50
C10H6O3S2	237.9758	0.52	1.00	0.60	0.30
C8H9NO6S	247.0151	1.43	0.83	1.13	0.75
C10H10O3	178.0630	2.99	1.00	1.00	0.30
C3H3NO3	101.0113	0.05	1.00	1.00	1.00
C3H4O6S	167.9729	0.37	0.33	1.33	2.00
C12H10O2	186.0681	7.16	1.00	0.83	0.17
C9H8O	132.0575	3.10	1.00	0.89	0.11
C11H18O5	230.1154	3.20	0.60	1.64	0.45
C5H10O4S	166.0300	0.39	0.25	2.00	0.80
C15H10O3	238.0630	7.99	1.00	0.67	0.20
C5H12O4S	168.0456	2.22	0.00	2.40	0.80
C15H10O2	222.0681	8.08	1.00	0.67	0.13
C5H12O5S	184.0405	0.53	0.00	2.40	1.00
C14H8O4	240.0423	4.25	1.00	0.57	0.29
C5H4N2O3	140.0222	1.16	1.00	0.80	0.60
C6H5NO2	123.0320	0.38	1.00	0.83	0.33
C6H5NO6S	218.9838	2.92	0.83	0.83	1.00
C4H10O4S	154.0300	1.30	0.00	2.50	1.00
C8H6O4	166.0266	1.89	1.00	0.75	0.50
C8H5NO4	179.0219	4.91	1.00	0.63	0.50
C6H6O4S	173.9987	0.98	1.00	1.00	0.67
C7H14O5S	210.0562	2.50	0.20	2.00	0.71
C5H7NO8	209.0172	0.35	0.38	1.40	1.60
C18H10O4	290.0579	7.68	1.00	0.56	0.22
C14H8O4	240.0423	6.38	1.00	0.57	0.29
C10H10O2	162.0681	3.61	1.00	1.00	0.20
C6H5NO4	155.0219	0.39	1.00	0.83	0.67
C6H5NO3	139.0269	0.59	1.00	0.83	0.50
C9H10O3	166.0630	3.30	1.00	1.11	0.33
C7H14O6S	226.0511	2.22	0.17	2.00	0.86
C7H6N2O4	182.0328	3.45	1.00	0.86	0.57
C13H8O3	212.0473	7.98	1.00	0.62	0.23
C16H8O3	248.0473	7.40	1.00	0.50	0.19
C4H4N2O3	128.0222	0.55	1.00	1.00	0.75
C15H25NO7S	363.1352	8.03	0.57	1.67	0.47
C9H18O6S	254.0824	3.52	0.17	2.00	0.67
C7H8O5	172.0372	0.38	0.80	1.14	0.71
C9H8O6S	244.0042	2.84	1.00	0.89	0.67
C13H8O4	228.0423	8.21	1.00	0.62	0.31
C7H7NO4	169.0375	6.30	1.00	1.00	0.57
C13H8O3	212.0473	6.52	1.00	0.62	0.23
C12H9NO4S	263.0252	2.94	1.00	0.75	0.33
C5H10O5S	182.0249	0.90	0.20	2.00	1.00
C10H10O3	178.0630	3.38	1.00	1.00	0.30
C11H7NO5	233.0324	7.21	1.00	0.64	0.45
C11H8O6	236.0321	2.86	1.00	0.73	0.55
C6H13NO7S	243.0413	3.33	0.14	2.17	1.17
C7H14O6S	226.0511	2.48	0.17	2.00	0.86
C9H8O6S	244.0042	0.81	1.00	0.89	0.67
C6H6O4	142.0266	0.39	1.00	1.00	0.67
C9H5NO4	191.0219	0.18	1.00	0.56	0.44
C14H10O5	258.0528	3.66	1.00	0.71	0.36
C11H8N2O5	248.0433	8.16	1.00	0.73	0.45
C9H7NO6	225.0273	3.16	1.00	0.78	0.67
C7H7NO3	153.0426	0.38	1.00	1.00	0.43
C10H20O5S	252.1031	3.86	0.20	2.00	0.50
C5H3N3O2	137.0225	3.19	1.00	0.60	0.40
C9H19NO8S	301.0831	3.36	0.13	2.11	0.89
C8H7NO3	165.0426	6.74	1.00	0.88	0.38
C9H15NO8S	297.0518	2.91	0.38	1.67	0.89
C12H14O4	222.0892	8.03	1.00	1.17	0.33
C9H9NO5	211.0481	6.99	1.00	1.00	0.56
C7H6O2	122.0368	1.34	1.00	0.86	0.29
C8H12O5	188.0685	1.29	0.60	1.50	0.63
C14H11NO3	241.0739	3.48	1.00	0.79	0.21
C10H16O7S	280.0617	2.48	0.43	1.60	0.70
C8H18O5S	226.0875	2.94	0.00	2.25	0.63
C7H7NO5	185.0324	2.62	1.00	1.00	0.71

7 Appendix

C5H12O3S	152.0507	1.88	0.00	2.40	0.60
C6H12O3	132.0786	2.59	0.33	2.00	0.50
C8H7NO3	165.0426	2.41	1.00	0.88	0.38
C6H12O4S	180.0456	2.55	0.25	2.00	0.67
C9H11NO4	197.0688	7.77	1.00	1.22	0.44
C14H8O5	256.0372	6.50	1.00	0.57	0.36
C16H8O4	264.0423	7.59	1.00	0.50	0.25
C17H10O2	246.0681	8.30	1.00	0.59	0.12
C2H4O4S	123.9830	3.52	0.25	2.00	2.00
C15H12O3	240.0786	7.70	1.00	0.80	0.20
C3H5NO3	103.0269	0.37	0.67	1.67	1.00
C9H7NO4	193.0375	2.36	1.00	0.78	0.44
C4H8O6S	184.0042	0.72	0.17	2.00	1.50
C9H16O4	188.1049	2.94	0.50	1.78	0.44
C7H7NO2	137.0477	2.39	1.00	1.00	0.29
C7H14O7S	242.0460	0.57	0.14	2.00	1.00
C7H6N2O6	214.0226	7.08	1.00	0.86	0.86
C10H7NO3	189.0426	3.21	1.00	0.70	0.30
C12H24O5S	280.1344	7.14	0.20	2.00	0.42
C8H4N2O	144.0324	3.70	1.00	0.50	0.13
C20H16O8	384.0845	8.25	1.00	0.80	0.40
C14H8O4	240.0423	7.96	1.00	0.57	0.29
C14H8O4	240.0423	3.96	1.00	0.57	0.29
C16H10O4	266.0579	6.98	1.00	0.63	0.25
C14H28O5S	308.1657	7.92	0.20	2.00	0.36
C8H7NO4	181.0375	2.14	1.00	0.88	0.50
C13H9NO4	243.0532	8.26	1.00	0.69	0.31
C9H16O6S	252.0668	2.65	0.33	1.78	0.67
C11H6O7	250.0114	2.83	1.00	0.55	0.64
C9H7NO	145.0528	3.47	1.00	0.78	0.11
C9H8N2O2	176.0586	7.46	1.00	0.89	0.22
C9H9NO4	195.0532	6.32	1.00	1.00	0.44
C9H7NO5	209.0324	0.57	1.00	0.78	0.56
C4H11NO3S	153.0460	0.64	0.00	2.75	0.75
C13H6O5	242.0215	3.77	1.00	0.46	0.38
C7H7NO3	153.0426	2.59	1.00	1.00	0.43
C13H8O5	244.0372	8.17	1.00	0.62	0.38
C8H7NO3	165.0426	2.65	1.00	0.88	0.38
C7H13NO7S	255.0413	3.41	0.29	1.86	1.00
C8H17NO8S	287.0675	2.98	0.13	2.13	1.00
C10H9NO5S	255.0201	2.84	1.00	0.90	0.50
C15H12O4	256.0736	6.95	1.00	0.80	0.27
C9H8O6S	244.0042	3.12	1.00	0.89	0.67
C7H7NO	121.0528	3.19	1.00	1.00	0.14
C5H6N2O	110.0480	0.14	1.00	1.20	0.20
C9H6O4	178.0266	2.43	1.00	0.67	0.44
C8H8O3	152.0473	1.75	1.00	1.00	0.38
C5H6N2O4S	190.0048	0.82	1.00	1.20	0.80
C8H4N2O	144.0324	3.43	1.00	0.50	0.13
C9H6N2O3	190.0378	2.75	1.00	0.67	0.33
C9H9NO7S	275.0100	3.70	0.86	1.00	0.78
C7H6O3	138.0317	0.16	1.00	0.86	0.43
C13H10O2	198.0681	7.97	1.00	0.77	0.15
C8H8O	120.0575	3.28	1.00	1.00	0.13
C9H7NO3	177.0426	2.75	1.00	0.78	0.33
C9H9NO3	179.0582	6.99	1.00	1.00	0.33
C13H6O5	242.0215	2.84	1.00	0.46	0.38
C5H5NO5	159.0168	0.39	0.80	1.00	1.00
C6H7NO4S	189.0096	0.39	1.00	1.17	0.67
C8H5NO6	211.0117	3.00	1.00	0.63	0.75
C9H17NO7S	283.0726	7.24	0.29	1.89	0.78
C8H16O6S	240.0668	3.28	0.17	2.00	0.75
C4H5NO2	99.0320	0.46	1.00	1.25	0.50
C6H12N4O10S	332.0274	5.04	0.30	2.00	1.67
C6H14O5S	198.0562	0.83	0.00	2.33	0.83
C6H4N2O5	184.0120	6.29	1.00	0.67	0.83
C15H8O5	268.0372	4.28	1.00	0.53	0.33
C5H5N3O4	171.0280	3.94	1.00	1.00	0.80
C5H4O3	112.0160	0.38	1.00	0.80	0.60
C7H5NO4	167.0219	3.80	1.00	0.71	0.57

7 Appendix

C5H8O3	116.0473	0.07	0.67	1.60	0.60
C8H8O3	152.0473	2.26	1.00	1.00	0.38
C8H8O6S	232.0042	3.09	0.83	1.00	0.75
C6H4N2O6	200.0069	4.82	1.00	0.67	1.00
C10H6O6	222.0164	1.35	1.00	0.60	0.60
C13H10O3	214.0630	7.61	1.00	0.77	0.23
C7H12O5	176.0685	1.15	0.40	1.71	0.71
C4H3NO2	97.0164	0.38	1.00	0.75	0.50
C8H6N2O5	210.0277	7.60	1.00	0.75	0.63
C8H6O3	150.0317	3.05	1.00	0.75	0.38
C6H12O6S	212.0355	2.55	0.17	2.00	1.00
C9H8O6S	244.0042	2.36	1.00	0.89	0.67
C4H6O3	102.0317	0.09	0.67	1.50	0.75
C4H3N3O4	157.0124	3.24	1.00	0.75	1.00
C6H12O6S	212.0355	1.62	0.17	2.00	1.00
C9H12O5S	232.0405	2.74	0.80	1.33	0.56
C9H9NO4	195.0532	6.61	1.00	1.00	0.44
C8H9NO4	183.0532	4.18	1.00	1.13	0.50
C12H10O6	250.0477	2.97	1.00	0.83	0.50
C7H7NO4	169.0375	6.68	1.00	1.00	0.57
C13H26O5S	294.1501	7.61	0.20	2.00	0.38
C5H4N2O3	140.0222	0.39	1.00	0.80	0.60
C5H10O3	118.0630	1.09	0.33	2.00	0.60
C8H7NO	133.0528	2.33	1.00	0.88	0.13
C8H8O4	168.0423	3.19	1.00	1.00	0.50
C10H5NO2S	203.0041	0.52	1.00	0.50	0.20
C12H6O5	230.0215	6.72	1.00	0.50	0.42
C9H10O5S	230.0249	2.77	1.00	1.11	0.56
C9H10O5S	230.0249	2.69	1.00	1.11	0.56
C14H10O5	258.0528	3.36	1.00	0.71	0.36
C9H7NO4S	225.0096	1.84	1.00	0.78	0.44
C3H4N2O3S	147.9943	0.41	1.00	1.33	1.00
C8H14O4	174.0892	2.32	0.50	1.75	0.50
C8H5NO4	179.0219	3.13	1.00	0.63	0.50
C8H14O4	174.0892	2.69	0.50	1.75	0.50
C7H8O4S	188.0143	2.57	1.00	1.14	0.57
C15H30O5S	322.1814	8.12	0.20	2.00	0.33
C6H8O3	128.0473	0.59	1.00	1.33	0.50
C6H5NO3	139.0269	0.08	1.00	0.83	0.50
C4H8O4S	152.0143	2.84	0.25	2.00	1.00
C8H8N2O4	196.0484	4.06	1.00	1.00	0.50
C12H24O6S	296.1294	6.96	0.17	2.00	0.50
C7H16O6S	228.0668	0.57	0.00	2.29	0.86
C16H10O6	298.0477	3.46	1.00	0.63	0.38
C7H8N2O3	168.0535	3.75	1.00	1.14	0.43
C10H14O5	214.0841	2.67	0.80	1.40	0.50
C10H10O7S	274.0147	1.02	0.86	1.00	0.70
C5H6O6S	193.9885	0.65	0.50	1.20	1.20
C10H18O6S	266.0824	3.00	0.33	1.80	0.60
C7H14O4	162.0892	0.87	0.25	2.00	0.57
C10H10O5S	242.0249	2.76	1.00	1.00	0.50
C8H8O4	168.0423	1.11	1.00	1.00	0.50
C13H8O4	228.0423	7.25	1.00	0.62	0.31
C6H12O6S	212.0355	2.82	0.17	2.00	1.00
C11H6O3	186.0317	6.60	1.00	0.55	0.27
C8H8O4S	200.0143	1.22	1.00	1.00	0.50
C7H6O2	122.0368	6.99	1.00	0.86	0.29
C12H8O4	216.0423	3.33	1.00	0.67	0.33
C15H10O4	254.0579	7.19	1.00	0.67	0.27
C8H7NO4S	213.0096	1.11	1.00	0.88	0.50
C8H18O3S	194.0977	5.17	0.00	2.25	0.38
C4H5NO2	99.0320	0.04	1.00	1.25	0.50
C6H10N2O3	158.0691	1.11	1.00	1.67	0.50
C15H8O5	268.0372	5.09	1.00	0.53	0.33
C6H3N3O7	228.9971	4.08	1.00	0.50	1.17
C9H16O8S	284.0566	2.48	0.25	1.78	0.89
C6H4O4S	171.9830	1.56	1.00	0.67	0.67
C13H12O2	200.0837	7.71	1.00	0.92	0.15
C17H12O3	264.0786	7.70	1.00	0.71	0.18
C6H6O3	126.0317	0.38	1.00	1.00	0.50

7 Appendix

C11H7NO3	201.0426	3.23	1.00	0.64	0.27
C14H30O5S	310.1814	7.83	0.00	2.14	0.36
C8H5NO7	227.0066	2.78	1.00	0.63	0.88
C11H5NO3	199.0269	3.02	1.00	0.45	0.27
C10H18O4	202.1205	2.88	0.50	1.80	0.40
C15H30O6S	338.1763	7.67	0.17	2.00	0.40
C9H10O2	150.0681	3.74	1.00	1.11	0.22
C12H8O3	200.0473	4.40	1.00	0.67	0.25
C7H12O7S	240.0304	0.91	0.29	1.71	1.00
C3H7NO7S	200.9943	0.85	0.14	2.33	2.33
C9H18O4	190.1205	2.81	0.25	2.00	0.44
C9H7NO6	225.0273	3.60	1.00	0.78	0.67
C6H7NO4	157.0375	0.69	1.00	1.17	0.67
C11H20O7S	296.0930	2.91	0.29	1.82	0.64
C10H17NO8S	311.0675	3.77	0.38	1.70	0.80
C10H9NO	159.0684	2.63	1.00	0.90	0.10
C8H8O5S	216.0092	2.58	1.00	1.00	0.63
C9H17NO9S	315.0624	2.54	0.22	1.89	1.00
C9H5NO5	207.0168	3.18	1.00	0.56	0.56
C7H14O6S	226.0511	0.60	0.17	2.00	0.86
C16H22O8S	374.1035	7.37	0.75	1.38	0.50
C12H20O5	244.1311	3.81	0.60	1.67	0.42
C4H9NO7S	215.0100	1.94	0.14	2.25	1.75
C6H5NO4	155.0219	1.84	1.00	0.83	0.67
C9H4N2O2	172.0273	2.95	1.00	0.44	0.22
C10H11NO3	193.0739	7.81	1.00	1.10	0.30
C7H16O5S	212.0718	3.01	0.00	2.29	0.71
C20H26O4	330.1831	7.61	1.00	1.30	0.20
C15H12O4S	288.0456	7.51	1.00	0.80	0.27
C8H8O5S	216.0092	1.08	1.00	1.00	0.63
C10H17NO10S	343.0573	2.68	0.30	1.70	1.00
C11H8O7	252.0270	2.65	1.00	0.73	0.64
C10H12O3	180.0786	7.82	1.00	1.20	0.30
C11H20N2O10	340.1118	6.79	0.30	1.82	0.91
C7H8N2O3	168.0535	3.35	1.00	1.14	0.43
C8H5NO5	195.0168	3.14	1.00	0.63	0.63
C10H6O4S	221.9987	3.88	1.00	0.60	0.40
C12H10O3	202.0630	8.13	1.00	0.83	0.25
C12H9NO3	215.0582	3.34	1.00	0.75	0.25
C11H7NO	169.0528	7.37	1.00	0.64	0.09
C16H9NO2	247.0633	7.08	1.00	0.56	0.13
C13H10O3	214.0630	3.47	1.00	0.77	0.23
C4H4N2O4S	175.9892	0.43	1.00	1.00	1.00
C15H12O3	240.0786	6.87	1.00	0.80	0.20
C9H6O8	242.0063	3.11	0.88	0.67	0.89
C7H6O2	122.0368	7.64	1.00	0.86	0.29
C15H7NOS2	280.9969	0.60	1.00	0.47	0.07
C8H10O3S	186.0351	2.78	1.00	1.25	0.38
C6H6O	94.0419	3.55	1.00	1.00	0.17
C9H10O	134.0732	3.80	1.00	1.11	0.11
C11H8O7	252.0270	1.17	1.00	0.73	0.64
C7H6O2	122.0368	1.91	1.00	0.86	0.29
C12H8O4	216.0423	2.84	1.00	0.67	0.33
C13H28O5S	296.1657	8.19	0.00	2.15	0.38
C9H10O4	182.0579	2.31	1.00	1.11	0.44
C4H6N2O2	114.0429	0.04	1.00	1.50	0.50
C15H8O3	236.0473	7.83	1.00	0.53	0.20
C8H14O7S	254.0460	1.07	0.29	1.75	0.88
C11H24O5S	268.1344	7.66	0.00	2.18	0.45
C10H20O6S	268.0981	3.79	0.17	2.00	0.60
C19H22O4	314.1518	7.70	1.00	1.16	0.21
C5H8O2	100.0524	0.68	1.00	1.60	0.40
C8H7NO4	181.0375	2.89	1.00	0.88	0.50
C4H6O8	182.0063	0.39	0.25	1.50	2.00
C8H6O6	198.0164	1.25	1.00	0.75	0.75
C8H10O5	186.0528	0.65	0.80	1.25	0.63
C7H8O4	156.0423	1.07	1.00	1.14	0.57
C8H12O6	204.0634	0.65	0.50	1.50	0.75
C15H10O5	270.0528	4.14	1.00	0.67	0.33
C10H7NO2	173.0477	3.45	1.00	0.70	0.20

7 Appendix

C6H4O5	156.0059	0.68	1.00	0.67	0.83
C11H18O4	214.1205	6.74	0.75	1.64	0.36
C6H13NO8S	259.0362	1.45	0.13	2.17	1.33
C13H28O5S	296.1657	7.55	0.00	2.15	0.38
C11H20O6S	280.0981	3.15	0.33	1.82	0.55
C6H9NO2	127.0633	0.20	1.00	1.50	0.33
C6H5NO7S	234.9787	2.81	0.71	0.83	1.17
C8H16O3	160.1099	3.14	0.33	2.00	0.38
C10H10O6S	258.0198	0.77	1.00	1.00	0.60
C10H9NO4	207.0532	2.44	1.00	0.90	0.40
C9H9NO4	195.0532	3.94	1.00	1.00	0.44
C8H10O3	154.0630	1.58	1.00	1.25	0.38
C10H16O4	200.1049	4.58	0.75	1.60	0.40
C4H10O3S	138.0351	0.70	0.00	2.50	0.75
C6H8O2	112.0524	1.03	1.00	1.33	0.33
C10H8O5	208.0372	3.63	1.00	0.80	0.50
C11H13NO3	207.0895	8.17	1.00	1.18	0.27
C15H8O2	220.0524	7.85	1.00	0.53	0.13
C7H7NO	121.0528	1.07	1.00	1.00	0.14
C15H31NO8S	385.1770	7.99	0.13	2.07	0.53
C5H10N2O11S	306.0005	2.60	0.18	2.00	2.20
C6H5N3O2	151.0382	3.88	1.00	0.83	0.33
C8H5NO7	227.0066	4.07	1.00	0.63	0.88
C13H9NO	195.0684	4.46	1.00	0.69	0.08
C5H14N2O6S	230.0573	6.64	0.00	2.80	1.20
C8H9NO2	151.0633	2.71	1.00	1.13	0.25
C6H7NO3	141.0426	2.47	1.00	1.17	0.50
C10H10O6S	258.0198	1.07	1.00	1.00	0.60
C9H4O5	192.0059	1.95	1.00	0.44	0.56
C6H11NO4S	193.0409	0.56	0.50	1.83	0.67
C23H10OS	334.0452	7.23	1.00	0.43	0.04
C14H8O5	256.0372	7.57	1.00	0.57	0.36
C17H12O4	280.0736	7.73	1.00	0.71	0.24
C8H8O4S	200.0143	1.69	1.00	1.00	0.50
C10H18O6S	266.0824	2.66	0.33	1.80	0.60
C8H9NO5S	231.0201	2.73	1.00	1.13	0.63
C9H18O6S	254.0824	4.28	0.17	2.00	0.67
C12H25NO7S	327.1352	8.10	0.14	2.08	0.58
C9H14O6	218.0790	0.89	0.50	1.56	0.67
C7H16O3S	180.0820	3.56	0.00	2.29	0.43
C10H6O4	190.0266	3.33	1.00	0.60	0.40
C9H16O8S	284.0566	2.65	0.25	1.78	0.89
C12H14N2O4	250.0954	5.27	1.00	1.17	0.33
C16H10O5	282.0528	7.47	1.00	0.63	0.31
C10H17NO8	279.0954	2.97	0.38	1.70	0.80
C10H6O5	206.0215	2.48	1.00	0.60	0.50
C8H5NO4	179.0219	2.56	1.00	0.63	0.50
C8H18O5S	226.0875	2.62	0.00	2.25	0.63
C15H32O5S	324.1970	8.07	0.00	2.13	0.33
C9H10O4S	214.0300	2.59	1.00	1.11	0.44
C12H20N2O2	224.1525	2.88	1.00	1.67	0.17
C4H4O5	132.0059	0.35	0.60	1.00	1.25
C8H16O4S	208.0769	6.80	0.25	2.00	0.50
C12H24O6S	296.1294	7.49	0.17	2.00	0.50
C8H11NO5S	233.0358	0.63	0.80	1.38	0.63
C10H6O6	222.0164	3.69	1.00	0.60	0.60
C12H10N2O2	214.0742	8.26	1.00	0.83	0.17
C12H14O4	222.0892	3.18	1.00	1.17	0.33
C12H8O3	200.0473	7.12	1.00	0.67	0.25
C8H16O5S	224.0718	3.74	0.20	2.00	0.63
C14H9NO5	271.0481	7.50	1.00	0.64	0.36
C17H24O3	276.1725	7.56	1.00	1.41	0.18
C5H5NO2	111.0320	0.38	1.00	1.00	0.40
C6H6O5S	189.9936	1.35	0.80	1.00	0.83
C7H7NO7S	248.9943	2.88	0.71	1.00	1.00
C7H16N2O5S	240.0780	8.00	0.20	2.29	0.71
C6H4O4	140.0110	0.38	1.00	0.67	0.67
C11H18O4	214.1205	4.41	0.75	1.64	0.36
C11H8O3	188.0473	5.16	1.00	0.73	0.27
C9H18O5S	238.0875	2.72	0.20	2.00	0.56

7 Appendix

C8H16O3	160.1099	5.84	0.33	2.00	0.38
C7H5N3O6	227.0178	3.31	1.00	0.71	0.86
C7H5N3O7	243.0127	5.68	1.00	0.71	1.00
C11H11NO4	221.0688	3.05	1.00	1.00	0.36
C8H16O4	176.1049	2.41	0.25	2.00	0.50
C5H12N2O8S	260.0314	7.59	0.13	2.40	1.60
C6H12O5S	196.0405	2.31	0.20	2.00	0.83
C10H8O3	176.0473	4.14	1.00	0.80	0.30
C23H13NO6S	431.0464	4.70	1.00	0.57	0.26
C7H7NO3	153.0426	3.35	1.00	1.00	0.43
C8H14O6S	238.0511	1.52	0.33	1.75	0.75
C4H9NO8S	231.0049	0.71	0.13	2.25	2.00
C6H7NO	109.0528	0.53	1.00	1.17	0.17
C9H8O2	148.0524	2.40	1.00	0.89	0.22
C10H9NO3	191.0582	4.43	1.00	0.90	0.30
C9H11NO4	197.0688	5.79	1.00	1.22	0.44
C5H7NO2	113.0477	0.44	1.00	1.40	0.40
C15H8O6	284.0321	3.45	1.00	0.53	0.40
C20H28O3	316.2038	8.42	1.00	1.40	0.15
C13H10O2	198.0681	7.20	1.00	0.77	0.15
C6H6O5S	189.9936	0.54	0.80	1.00	0.83
C8H6N2O6	226.0226	3.00	1.00	0.75	0.75
C9H7NO5	209.0324	4.00	1.00	0.78	0.56
C8H16O6S	240.0668	1.22	0.17	2.00	0.75
C13H8O3	212.0473	5.77	1.00	0.62	0.23
C11H20O4	216.1362	3.17	0.50	1.82	0.36
C6H4O3	124.0160	3.08	1.00	0.67	0.50
C10H17NO8S	311.0675	3.45	0.38	1.70	0.80
C8H9NO3	167.0582	0.76	1.00	1.13	0.38
C12H7NO3	213.0426	3.46	1.00	0.58	0.25
C10H14O6	230.0790	2.81	0.67	1.40	0.60
C11H8O6	236.0321	2.48	1.00	0.73	0.55
C5H14N2O6S	230.0573	6.27	0.00	2.80	1.20
C11H22O5S	266.1188	5.46	0.20	2.00	0.45
C13H13NO3	231.0895	8.33	1.00	1.00	0.23
C7H5NO5	183.0168	1.28	1.00	0.71	0.71
C10H22O4S	238.1239	7.64	0.00	2.20	0.40
C10H17NO3	199.1208	6.95	1.00	1.70	0.30
C10H20O6S	268.0981	2.71	0.17	2.00	0.60
C14H9NO2	223.0633	7.59	1.00	0.64	0.14
C10H20N2O8S	328.0940	8.16	0.25	2.00	0.80
C5H10O3	118.0630	0.14	0.33	2.00	0.60
C9H6N2O3	190.0378	3.04	1.00	0.67	0.33
C7H8N4O8S2	339.9784	2.78	0.75	1.14	1.14
C11H18O6	246.1103	4.37	0.50	1.64	0.55
C10H6O6	222.0164	2.44	1.00	0.60	0.60
C9H8O5S	228.0092	1.69	1.00	0.89	0.56
C14H6O3S2	285.9758	2.62	1.00	0.43	0.21
C6H10O2	114.0681	1.23	1.00	1.67	0.33
C3H6O4S	137.9987	1.64	0.25	2.00	1.33
C7H4N2O6	212.0069	2.81	1.00	0.57	0.86
C12H10O3	202.0630	7.81	1.00	0.83	0.25
C7H10O6	190.0477	0.99	0.50	1.43	0.86
C10H6O5	206.0215	2.89	1.00	0.60	0.50
C11H22O5S	266.1188	6.43	0.20	2.00	0.45
C11H8O8S	299.9940	3.85	1.00	0.73	0.73
C13H10O2	198.0681	7.48	1.00	0.77	0.15
C9H18O6S	254.0824	2.49	0.17	2.00	0.67
C6H6O	94.0419	2.34	1.00	1.00	0.17
C8H14O4	174.0892	3.96	0.50	1.75	0.50
C7H7NO3	153.0426	4.70	1.00	1.00	0.43
C8H6N2O	146.0480	3.00	1.00	0.75	0.13
C11H11NO4	221.0688	8.03	1.00	1.00	0.36
C10H18O5	218.1154	2.84	0.40	1.80	0.50
C8H18O6S	242.0824	1.52	0.00	2.25	0.75
C4H4N2O4	144.0171	0.92	1.00	1.00	1.00
C7H12O2	128.0837	2.47	1.00	1.71	0.29
C9H18N2O9S	330.0733	7.35	0.22	2.00	1.00
C12H12O6	252.0634	4.82	1.00	1.00	0.50
C13H8O4	228.0423	6.71	1.00	0.62	0.31

7 Appendix

C8H7NO5	197.0324	5.56	1.00	0.88	0.63
C13H27NO7S	341.1508	8.34	0.14	2.08	0.54
C18H12O3	276.0786	8.06	1.00	0.67	0.17
C20H30O4	334.2144	8.12	1.00	1.50	0.20
C12H20O4	228.1362	6.61	0.75	1.67	0.33
C13H9NO2	211.0633	7.95	1.00	0.69	0.15
C14H22O4	254.1518	6.66	1.00	1.57	0.29
C6H8N2O5	188.0433	2.77	0.80	1.33	0.83
C3H6O9S	217.9733	4.06	0.11	2.00	3.00
C5H8N2O3	144.0535	0.57	1.00	1.60	0.60
C7H6O4	154.0266	2.11	1.00	0.86	0.57
C16H14O4	270.0892	7.54	1.00	0.88	0.25
C11H18N2O4	242.1267	2.87	1.00	1.64	0.36
C9H11NO7S	277.0256	2.21	0.71	1.22	0.78
C8H8N2O6	228.0382	4.68	1.00	1.00	0.75
C13H9NO	195.0684	7.65	1.00	0.69	0.08
C10H7NO2	173.0477	2.96	1.00	0.70	0.20
C7H8O5	172.0372	1.04	0.80	1.14	0.71
C7H9NO5S	219.0201	1.26	0.80	1.29	0.71
C12H10O2	186.0681	5.66	1.00	0.83	0.17
C7H12N2O7S	268.0365	5.07	0.43	1.71	1.00
C5H10O4S	166.0300	0.72	0.25	2.00	0.80
C10H13NO4	211.0845	7.84	1.00	1.30	0.40
C6H14O5S	198.0562	2.20	0.00	2.33	0.83
C15H6O4S2	313.9707	0.82	1.00	0.40	0.27
C8H7NO3	165.0426	7.38	1.00	0.88	0.38
C3H4N2O3	116.0222	0.64	1.00	1.33	1.00
C11H23NO7S	313.1195	7.96	0.14	2.09	0.64
C8H8O5S	216.0092	1.55	1.00	1.00	0.63
C12H8O2	184.0524	5.15	1.00	0.67	0.17
C10H17N3O13S	419.0482	7.61	0.31	1.70	1.30
C10H6O7	238.0114	1.10	1.00	0.60	0.70
C16H32O5S	336.1970	8.27	0.20	2.00	0.31
C12H8O3	200.0473	8.05	1.00	0.67	0.25
C11H8O2	172.0524	6.82	1.00	0.73	0.18
C9H11NO4	197.0688	6.64	1.00	1.22	0.44
C9H12O5	200.0685	2.49	0.80	1.33	0.56
C13H26O6S	310.1450	7.39	0.17	2.00	0.46
C11H7NO6	249.0273	2.75	1.00	0.64	0.55
C11H10O2	174.0681	3.34	1.00	0.91	0.18
C16H10O4S	298.0300	7.48	1.00	0.63	0.25
C11H22O6S	282.1137	6.97	0.17	2.00	0.55
C16H9NO2	247.0633	8.16	1.00	0.56	0.13
C12H8O2	184.0524	8.05	1.00	0.67	0.17
C15H16O2S2	292.0592	2.79	1.00	1.07	0.13
C7H8N4O7S2	323.9834	2.94	0.86	1.14	1.00
C10H19NO7S	297.0882	7.46	0.29	1.90	0.70
C11H6O7S2	313.9555	2.59	1.00	0.55	0.64
C6H5N3O2	151.0382	4.22	1.00	0.83	0.33
C6H16N2O7S2	292.0399	3.58	0.00	2.67	1.17
C10H14N2O7S	306.0522	7.83	0.71	1.40	0.70
C9H14O7S	266.0460	1.34	0.43	1.56	0.78
C12H20O6	260.1260	3.43	0.50	1.67	0.50
C11H6O4	202.0266	2.79	1.00	0.55	0.36
C6H4N2O	120.0324	2.26	1.00	0.67	0.17
C19H6OS	282.0139	7.09	1.00	0.32	0.05
C10H7NO5	221.0324	4.17	1.00	0.70	0.50
C11H6O6	234.0164	1.00	1.00	0.55	0.55
C10H18O6	234.1103	2.74	0.33	1.80	0.60
C5H3N3O2	137.0225	2.82	1.00	0.60	0.40
C12H7NO2	197.0477	3.84	1.00	0.58	0.17
C8H6N2O2	162.0429	3.13	1.00	0.75	0.25
C15H22O2	234.1620	0.13	1.00	1.47	0.13
C4H4N2O	96.0324	0.55	1.00	1.00	0.25
C5H4O2S	127.9932	1.57	1.00	0.80	0.40
C10H7NO5	221.0324	3.45	1.00	0.70	0.50
C9H6O6	210.0164	3.06	1.00	0.67	0.67
C4H5N3O2	127.0382	1.08	1.00	1.25	0.50
C8H8O6S	232.0042	3.49	0.83	1.00	0.75
C15H5NOS2	278.9813	1.76	1.00	0.33	0.07

7 Appendix

C8H18O5S	226.0875	3.71	0.00	2.25	0.63
C6H8N2O5S2	188.0078	2.59	1.00	1.33	0.17
C9H19NO7S	285.0882	7.41	0.14	2.11	0.78
C8H6N2O3	178.0378	6.49	1.00	0.75	0.38
C10H18O4	202.1205	7.45	0.50	1.80	0.40
C6H7NO5	173.0324	0.77	0.80	1.17	0.83
C11H8O3	188.0473	3.82	1.00	0.73	0.27
C7H8O9S	267.9889	3.55	0.44	1.14	1.29
C23H28N4O5S2	440.1705	7.16	1.00	1.22	0.04
C9H11NO5	213.0637	3.59	1.00	1.22	0.56
C10H7NO5	221.0324	3.05	1.00	0.70	0.50
C5H4N2O4	156.0171	1.24	1.00	0.80	0.80
C9H10O6S	246.0198	2.88	0.83	1.11	0.67
C14H9NO5	271.0481	7.89	1.00	0.64	0.36
C16H14O3	254.0943	8.03	1.00	0.88	0.19
C7H7NO7S	248.9943	2.50	0.71	1.00	1.00
C9H6N2O3	190.0378	4.44	1.00	0.67	0.33
C8H10O5	186.0528	3.04	0.80	1.25	0.63
C11H6N2O3	214.0378	3.52	1.00	0.55	0.27
C7H7NO2	137.0477	2.92	1.00	1.00	0.29
C13H8O5	244.0372	3.68	1.00	0.62	0.38
C9H8O4S	212.0143	1.59	1.00	0.89	0.44
C9H20O3S	208.1133	7.12	0.00	2.22	0.33
C15H5NOS2	278.9813	1.11	1.00	0.33	0.07
C8H12N2O5S2	216.0391	3.63	1.00	1.50	0.13
C8H18O6S	242.0824	1.08	0.00	2.25	0.75
C7H13NO9S	287.0311	2.69	0.22	1.86	1.29
C14H8O3	224.0473	7.86	1.00	0.57	0.21
C9H8O6	212.0321	3.70	1.00	0.89	0.67
C6H15N3O5S	241.0732	7.67	0.20	2.50	0.83
C10H20O6S	268.0981	4.91	0.17	2.00	0.60
C7H9NO5S	219.0201	2.47	0.80	1.29	0.71
C15H10O7	302.0427	3.03	1.00	0.67	0.47
C9H10O3	166.0630	4.30	1.00	1.11	0.33
C11H9NO5	235.0481	7.48	1.00	0.82	0.45
C13H16O4	236.1049	7.80	1.00	1.23	0.31
C16H24O8	344.1471	3.49	0.63	1.50	0.50
C10H14O4	198.0892	2.64	1.00	1.40	0.40
C9H7NO	145.0528	4.14	1.00	0.78	0.11
C9H9NO6	227.0430	2.99	1.00	1.00	0.67
C7H12N2O7S	268.0365	4.44	0.43	1.71	1.00
C13H26O6S	310.1450	7.79	0.17	2.00	0.46
C14H10O	194.0732	7.08	1.00	0.71	0.07
C10H7NO7S	284.9943	6.68	1.00	0.70	0.70
C18H13NO3	291.0895	7.35	1.00	0.72	0.17
C18H14O3	278.0943	8.02	1.00	0.78	0.17
C9H18O3	174.1256	3.80	0.33	2.00	0.33
C14H29NO8S	371.1614	7.84	0.13	2.07	0.57
C8H6N2O3	178.0378	2.50	1.00	0.75	0.38
C5H7NO2	113.0477	0.10	1.00	1.40	0.40
C7H10N2O5	202.0590	3.13	0.80	1.43	0.71
C8H11NO4S	217.0409	0.91	1.00	1.38	0.50
C8H8N2O8S	292.0001	2.98	0.75	1.00	1.00
C7H16O5S	212.0718	1.52	0.00	2.29	0.71
C11H22O6S	282.1137	7.89	0.17	2.00	0.55
C12H8O5	232.0372	3.87	1.00	0.67	0.42
C14H11NO3	241.0739	8.34	1.00	0.79	0.21
C13H8O5	244.0372	6.70	1.00	0.62	0.38
C9H6O2	146.0368	3.07	1.00	0.67	0.22
C4H4O3	100.0160	0.11	1.00	1.00	0.75
C6H6N2O4	170.0328	0.39	1.00	1.00	0.67
C7H7NO2	137.0477	3.18	1.00	1.00	0.29
C7H16O15	340.0489	7.15	0.00	2.29	2.14
C9H6O2S	178.0088	3.89	1.00	0.67	0.22
C8H7NO4	181.0375	4.76	1.00	0.88	0.50
C10H12O4	196.0736	2.67	1.00	1.20	0.40
C5H10N2O11S	306.0005	2.37	0.18	2.00	2.20
C10H11NO5	225.0637	3.49	1.00	1.10	0.50
C12H7NO4	229.0375	7.41	1.00	0.58	0.33
C7H9NO3S	187.0303	0.92	1.00	1.29	0.43

7 Appendix

C5H2N2O3	138.0065	0.47	1.00	0.40	0.60
C5H4N2O4	156.0171	0.39	1.00	0.80	0.80
C11H5NO4	215.0219	3.15	1.00	0.45	0.36
C6H8O4	144.0423	2.43	0.75	1.33	0.67
C14H24O5	272.1624	7.35	0.60	1.71	0.36
C16H14O3	254.0943	7.59	1.00	0.88	0.19
C9H8O5	196.0372	5.42	1.00	0.89	0.56
C8H8O6S	232.0042	1.34	0.83	1.00	0.75
C14H9NO4	255.0532	8.07	1.00	0.64	0.29
C13H8O4	228.0423	4.29	1.00	0.62	0.31
C6H9NO3	143.0582	0.63	1.00	1.50	0.50
C8H14N2O10S	330.0369	3.13	0.30	1.75	1.25
C8H14O7S	254.0460	2.32	0.29	1.75	0.88
C18H32O6S	376.1920	7.54	0.50	1.78	0.33
C7H4O7	199.9957	2.22	0.86	0.57	1.00
C7H6N4O6S	274.0008	3.85	1.00	0.86	0.86
C9H11NO5	213.0637	3.24	1.00	1.22	0.56
C9H6O4	178.0266	0.80	1.00	0.67	0.44
C13H24O5S2	324.1065	6.57	0.40	1.85	0.38
C9H7NO4	193.0375	2.10	1.00	0.78	0.44
C8H9NO2	151.0633	1.80	1.00	1.13	0.25
C13H4N4OS2	295.9827	3.85	1.00	0.31	0.08
C8H10O4S	202.0300	3.17	1.00	1.25	0.50
C9H8O5	196.0372	4.11	1.00	0.89	0.56
C11H22O6S	282.1137	7.39	0.17	2.00	0.55
C7H8O5S	204.0092	2.77	0.80	1.14	0.71
C12H12O6	252.0634	3.37	1.00	1.00	0.50
C12H10O7	266.0427	2.90	1.00	0.83	0.58
C6H7NO3S	173.0147	0.60	1.00	1.17	0.50
C10H5NO2	171.0320	2.92	1.00	0.50	0.20
C6H6O	94.0419	2.78	1.00	1.00	0.17
C8H8O4	168.0423	1.60	1.00	1.00	0.50
C10H22N2O11S2	410.0665	7.96	0.09	2.20	1.10
C10H20O4	204.1362	3.15	0.25	2.00	0.40
C11H13NO8	287.0641	2.65	0.75	1.18	0.73
C8H4N2O2	160.0273	3.15	1.00	0.50	0.25
C9H14O8S	282.0409	0.90	0.38	1.56	0.89
C14H8O4S	272.0143	7.17	1.00	0.57	0.29
C7H7NO4S	201.0096	0.55	1.00	1.00	0.57
C9H11NO7S	277.0256	4.93	0.71	1.22	0.78
C6H4N2O	120.0324	0.39	1.00	0.67	0.17
C7H12N2O9S	300.0264	3.44	0.33	1.71	1.29
C9H8O7S	259.9991	1.15	0.86	0.89	0.78
C4H8O4S	152.0143	7.83	0.25	2.00	1.00
C12H22O4	230.1518	3.72	0.50	1.83	0.33
C5H4O3	112.0160	0.67	1.00	0.80	0.60
C16H12O2	236.0837	8.19	1.00	0.75	0.13
C11H22O5S	266.1188	6.81	0.20	2.00	0.45
C7H8O3S	172.0194	1.33	1.00	1.14	0.43
C9H16O6S	252.0668	0.79	0.33	1.78	0.67
C10H19NO9S	329.0781	2.69	0.22	1.90	0.90
C15H10O2	222.0681	5.66	1.00	0.67	0.13
C9H10N4O4S	270.0423	3.72	1.00	1.11	0.44
C10H9NO	159.0684	2.87	1.00	0.90	0.10
C11H7NO5	233.0324	4.53	1.00	0.64	0.45
C10H10O4	194.0579	1.12	1.00	1.00	0.40
C7H9NO9S	282.9998	3.21	0.44	1.29	1.29
C16H32O7S	368.1869	7.08	0.14	2.00	0.44
C4H3NO2	97.0164	0.08	1.00	0.75	0.50
C7H16O5S	212.0718	1.97	0.00	2.29	0.71
C6H9NO4	159.0532	0.88	0.75	1.50	0.67
C13H9NO5	259.0481	7.63	1.00	0.69	0.38
C8H6N2O5	210.0277	6.96	1.00	0.75	0.63
C7H9NO	123.0684	0.72	1.00	1.29	0.14
C7H10O5S	206.0249	0.56	0.60	1.43	0.71
C15H9NO	219.0684	8.19	1.00	0.60	0.07
C8H6O5	182.0215	3.70	1.00	0.75	0.63
C7H4N2O5	196.0120	3.38	1.00	0.57	0.71
C9H4O6	208.0008	1.06	1.00	0.44	0.67
C8H6N2O5	210.0277	3.39	1.00	0.75	0.63

7 Appendix

C12H26O3S	250.1603	8.13	0.00	2.17	0.25
C15H14O4	258.0892	7.71	1.00	0.93	0.27
C10H21NO8S	315.0988	3.76	0.13	2.10	0.80
C3H5NO2	87.0320	0.04	1.00	1.67	0.67
C18H18O4S	330.0926	8.07	1.00	1.00	0.22
C9H16N2O5S	264.0780	7.92	0.60	1.78	0.56
C11H10O3	190.0630	2.67	1.00	0.91	0.27
C13H8O3	212.0473	4.23	1.00	0.62	0.23
C5H6N4O6S	250.0008	3.09	0.83	1.20	1.20
C12H18O6	258.1103	2.95	0.67	1.50	0.50
C9H8N2O3	192.0535	2.49	1.00	0.89	0.33
C20H28O4	332.1988	7.58	1.00	1.40	0.20
C13H10O2	198.0681	5.03	1.00	0.77	0.15
C7H5NO6	199.0117	1.49	1.00	0.71	0.86
C7H6O	106.0419	0.82	1.00	0.86	0.14
C6H7NO	109.0528	2.48	1.00	1.17	0.17
C4H4N2O3	128.0222	0.11	1.00	1.00	0.75
C5H11NO8S	245.0205	0.81	0.13	2.20	1.60
C19H24O3	300.1725	8.19	1.00	1.26	0.16
C13H6O5	242.0215	4.65	1.00	0.46	0.38
C16H8O6	296.0321	4.24	1.00	0.50	0.38
C10H10O6S	258.0198	2.78	1.00	1.00	0.60
C10H10O5	210.0528	6.63	1.00	1.00	0.50
C10H7NO4	205.0375	3.62	1.00	0.70	0.40
C7H5NO6	199.0117	0.66	1.00	0.71	0.86
C5H6O4S	161.9987	0.66	0.75	1.20	0.80
C10H7NO7S	284.9943	1.99	1.00	0.70	0.70
C14H11NO4	257.0688	8.08	1.00	0.79	0.29
C5H3NO3	125.0113	0.42	1.00	0.60	0.60
C10H11NO3	193.0739	4.08	1.00	1.10	0.30
C8H6N2O6	226.0226	2.43	1.00	0.75	0.75
C9H6O7S	257.9834	0.71	1.00	0.67	0.78
C8H7NO2	149.0477	1.43	1.00	0.88	0.25
C5H6N2O5	174.0277	2.54	0.80	1.20	1.00
C6H8O6S	208.0042	1.38	0.50	1.33	1.00
C6H6O4	142.0266	0.88	1.00	1.00	0.67
C6H6O2	110.0368	0.39	1.00	1.00	0.33
C13H22O5	258.1467	6.47	0.60	1.69	0.38
C7H9NO3	155.0582	0.54	1.00	1.29	0.43
C4H5N3O2	127.0382	0.81	1.00	1.25	0.50
C8H6O2	134.0368	2.98	1.00	0.75	0.25
C7H12O5	176.0685	2.41	0.40	1.71	0.71
C9H12O3	168.0786	2.80	1.00	1.33	0.33
C12H20O7S	308.0930	2.85	0.43	1.67	0.58
C11H7NO5	233.0324	2.89	1.00	0.64	0.45
C5H8O	84.0575	0.56	1.00	1.60	0.20
C13H7NO2	209.0477	8.00	1.00	0.54	0.15
C10H6O6	222.0164	2.86	1.00	0.60	0.60
C10H11NO7S	289.0256	2.54	0.86	1.10	0.70
C12H11NO5	249.0637	2.68	1.00	0.92	0.42
C13H8O2S	228.0245	8.10	1.00	0.62	0.15
C10H6N2O	170.0480	2.75	1.00	0.60	0.10
C7H15NO7S	257.0569	4.10	0.14	2.14	1.00
C9H10O6S	246.0198	0.96	0.83	1.11	0.67
C8H8O6S	232.0042	0.59	0.83	1.00	0.75
C8H16O6S	240.0668	4.06	0.17	2.00	0.75
C18H10O5	274.0452	3.67	1.00	0.56	0.06
C9H18N2O10S	346.0682	7.40	0.20	2.00	1.11
C9H5NO6	223.0117	2.62	1.00	0.56	0.67
C8H6N2O3	178.0378	5.58	1.00	0.75	0.38
C24H34O2	354.2559	9.06	1.00	1.42	0.08
C10H17NO9S	327.0624	3.17	0.33	1.70	0.90
C11H8O2	172.0524	4.46	1.00	0.73	0.18
C8H14O5	190.0841	0.67	0.40	1.75	0.63
C15H26O5	286.1780	7.35	0.60	1.73	0.33
C10H19NO10S	345.0730	1.05	0.20	1.90	1.00
C10H11NO5	225.0637	6.78	1.00	1.10	0.50
C4H4O6S	179.9729	0.41	0.50	1.00	1.50
C9H11NO4	197.0688	4.41	1.00	1.22	0.44
C12H10O6	250.0477	3.45	1.00	0.83	0.50

7 Appendix

C18H13NO3	291.0895	7.79	1.00	0.72	0.17
C11H21NO7S	311.1039	7.71	0.29	1.91	0.64
C10H8N2O6	252.0382	7.80	1.00	0.80	0.60
C8H8N2O3	180.0535	2.53	1.00	1.00	0.38
C11H8O2	172.0524	7.42	1.00	0.73	0.18
C12H8O3S2	263.9915	0.69	1.00	0.67	0.25
C8H8O6S	232.0042	2.85	0.83	1.00	0.75
C12H24O6S	296.1294	8.14	0.17	2.00	0.50
C13H27NO8S	357.1457	7.55	0.13	2.08	0.62
C13H8O3	212.0473	4.93	1.00	0.62	0.23
C10H6N2O2	186.0429	3.48	1.00	0.60	0.20
C8H7NO2	149.0477	2.94	1.00	0.88	0.25
C11H14N2O7S	318.0522	7.64	0.86	1.27	0.64
C14H10O	194.0732	8.15	1.00	0.71	0.07
C18H12O4S	324.0456	7.78	1.00	0.67	0.22
C5H10N2O10	258.0335	2.39	0.20	2.00	2.00
C6H8N2O	124.0637	0.46	1.00	1.33	0.17
C9H6O7S	257.9834	2.28	1.00	0.67	0.78
C14H27NO8S	369.1457	7.79	0.25	1.93	0.57
C10H16O7S	280.0617	1.06	0.43	1.60	0.70
C6H7NO10S	284.9791	3.08	0.40	1.17	1.67
C14H12O2	212.0837	8.20	1.00	0.86	0.14
C7H7NO7S	248.9943	3.37	0.71	1.00	1.00
C5H9NO3	131.0582	0.89	0.67	1.80	0.60
C11H14O3	194.0943	8.28	1.00	1.27	0.27
C9H8N2O3	192.0535	4.81	1.00	0.89	0.33
C9H11NO7S	277.0256	4.42	0.71	1.22	0.78
C7H8N4O8S2	339.9784	1.07	0.75	1.14	1.14
C11H8O2	172.0524	5.13	1.00	0.73	0.18
C8H7NO4	181.0375	6.13	1.00	0.88	0.50
C6H7NO4S	189.0096	0.78	1.00	1.17	0.67
C10H9NO3	191.0582	2.85	1.00	0.90	0.30
C13H12OS2	248.0330	2.21	1.00	0.92	0.08
C7H8N2O2	152.0586	1.73	1.00	1.14	0.29
C10H6O7	238.0114	2.78	1.00	0.60	0.70
C14H9NO2	223.0633	7.17	1.00	0.64	0.14
C12H18N2O6S	318.0886	7.97	0.83	1.50	0.50
C12H12O4	220.0736	7.72	1.00	1.00	0.33
C8H6N2O7	242.0175	6.46	1.00	0.75	0.88
C13H22O7S	322.1086	3.07	0.43	1.69	0.54
C11H11N3O4	249.0750	2.98	1.00	1.00	0.36
C9H7NO3	177.0426	6.98	1.00	0.78	0.33
C5H5NO4	143.0219	1.21	1.00	1.00	0.80
C8H16O3S	192.0820	3.98	0.33	2.00	0.38
C14H9NO3	239.0582	2.69	1.00	0.64	0.21
C5H10O8S	230.0096	1.70	0.13	2.00	1.60
C12H7NO6	261.0273	2.92	1.00	0.58	0.50
C8H8O4S	200.0143	2.65	1.00	1.00	0.50
C12H16O7	272.0896	2.66	0.71	1.33	0.58
C10H12O4	196.0736	3.34	1.00	1.20	0.40
C7H8N2O2	152.0586	0.55	1.00	1.14	0.29
C10H6N4O5S	294.0059	3.07	1.00	0.60	0.50
C12H8O6	248.0321	3.27	1.00	0.67	0.50
C14H10O3	226.0630	4.17	1.00	0.71	0.21
C7H12N2O7S	268.0365	7.09	0.43	1.71	1.00
C5H5N3O3	155.0331	1.69	1.00	1.00	0.60
C10H16O7S	280.0617	1.55	0.43	1.60	0.70
C14H11NO4	257.0688	8.36	1.00	0.79	0.29
C17H8O3S	292.0194	2.87	1.00	0.47	0.18
C14H10O3	226.0630	5.28	1.00	0.71	0.21
C8H14O2	142.0994	2.95	1.00	1.75	0.25
C10H11NO7S	289.0256	6.11	0.86	1.10	0.70
C6H12O4S	180.0456	0.55	0.25	2.00	0.67
C12H10O3	202.0630	7.18	1.00	0.83	0.25
C11H22N2O10S	374.0995	7.95	0.20	2.00	0.91
C7H18N2O7S	274.0835	3.89	0.00	2.57	1.00
C8H8O4	168.0423	4.40	1.00	1.00	0.50
C7H13NO8S	271.0362	2.77	0.25	1.86	1.14
C16H31NO9S	413.1720	8.07	0.22	1.94	0.56
C10H7NO5	221.0324	6.27	1.00	0.70	0.50

7 Appendix

C22H33NO5S2	455.1800	7.59	1.00	1.50	0.23
C17H34O5S	350.2127	8.38	0.20	2.00	0.29
C7H8O	108.0575	2.73	1.00	1.14	0.14
C7H6N2O4	182.0328	4.70	1.00	0.86	0.57
C8H5NO7	227.0066	2.21	1.00	0.63	0.88
C11H13NO5	239.0794	7.35	1.00	1.18	0.45
C8H6O5S	213.9936	2.74	1.00	0.75	0.63
C8H7NO8S	276.9892	3.26	0.75	0.88	1.00
C17H14O7	330.0740	8.06	1.00	0.82	0.41
C7H14O7S	242.0460	2.60	0.14	2.00	1.00
C8H12N2O8S	296.0314	3.48	0.50	1.50	1.00
C9H6O5	194.0215	3.17	1.00	0.67	0.56
C7H5NO3	151.0269	2.89	1.00	0.71	0.43
C4H4N4O7S	251.9801	0.83	0.71	1.00	1.75
C6H12N2O18S	431.9806	6.48	0.11	2.00	3.00
C7H9NO4	171.0532	1.38	1.00	1.29	0.57
C12H20O8S	324.0879	2.84	0.38	1.67	0.67
C10H15N3O7S	321.0631	8.07	0.71	1.50	0.70
C12H10O4	218.0579	3.21	1.00	0.83	0.33
C7H9NO2	139.0633	1.02	1.00	1.29	0.29
C4H5NO5	147.0168	0.34	0.60	1.25	1.25
C8H11NO3	169.0739	2.70	1.00	1.38	0.38
C15H14O5	274.0841	6.76	1.00	0.93	0.33
C7H14O4	162.0892	2.45	0.25	2.00	0.57
C9H6O2S2	209.9809	0.63	1.00	0.67	0.22
C3H5NO4S	150.9939	0.50	0.50	1.67	1.33
C9H16O6S	252.0668	4.08	0.33	1.78	0.67
C18H35NO8S	425.2083	8.26	0.25	1.94	0.44
C10H5NO3	187.0269	2.95	1.00	0.50	0.30
C12H7NO4	229.0375	3.42	1.00	0.58	0.33
C7H5NO5	183.0168	0.66	1.00	0.71	0.71
C14H13NO4	259.0845	8.13	1.00	0.93	0.29
C14H26O5	274.1780	7.40	0.40	1.86	0.36
C8H6N2O3	178.0378	5.40	1.00	0.75	0.38
C15H14O3	242.0943	8.22	1.00	0.93	0.20
C8H6N2O3	178.0378	6.24	1.00	0.75	0.38
C12H16N2O7S	332.0678	8.00	0.86	1.33	0.58
C13H4N4O6	312.0131	2.72	1.00	0.31	0.46
C9H18O6S	254.0824	6.92	0.17	2.00	0.67
C8H7N3O2	177.0538	3.38	1.00	0.88	0.25
C7H10O	110.0732	2.49	1.00	1.43	0.14
C8H6O10S	293.9682	1.95	0.60	0.75	1.25
C9H11NO4	197.0688	4.76	1.00	1.22	0.44
C8H16O6S	240.0668	4.65	0.17	2.00	0.75
C6H5N3O5	199.0229	7.41	1.00	0.83	0.83
C11H5NO4	215.0219	3.59	1.00	0.45	0.36
C8H16O3S2	224.0541	2.86	0.33	2.00	0.38
C8H10O6S	234.0198	0.63	0.67	1.25	0.75
C8H6N2O6	226.0226	4.75	1.00	0.75	0.75
C10H9NO2	175.0633	3.18	1.00	0.90	0.20
C6H5N3O2	151.0382	3.37	1.00	0.83	0.33
C6H12O5S	196.0405	2.79	0.20	2.00	0.83
C9H7NO5	209.0324	3.41	1.00	0.78	0.56
C3H6O4S	137.9987	2.76	0.25	2.00	1.33
C12H18O4	226.1205	5.86	1.00	1.50	0.33
C14H25NO7S	351.1352	8.11	0.43	1.79	0.50
C10H17NO8S	311.0675	3.10	0.38	1.70	0.80
C14H14O2	214.0994	8.12	1.00	1.00	0.14
C10H7NO2	173.0477	5.02	1.00	0.70	0.20
C12H12O3	204.0786	3.37	1.00	1.00	0.25
C7H12N2O8S2	316.0035	5.35	0.38	1.71	1.14
C15H9NO5	283.0481	3.24	1.00	0.60	0.33
C10H12O5	212.0685	2.62	1.00	1.20	0.50
C9H5NO5	207.0168	1.85	1.00	0.56	0.56
C8H6N2O6	226.0226	4.96	1.00	0.75	0.75
C14H16O4	248.1049	7.71	1.00	1.14	0.29
C8H12N2O6S	264.0416	6.99	0.67	1.50	0.75
C4H8O4S	152.0143	5.11	0.25	2.00	1.00
C8H16O4	176.1049	1.48	0.25	2.00	0.50
C10H11NO6	241.0586	4.16	1.00	1.10	0.60

7 Appendix

C13H6N4O5S2	297.9983	1.72	1.00	0.46	0.08
C12H11NO6	265.0586	2.64	1.00	0.92	0.50
C12H16N2O5S	300.0780	8.11	1.00	1.33	0.42
C8H12O2	140.0837	2.77	1.00	1.50	0.25
C7H6N2O6	214.0226	6.75	1.00	0.86	0.86
C8H12N2O8S	296.0314	7.38	0.50	1.50	1.00
C8H9NO2	151.0633	0.75	1.00	1.13	0.25
C8H8N2O4	196.0484	2.94	1.00	1.00	0.50
C6H13NO8S	259.0362	2.60	0.13	2.17	1.33
C12H8O3	200.0473	3.09	1.00	0.67	0.25
C7H6O	106.0419	2.64	1.00	0.86	0.14
C6H7NO9S	268.9842	3.75	0.44	1.17	1.50
C18H18O4	298.1205	7.67	1.00	1.00	0.22
C8H4O3	148.0160	1.94	1.00	0.50	0.38
C10H18N2O6S	294.0886	8.00	0.50	1.80	0.60
C8H12N2O10S	328.0213	3.16	0.40	1.50	1.25
C13H10O8S	326.0096	5.04	1.00	0.77	0.62
C18H36O5S	364.2283	8.26	0.20	2.00	0.28
C17H14O12S	442.0206	7.43	0.92	0.82	0.71
C6H4N2O5	184.0120	3.99	1.00	0.67	0.83
C10H20N2O8S	328.0940	7.25	0.25	2.00	0.80
C10H10O6S	258.0198	3.65	1.00	1.00	0.60
C10H8O2	160.0524	3.55	1.00	0.80	0.20
C8H6O6S	229.9885	1.34	1.00	0.75	0.75
C5H9NO7S	227.0100	3.10	0.29	1.80	1.40
C6H13NO7S	243.0413	3.97	0.14	2.17	1.17
C20H30O5	350.2093	7.89	1.00	1.50	0.25
C9H8O5S	228.0092	1.50	1.00	0.89	0.56
C7H15NO8S	273.0518	2.04	0.13	2.14	1.14
C5H9NO8S	243.0049	1.68	0.25	1.80	1.60
C12H9NO5	247.0481	7.70	1.00	0.75	0.42
C14H14O6	278.0790	3.30	1.00	1.00	0.43
C12H7NO2	197.0477	6.84	1.00	0.58	0.17
C4H8O2	88.0524	1.09	0.50	2.00	0.50
C8H8O6S	232.0042	2.31	0.83	1.00	0.75
C13H6O7	274.0114	5.15	1.00	0.46	0.54
C9H18N2O9S	330.0733	6.92	0.22	2.00	1.00
C8H15NO9S	301.0468	3.11	0.22	1.88	1.13
C12H10O7S	298.0147	2.36	1.00	0.83	0.58
C8H9NO7S	263.0100	4.84	0.71	1.13	0.88
C7H9NO3	155.0582	1.38	1.00	1.29	0.43
C7H12N2O8S2	316.0035	5.63	0.38	1.71	1.14
C7H12N2O6S	252.0416	6.62	0.50	1.71	0.86
C12H8O4	216.0423	6.72	1.00	0.67	0.33
C7H14O3S2	210.0384	2.59	0.33	2.00	0.43
C6H5NO6S	218.9838	0.38	0.83	0.83	1.00
C17H16O3	268.1099	8.22	1.00	0.94	0.18
C14H10O5	258.0528	7.61	1.00	0.71	0.36
C9H9NO4S	227.0252	1.66	1.00	1.00	0.44
C10H14N2O5S	274.0623	6.99	1.00	1.40	0.50
C8H5NO8	243.0015	4.16	0.88	0.63	1.00
C7H9N3O3	183.0644	3.10	1.00	1.29	0.43
C10H17NO5	231.1107	2.62	0.60	1.70	0.50
C15H8O7S2	363.9711	2.94	1.00	0.53	0.47
C17H28O5	312.1937	7.80	0.80	1.65	0.29
C9H20N2O5S	268.1093	7.86	0.20	2.22	0.56
C11H10O6S	270.0198	2.57	1.00	0.91	0.55
C9H8O2	148.0524	3.78	1.00	0.89	0.22
C9H9NO4S	227.0252	2.21	1.00	1.00	0.44
C12H22O5	246.1467	3.02	0.40	1.83	0.42
C13H24O5	260.1624	6.77	0.40	1.85	0.38
C4H4N4O8S	267.9750	1.94	0.63	1.00	2.00
C11H21NO9	311.1216	2.51	0.22	1.91	0.82
C6H6O2	110.0368	2.60	1.00	1.00	0.33
C11H18O7S	294.0773	2.62	0.43	1.64	0.64
C10H17NO9S	327.0624	3.50	0.33	1.70	0.90
C8H11NO5	201.0637	0.79	0.80	1.38	0.63
C9H10O2	150.0681	5.00	1.00	1.11	0.22
C10H8N2O4	220.0484	1.22	1.00	0.80	0.40
C14H7NO5	269.0324	7.83	1.00	0.50	0.36

7 Appendix

C16H14O2	238.0994	8.26	1.00	0.88	0.13
C9H9NO4	195.0532	7.34	1.00	1.00	0.44
C4H12N2O7S	232.0365	3.49	0.00	3.00	1.75
C15H18O4	262.1205	8.01	1.00	1.20	0.27
C11H7NO6	249.0273	2.46	1.00	0.64	0.55
C11H20O5S	264.1031	3.90	0.40	1.82	0.45
C8H9NO4	183.0532	0.55	1.00	1.13	0.50
C15H25NO8S	379.1301	7.56	0.50	1.67	0.53
C7H7NO5S	217.0045	2.29	1.00	1.00	0.71
C13H10O	182.0732	7.10	1.00	0.77	0.08
C10H6N4O5S	294.0059	3.28	1.00	0.60	0.50
C9H7NO	145.0528	0.91	1.00	0.78	0.11
C12H13NO4	235.0845	8.23	1.00	1.08	0.33
C13H22O5	258.1467	3.16	0.60	1.69	0.38
C9H7NO5	209.0324	1.10	1.00	0.78	0.56
C7H5NO4	167.0219	2.93	1.00	0.71	0.57
C8H14O10S	302.0308	2.48	0.20	1.75	1.25
C8H16O4S	208.0769	6.31	0.25	2.00	0.50
C7H6N2O	134.0480	2.85	1.00	0.86	0.14
C10H20O3	188.1412	5.47	0.33	2.00	0.30
C5H10N2O10	258.0335	2.96	0.20	2.00	2.00
C7H8O2	124.0524	0.63	1.00	1.14	0.29
C13H25NO9S	371.1250	7.24	0.22	1.92	0.69
C9H7NO	145.0528	3.01	1.00	0.78	0.11
C6H12O2	116.0837	2.71	0.50	2.00	0.33
C12H13NO4	235.0845	2.91	1.00	1.08	0.33
C8H11NO8S	281.0205	3.04	0.50	1.38	1.00
C3H6O9S	217.9733	7.58	0.11	2.00	3.00
C6H5NO5	171.0168	0.41	1.00	0.83	0.83
C9H13NO5S	247.0514	1.02	0.80	1.44	0.56
C16H12O5	284.0685	4.32	1.00	0.75	0.31
C4H11N3O8S	261.0267	4.27	0.13	2.75	2.00
C17H14O3	266.0943	8.08	1.00	0.82	0.18
C6H7NO5S	205.0045	1.07	0.80	1.17	0.83
C10H20O4	204.1362	6.68	0.25	2.00	0.40
C11H22O4	218.1518	3.79	0.25	2.00	0.36
C10H9NO5	223.0481	5.90	1.00	0.90	0.50
C4H3NO2S	128.9884	0.55	1.00	0.75	0.50
C8H7N3O7	257.0284	6.95	1.00	0.88	0.88
C14H10O2	210.0681	6.88	1.00	0.71	0.14
C9H6O2	146.0368	2.51	1.00	0.67	0.22
C5H6O2	98.0368	0.39	1.00	1.20	0.40
C20H10O5S2	393.9970	5.04	1.00	0.50	0.25
C7H14O4	162.0892	2.74	0.25	2.00	0.57
C17H24O4	292.1675	6.83	1.00	1.41	0.24
C10H8N2O5S2	299.9875	1.49	1.00	0.80	0.50
C10H10O6S	258.0198	3.44	1.00	1.00	0.60
C15H6OS2	265.9860	0.81	1.00	0.40	0.07
C11H10N2O8S	330.0158	3.71	1.00	0.91	0.73
C14H26O7S	338.1399	3.11	0.29	1.86	0.50
C15H10O4S	286.0300	7.18	1.00	0.67	0.27
C8H6N2O2	162.0429	1.16	1.00	0.75	0.25
C4H8O7	168.0270	1.12	0.14	2.00	1.75
C13H27NO5S	309.1610	3.68	0.20	2.08	0.38
C9H18O8S	286.0722	5.22	0.13	2.00	0.89
C15H15NO3	257.1052	8.40	1.00	1.00	0.20
C26H50O4	426.3709	10.38	0.50	1.92	0.15
C7H7NO	121.0528	2.65	1.00	1.00	0.14
C12H20O6S	292.0981	2.98	0.50	1.67	0.50
C7H6N2O3	166.0378	1.11	1.00	0.86	0.43
C11H19NO5	245.1263	3.04	0.60	1.73	0.45
C11H14O7	258.0740	2.59	0.71	1.27	0.64
C8H6N2O	146.0480	2.40	1.00	0.75	0.13
C8H12N2O6S	264.0416	8.37	0.67	1.50	0.75
C12H10O2	186.0681	7.55	1.00	0.83	0.17
C7H6N4OS2	225.9983	1.71	1.00	0.86	0.14
C10H9NO6S	271.0151	2.36	1.00	0.90	0.60
C20H6O3S2	357.9758	6.99	1.00	0.30	0.15
C10H14O3	182.0943	3.07	1.00	1.40	0.30
C4H7NO3S	149.0147	0.62	0.67	1.75	0.75

7 Appendix

C16H22O5	294.1467	8.41	1.00	1.38	0.31
C7H6O5	170.0215	1.42	1.00	0.86	0.71
C10H12O6	228.0634	2.65	0.83	1.20	0.60
C29H9NO3S	451.0303	3.57	1.00	0.31	0.10
C13H25NO7S	339.1352	8.22	0.29	1.92	0.54
C13H12O4	232.0736	3.90	1.00	0.92	0.31
C7H9NO2	139.0633	2.52	1.00	1.29	0.29
C15H5NO3S	278.9990	0.85	1.00	0.33	0.20
C12H24O5S	280.1344	8.19	0.20	2.00	0.42
C12H12O2	188.0837	4.24	1.00	1.00	0.17
C16H30O5	302.2093	7.51	0.40	1.88	0.31
C16H9NO2S	279.0354	6.38	1.00	0.56	0.13
C16H10O7	314.0427	3.52	1.00	0.63	0.44
C6H13N3O6S	255.0525	6.91	0.33	2.17	1.00
C10H16N2O10S	356.0526	7.71	0.40	1.60	1.00
C8H14N2O10S	330.0369	3.73	0.30	1.75	1.25
C11H13NO5	239.0794	4.58	1.00	1.18	0.45
C7H8O5S	204.0092	0.99	0.80	1.14	0.71
C18H28O3	292.2038	8.29	1.00	1.56	0.17
C8H7NO2	149.0477	0.66	1.00	0.88	0.25
C10H16O3	184.1099	7.89	1.00	1.60	0.30
C12H22O7S	310.1086	3.94	0.29	1.83	0.58
C9H19NO4S	237.1035	6.86	0.25	2.11	0.44
C11H8O3	188.0473	6.44	1.00	0.73	0.27
C8H13NO4	187.0845	2.70	0.75	1.63	0.50
C11H8O7	252.0270	3.34	1.00	0.73	0.64
C10H9NO6	239.0430	4.25	1.00	0.90	0.60
C8H10O6	202.0477	1.59	0.67	1.25	0.75
C11H13NO4	223.0845	7.85	1.00	1.18	0.36
C7H8O	108.0575	4.37	1.00	1.14	0.14
C6H8N2O7	220.0332	0.68	0.57	1.33	1.17
C10H19NO13S2	425.0298	4.68	0.15	1.90	1.30
C15H27NO7S	365.1508	8.24	0.43	1.80	0.47
C7H6O4S	185.9987	1.42	1.00	0.86	0.57
C18H10O4S	322.0300	7.72	1.00	0.56	0.22
C9H16O4S	220.0769	2.06	0.50	1.78	0.44
C8H15NO9S	301.0468	2.37	0.22	1.88	1.13
C8H13NO2	155.0946	3.34	1.00	1.63	0.25
C4H8O2	88.0524	0.39	0.50	2.00	0.50
C9H13NO3	183.0895	2.73	1.00	1.44	0.33
C8H9NO7S	263.0100	3.13	0.71	1.13	0.88
C14H22O7	302.1366	3.08	0.57	1.57	0.50
C8H16O5S	224.0718	1.81	0.20	2.00	0.63
C8H10N2O2	166.0742	2.79	1.00	1.25	0.25
C9H5NO6	223.0117	2.33	1.00	0.56	0.67
C16H10O7	314.0427	3.32	1.00	0.63	0.44
C9H20O5S	240.1031	5.60	0.00	2.22	0.56
C11H22O6S	282.1137	6.17	0.17	2.00	0.55
C13H7NO4	241.0375	3.41	1.00	0.54	0.31
C14H8O4	240.0423	3.54	1.00	0.57	0.29
C15H9NO5	283.0481	3.57	1.00	0.60	0.33
C14H16O4	248.1049	7.80	1.00	1.14	0.29
C9H11NO5	213.0637	4.33	1.00	1.22	0.56
C15H28O6	304.1886	7.30	0.33	1.87	0.40
C9H11NO4	197.0688	3.60	1.00	1.22	0.44
C5H14N2O7S	246.0522	3.43	0.00	2.80	1.40
C13H22O5	258.1467	7.26	0.60	1.69	0.38
C7H4O3	136.0160	3.12	1.00	0.57	0.43
C9H11NO6	229.0586	2.62	0.83	1.22	0.67
C15H20O4	264.1362	8.19	1.00	1.33	0.27
C9H8N2O3	192.0535	6.89	1.00	0.89	0.33
C8H8N4O5S2	240.0140	2.72	1.00	1.00	0.13
C9H11NO2	165.0790	3.26	1.00	1.22	0.22
C8H9NO5	199.0481	5.42	1.00	1.13	0.63
C5H7NO8S	240.9892	1.10	0.38	1.40	1.60
C10H18O6S	266.0824	5.42	0.33	1.80	0.60
C17H30O4	298.2144	8.18	0.75	1.76	0.24
C14H13NO7S	339.0413	7.47	1.00	0.93	0.50
C12H13NO4	235.0845	7.54	1.00	1.08	0.33
C16H8OS	248.0296	3.92	1.00	0.50	0.06

7 Appendix

C7H7N3O2	165.0538	3.72	1.00	1.00	0.29
C11H12O5S	256.0405	2.73	1.00	1.09	0.45
C6H10O7	194.0427	2.90	0.29	1.67	1.17
C9H7NO5S	241.0045	2.48	1.00	0.78	0.56
C15H5NOS2	278.9813	2.69	1.00	0.33	0.07
C4H12N2O7S	232.0365	4.93	0.00	3.00	1.75
C11H8O3S2	251.9915	1.09	1.00	0.73	0.27
C11H20O6S	280.0981	7.03	0.33	1.82	0.55
C7H10O5S	206.0249	0.96	0.60	1.43	0.71
C9H11NO3	181.0739	2.57	1.00	1.22	0.33
C5H14N2O9S	278.0420	2.77	0.00	2.80	1.80
C11H19NO7S	309.0882	7.60	0.43	1.73	0.64
C7H5NO6	199.0117	0.97	1.00	0.71	0.86
C11H11NO5	237.0637	7.46	1.00	1.00	0.45
C3H7NO8S	216.9892	4.53	0.13	2.33	2.67
C4H8O4S	152.0143	1.20	0.25	2.00	1.00
C13H24O5	260.1624	7.21	0.40	1.85	0.38
C8H12N2O8S	296.0314	5.27	0.50	1.50	1.00
C8H12N2O8S	296.0314	3.96	0.50	1.50	1.00
C12H16O4	224.1049	3.03	1.00	1.33	0.33
C7H7NO7S	248.9943	3.80	0.71	1.00	1.00
C7H6O5	170.0215	2.13	1.00	0.86	0.71
C8H14N2O6S	266.0573	3.54	0.50	1.75	0.75
C15H11NO5	285.0637	7.79	1.00	0.73	0.33
C16H14O6	302.0790	5.12	1.00	0.88	0.38
C8H14O8	238.0689	3.10	0.25	1.75	1.00
C14H9NO2	223.0633	6.82	1.00	0.64	0.14
C14H26N4O12	442.1547	3.71	0.33	1.86	0.86
C10H6O9S	301.9733	0.48	0.89	0.60	0.90
C9H12O7	232.0583	2.52	0.57	1.33	0.78
C23H13NO6S	431.0464	6.33	1.00	0.57	0.26
C8H6N2O3	178.0378	4.26	1.00	0.75	0.38
C11H22O4	218.1518	3.29	0.25	2.00	0.36
C12H23NO9S	357.1094	3.50	0.22	1.92	0.75
C7H9NO	123.0684	0.95	1.00	1.29	0.14
C5H2N4OS2	197.9670	0.53	1.00	0.40	0.20
C5H9NO9S	258.9998	0.74	0.22	1.80	1.80
C10H12O7	244.0583	0.63	0.71	1.20	0.70
C9H11NO4	197.0688	4.12	1.00	1.22	0.44
C13H18O5	254.1154	3.13	1.00	1.38	0.38
C9H8N2O3	192.0535	7.32	1.00	0.89	0.33
C12H8O2S2	247.9966	0.52	1.00	0.67	0.17
C13H23NO2	225.1729	8.19	1.00	1.77	0.15
C4H8O5S	168.0092	0.85	0.20	2.00	1.25
C12H18O4	226.1205	3.17	1.00	1.50	0.33
C16H16O5	288.0998	7.49	1.00	1.00	0.31
C10H15NO4	213.1001	3.82	1.00	1.50	0.40
C7H12O8	224.0532	2.98	0.25	1.71	1.14
C15H15NO4	273.1001	8.27	1.00	1.00	0.27
C7H6N2O6	214.0226	4.34	1.00	0.86	0.86
C7H13N3O4S	235.0627	7.57	0.75	1.86	0.57
C11H20O8S	312.0879	3.79	0.25	1.82	0.73
C14H12O3	228.0786	4.41	1.00	0.86	0.21
C7H4N2O5	196.0120	3.57	1.00	0.57	0.71
C6H7NO3S	173.0147	1.30	1.00	1.17	0.50
C14H28O4	260.1988	7.52	0.25	2.00	0.29
C9H11N3OS2	241.0344	0.58	1.00	1.22	0.11
C11H8O3	188.0473	3.15	1.00	0.73	0.27
C5H8O	84.0575	1.71	1.00	1.60	0.20
C9H6O7S	257.9834	1.71	1.00	0.67	0.78
C11H12O4	208.0736	7.58	1.00	1.09	0.36
C13H23N3O3	269.1739	6.71	1.00	1.77	0.23
C5H14N2O9S	278.0420	3.01	0.00	2.80	1.80
C12H12O3	204.0786	4.07	1.00	1.00	0.25
C10H9NO5	223.0481	5.01	1.00	0.90	0.50
C16H30O5	302.2093	7.96	0.40	1.88	0.31
C8H6O6S	229.9885	0.92	1.00	0.75	0.75
C9H6O3	162.0317	1.07	1.00	0.67	0.33
C11H9NO6	251.0430	2.73	1.00	0.82	0.55
C6H7NO4S	189.0096	1.34	1.00	1.17	0.67

7 Appendix

C8H15NO6	221.0899	3.73	0.33	1.88	0.75
C15H16O4	260.1049	7.83	1.00	1.07	0.27
C7H14N2O8S	286.0471	4.94	0.25	2.00	1.14
C12H4O13	355.9652	0.18	0.85	0.33	1.08
C20H20N4O3	364.1535	7.50	1.00	1.00	0.15
C14H10O3	226.0630	3.55	1.00	0.71	0.21
C5H13N3O7S	259.0474	6.98	0.14	2.60	1.40
C16H10N4O6	354.0600	5.21	1.00	0.63	0.38
C11H6O6	234.0164	1.59	1.00	0.55	0.55
C9H20N2OS2	236.1017	6.75	1.00	2.22	0.11
C9H8N2O3	192.0535	7.63	1.00	0.89	0.33
C11H12N2O10	332.0492	6.18	0.70	1.09	0.91
C8H6N2O7	242.0175	2.26	1.00	0.75	0.88
C10H8O8S	287.9940	1.51	0.88	0.80	0.80
C13H12O3	216.0786	7.80	1.00	0.92	0.23
C11H10O2	174.0681	3.55	1.00	0.91	0.18
C6H5NO5	171.0168	1.06	1.00	0.83	0.83
C8H8O11S2	343.9508	1.59	0.45	1.00	1.38
C6H13NO9S	275.0311	0.71	0.11	2.17	1.50
C20H26OS2	346.1425	7.49	1.00	1.30	0.05
C8H8O5	184.0372	1.82	1.00	1.00	0.63
C9H13NO5S	247.0514	1.29	0.80	1.44	0.56
C8H7NO2	149.0477	2.44	1.00	0.88	0.25
C9H8O6	212.0321	4.14	1.00	0.89	0.67
C5H8O10S2	291.9559	8.87	0.20	1.60	2.00
C4H7NO8S	228.9892	0.86	0.25	1.75	2.00
C10H9NO6S	271.0151	0.89	1.00	0.90	0.60
C16H30O6	318.2042	7.62	0.33	1.88	0.38
C4H4N4O8S	267.9750	1.09	0.63	1.00	2.00
C16H20O4	276.1362	8.30	1.00	1.25	0.25
C8H6N2O3	178.0378	3.88	1.00	0.75	0.38
C8H15N3O5S	265.0732	8.44	0.60	1.88	0.63
C18H10O5	274.0452	4.15	1.00	0.56	0.06
C14H16O3	232.1099	7.40	1.00	1.14	0.21
C6H12N2O10	272.0492	3.33	0.20	2.00	1.67
C7H7NO5S	217.0045	1.09	1.00	1.00	0.71
C5H3NO4S	172.9783	0.56	1.00	0.60	0.80
C15H26O3	254.1882	8.37	1.00	1.73	0.20
C10H6O4	190.0266	4.24	1.00	0.60	0.40
C10H22N2O2S2	266.1123	3.80	0.50	2.20	0.20
C14H16O4	248.1049	6.78	1.00	1.14	0.29
C11H12O6S	272.0355	1.07	1.00	1.09	0.55
C21H22N4O3	378.1692	7.81	1.00	1.05	0.14
C9H9NO4	195.0532	7.56	1.00	1.00	0.44
C10H6O12S2	381.9301	0.13	0.67	0.60	1.20
C9H16O4	188.1049	3.72	0.50	1.78	0.44
C6H5NO3	139.0269	3.75	1.00	0.83	0.50
C4H6O4	118.0266	0.52	0.50	1.50	1.00
C7H12O4	160.0736	2.72	0.50	1.71	0.57
C6H10O4	146.0579	1.70	0.50	1.67	0.67
C4H8O4	120.0423	0.38	0.25	2.00	1.00
C10H18O4	202.1205	5.21	0.50	1.80	0.40
C4H4O4	116.0110	0.38	0.75	1.00	1.00
C5H8O4	132.0423	0.76	0.50	1.60	0.80
C7H7NO3	153.0426	6.04	1.00	1.00	0.43
C5H10O4	134.0579	0.38	0.25	2.00	0.80
C8H7NO5	197.0324	3.66	1.00	0.88	0.63
C8H12O6	204.0634	2.33	0.50	1.50	0.75
C7H7NO3	153.0426	5.21	1.00	1.00	0.43
C9H8O4	180.0423	3.15	1.00	0.89	0.44
C7H14O3	146.0943	3.23	0.33	2.00	0.43
C3H6O5S	153.9936	0.36	0.20	2.00	1.67
C2H3NO4S	136.9783	0.38	0.50	1.50	2.00
C5H8O5	148.0372	0.38	0.40	1.60	1.00
C8H9NO3	167.0582	7.56	1.00	1.13	0.38
C12H14O4	222.0892	7.43	1.00	1.17	0.33
C8H9NO3	167.0582	7.26	1.00	1.13	0.38
C16H6N4O6S2	413.9729	7.95	1.00	0.38	0.38
C6H5NO4	155.0219	3.08	1.00	0.83	0.67
C17H24O4	292.1675	8.56	1.00	1.41	0.24

7 Appendix

C4H8O4S	152.0143	0.38	0.25	2.00	1.00
C9H14O5	202.0841	2.69	0.60	1.56	0.56
C15H16O5S2	340.0439	3.72	1.00	1.07	0.33
C13H26O3	230.1882	7.99	0.33	2.00	0.23
C7H5NO5	183.0168	3.26	1.00	0.71	0.71
C10H16O5	216.0998	2.94	0.60	1.60	0.50
C6H12O5	164.0685	0.36	0.20	2.00	0.83
C7H5NO5	183.0168	2.94	1.00	0.71	0.71
C10H12N4OS2	268.0453	3.71	1.00	1.20	0.10
C6H12O4	148.0736	0.58	0.25	2.00	0.67
C6H10O5	162.0528	0.49	0.40	1.67	0.83
C11H20O5	232.1311	3.53	0.40	1.82	0.45
C14H28O4S	292.1708	8.27	0.25	2.00	0.29
C14H13NO3	243.0895	8.31	1.00	0.93	0.21
C2H6O4S	125.9987	0.38	0.00	3.00	2.00
C22H8N4O3S	408.0317	3.71	1.00	0.36	0.14
C5H8O6S	196.0042	0.36	0.33	1.60	1.20
C3H3N3O3	129.0174	0.36	1.00	1.00	1.00
C8H14O	126.1045	3.71	1.00	1.75	0.13
C7H6N2O6	214.0226	4.82	1.00	0.86	0.86
C5H6O5	146.0215	0.37	0.60	1.20	1.00
C7H10O5	174.0528	0.95	0.60	1.43	0.71
C13H16O3	220.1099	8.07	1.00	1.23	0.23
C3H4O4	104.0110	0.37	0.50	1.33	1.33
C2H4O5S	139.9779	0.34	0.20	2.00	2.50
C7H6O3	138.0317	3.55	1.00	0.86	0.43
C7H6O2	122.0368	2.67	1.00	0.86	0.29
C8H6O4	166.0266	2.64	1.00	0.75	0.50
C4H8O6S	184.0042	0.38	0.17	2.00	1.50
C9H14O4	186.0892	2.96	0.75	1.56	0.44
C5H10O5	150.0528	0.34	0.20	2.00	1.00
C3H6O4S	137.9987	0.35	0.25	2.00	1.33
C2H4O6S	155.9729	0.35	0.17	2.00	3.00
C5H8O4	132.0423	0.39	0.50	1.60	0.80
C5H8O4	132.0423	1.10	0.50	1.60	0.80
C8H6O3	150.0317	2.63	1.00	0.75	0.38
C7H7NO4	169.0375	4.11	1.00	1.00	0.57
C7H10O4	158.0579	1.69	0.75	1.43	0.57
C7H7NO4	169.0375	2.94	1.00	1.00	0.57
C18H30O5	326.2093	8.01	0.80	1.67	0.28
C8H6O3	150.0317	1.14	1.00	0.75	0.38
C9H8O3	164.0473	3.06	1.00	0.89	0.33
C4H8O5S	168.0092	0.39	0.20	2.00	1.25
C8H7NO3	165.0426	1.07	1.00	0.88	0.38
C4H6O5S	165.9936	0.36	0.40	1.50	1.25
C12H9NO3	215.0582	8.09	1.00	0.75	0.25
C13H28O4S	280.1708	8.59	0.00	2.15	0.31
C13H22O4	242.1518	7.48	0.75	1.69	0.31
C7H5NO	119.0371	3.13	1.00	0.71	0.14
C6H8O5	160.0372	0.39	0.60	1.33	0.83
C9H10N2O5	226.0590	8.15	1.00	1.11	0.56
C9H9NO3	179.0582	2.88	1.00	1.00	0.33
C7H6N2O4	182.0328	3.12	1.00	0.86	0.57
C8H7NO3	165.0426	3.19	1.00	0.88	0.38
C8H7NO4	181.0375	3.91	1.00	0.88	0.50
C7H12O6	192.0634	0.37	0.33	1.71	0.86
C6H6N2O2	138.0429	0.92	1.00	1.00	0.33
C9H16O5	204.0998	2.58	0.40	1.78	0.56
C5H12O4S	168.0456	2.81	0.00	2.40	0.80
C10H18O4	202.1205	6.80	0.50	1.80	0.40
C12H20O4	228.1362	7.36	0.75	1.67	0.33
C8H12O5	188.0685	1.91	0.60	1.50	0.63
C5H3NO4	141.0062	0.37	1.00	0.60	0.80
C3H3NO4	117.0062	0.39	0.75	1.00	1.33
C6H9NO4	159.0532	0.38	0.75	1.50	0.67
C16H32O6S	352.1920	7.86	0.17	2.00	0.38
C9H18O4	190.1205	3.47	0.25	2.00	0.44
C12H8N2O5	260.0433	8.31	1.00	0.67	0.42
C6H5NO4	155.0219	3.81	1.00	0.83	0.67
C3H8O4S	140.0143	0.50	0.00	2.67	1.33

7 Appendix

C10H11NO5	225.0637	4.15	1.00	1.10	0.50
C10H10O4	194.0579	6.38	1.00	1.00	0.40
C8H8N2O6	228.0382	7.67	1.00	1.00	0.75
C12H12N2O3	232.0848	7.63	1.00	1.00	0.25
C5H4O4	128.0110	0.37	1.00	0.80	0.80
C14H26O3	242.1882	8.40	0.67	1.86	0.21
C11H8O2	172.0524	3.84	1.00	0.73	0.18
C16H32O4	288.2301	7.56	0.25	2.00	0.25
C12H20O5	244.1311	4.34	0.60	1.67	0.42
C8H14O5	190.0841	2.24	0.40	1.75	0.63
C13H5NOS	223.0092	3.55	1.00	0.38	0.08
C8H6O5	182.0215	2.78	1.00	0.75	0.63
C7H12O	112.0888	3.12	1.00	1.71	0.14
C9H15NO2	169.1103	4.41	1.00	1.67	0.22

Table S4.3.5 Molecular formulas of organic compounds detected in Guangzhou OA in ESI⁻ mode.

Formula [M]	Neutral mass (Da)	RT (min)	MCR	H/C	O/C
C7H5NO5	183.0168	3.23	1.00	0.71	0.71
C7H7NO4	169.0375	2.93	1.00	1.00	0.57
C10H7NO3	189.0426	7.73	1.00	0.70	0.30
C7H5NO5	183.0168	2.93	1.00	0.71	0.71
C8H9NO5	199.0481	2.49	1.00	1.13	0.63
C8H9NO4	183.0532	7.04	1.00	1.13	0.50
C10H10O5	210.0528	3.01	1.00	1.00	0.50
C8H12O4	172.0736	2.46	0.75	1.50	0.50
C5H4N2O3	140.0222	2.38	1.00	0.80	0.60
C7H7NO5	185.0324	3.28	1.00	1.00	0.71
C13H25NO3	243.1834	7.36	0.67	1.92	0.23
C8H10O5S	218.0249	1.40	0.80	1.25	0.63
C6H12O7S	228.0304	0.38	0.14	2.00	1.17
C7H6O3	138.0317	2.23	1.00	0.86	0.43
C18H14O8	358.0689	7.43	1.00	0.78	0.44
C8H9NO4	183.0532	5.66	1.00	1.13	0.50
C5H6O7S	209.9834	0.37	0.43	1.20	1.40
C9H6O6	210.0164	1.08	1.00	0.67	0.67
C8H8O3	152.0473	2.63	1.00	1.00	0.38
C6H6O6	174.0164	0.37	0.67	1.00	1.00
C9H6O6	210.0164	1.90	1.00	0.67	0.67
C6H6O5	158.0215	0.38	0.80	1.00	0.83
C17H14O6	314.0790	7.96	1.00	0.82	0.35
C14H10O4S	274.0300	7.08	1.00	0.71	0.29
C4H10O5S	170.0249	0.38	0.00	2.50	1.25
C9H14O4	186.0892	2.92	0.75	1.56	0.44
C8H7NO5	197.0324	4.69	1.00	0.88	0.63
C10H17NO10S	343.0573	2.71	0.30	1.70	1.00
C5H10O7S	214.0147	0.37	0.14	2.00	1.40
C6H5N3O4	183.0280	4.90	1.00	0.83	0.67
C7H6O3	138.0317	2.76	1.00	0.86	0.43
C6H5NO5	171.0168	2.29	1.00	0.83	0.83
C9H11NO4	197.0688	7.36	1.00	1.22	0.44
C11H9NO3	203.0582	7.98	1.00	0.82	0.27
C10H17NO7S	295.0726	6.58	0.43	1.70	0.70
C13H8O2	196.0524	7.54	1.00	0.62	0.15
C9H16O5S	236.0718	2.64	0.40	1.78	0.56
C6H8O4	144.0423	0.69	0.75	1.33	0.67
C7H6N2O6	214.0226	3.53	1.00	0.86	0.86
C3H4O3	88.0160	0.36	0.67	1.33	1.00
C9H15NO8S	297.0518	3.26	0.38	1.67	0.89
C9H8O2	148.0524	3.08	1.00	0.89	0.22
C9H9NO7S	275.0100	4.19	0.86	1.00	0.78
C7H8O6	188.0321	0.39	0.67	1.14	0.86
C5H8O4	132.0423	0.39	0.50	1.60	0.80
C9H7NO4	193.0375	3.46	1.00	0.78	0.44
C4H6O6S	181.9885	0.38	0.33	1.50	1.50

7 Appendix

C8H5NO3	163.0269	2.66	1.00	0.63	0.38
C5H4N4O3	168.0283	0.37	1.00	0.80	0.60
C12H10O5S	266.0249	3.32	1.00	0.83	0.42
C9H16O6S	252.0668	2.60	0.33	1.78	0.67
C7H4N2O3	164.0222	3.99	1.00	0.57	0.43
C7H6O4	154.0266	1.28	1.00	0.86	0.57
C9H18O6S	254.0824	3.20	0.17	2.00	0.67
C8H7NO5	197.0324	3.25	1.00	0.88	0.63
C10H18O5S	250.0875	3.08	0.40	1.80	0.50
C8H5NO2	147.0320	3.25	1.00	0.63	0.25
C10H17N3O13S	419.0482	7.61	0.31	1.70	1.30
C8H9NO4	183.0532	6.51	1.00	1.13	0.50
C8H8O2	136.0524	3.10	1.00	1.00	0.25
C13H8O2	196.0524	7.18	1.00	0.62	0.15
C22H10O3S	354.0351	2.62	1.00	0.45	0.14
C5H10O6S	198.0198	0.44	0.17	2.00	1.20
C11H18O5	230.1154	3.20	0.60	1.64	0.45
C7H4N2O4	180.0171	3.51	1.00	0.57	0.57
C10H16O5S	248.0718	2.98	0.60	1.60	0.50
C11H8O2	172.0524	3.84	1.00	0.73	0.18
C3H5NO5	135.0168	0.38	0.40	1.67	1.67
C8H12O5	188.0685	2.34	0.60	1.50	0.63
C6H10O4	146.0579	0.58	0.50	1.67	0.67
C8H10O5	186.0528	3.03	0.80	1.25	0.63
C10H10O4	194.0579	3.66	1.00	1.00	0.40
C8H8N2O6	228.0382	7.58	1.00	1.00	0.75
C4H8O5S	168.0092	0.42	0.20	2.00	1.25
C5H3N3O2	137.0225	3.18	1.00	0.60	0.40
C7H12O7S	240.0304	0.57	0.29	1.71	1.00
C10H8O4	192.0423	3.08	1.00	0.80	0.40
C8H9NO4	183.0532	5.95	1.00	1.13	0.50
C10H8O5	208.0372	2.54	1.00	0.80	0.50
C7H6O5S	201.9936	0.62	1.00	0.86	0.71
C10H18N2O11S	374.0631	4.36	0.27	1.80	1.10
C9H8O3	164.0473	2.47	1.00	0.89	0.33
C10H8O6	224.0321	2.86	1.00	0.80	0.60
C9H5NO4	191.0219	2.64	1.00	0.56	0.44
C5H4O4	128.0110	0.37	1.00	0.80	0.80
C9H8O3	164.0473	3.06	1.00	0.89	0.33
C8H6O5	182.0215	1.89	1.00	0.75	0.63
C10H19NO8S	313.0831	3.38	0.25	1.90	0.80
C7H5NO6	199.0117	3.41	1.00	0.71	0.86
C9H9NO6	227.0430	3.36	1.00	1.00	0.67
C14H10O4	242.0579	5.03	1.00	0.71	0.29
C7H5NO6	199.0117	2.65	1.00	0.71	0.86
C4H6O3	102.0317	0.39	0.67	1.50	0.75
C4H10O4S	154.0300	0.92	0.00	2.50	1.00
C14H8O3	224.0473	7.56	1.00	0.57	0.21
C6H5NO3	139.0269	0.39	1.00	0.83	0.50
C8H15NO8S	285.0518	2.97	0.25	1.88	1.00
C5H10O5S	182.0249	0.52	0.20	2.00	1.00
C10H6O5	206.0215	3.13	1.00	0.60	0.50
C8H6O3	150.0317	0.81	1.00	0.75	0.38
C9H16O5	204.0998	2.76	0.40	1.78	0.56
C12H6O4	214.0266	5.46	1.00	0.50	0.33
C10H6O3S2	237.9758	0.52	1.00	0.60	0.30
C9H6O3	162.0317	3.14	1.00	0.67	0.33
C9H8O4	180.0423	2.75	1.00	0.89	0.44
C3H3NO2	85.0164	0.05	1.00	1.00	0.67
C6H4N2O5	184.0120	6.28	1.00	0.67	0.83
C3H4O8S	199.9627	0.31	0.25	1.33	2.67
C9H11NO4	197.0688	7.76	1.00	1.22	0.44
C6H12O5S	196.0405	0.97	0.20	2.00	0.83
C7H10O4	158.0579	1.67	0.75	1.43	0.57
C5H5N3O4	171.0280	3.93	1.00	1.00	0.80
C8H9NO4	183.0532	4.16	1.00	1.13	0.50
C7H6N2O6	214.0226	7.13	1.00	0.86	0.86
C9H15NO8S	297.0518	2.90	0.38	1.67	0.89
C8H7NO3	165.0426	3.18	1.00	0.88	0.38
C3H5NO5S	166.9888	0.36	0.40	1.67	1.67

7 Appendix

C5H4N2O3	140.0222	1.14	1.00	0.80	0.60
C9H7NO4	193.0375	7.16	1.00	0.78	0.44
C8H5NO4	179.0219	5.38	1.00	0.63	0.50
C7H4N2O7	228.0019	4.05	1.00	0.57	1.00
C4H3N3O4	157.0124	3.23	1.00	0.75	1.00
C9H6O3	162.0317	2.96	1.00	0.67	0.33
C6H8O7S	223.9991	0.38	0.43	1.33	1.17
C7H14O6S	226.0511	2.18	0.17	2.00	0.86
C10H16O4	200.1049	3.39	0.75	1.60	0.40
C7H12O6S	224.0355	0.82	0.33	1.71	0.86
C10H17NO7S	295.0726	6.29	0.43	1.70	0.70
C10H11NO4	209.0688	7.17	1.00	1.10	0.40
C8H8O3	152.0473	3.22	1.00	1.00	0.38
C10H14O5	214.0841	2.66	0.80	1.40	0.50
C9H13NO16	391.0234	3.08	0.25	1.44	1.78
C6H10O2	114.0681	2.74	1.00	1.67	0.33
C7H5NO4	167.0219	3.79	1.00	0.71	0.57
C9H14O6	218.0790	2.72	0.50	1.56	0.67
C8H5NO5	195.0168	3.13	1.00	0.63	0.63
C2H6O3S	110.0038	0.35	0.00	3.00	1.50
C11H24O4S	252.1395	8.19	0.00	2.18	0.36
C10H18N2O11S	374.0631	3.23	0.27	1.80	1.10
C10H4N2O4	216.0171	0.12	1.00	0.40	0.40
C5H8O3	116.0473	0.39	0.67	1.60	0.60
C10H8O4	192.0423	6.98	1.00	0.80	0.40
C7H10O4	158.0579	1.22	0.75	1.43	0.57
C8H9NO5	199.0481	4.23	1.00	1.13	0.63
C10H19NO8S	313.0831	3.08	0.25	1.90	0.80
C7H7NO5	185.0324	2.61	1.00	1.00	0.71
C8H8O10S	295.9838	2.65	0.50	1.00	1.25
C8H5NO4	179.0219	4.90	1.00	0.63	0.50
C7H12O7S	240.0304	0.89	0.29	1.71	1.00
C6H3N3O7	228.9971	4.07	1.00	0.50	1.17
C8H18O3S	194.0977	5.17	0.00	2.25	0.38
C8H6N2O5	210.0277	7.59	1.00	0.75	0.63
C10H10O3	178.0630	2.98	1.00	1.00	0.30
C4H4O5	132.0059	0.35	0.60	1.00	1.25
C10H14O6	230.0790	2.79	0.67	1.40	0.60
C7H5NO2	135.0320	2.67	1.00	0.71	0.29
C5H5NO3	127.0269	1.01	1.00	1.00	0.60
C8H6O4	166.0266	1.33	1.00	0.75	0.50
C11H20O6	248.1260	3.03	0.33	1.82	0.55
C9H18O6S	254.0824	3.51	0.17	2.00	0.67
C13H8O2	196.0524	4.86	1.00	0.62	0.15
C8H10O3	154.0630	1.56	1.00	1.25	0.38
C9H16O6S	252.0668	4.01	0.33	1.78	0.67
C14H10O3	226.0630	7.14	1.00	0.71	0.21
C6H12O4	148.0736	0.53	0.25	2.00	0.67
C8H17NO8S	287.0675	2.99	0.13	2.13	1.00
C5H4O3	112.0160	0.38	1.00	0.80	0.60
C7H12O4	160.0736	0.91	0.50	1.71	0.57
C9H6O7	226.0114	1.05	1.00	0.67	0.78
C4H8O3	104.0473	0.60	0.33	2.00	0.75
C9H18O7S	270.0773	3.03	0.14	2.00	0.78
C12H8O4	216.0423	4.04	1.00	0.67	0.33
C9H10O3	166.0630	3.23	1.00	1.11	0.33
C8H6O2	134.0368	1.79	1.00	0.75	0.25
C13H11NO3	229.0739	8.12	1.00	0.85	0.23
C8H5NO3	163.0269	2.99	1.00	0.63	0.38
C5H8O2	100.0524	0.67	1.00	1.60	0.40
C5H4N2O3	140.0222	0.39	1.00	0.80	0.60
C8H10O5	186.0528	0.65	0.80	1.25	0.63
C8H6O4	166.0266	1.86	1.00	0.75	0.50
C6H6O7	190.0114	0.35	0.57	1.00	1.17
C6H14O4S	182.0613	3.49	0.00	2.33	0.67
C5H4N2O4	156.0171	1.22	1.00	0.80	0.80
C9H16O7S	268.0617	2.35	0.29	1.78	0.78
C9H7NO4	193.0375	6.77	1.00	0.78	0.44
C6H5NO3	139.0269	2.96	1.00	0.83	0.50
C6H6O4	142.0266	0.39	1.00	1.00	0.67

7 Appendix

C7H6O2	122.0368	0.81	1.00	0.86	0.29
C9H7NO6	225.0273	3.19	1.00	0.78	0.67
C10H8O3	176.0473	3.23	1.00	0.80	0.30
C10H9NO4	207.0532	4.54	1.00	0.90	0.40
C6H4O5	156.0059	0.67	1.00	0.67	0.83
C5H11NO7S	229.0256	2.73	0.14	2.20	1.40
C13H9NO3	227.0582	8.23	1.00	0.69	0.23
C9H17NO9S	315.0624	2.52	0.22	1.89	1.00
C10H10N2O6	254.0539	7.79	1.00	1.00	0.60
C10H14O4	198.0892	3.73	1.00	1.40	0.40
C9H9NO6	227.0430	2.98	1.00	1.00	0.67
C7H12O5	176.0685	1.06	0.40	1.71	0.71
C9H7NO5	209.0324	4.07	1.00	0.78	0.56
C7H14O4	162.0892	0.84	0.25	2.00	0.57
C9H7NO3	177.0426	3.24	1.00	0.78	0.33
C10H9NO4	207.0532	7.65	1.00	0.90	0.40
C7H6O4	154.0266	2.59	1.00	0.86	0.57
C9H16O4	188.1049	2.60	0.50	1.78	0.44
C3H4O3	88.0160	0.07	0.67	1.33	1.00
C7H12O5	176.0685	1.65	0.40	1.71	0.71
C9H9NO7S	275.0100	3.69	0.86	1.00	0.78
C7H6O3	138.0317	1.05	1.00	0.86	0.43
C9H8O	132.0575	3.09	1.00	0.89	0.11
C9H19NO8S	301.0831	3.20	0.13	2.11	0.89
C10H8O6	224.0321	2.44	1.00	0.80	0.60
C8H5NO6	211.0117	2.57	1.00	0.63	0.75
C7H10O4	158.0579	2.75	0.75	1.43	0.57
C6H8O3	128.0473	0.52	1.00	1.33	0.50
C3H6O3S	122.0038	0.38	0.33	2.00	1.00
C12H20O5	244.1311	3.80	0.60	1.67	0.42
C6H5NO4	155.0219	0.40	1.00	0.83	0.67
C2H3NO3	89.0113	0.02	0.67	1.50	1.50
C8H14O7S	254.0460	2.30	0.29	1.75	0.88
C6H6O3	126.0317	0.37	1.00	1.00	0.50
C8H14O7S	254.0460	1.04	0.29	1.75	0.88
C9H8N2O2	176.0586	7.46	1.00	0.89	0.22
C11H18N2O2	210.1368	2.70	1.00	1.64	0.18
C7H7NO3	153.0426	0.38	1.00	1.00	0.43
C6H8O4	144.0423	1.32	0.75	1.33	0.67
C9H16O4	188.1049	2.94	0.50	1.78	0.44
C8H5NO6	211.0117	3.00	1.00	0.63	0.75
C10H8O5	208.0372	2.14	1.00	0.80	0.50
C8H8N2O6	228.0382	4.68	1.00	1.00	0.75
C13H9NO4	243.0532	7.74	1.00	0.69	0.31
C8H14O4	174.0892	2.69	0.50	1.75	0.50
C9H6N2O3	190.0378	2.76	1.00	0.67	0.33
C14H5NO2S	251.0041	2.62	1.00	0.36	0.14
C13H22O4	242.1518	7.48	0.75	1.69	0.31
C6H6O3S	158.0038	0.74	1.00	1.00	0.50
C7H8N2O3	168.0535	3.74	1.00	1.14	0.43
C5H9NO7S	227.0100	3.08	0.29	1.80	1.40
C8H7NO3	165.0426	6.75	1.00	0.88	0.38
C10H7NO5	221.0324	3.45	1.00	0.70	0.50
C7H16O4S	196.0769	5.12	0.00	2.29	0.57
C10H5NO2S	203.0041	0.52	1.00	0.50	0.20
C10H9NO4	207.0532	4.85	1.00	0.90	0.40
C9H16O8S	284.0566	2.49	0.25	1.78	0.89
C13H26O5S	294.1501	7.59	0.20	2.00	0.38
C9H18O7S	270.0773	2.52	0.14	2.00	0.78
C10H18O6S	266.0824	2.96	0.33	1.80	0.60
C9H17NO8S	299.0675	3.34	0.25	1.89	0.89
C16H16O4	272.1049	8.15	1.00	1.00	0.25
C14H10O4	242.0579	6.91	1.00	0.71	0.29
C10H7NO5	221.0324	5.83	1.00	0.70	0.50
C12H20O5	244.1311	4.34	0.60	1.67	0.42
C8H6O6	198.0164	0.89	1.00	0.75	0.75
C8H8O4	168.0423	3.08	1.00	1.00	0.50
C11H16O5	228.0998	2.85	0.80	1.45	0.45
C10H8N2O6	252.0382	7.80	1.00	0.80	0.60
C3H3NO3	101.0113	0.07	1.00	1.00	1.00

7 Appendix

C4H4N2O3	128.0222	0.55	1.00	1.00	0.75
C6H5NO2	123.0320	0.38	1.00	0.83	0.33
C9H10O6S	246.0198	2.87	0.83	1.11	0.67
C10H13NO4	211.0845	7.85	1.00	1.30	0.40
C6H10O5	162.0528	0.91	0.40	1.67	0.83
C7H6N2O4	182.0328	3.45	1.00	0.86	0.57
C9H10O4	182.0579	2.79	1.00	1.11	0.44
C7H12O4	160.0736	1.32	0.50	1.71	0.57
C14H9NO3	239.0582	8.21	1.00	0.64	0.21
C8H14O6S	238.0511	1.50	0.33	1.75	0.75
C5H11NO9S	261.0155	0.53	0.11	2.20	1.80
C11H8N2O5	248.0433	8.16	1.00	0.73	0.45
C6H7NO5	173.0324	0.37	0.80	1.17	0.83
C9H6O6	210.0164	2.20	1.00	0.67	0.67
C10H11NO4	209.0688	7.55	1.00	1.10	0.40
C9H7NO	145.0528	2.22	1.00	0.78	0.11
C10H16O4	200.1049	4.58	0.75	1.60	0.40
C8H6O6	198.0164	3.08	1.00	0.75	0.75
C5H3N3O2	137.0225	2.79	1.00	0.60	0.40
C10H7NO4	205.0375	3.04	1.00	0.70	0.40
C9H10O7S	262.0147	2.65	0.71	1.11	0.78
C10H10O2	162.0681	3.61	1.00	1.00	0.20
C10H18O6S	266.0824	2.65	0.33	1.80	0.60
C9H6N2O6	238.0226	7.25	1.00	0.67	0.67
C10H11NO3	193.0739	7.79	1.00	1.10	0.30
C5H12O4S	168.0456	2.19	0.00	2.40	0.80
C7H7NO5	185.0324	2.42	1.00	1.00	0.71
C8H5NO8	243.0015	2.88	0.88	0.63	1.00
C7H6N2O3	166.0378	3.45	1.00	0.86	0.43
C8H6O6	198.0164	1.22	1.00	0.75	0.75
C14H10O2	210.0681	7.79	1.00	0.71	0.14
C9H11NO5	213.0637	3.58	1.00	1.22	0.56
C15H5NOS2	278.9813	1.09	1.00	0.33	0.07
C12H14O4	222.0892	8.04	1.00	1.17	0.33
C15H10O6	286.0477	3.49	1.00	0.67	0.40
C8H4N2O6	224.0069	4.13	1.00	0.50	0.75
C5H3NO4	141.0062	0.37	1.00	0.60	0.80
C12H5NO6	259.0117	3.85	1.00	0.42	0.50
C6H8O2	112.0524	1.02	1.00	1.33	0.33
C15H5NOS2	278.9813	1.73	1.00	0.33	0.07
C12H8O4	216.0423	4.44	1.00	0.67	0.33
C9H8O4	180.0423	4.11	1.00	0.89	0.44
C15H28O8S	368.1505	7.56	0.25	1.87	0.53
C31H22O3	442.1569	7.86	1.00	0.71	0.10
C7H7NO4	169.0375	6.29	1.00	1.00	0.57
C11H20O5	232.1311	3.52	0.40	1.82	0.45
C8H6N2O5	210.0277	6.96	1.00	0.75	0.63
C7H12O2	128.0837	2.45	1.00	1.71	0.29
C4H4O3	100.0160	0.46	1.00	1.00	0.75
C10H18O4	202.1205	2.88	0.50	1.80	0.40
C9H7NO	145.0528	3.46	1.00	0.78	0.11
C20H18O9	402.0951	7.43	1.00	0.90	0.45
C13H8O3	212.0473	7.08	1.00	0.62	0.23
C9H12O5S	232.0405	2.74	0.80	1.33	0.56
C6H5N3O2	151.0382	3.87	1.00	0.83	0.33
C8H6O3	150.0317	1.13	1.00	0.75	0.38
C6H10O2	114.0681	1.26	1.00	1.67	0.33
C9H4N4O13	375.9775	3.26	0.77	0.44	1.44
C4H4N2O4	144.0171	0.91	1.00	1.00	1.00
C13H8O3	212.0473	6.53	1.00	0.62	0.23
C12H8N2O6	276.0382	7.94	1.00	0.67	0.50
C13H8O3	212.0473	7.51	1.00	0.62	0.23
C5H10O3	118.0630	0.80	0.33	2.00	0.60
C13H20O6	272.1260	3.11	0.67	1.54	0.46
C15H16OS2	276.0643	3.20	1.00	1.07	0.07
C8H8N2O4	196.0484	4.03	1.00	1.00	0.50
C8H16O3	160.1099	3.13	0.33	2.00	0.38
C8H8O3	152.0473	1.72	1.00	1.00	0.38
C13H9NO4	243.0532	8.26	1.00	0.69	0.31
C21H36O9	432.2359	7.62	0.44	1.71	0.43

7 Appendix

C6H12N2O6S	240.0416	7.24	0.33	2.00	1.00
C5H5NO4	143.0219	1.19	1.00	1.00	0.80
C18H34O8S	410.1974	8.18	0.25	1.89	0.44
C12H20N2O10S	384.0839	8.25	0.40	1.67	0.83
C12H12O5	236.0685	3.14	1.00	1.00	0.42
C11H6O3	186.0317	6.60	1.00	0.55	0.27
C16H10O4	266.0579	7.39	1.00	0.63	0.25
C15H10O2	222.0681	7.23	1.00	0.67	0.13
C9H10O4S	214.0300	2.58	1.00	1.11	0.44
C7H12O5	176.0685	2.39	0.40	1.71	0.71
C8H4N2O	144.0324	3.69	1.00	0.50	0.13
C16H10O4S	298.0300	7.48	1.00	0.63	0.25
C10H20O6S	268.0981	3.43	0.17	2.00	0.60
C12H8O3	200.0473	4.40	1.00	0.67	0.25
C15H8O4	252.0423	5.27	1.00	0.53	0.27
C6H4N2O6	200.0069	4.78	1.00	0.67	1.00
C8H5NO7	227.0066	4.07	1.00	0.63	0.88
C5H6O4	130.0266	0.96	0.75	1.20	0.80
C5H6O2	98.0368	0.39	1.00	1.20	0.40
C7H8O4	156.0423	1.04	1.00	1.14	0.57
C8H6N2O3	178.0378	6.48	1.00	0.75	0.38
C11H8O3	188.0473	7.77	1.00	0.73	0.27
C6H5N3O2	151.0382	4.22	1.00	0.83	0.33
C6H6N2O2	138.0429	0.91	1.00	1.00	0.33
C6H4O4	140.0110	0.38	1.00	0.67	0.67
C7H13NO9S	287.0311	2.68	0.22	1.86	1.29
C5H6O6S	193.9885	0.63	0.50	1.20	1.20
C9H6O6	210.0164	2.53	1.00	0.67	0.67
C12H18O6	258.1103	2.93	0.67	1.50	0.50
C4H7NO6	165.0273	0.38	0.33	1.75	1.50
C9H4O5	192.0059	1.89	1.00	0.44	0.56
C9H7NO6	225.0273	3.59	1.00	0.78	0.67
C6H13NO8S	259.0362	2.62	0.13	2.17	1.33
C10H10O7S	274.0147	2.78	0.86	1.00	0.70
C7H7NO4	169.0375	6.67	1.00	1.00	0.57
C9H15NO9S	313.0468	3.20	0.33	1.67	1.00
C19H16O7	356.0896	7.78	1.00	0.84	0.37
C6H12O3	132.0786	2.58	0.33	2.00	0.50
C4H5NO5	147.0168	0.34	0.60	1.25	1.25
C15H12N2O14S	476.0009	3.08	0.79	0.80	0.93
C6H7NO4	157.0375	0.71	1.00	1.17	0.67
C9H9NO3	179.0582	3.32	1.00	1.00	0.33
C9H16O7S	268.0617	0.71	0.29	1.78	0.78
C8H8O4	168.0423	1.09	1.00	1.00	0.50
C11H10O2	174.0681	3.33	1.00	0.91	0.18
C18H13NO6	339.0743	7.85	1.00	0.72	0.33
C7H7N3O4	197.0437	6.94	1.00	1.00	0.57
C14H10O5	258.0528	3.66	1.00	0.71	0.36
C7H7NO2	137.0477	2.36	1.00	1.00	0.29
C8H10O5	186.0528	2.31	0.80	1.25	0.63
C10H16O7S	280.0617	2.05	0.43	1.60	0.70
C11H9NO5	235.0481	7.48	1.00	0.82	0.45
C16H20O5	292.1311	7.51	1.00	1.25	0.31
C5H10O3	118.0630	2.91	0.33	2.00	0.60
C8H9NO2	151.0633	1.76	1.00	1.13	0.25
C10H15NO10S	341.0417	2.98	0.40	1.50	1.00
C9H8N2O2	176.0586	6.72	1.00	0.89	0.22
C13H11NO4	245.0688	7.89	1.00	0.85	0.31
C6H7NO3	141.0426	0.47	1.00	1.17	0.50
C8H15NO9S	301.0468	3.09	0.22	1.88	1.13
C9H5N3O2	187.0382	3.99	1.00	0.56	0.22
C6H9NO3	143.0582	0.58	1.00	1.50	0.50
C11H11NO4	221.0688	6.97	1.00	1.00	0.36
C9H18O6S	254.0824	4.27	0.17	2.00	0.67
C13H20O5	256.1311	7.91	0.80	1.54	0.38
C8H12O9S	284.0202	1.08	0.33	1.50	1.13
C9H6N2O3	190.0378	4.44	1.00	0.67	0.33
C9H10O2	150.0681	3.71	1.00	1.11	0.22
C9H10N2O5	226.0590	8.17	1.00	1.11	0.56
C8H7NO6	213.0273	4.60	1.00	0.88	0.75

7 Appendix

C5H8O3	116.0473	0.05	0.67	1.60	0.60
C15H5NOS2	278.9813	2.69	1.00	0.33	0.07
C11H7NO4	217.0375	6.97	1.00	0.64	0.36
C20H30O4	334.2144	8.13	1.00	1.50	0.20
C6H5NO4	155.0219	1.79	1.00	0.83	0.67
C8H12O9S	284.0202	0.69	0.33	1.50	1.13
C9H7NO3	177.0426	6.97	1.00	0.78	0.33
C11H8O6	236.0321	2.57	1.00	0.73	0.55
C12H8O3S2	263.9915	0.67	1.00	0.67	0.25
C8H8N2O6	228.0382	3.68	1.00	1.00	0.75
C7H6O2	122.0368	1.87	1.00	0.86	0.29
C6H7NO5	173.0324	0.76	0.80	1.17	0.83
C8H4N2O	144.0324	3.42	1.00	0.50	0.13
C7H16O5S	212.0718	1.48	0.00	2.29	0.71
C15H8O4	252.0423	7.60	1.00	0.53	0.27
C14H10O3S	258.0351	0.53	1.00	0.71	0.21
C10H9NO4	207.0532	2.82	1.00	0.90	0.40
C6H6O4S	173.9987	0.97	1.00	1.00	0.67
C10H9NO5	223.0481	5.89	1.00	0.90	0.50
C11H13NO4	223.0845	7.87	1.00	1.18	0.36
C11H8O3	188.0473	7.28	1.00	0.73	0.27
C13H11NO7	293.0536	7.66	1.00	0.85	0.54
C4H8O2	88.0524	0.39	0.50	2.00	0.50
C9H7NO4	193.0375	2.34	1.00	0.78	0.44
C4H8O3	104.0473	0.09	0.33	2.00	0.75
C8H16O4	176.1049	2.40	0.25	2.00	0.50
C13H22O5	258.1467	6.47	0.60	1.69	0.38
C8H8O4S	200.0143	1.20	1.00	1.00	0.50
C6H4O3	124.0160	3.07	1.00	0.67	0.50
C9H6N2O6	238.0226	6.99	1.00	0.67	0.67
C7H16O4S	196.0769	3.67	0.00	2.29	0.57
C14H8O3	224.0473	4.49	1.00	0.57	0.21
C9H10O5S	230.0249	2.53	1.00	1.11	0.56
C8H8O3	152.0473	4.36	1.00	1.00	0.38
C8H16O4	176.1049	1.44	0.25	2.00	0.50
C6H7NO3	141.0426	2.46	1.00	1.17	0.50
C14H8O4	240.0423	6.38	1.00	0.57	0.29
C8H6O	118.0419	3.13	1.00	0.75	0.13
C8H15NO9S	301.0468	2.36	0.22	1.88	1.13
C17H22O4	290.1518	7.24	1.00	1.29	0.24
C8H8O3	152.0473	5.32	1.00	1.00	0.38
C8H5NO4	179.0219	3.12	1.00	0.63	0.50
C8H8O	120.0575	3.06	1.00	1.00	0.13
C4H5NO2	99.0320	0.09	1.00	1.25	0.50
C5H5N3O3	155.0331	1.67	1.00	1.00	0.60
C10H16N2O10S	356.0526	7.72	0.40	1.60	1.00
C9H8N2O6	240.0382	7.70	1.00	0.89	0.67
C10H9NO3	191.0582	4.43	1.00	0.90	0.30
C4H4O4S	147.9830	0.40	0.75	1.00	1.00
C6H6N2O4	170.0328	2.35	1.00	1.00	0.67
C4H6N2O2	114.0429	0.05	1.00	1.50	0.50
C8H9NO4	183.0532	2.34	1.00	1.13	0.50
C13H10O2	198.0681	7.97	1.00	0.77	0.15
C12H11NO7S	313.0256	7.11	1.00	0.92	0.58
C7H14O6S	226.0511	0.84	0.17	2.00	0.86
C13H8O4	228.0423	7.86	1.00	0.62	0.31
C7H7N3O4	197.0437	5.74	1.00	1.00	0.57
C7H6O2	122.0368	6.99	1.00	0.86	0.29
C9H6O4	178.0266	2.42	1.00	0.67	0.44
C9H7NO6	225.0273	4.06	1.00	0.78	0.67
C11H8O2	172.0524	6.77	1.00	0.73	0.18
C15H8O4	252.0423	7.25	1.00	0.53	0.27
C12H10O2	186.0681	7.25	1.00	0.83	0.17
C14H9NO5	271.0481	7.51	1.00	0.64	0.36
C10H9NO3	191.0582	3.52	1.00	0.90	0.30
C4H8O4S	152.0143	2.83	0.25	2.00	1.00
C9H8N2O3	192.0535	4.80	1.00	0.89	0.33
C6H5NO6S	218.9838	2.92	0.83	0.83	1.00
C8H5NO4	179.0219	2.55	1.00	0.63	0.50
C5H5NO4	143.0219	0.38	1.00	1.00	0.80

7 Appendix

C9H8O6	212.0321	2.92	1.00	0.89	0.67
C8H8O	120.0575	3.27	1.00	1.00	0.13
C14H6O3S2	285.9758	2.61	1.00	0.43	0.21
C9H16O4S	220.0769	2.02	0.50	1.78	0.44
C7H14O3	146.0943	3.22	0.33	2.00	0.43
C9H14O2	154.0994	3.13	1.00	1.56	0.22
C10H15NO8S	309.0518	3.22	0.50	1.50	0.80
C8H10O5S	218.0249	1.81	0.80	1.25	0.63
C16H24O8	344.1471	3.47	0.63	1.50	0.50
C13H6O6	258.0164	3.26	1.00	0.46	0.46
C6H8O4	144.0423	2.40	0.75	1.33	0.67
C10H19NO7S	297.0882	7.48	0.29	1.90	0.70
C6H10N2O3	158.0691	1.09	1.00	1.67	0.50
C18H16O6	328.0947	8.16	1.00	0.89	0.33
C10H14O3	182.0943	3.07	1.00	1.40	0.30
C12H8O3	200.0473	5.95	1.00	0.67	0.25
C8H5NO3S	194.9990	7.41	1.00	0.63	0.38
C10H19NO10S	345.0730	1.04	0.20	1.90	1.00
C8H16O6S	240.0668	1.17	0.17	2.00	0.75
C11H7NO7	265.0223	6.71	1.00	0.64	0.64
C6H9NO2	127.0633	0.12	1.00	1.50	0.33
C8H14O10S	302.0308	2.46	0.20	1.75	1.25
C13H10O2	198.0681	7.20	1.00	0.77	0.15
C10H12O6	228.0634	2.64	0.83	1.20	0.60
C9H8O2	148.0524	2.38	1.00	0.89	0.22
C4H5N3O2	127.0382	1.06	1.00	1.25	0.50
C4H10O3S	138.0351	0.69	0.00	2.50	0.75
C13H18O6	270.1103	3.05	0.83	1.38	0.46
C12H9NO7	279.0379	7.47	1.00	0.75	0.58
C12H22O5	246.1467	4.69	0.40	1.83	0.42
C10H12O4	196.0736	3.31	1.00	1.20	0.40
C13H9NO5	259.0481	7.63	1.00	0.69	0.38
C6H11NO8S	257.0205	2.11	0.25	1.83	1.33
C14H26O6	290.1729	6.52	0.33	1.86	0.43
C12H22O4	230.1518	3.72	0.50	1.83	0.33
C5H10O8S	230.0096	1.68	0.13	2.00	1.60
C6H8O5S	192.0092	0.89	0.60	1.33	0.83
C13H12O2	200.0837	7.73	1.00	0.92	0.15
C6H7NO	109.0528	0.45	1.00	1.17	0.17
C12H14N2O4	250.0954	5.26	1.00	1.17	0.33
C10H16O5S	248.0718	2.61	0.60	1.60	0.50
C7H10O6	190.0477	1.48	0.50	1.43	0.86
C12H12O3	204.0786	3.31	1.00	1.00	0.25
C11H17NO7S	307.0726	6.70	0.57	1.55	0.64
C7H7NO7S	248.9943	2.87	0.71	1.00	1.00
C7H16O3S	180.0820	3.55	0.00	2.29	0.43
C12H25NO3S2	295.1276	3.04	0.33	2.08	0.25
C12H15N3O4S	297.0783	4.67	1.00	1.25	0.33
C11H11NO4	221.0688	6.46	1.00	1.00	0.36
C12H13N3O4	263.0906	7.94	1.00	1.08	0.33
C9H8N2O5	224.0433	7.71	1.00	0.89	0.56
C15H8O5	268.0372	5.08	1.00	0.53	0.33
C5H5NO5	159.0168	0.43	0.80	1.00	1.00
C6H7NO3	141.0426	0.94	1.00	1.17	0.50
C9H8O6S	244.0042	2.37	1.00	0.89	0.67
C10H9NO5	223.0481	5.02	1.00	0.90	0.50
C9H10O4	182.0579	4.17	1.00	1.11	0.44
C6H6O2	110.0368	0.38	1.00	1.00	0.33
C9H8N2O3	192.0535	2.48	1.00	0.89	0.33
C6H8N2O5	188.0433	2.77	0.80	1.33	0.83
C9H18O3	174.1256	3.80	0.33	2.00	0.33
C18H10O3	274.0630	7.98	1.00	0.56	0.17
C9H12O7	232.0583	2.51	0.57	1.33	0.78
C8H8O4S	200.0143	1.67	1.00	1.00	0.50
C14H8O3	224.0473	6.88	1.00	0.57	0.21
C8H14O4	174.0892	3.95	0.50	1.75	0.50
C10H17NO4	215.1158	3.61	0.75	1.70	0.40
C11H12O3	192.0786	3.69	1.00	1.09	0.27
C15H10O3	238.0630	7.98	1.00	0.67	0.20
C10H6O5	206.0215	2.42	1.00	0.60	0.50

7 Appendix

C7H10O2	126.0681	1.25	1.00	1.43	0.29
C18H34O7S	394.2025	7.66	0.29	1.89	0.39
C7H6O4	154.0266	2.07	1.00	0.86	0.57
C10H7N3O4	233.0437	7.61	1.00	0.70	0.40
C7H5NO6	199.0117	0.96	1.00	0.71	0.86
C10H16N2O10S	356.0526	7.36	0.40	1.60	1.00
C10H11NO7S	289.0256	6.10	0.86	1.10	0.70
C6H5NO7S	234.9787	1.08	0.71	0.83	1.17
C14H8O3	224.0473	5.82	1.00	0.57	0.21
C13H9NO5	259.0481	8.07	1.00	0.69	0.38
C5H8O	84.0575	0.55	1.00	1.60	0.20
C13H24O6	276.1573	4.37	0.33	1.85	0.46
C21H32O7	396.2148	7.87	0.86	1.52	0.33
C15H12O4	256.0736	6.95	1.00	0.80	0.27
C15H14O5	274.0841	6.76	1.00	0.93	0.33
C17H24O4	292.1675	8.59	1.00	1.41	0.24
C10H14N2O4	226.0954	1.03	1.00	1.40	0.40
C13H6O6	258.0164	4.37	1.00	0.46	0.46
C15H24O3	252.1725	8.04	1.00	1.60	0.20
C13H8O4	228.0423	7.26	1.00	0.62	0.31
C13H6O5	242.0215	3.77	1.00	0.46	0.38
C8H6N2O4	194.0328	5.21	1.00	0.75	0.50
C20H14N2O5	330.0827	6.79	1.00	0.70	0.05
C10H11NO7S	289.0256	4.98	0.86	1.10	0.70
C15H32O5S	324.1970	8.07	0.00	2.13	0.33
C15H23NO8S	377.1144	7.34	0.63	1.53	0.53
C10H12O5	212.0685	2.58	1.00	1.20	0.50
C10H20O5S	252.1031	3.60	0.20	2.00	0.50
C7H8O5S	204.0092	2.77	0.80	1.14	0.71
C15H10O2	222.0681	8.08	1.00	0.67	0.13
C8H9NO2	151.0633	0.74	1.00	1.13	0.25
C11H20N2O11	356.1067	4.81	0.27	1.82	1.00
C5H10O4S	166.0300	0.72	0.25	2.00	0.80
C9H4N2O2	172.0273	0.10	1.00	0.44	0.22
C7H5NO4	167.0219	2.93	1.00	0.71	0.57
C8H12N2O4	200.0797	2.37	1.00	1.50	0.50
C15H24O9	348.1420	3.25	0.44	1.60	0.60
C7H9NO4S	203.0252	0.53	1.00	1.29	0.57
C11H10O6	238.0477	4.09	1.00	0.91	0.55
C15H15NO2S	273.0823	3.71	1.00	1.00	0.13
C10H12O7	244.0583	0.69	0.71	1.20	0.70
C10H20O6S	268.0981	4.90	0.17	2.00	0.60
C7H7N3O2	165.0538	3.72	1.00	1.00	0.29
C13H24N2O10S	400.1152	7.99	0.30	1.85	0.77
C5H10O3	118.0630	0.11	0.33	2.00	0.60
C9H20O3S	208.1133	7.12	0.00	2.22	0.33
C10H21NO8S	315.0988	3.79	0.13	2.10	0.80
C13H8O3	212.0473	5.77	1.00	0.62	0.23
C9H15NO18	425.0289	4.67	0.17	1.67	2.00
C7H7NO7S	248.9943	3.34	0.71	1.00	1.00
C7H8O3S	172.0194	1.32	1.00	1.14	0.43
C8H9NO5S	231.0201	2.72	1.00	1.13	0.63
C12H21NO9S	355.0937	6.47	0.33	1.75	0.75
C11H13NO3	207.0895	8.18	1.00	1.18	0.27
C15H8O3	236.0473	7.80	1.00	0.53	0.20
C10H6O5	206.0215	2.89	1.00	0.60	0.50
C13H8O3	212.0473	7.98	1.00	0.62	0.23
C14H13NO4	259.0845	8.13	1.00	0.93	0.29
C10H13NO5	227.0794	4.01	1.00	1.30	0.50
C8H16O3	160.1099	5.85	0.33	2.00	0.38
C6H9NO4	159.0532	0.87	0.75	1.50	0.67
C8H11NO13S2	392.9672	3.59	0.31	1.38	1.63
C13H7NO5	257.0324	7.25	1.00	0.54	0.38
C7H5NO6	199.0117	0.65	1.00	0.71	0.86
C17H24O4	292.1675	6.82	1.00	1.41	0.24
C12H6N4O12	397.9982	2.57	1.00	0.50	1.00
C9H18O4S	222.0926	8.11	0.25	2.00	0.44
C9H15NO2	169.1103	4.41	1.00	1.67	0.22
C13H24O5	260.1624	6.77	0.40	1.85	0.38
C11H9NO5	235.0481	7.13	1.00	0.82	0.45

7 Appendix

C10H20O6S	268.0981	7.36	0.17	2.00	0.60
C15H10O4	254.0579	7.15	1.00	0.67	0.27
C11H8O5S2	283.9813	0.76	1.00	0.73	0.45
C6H5NO2	123.0320	1.56	1.00	0.83	0.33
C15H10O6	286.0477	4.01	1.00	0.67	0.40
C10H10N2O3	206.0691	2.83	1.00	1.00	0.30
C4H6N4O6S	238.0008	3.15	0.67	1.50	1.50
C7H9NO10S	298.9947	3.81	0.40	1.29	1.43
C12H13NO4	235.0845	7.60	1.00	1.08	0.33
C8H8N4O6S	288.0165	2.31	1.00	1.00	0.75
C5H4N2O4	156.0171	2.59	1.00	0.80	0.80
C12H7NO2S	229.0197	0.68	1.00	0.58	0.17
C9H4O6	208.0008	1.06	1.00	0.44	0.67
C11H18N2O10	338.0961	7.49	0.40	1.64	0.91
C17H10O2	246.0681	7.65	1.00	0.59	0.12
C10H7NO5	221.0324	2.74	1.00	0.70	0.50
C15H31NO8S	385.1770	7.99	0.13	2.07	0.53
C7H10N2O4	186.0641	0.97	1.00	1.43	0.57
C9H8O5	196.0372	1.77	1.00	0.89	0.56
C9H7NO4	193.0375	0.64	1.00	0.78	0.44
C6H5N3O2	151.0382	3.36	1.00	0.83	0.33
C16H12O5S	316.0405	6.46	1.00	0.75	0.31
C16H31NO9S	413.1720	8.13	0.22	1.94	0.56
C10H17N3O3	227.1270	3.11	1.00	1.70	0.30
C3H5NO3	103.0269	0.03	0.67	1.67	1.00
C16H30O5	302.2093	7.50	0.40	1.88	0.31
C13H9NO	195.0684	4.46	1.00	0.69	0.08
C7H12O8	224.0532	2.85	0.25	1.71	1.14
C9H6O8	242.0063	3.10	0.88	0.67	0.89
C3H7NO8S	216.9892	0.48	0.13	2.33	2.67
C20H13NOS2	347.0439	4.32	1.00	0.65	0.05
C6H6O2	110.0368	1.28	1.00	1.00	0.33
C9H10N4OS2	254.0296	3.11	1.00	1.11	0.11
C7H8N4O8S2	339.9784	1.05	0.75	1.14	1.14
C7H9NO8S	267.0049	2.50	0.50	1.29	1.14
C10H15NO9S	325.0468	3.01	0.44	1.50	0.90
C13H25NO8S	355.1301	7.63	0.25	1.92	0.62
C7H9NO	123.0684	0.69	1.00	1.29	0.14
C12H9NO5	247.0481	7.70	1.00	0.75	0.42
C14H11NO3	241.0739	8.34	1.00	0.79	0.21
C12H7NO2	197.0477	3.83	1.00	0.58	0.17
C8H9NO2	151.0633	2.70	1.00	1.13	0.25
C6H11NO9S	273.0155	2.19	0.22	1.83	1.50
C4H8O2	88.0524	1.08	0.50	2.00	0.50
C14H24O3	240.1725	7.90	1.00	1.71	0.21
C10H20O6S	268.0981	7.60	0.17	2.00	0.60
C19H24O4	316.1675	7.61	1.00	1.26	0.21
C13H24N2O4	272.1736	1.46	0.75	1.85	0.31
C7H6N4OS2	225.9983	1.68	1.00	0.86	0.14
C14H8O4	240.0423	4.24	1.00	0.57	0.29
C11H8O3	188.0473	6.44	1.00	0.73	0.27
C14H14O4	246.0892	7.41	1.00	1.00	0.29
C16H30O8S	382.1661	7.76	0.25	1.88	0.50
C14H16O4	248.1049	8.25	1.00	1.14	0.29
C8H8O4	168.0423	4.40	1.00	1.00	0.50
C6H11NO3	145.0739	1.47	0.67	1.83	0.50
C10H8O7	240.0270	2.87	1.00	0.80	0.70
C12H25NO8S	343.1301	6.88	0.13	2.08	0.67
C9H8N2O3	192.0535	6.89	1.00	0.89	0.33
C9H8N2O3	192.0535	7.32	1.00	0.89	0.33
C15H6O7S2	361.9555	1.89	1.00	0.40	0.47
C9H19NO7S	285.0882	7.41	0.14	2.11	0.78
C11H8O3	188.0473	5.15	1.00	0.73	0.27
C9H7NO	145.0528	4.13	1.00	0.78	0.11
C6H6O	94.0419	2.32	1.00	1.00	0.17
C14H13NO3S	275.0616	3.11	1.00	0.93	0.21
C6H4N2O	120.0324	2.24	1.00	0.67	0.17
C12H14O3	206.0943	7.26	1.00	1.17	0.25
C12H16O4	224.1049	3.04	1.00	1.33	0.33
C8H5NO8	243.0015	3.31	0.88	0.63	1.00

7 Appendix

C19H18O6	342.1103	8.30	1.00	0.95	0.32
C15H8O6	284.0321	3.43	1.00	0.53	0.40
C15H12O3	240.0786	6.87	1.00	0.80	0.20
C7H3NO5S	212.9732	6.63	1.00	0.43	0.71
C7H7NO	121.0528	3.18	1.00	1.00	0.14
C11H8O2	172.0524	5.13	1.00	0.73	0.18
C15H24O3	252.1725	7.88	1.00	1.60	0.20
C20H36O8	404.2410	7.43	0.38	1.80	0.40
C10H21NO7S	299.1039	7.73	0.14	2.10	0.70
C6H4N4OS2	211.9827	0.76	1.00	0.67	0.17
C9H14O	138.1045	2.76	1.00	1.56	0.11
C10H9NO3	191.0582	6.77	1.00	0.90	0.30
C6H12O5S	196.0405	2.29	0.20	2.00	0.83
C8H11NO8S	281.0205	3.01	0.50	1.38	1.00
C9H18O8S	286.0722	5.20	0.13	2.00	0.89
C8H18N2O4S2	270.0708	1.41	0.25	2.25	0.50
C7H9NO2	139.0633	1.00	1.00	1.29	0.29
C12H7NO2	197.0477	3.63	1.00	0.58	0.17
C13H7NO5	257.0324	7.66	1.00	0.54	0.38
C16H34O5S	338.2127	8.25	0.00	2.13	0.31
C8H11NO4S	217.0409	0.90	1.00	1.38	0.50
C8H4O3	148.0160	1.91	1.00	0.50	0.38
C12H12O2	188.0837	4.23	1.00	1.00	0.17
C11H13NO5	239.0794	4.59	1.00	1.18	0.45
C5H7NO2	113.0477	0.12	1.00	1.40	0.40
C10H10N2O3	206.0691	6.55	1.00	1.00	0.30
C7H14O4	162.0892	2.43	0.25	2.00	0.57
C4H4N4O7S	251.9801	0.81	0.71	1.00	1.75
C9H16O10S	316.0464	8.07	0.20	1.78	1.11
C12H18O8	290.1002	2.63	0.50	1.50	0.67
C9H8N2O3	192.0535	7.62	1.00	0.89	0.33
C11H14O4	210.0892	3.01	1.00	1.27	0.36
C9H17NO9S	315.0624	6.29	0.22	1.89	1.00
C9H7NO5	209.0324	6.22	1.00	0.78	0.56
C4H7NO5	149.0324	0.52	0.40	1.75	1.25
C13H10O2	198.0681	7.48	1.00	0.77	0.15
C13H8O4	228.0423	8.21	1.00	0.62	0.31
C23H10OS	334.0452	7.23	1.00	0.43	0.04
C4H8O4S	152.0143	5.12	0.25	2.00	1.00
C13H8O4	228.0423	6.73	1.00	0.62	0.31
C10H20O6S	268.0981	6.61	0.17	2.00	0.60
C9H7NO5	209.0324	0.57	1.00	0.78	0.56
C15H16O3S2	308.0541	3.71	1.00	1.07	0.20
C19H18O7	358.1053	7.83	1.00	0.95	0.37
C5H3NO3	125.0113	0.42	1.00	0.60	0.60
C10H11NO7S	289.0256	4.44	0.86	1.10	0.70
C8H10O6S	234.0198	0.70	0.67	1.25	0.75
C8H9NO5	199.0481	5.41	1.00	1.13	0.63
C7H6O	106.0419	0.82	1.00	0.86	0.14
C11H23NO7S	313.1195	7.93	0.14	2.09	0.64
C11H8O3S2	251.9915	1.09	1.00	0.73	0.27
C9H20O4S	224.1082	7.19	0.00	2.22	0.44
C7H5NO3	151.0269	2.89	1.00	0.71	0.43
C12H8N2O6	276.0382	7.60	1.00	0.67	0.50
C14H11NO3	241.0739	3.47	1.00	0.79	0.21
C17H16O5	300.0998	7.78	1.00	0.94	0.29
C9H6O2	146.0368	3.06	1.00	0.67	0.22
C7H4N2O5	196.0120	3.37	1.00	0.57	0.71
C8H6N2O2	162.0429	3.11	1.00	0.75	0.25
C12H9NO5	247.0481	4.12	1.00	0.75	0.42
C16H18OS2	290.0799	3.43	1.00	1.13	0.06
C8H13NO5	203.0794	2.51	0.60	1.63	0.63
C9H10O	134.0732	3.80	1.00	1.11	0.11
C11H12N2O4	236.0797	4.25	1.00	1.09	0.36
C6H7NO2	125.0477	2.92	1.00	1.17	0.33
C8H6O2	134.0368	2.95	1.00	0.75	0.25
C16H30O5S	334.1814	8.04	0.40	1.88	0.31
C6H10O8	210.0376	2.54	0.25	1.67	1.33
C9H8N2O5	224.0433	3.68	1.00	0.89	0.56
C8H10O4S	202.0300	3.14	1.00	1.25	0.50

7 Appendix

C5H8O	84.0575	1.67	1.00	1.60	0.20
C6H6O	94.0419	2.77	1.00	1.00	0.17
C11H18N2O10	338.0961	7.15	0.40	1.64	0.91
C7H4N2O3	164.0222	1.10	1.00	0.57	0.43
C18H28O3	292.2038	8.29	1.00	1.56	0.17
C11H8O5S2	283.9813	1.09	1.00	0.73	0.45
C10H20N2O10S	360.0839	7.64	0.20	2.00	1.00
C8H16O6S	240.0668	4.03	0.17	2.00	0.75
C9H8O6	212.0321	3.69	1.00	0.89	0.67
C7H6O6S	217.9885	1.17	0.83	0.86	0.86
C11H21NO7S	311.1039	7.71	0.29	1.91	0.64
C19H32O9	404.2046	7.09	0.44	1.68	0.47
C9H7NO	145.0528	0.90	1.00	0.78	0.11
C13H20O11	352.1006	0.60	0.36	1.54	0.85
C12H8O4	216.0423	5.80	1.00	0.67	0.33
C11H10O15S	413.9740	7.95	0.47	0.91	1.36
C6H6O2	110.0368	1.84	1.00	1.00	0.33
C12H25NO7S	327.1352	8.09	0.14	2.08	0.58
C10H19NO9S	329.0781	1.43	0.22	1.90	0.90
C4H8O4S	152.0143	1.18	0.25	2.00	1.00
C11H6O3	186.0317	5.69	1.00	0.55	0.27
C9H7NO7	241.0223	3.62	1.00	0.78	0.78
C6H7NO	109.0528	2.47	1.00	1.17	0.17
C8H4N2O10S	319.9587	0.10	0.80	0.50	1.25
C7H14O4	162.0892	2.74	0.25	2.00	0.57
C13H20O3	224.1412	7.36	1.00	1.54	0.23
C11H10O2	174.0681	3.55	1.00	0.91	0.18
C19H14O4	306.0892	7.73	1.00	0.74	0.21
C7H10N2O5	202.0590	3.15	0.80	1.43	0.71
C8H16O2	144.1150	4.06	0.50	2.00	0.25
C15H6O6S2	345.9606	0.81	1.00	0.40	0.40
C12H7NO3	213.0426	3.46	1.00	0.58	0.25
C11H20N2O10	340.1118	8.15	0.30	1.82	0.91
C15H24O13	412.1217	0.55	0.31	1.60	0.87
C12H21NO9S	355.0937	5.17	0.33	1.75	0.75
C6H10O	98.0732	0.91	1.00	1.67	0.17
C7H6N2O5	198.0277	2.68	1.00	0.86	0.71
C12H20O6	260.1260	6.52	0.50	1.67	0.50
C10H11NO7S	289.0256	5.67	0.86	1.10	0.70
C12H8O5	232.0372	3.49	1.00	0.67	0.42
C9H8O5S	228.0092	1.97	1.00	0.89	0.56
C10H17NO8	279.0954	5.40	0.38	1.70	0.80
C8H6N2O8	258.0124	7.55	0.88	0.75	1.00
C10H18N2O11S	374.0631	7.67	0.27	1.80	1.10
C9H8N2O4	208.0484	3.60	1.00	0.89	0.44
C9H9NO6	227.0430	4.34	1.00	1.00	0.67
C13H26O4	246.1831	7.07	0.25	2.00	0.31
C17H22O3	274.1569	7.60	1.00	1.29	0.18
C14H8O3	224.0473	3.30	1.00	0.57	0.21
C10H8O7	240.0270	3.81	1.00	0.80	0.70
C9H8O5S	228.0092	2.57	1.00	0.89	0.56
C9H17NO9S	315.0624	4.79	0.22	1.89	1.00
C14H14O2	214.0994	8.11	1.00	1.00	0.14
C9H8O5	196.0372	5.40	1.00	0.89	0.56
C8H5NO8	243.0015	4.14	0.88	0.63	1.00
C6H8N2O7	220.0332	0.68	0.57	1.33	1.17
C10H17NO7S	295.0726	3.29	0.43	1.70	0.70
C13H20O7	288.1209	6.22	0.57	1.54	0.54
C15H22O4S2	330.0959	2.70	1.00	1.47	0.27
C7H12O	112.0888	2.64	1.00	1.71	0.14
C18H12O4	292.0736	7.86	1.00	0.67	0.22
C5H4O2S	127.9932	1.53	1.00	0.80	0.40
C11H17NO9	307.0903	3.19	0.44	1.55	0.82
C14H20O3	236.1412	7.94	1.00	1.43	0.21
C16H8O4	264.0423	7.87	1.00	0.50	0.25
C16H31NO8S	397.1770	8.21	0.25	1.94	0.50
C8H9NO6	215.0430	1.50	0.83	1.13	0.75
C7H11NO9S	285.0155	1.69	0.33	1.57	1.29
C14H7NO2	221.0477	7.65	1.00	0.50	0.14
C19H34O7	374.2305	8.26	0.43	1.79	0.37

7 Appendix

C15H15NO4	273.1001	8.28	1.00	1.00	0.27
C11H6O4	202.0266	2.79	1.00	0.55	0.36
C11H11NO6	253.0586	6.95	1.00	1.00	0.55
C8H7NO6	213.0273	5.35	1.00	0.88	0.75
C6H6N2O7	218.0175	0.69	0.71	1.00	1.17
C12H21N3O3	255.1583	4.43	1.00	1.75	0.25
C8H18O4S	210.0926	6.37	0.00	2.25	0.50
C12H8O8	280.0219	1.27	1.00	0.67	0.67
C7H9NO2	139.0633	2.50	1.00	1.29	0.29
C12H14O5	238.0841	2.60	1.00	1.17	0.42
C12H22O5	246.1467	4.19	0.40	1.83	0.42
C12H13NO5	251.0794	7.83	1.00	1.08	0.42
C6H3NO7	200.9910	1.93	0.86	0.50	1.17
C8H6N2O	146.0480	2.99	1.00	0.75	0.13
C8H8N2O3	180.0535	2.52	1.00	1.00	0.38
C7H7NO	121.0528	2.64	1.00	1.00	0.14
C8H7NO2	149.0477	3.79	1.00	0.88	0.25
C15H6O5S2	329.9657	1.07	1.00	0.40	0.33
C6H12O4	148.0736	0.93	0.25	2.00	0.67
C18H30O9	390.1890	6.56	0.44	1.67	0.50
C9H14N2O5S	262.0623	7.84	0.80	1.56	0.56
C7H7N3O2	165.0538	6.52	1.00	1.00	0.29
C8H16O5	192.0998	0.61	0.20	2.00	0.63
C10H7NO4	205.0375	5.86	1.00	0.70	0.40
C13H27NO7S	341.1508	8.25	0.14	2.08	0.54
C9H14N2O5S	262.0623	8.12	0.80	1.56	0.56
C10H8N2O3	204.0535	5.57	1.00	0.80	0.30
C13H15NO4	249.1001	7.94	1.00	1.15	0.31
C21H30O7S	426.1712	7.61	1.00	1.43	0.33
C8H7NO2	149.0477	0.61	1.00	0.88	0.25
C10H13NO9S	323.0311	2.30	0.56	1.30	0.90
C15H26O3	254.1882	8.35	1.00	1.73	0.20
C10H12O7	244.0583	2.60	0.71	1.20	0.70
C15H10O4	254.0579	4.46	1.00	0.67	0.27
C16H16N2O5S2	380.0501	4.68	1.00	1.00	0.31
C9H6O8S	273.9783	2.50	0.88	0.67	0.89
C9H16N2O6S	280.0729	7.74	0.50	1.78	0.67
C10H8O8S	287.9940	1.45	0.88	0.80	0.80
C13H6O5	242.0215	4.65	1.00	0.46	0.38
C9H13NO4	199.0845	2.57	1.00	1.44	0.44
C17H32O5	316.2250	8.14	0.40	1.88	0.29
C15H6O5S2	329.9657	1.90	1.00	0.40	0.33
C14H16O5	264.0998	7.42	1.00	1.14	0.36
C10H7NO2	173.0477	3.48	1.00	0.70	0.20
C15H15NO3	257.1052	8.38	1.00	1.00	0.20
C13H25NO7S	339.1352	8.18	0.29	1.92	0.54
C5H10O2	102.0681	1.68	0.50	2.00	0.40
C15H26N2O11S	442.1257	7.59	0.36	1.73	0.73
C11H12N2O2	204.0899	8.00	1.00	1.09	0.18
C18H16O7	344.0896	7.32	1.00	0.89	0.39
C6H11NO8S	257.0205	2.80	0.25	1.83	1.33
C12H22O7	278.1366	2.75	0.29	1.83	0.58
C17H8O5	292.0372	3.98	1.00	0.47	0.29
C14H11NO3S	273.0460	1.25	1.00	0.79	0.21
C18H8N4O6S2	439.9885	1.68	1.00	0.44	0.33
C12H10O2	186.0681	5.65	1.00	0.83	0.17
C6H11NO8S	257.0205	1.74	0.25	1.83	1.33
C13H10O2	198.0681	5.02	1.00	0.77	0.15
C11H20O6	248.1260	1.67	0.33	1.82	0.55
C9H11NO2	165.0790	3.21	1.00	1.22	0.22
C13H24O6	276.1573	3.10	0.33	1.85	0.46
C10H13NO4	211.0845	5.35	1.00	1.30	0.40
C13H26N2O10	370.1587	8.18	0.20	2.00	0.77
C8H15NO7S	269.0569	4.13	0.29	1.88	0.88
C9H6O3	162.0317	1.05	1.00	0.67	0.33
C11H6N4OS	242.0262	0.89	1.00	0.55	0.09
C9H8O	132.0575	3.55	1.00	0.89	0.11
C4H8O4S	152.0143	7.84	0.25	2.00	1.00
C13H23NO8S	353.1144	7.39	0.38	1.77	0.62
C9H8N4O6S	300.0165	5.04	1.00	0.89	0.67

7 Appendix

C3H5NO4S	150.9939	0.51	0.50	1.67	1.33
C7H9NO	123.0684	0.95	1.00	1.29	0.14
C15H12O4	256.0736	4.35	1.00	0.80	0.27
C15H24O4	268.1675	4.08	1.00	1.60	0.27
C12H9NO5	247.0481	7.41	1.00	0.75	0.42
C13H23NO7S	337.1195	7.99	0.43	1.77	0.54
C7H11NO9S	285.0155	2.78	0.33	1.57	1.29
C14H10O3	226.0630	5.27	1.00	0.71	0.21
C7H6O6S	217.9885	0.87	0.83	0.86	0.86
C9H11NO2	165.0790	2.87	1.00	1.22	0.22
C7H12N2O4	188.0797	0.99	0.75	1.71	0.57
C19H22O5	330.1467	7.98	1.00	1.16	0.26
C7H5NO3S	182.9990	0.97	1.00	0.71	0.43
C9H8O5	196.0372	4.10	1.00	0.89	0.56
C7H6O	106.0419	2.63	1.00	0.86	0.14
C6H4O6	172.0008	0.68	0.83	0.67	1.00
C14H10O5	258.0528	5.01	1.00	0.71	0.36
C10H18N2O12S	390.0580	4.44	0.25	1.80	1.20
C14H10O5	258.0528	7.21	1.00	0.71	0.36
C7H6N2O	134.0480	2.85	1.00	0.86	0.14
C7H6N2O4	182.0328	4.69	1.00	0.86	0.57
C15H14O3	242.0943	8.21	1.00	0.93	0.20
C13H9NO2S	243.0354	1.67	1.00	0.69	0.15
C16H5NO3S	290.9990	3.98	1.00	0.31	0.19
C18H8O5S2	367.9813	3.83	1.00	0.44	0.28
C18H12O4	292.0736	6.85	1.00	0.67	0.22
C15H20O10	360.1056	2.74	0.60	1.33	0.67
C9H9NO6	227.0430	6.85	1.00	1.00	0.67
C15H18O4	262.1205	8.05	1.00	1.20	0.27
C15H14O7	306.0740	3.73	1.00	0.93	0.47
C5H10O2	102.0681	0.81	0.50	2.00	0.40
C10H10O5	210.0528	6.62	1.00	1.00	0.50
C20H32O4	336.2301	8.31	1.00	1.60	0.20
C17H20O4	288.1362	7.38	1.00	1.18	0.24
C6H4N4OS2	211.9827	1.09	1.00	0.67	0.17
C7H4N2O3	164.0222	1.36	1.00	0.57	0.43
C13H20O3	224.1412	4.74	1.00	1.54	0.23
C9H6O2	146.0368	2.51	1.00	0.67	0.22
C13H10O8S	326.0096	5.04	1.00	0.77	0.62
C23H10N4O3S	422.0474	5.20	1.00	0.43	0.13
C17H20O5	304.1311	7.50	1.00	1.18	0.29
C12H20N2O12S	416.0737	7.43	0.33	1.67	1.00
C4H3NO2S	128.9884	0.53	1.00	0.75	0.50
C17H20O4	288.1362	8.14	1.00	1.18	0.24
C6H5NO4	155.0219	3.07	1.00	0.83	0.67
C6H5NO3	139.0269	3.74	1.00	0.83	0.50
C2H4O6S	155.9729	0.33	0.17	2.00	3.00
C4H6O5	134.0215	0.36	0.40	1.50	1.25
C3H4O4	104.0110	0.36	0.50	1.33	1.33
C4H6O4	118.0266	0.53	0.50	1.50	1.00
C4H4O4	116.0110	0.38	0.75	1.00	1.00
C5H8O5	148.0372	0.38	0.40	1.60	1.00
C7H6N2O5	198.0277	7.41	1.00	0.86	0.71
C9H8O4	180.0423	3.14	1.00	0.89	0.44
C8H18O4S	210.0926	7.15	0.00	2.25	0.50
C8H14O4	174.0892	3.11	0.50	1.75	0.50
C7H6O2	122.0368	2.63	1.00	0.86	0.29
C3H6O5S	153.9936	0.36	0.20	2.00	1.67
C10H17NO7S	295.0726	4.67	0.43	1.70	0.70
C2H2O4	89.9953	0.36	0.50	1.00	2.00
C9H17NO3	187.1208	2.98	0.67	1.89	0.33
C5H8O4	132.0423	0.77	0.50	1.60	0.80
C7H7NO4	169.0375	4.11	1.00	1.00	0.57
C5H6O5	146.0215	0.37	0.60	1.20	1.00
C5H7NO3	129.0426	0.38	1.00	1.40	0.60
C8H6O5	182.0215	2.77	1.00	0.75	0.63
C2H4O5S	139.9779	0.33	0.20	2.00	2.50
C6H10O4	146.0579	1.69	0.50	1.67	0.67
C6H8O5	160.0372	0.38	0.60	1.33	0.83
C3H8O5S	156.0092	0.36	0.00	2.67	1.67

7 Appendix

C5H8O6	164.0321	0.36	0.33	1.60	1.20
C2H6O4S	125.9987	0.38	0.00	3.00	2.00
C5H6O3	114.0317	0.38	1.00	1.20	0.60
C8H6N2O2	162.0429	6.07	1.00	0.75	0.25
C7H7NO3	153.0426	5.20	1.00	1.00	0.43
C5H8O4	132.0423	1.08	0.50	1.60	0.80
C10H6N2O5	234.0277	7.60	1.00	0.60	0.50
C3H6O4S	137.9987	0.35	0.25	2.00	1.33
C9H14O5	202.0841	2.68	0.60	1.56	0.56
C8H9NO4	183.0532	3.49	1.00	1.13	0.50
C7H6N2O4	182.0328	3.12	1.00	0.86	0.57
C8H6O3	150.0317	2.62	1.00	0.75	0.38
C12H22O6	262.1416	3.42	0.33	1.83	0.50
C7H12O7	208.0583	0.37	0.29	1.71	1.00
C5H10O5	150.0528	0.34	0.20	2.00	1.00
C6H10O6	178.0477	0.38	0.33	1.67	1.00
C7H10O6	190.0477	0.38	0.50	1.43	0.86
C7H6O3	138.0317	3.54	1.00	0.86	0.43
C10H16O5	216.0998	2.93	0.60	1.60	0.50
C5H12O4S	168.0456	2.80	0.00	2.40	0.80
C6H10O5	162.0528	0.49	0.40	1.67	0.83
C8H9NO3	167.0582	7.25	1.00	1.13	0.38
C16H22O4	278.1518	8.48	1.00	1.38	0.25
C15H22O8	330.1315	3.07	0.63	1.47	0.53
C3H8O4S	140.0143	0.50	0.00	2.67	1.33
C12H22O4	230.1518	7.58	0.50	1.83	0.33
C6H5NO4	155.0219	3.80	1.00	0.83	0.67
C4H8O4	120.0423	0.38	0.25	2.00	1.00
C5H10O4	134.0579	0.38	0.25	2.00	0.80
C8H7NO5	197.0324	3.61	1.00	0.88	0.63
C12H14O4	222.0892	7.46	1.00	1.17	0.33
C4H6O5S	165.9936	0.37	0.40	1.50	1.25
C3H6O4	106.0266	0.35	0.25	2.00	1.33
C9H20O4S	224.1082	7.64	0.00	2.22	0.44
C4H8O4S	152.0143	0.38	0.25	2.00	1.00
C3H3NO4	117.0062	0.38	0.75	1.00	1.33
C16H32O6S	352.1920	7.86	0.17	2.00	0.38
C9H11NO3	181.0739	8.04	1.00	1.22	0.33
C2H3NO3	89.0113	0.32	0.67	1.50	1.50
C8H16O8S	272.0566	3.71	0.13	2.00	1.00
C7H5NO3S2	214.9711	2.79	1.00	0.71	0.43
C6H10O4	146.0579	2.48	0.50	1.67	0.67
C10H22O4S	238.1239	7.95	0.00	2.20	0.40
C15H8N4O6	340.0444	3.71	1.00	0.53	0.40
C2H3NO4S	136.9783	0.37	0.50	1.50	2.00
C5H7NO5	161.0324	0.36	0.60	1.40	1.00
C7H6N2O6	214.0226	4.81	1.00	0.86	0.86
C16H30O4	286.2144	7.82	0.50	1.88	0.25
C8H14O	126.1045	3.71	1.00	1.75	0.13
C6H6N2O2	138.0429	0.38	1.00	1.00	0.33
C6H9NO4	159.0532	0.38	0.75	1.50	0.67
C4H4N2O2	112.0273	0.38	1.00	1.00	0.50
C10H10O4	194.0579	6.37	1.00	1.00	0.40
C10H18O6	234.1103	2.73	0.33	1.80	0.60
C14H21NO6	299.1369	4.59	0.83	1.50	0.43
C11H18O6	246.1103	4.36	0.50	1.64	0.55
C7H5NO	119.0371	3.13	1.00	0.71	0.14
C18H30O5	326.2093	8.01	0.80	1.67	0.28
C18H34O5	330.2406	7.44	0.40	1.89	0.28
C5H4N2O4	156.0171	0.39	1.00	0.80	0.80
C15H28O4	272.1988	8.28	0.50	1.87	0.27
C14H28O3	244.2038	8.21	0.33	2.00	0.21
C12H14O4	222.0892	3.95	1.00	1.17	0.33
C7H8O3S	172.0194	1.74	1.00	1.14	0.43
C10H11NO3	193.0739	3.04	1.00	1.10	0.30
C8H16O3	160.1099	4.43	0.33	2.00	0.38
C7H13NO3	159.0895	1.33	0.67	1.86	0.43
C18H32O4	312.2301	8.29	0.75	1.78	0.22
C7H12O	112.0888	3.11	1.00	1.71	0.14
C11H15NO3	209.1052	8.37	1.00	1.36	0.27

7 Appendix

C15H30O3	258.2195	8.38	0.33	2.00	0.20
C15H28O3	256.2038	8.27	0.67	1.87	0.20
C18H26O4	306.1831	8.71	1.00	1.44	0.22

Table S4.3.6 Molecular formulas of organic compounds detected in Xi'an OA in ESI⁻ mode.

Formula [M]	Neutral mass (Da)	RT (min)	MCR	H/C	O/C
C2H4O6S	155.9729	0.39	0.17	2.00	3.00
C7H7NO4	169.0375	2.92	1.00	1.00	0.57
C10H7NO3	189.0426	7.72	1.00	0.70	0.30
C9H12O4	184.0736	1.07	1.00	1.33	0.44
C5H12O4S	168.0456	2.80	0.00	2.40	0.80
C10H17NO7S	295.0726	4.70	0.43	1.70	0.70
C8H7NO3	165.0426	5.03	1.00	0.88	0.38
C7H7NO4	169.0375	3.79	1.00	1.00	0.57
C3H6O6S	169.9885	0.39	0.17	2.00	2.00
C9H15NO8S	297.0518	3.27	0.38	1.67	0.89
C10H17NO7S	295.0726	6.31	0.43	1.70	0.70
C3H8O5S	156.0092	0.38	0.00	2.67	1.67
C4H8O6S	184.0042	0.40	0.17	2.00	1.50
C8H9NO3	167.0582	7.24	1.00	1.13	0.38
C8H12O5	188.0685	1.21	0.60	1.50	0.63
C17H14O6	314.0790	7.96	1.00	0.82	0.35
C8H5NO2	147.0320	3.25	1.00	0.63	0.25
C7H7NO4	169.0375	4.60	1.00	1.00	0.57
C8H18O5S	226.0875	2.95	0.00	2.25	0.63
C8H9NO3	167.0582	7.55	1.00	1.13	0.38
C10H20N2O4	232.1423	3.00	0.50	2.00	0.40
C10H17NO7S	295.0726	6.63	0.43	1.70	0.70
C9H15NO8S	297.0518	2.91	0.38	1.67	0.89
C4H4O6S	179.9729	0.41	0.50	1.00	1.50
C6H10O8S	242.0096	0.39	0.25	1.67	1.33
C9H16O6S	252.0668	2.60	0.33	1.78	0.67
C8H9NO5	199.0481	2.81	1.00	1.13	0.63
C4H10O5S	170.0249	0.40	0.00	2.50	1.25
C10H17NO10S	343.0573	2.67	0.30	1.70	1.00
C6H12O7S	228.0304	0.40	0.14	2.00	1.17
C10H15NO9S	325.0468	2.99	0.44	1.50	0.90
C7H12O7S	240.0304	0.59	0.29	1.71	1.00
C8H16O4S	208.0769	4.86	0.25	2.00	0.50
C6H5N3O4	183.0280	4.85	1.00	0.83	0.67
C10H8O4	192.0423	6.96	1.00	0.80	0.40
C5H4N2O3	140.0222	2.34	1.00	0.80	0.60
C6H8O6	176.0321	0.38	0.50	1.33	1.00
C10H16O7S	280.0617	2.48	0.43	1.60	0.70
C10H14O6S	262.0511	3.00	0.67	1.40	0.60
C8H7NO5	197.0324	4.71	1.00	0.88	0.63
C10H18N2O11S	374.0631	4.40	0.27	1.80	1.10
C6H6O5	158.0215	0.39	0.80	1.00	0.83
C10H17NO8S	311.0675	3.78	0.38	1.70	0.80
C8H7NO4	181.0375	3.87	1.00	0.88	0.50
C8H9NO4	183.0532	5.59	1.00	1.13	0.50
C9H9NO7S	275.0100	4.22	0.86	1.00	0.78
C8H8O3	152.0473	2.63	1.00	1.00	0.38
C11H9NO3	203.0582	8.05	1.00	0.82	0.27
C5H11NO7S	229.0256	2.73	0.14	2.20	1.40
C8H16O5S	224.0718	2.55	0.20	2.00	0.63
C10H19NO8S	313.0831	3.40	0.25	1.90	0.80
C10H18O7S	282.0773	2.79	0.29	1.80	0.70
C4H8O5S	168.0092	0.40	0.20	2.00	1.25
C10H18O4	202.1205	7.12	0.50	1.80	0.40
C8H12O5	188.0685	2.41	0.60	1.50	0.63
C8H5NO3	163.0269	2.66	1.00	0.63	0.38
C9H18O6S	254.0824	2.67	0.17	2.00	0.67
C4H6O6S	181.9885	0.40	0.33	1.50	1.50

7 Appendix

C3H5NO5	135.0168	0.40	0.40	1.67	1.67
C5H8O6	164.0321	0.37	0.33	1.60	1.20
C10H18N2O11S	374.0631	3.27	0.27	1.80	1.10
C10H6O3S2	237.9758	0.54	1.00	0.60	0.30
C5H10O6S	198.0198	0.44	0.17	2.00	1.20
C5H12O5S	184.0405	0.44	0.00	2.40	1.00
C4H6O5S	165.9936	0.38	0.40	1.50	1.25
C6H11NO8	225.0485	0.37	0.25	1.83	1.33
C6H8O6S	208.0042	0.40	0.50	1.33	1.00
C8H12O7	220.0583	0.40	0.43	1.50	0.88
C8H9NO7S	263.0100	3.61	0.71	1.13	0.88
C9H19NO8S	301.0831	3.41	0.13	2.11	0.89
C6H6O6	174.0164	0.40	0.67	1.00	1.00
C6H5NO4	155.0219	3.78	1.00	0.83	0.67
C10H16O7S	280.0617	1.02	0.43	1.60	0.70
C9H18O6S	254.0824	3.22	0.17	2.00	0.67
C8H17NO5S	239.0827	2.24	0.20	2.13	0.63
C10H18O6S	266.0824	1.19	0.33	1.80	0.60
C10H18O6S	266.0824	0.63	0.33	1.80	0.60
C7H6O5S	201.9936	0.66	1.00	0.86	0.71
C7H8O6	188.0321	0.40	0.67	1.14	0.86
C9H14O5	202.0841	1.61	0.60	1.56	0.56
C14H14N2O5S2	354.0344	2.68	1.00	1.00	0.36
C10H10O4	194.0579	6.33	1.00	1.00	0.40
C3H8O3S	124.0194	0.40	0.00	2.67	1.00
C7H6N2O4	182.0328	3.11	1.00	0.86	0.57
C5H6O6S	193.9885	0.59	0.50	1.20	1.20
C10H19NO9S	329.0781	2.70	0.22	1.90	0.90
C7H8O5	172.0372	0.40	0.80	1.14	0.71
C7H12O5	176.0685	0.77	0.40	1.71	0.71
C5H8O5S	180.0092	0.40	0.40	1.60	1.00
C7H12O6S	224.0355	0.80	0.33	1.71	0.86
C12H9NO3	215.0582	7.85	1.00	0.75	0.25
C12H11NO3	217.0739	8.21	1.00	0.92	0.25
C10H20O5S	252.1031	7.03	0.20	2.00	0.50
C10H18N2O11S	374.0631	3.88	0.27	1.80	1.10
C2H2O3	74.0004	0.38	0.67	1.00	1.50
C14H10O4S	274.0300	7.12	1.00	0.71	0.29
C9H7NO4	193.0375	3.45	1.00	0.78	0.44
C9H18O6S	254.0824	3.54	0.17	2.00	0.67
C7H7NO5	185.0324	3.27	1.00	1.00	0.71
C6H6N2O3	154.0378	2.82	1.00	1.00	0.50
C7H4N2O7	228.0019	4.12	1.00	0.57	1.00
C9H16O3	172.1099	4.17	0.67	1.78	0.33
C7H14O7S	242.0460	0.54	0.14	2.00	1.00
C6H4O5	156.0059	0.68	1.00	0.67	0.83
C3H3NO4	117.0062	0.40	0.75	1.00	1.33
C12H10N2O6	278.0539	3.72	1.00	0.83	0.50
C9H16O3	172.1099	2.67	0.67	1.78	0.33
C9H6O3	162.0317	2.96	1.00	0.67	0.33
C12H7NO4	229.0375	7.98	1.00	0.58	0.33
C10H16N2O10S	356.0526	7.40	0.40	1.60	1.00
C14H8O3	224.0473	7.56	1.00	0.57	0.21
C10H16O5S	248.0718	2.99	0.60	1.60	0.50
C17H26O5	310.1780	8.07	1.00	1.53	0.29
C6H11NO8S	257.0205	2.05	0.25	1.83	1.33
C8H7NO5	197.0324	4.32	1.00	0.88	0.63
C10H19NO9S	329.0781	3.04	0.22	1.90	0.90
C7H14O6S	226.0511	2.09	0.17	2.00	0.86
C6H8O7S	223.9991	0.40	0.43	1.33	1.17
C6H11NO9S	273.0155	2.15	0.22	1.83	1.50
C8H16O3S	192.0820	3.61	0.33	2.00	0.38
C9H8O4	180.0423	4.11	1.00	0.89	0.44
C11H23NO5S	281.1297	2.91	0.20	2.09	0.45
C8H6O6S	229.9885	2.51	1.00	0.75	0.75
C10H14O6	230.0790	2.16	0.67	1.40	0.60
C8H12O8S	268.0253	0.63	0.38	1.50	1.00
C7H16O4S	196.0769	5.15	0.00	2.29	0.57
C5H4N4O3	168.0283	0.38	1.00	0.80	0.60
C8H16O3S	192.0820	4.01	0.33	2.00	0.38

7 Appendix

C8H12O5	188.0685	1.81	0.60	1.50	0.63
C9H11NO4	197.0688	7.34	1.00	1.22	0.44
C9H8O4	180.0423	2.77	1.00	0.89	0.44
C8H7NO5	197.0324	3.33	1.00	0.88	0.63
C10H18N2O11S	374.0631	4.99	0.27	1.80	1.10
C4H10O4S	154.0300	0.91	0.00	2.50	1.00
C4H5NO3	115.0269	0.39	1.00	1.25	0.75
C9H17NO9S	315.0624	2.50	0.22	1.89	1.00
C9H16O7S	268.0617	0.60	0.29	1.78	0.78
C7H5NO4	167.0219	3.77	1.00	0.71	0.57
C6H14O5S	198.0562	0.81	0.00	2.33	0.83
C8H17NO8S	287.0675	2.99	0.13	2.13	1.00
C9H7NO4	193.0375	7.14	1.00	0.78	0.44
C9H6N2O3	190.0378	2.75	1.00	0.67	0.33
C6H5NO4	155.0219	0.41	1.00	0.83	0.67
C10H15NO10S	341.0417	2.99	0.40	1.50	1.00
C3H7NO7S	200.9943	0.85	0.14	2.33	2.33
C11H18O5	230.1154	3.20	0.60	1.64	0.45
C7H5NO6	199.0117	3.46	1.00	0.71	0.86
C8H16O4S	208.0769	6.33	0.25	2.00	0.50
C5H6O5S	177.9936	0.42	0.60	1.20	1.00
C5H6O4S	161.9987	0.64	0.75	1.20	0.80
C10H16O8S	296.0566	0.59	0.38	1.60	0.80
C6H13NO8S	259.0362	1.38	0.13	2.17	1.33
C5H12O3S	152.0507	1.80	0.00	2.40	0.60
C6H3N3O7	228.9971	4.12	1.00	0.50	1.17
C24H24O3S	392.1446	8.14	1.00	1.00	0.13
C9H8O5	196.0372	2.76	1.00	0.89	0.56
C8H9NO4	183.0532	6.43	1.00	1.13	0.50
C8H11NO7	233.0536	3.01	0.57	1.38	0.88
C6H13NO7S	243.0413	3.25	0.14	2.17	1.17
C11H18N2O2	210.1368	2.69	1.00	1.64	0.18
C6H10O3	130.0630	0.66	0.67	1.67	0.50
C15H28O8S	368.1505	7.60	0.25	1.87	0.53
C7H15NO8S	273.0518	2.68	0.13	2.14	1.14
C10H22O4S	238.1239	8.01	0.00	2.20	0.40
C8H5NO4	179.0219	4.87	1.00	0.63	0.50
C9H8N2O2	176.0586	7.45	1.00	0.89	0.22
C10H18O7S	282.0773	0.68	0.29	1.80	0.70
C11H20O6S	280.0981	3.85	0.33	1.82	0.55
C11H21NO8	295.1267	3.01	0.25	1.91	0.73
C13H19NO6	285.1212	7.37	0.83	1.46	0.46
C7H6N2O6	214.0226	3.51	1.00	0.86	0.86
C7H14O6S	226.0511	2.46	0.17	2.00	0.86
C8H14O10S	302.0308	2.25	0.20	1.75	1.25
C9H18N2O4	218.1267	2.67	0.50	2.00	0.44
C16H10O	218.0732	8.36	1.00	0.63	0.06
C7H14O5S	210.0562	1.83	0.20	2.00	0.71
C13H10O4	230.0579	5.34	1.00	0.77	0.31
C13H9NO3	227.0582	8.23	1.00	0.69	0.23
C18H36O2	284.2715	9.53	0.50	2.00	0.11
C9H6O6	210.0164	1.15	1.00	0.67	0.67
C9H8O5	196.0372	3.30	1.00	0.89	0.56
C8H6O3	150.0317	3.01	1.00	0.75	0.38
C5H5NO4	143.0219	1.22	1.00	1.00	0.80
C11H10O5	222.0528	2.92	1.00	0.91	0.45
C9H16O6S	252.0668	0.83	0.33	1.78	0.67
C10H20O6S	268.0981	3.83	0.17	2.00	0.60
C9H9NO6	227.0430	3.36	1.00	1.00	0.67
C7H13NO7S	255.0413	3.42	0.29	1.86	1.00
C7H14O4	162.0892	0.81	0.25	2.00	0.57
C7H7NO3	153.0426	2.57	1.00	1.00	0.43
C8H6O5S	213.9936	1.54	1.00	0.75	0.63
C6H8O2	112.0524	1.01	1.00	1.33	0.33
C8H8O2	136.0524	3.50	1.00	1.00	0.25
C11H20O7S	296.0930	2.90	0.29	1.82	0.64
C6H13NO8S	259.0362	2.61	0.13	2.17	1.33
C12H14O5	238.0841	3.39	1.00	1.17	0.42
C7H12O2	128.0837	1.71	1.00	1.71	0.29
C7H5NO	119.0371	3.12	1.00	0.71	0.14

7 Appendix

C7H4N2O4	180.0171	3.49	1.00	0.57	0.57
C10H18O7S	282.0773	1.43	0.29	1.80	0.70
C10H19NO9S	329.0781	2.30	0.22	1.90	0.90
C8H10O5	186.0528	0.62	0.80	1.25	0.63
C9H16O7S	268.0617	2.39	0.29	1.78	0.78
C13H11NO3	229.0739	8.12	1.00	0.85	0.23
C13H8O10	324.0117	2.26	1.00	0.62	0.77
C14H22O4	254.1518	6.61	1.00	1.57	0.29
C9H16O6S	252.0668	3.71	0.33	1.78	0.67
C7H6O4	154.0266	2.58	1.00	0.86	0.57
C8H8N2O4	196.0484	3.18	1.00	1.00	0.50
C10H6O4	190.0266	3.34	1.00	0.60	0.40
C20H18O9	402.0951	7.44	1.00	0.90	0.45
C8H6O3	150.0317	0.83	1.00	0.75	0.38
C8H5NO4	179.0219	5.33	1.00	0.63	0.50
C5H5N3O4	171.0280	3.93	1.00	1.00	0.80
C8H6O2	134.0368	1.77	1.00	0.75	0.25
C10H11NO4	209.0688	7.16	1.00	1.10	0.40
C9H14O5S	234.0562	2.53	0.60	1.56	0.56
C8H9NO5	199.0481	4.22	1.00	1.13	0.63
C5H4N2O3	140.0222	1.13	1.00	0.80	0.60
C9H7NO	145.0528	3.46	1.00	0.78	0.11
C13H11NO3S	261.0460	2.65	1.00	0.85	0.23
C9H17NO8S	299.0675	3.36	0.25	1.89	0.89
C6H12O6S	212.0355	1.52	0.17	2.00	1.00
C9H10O7S	262.0147	2.68	0.71	1.11	0.78
C8H14O7S	254.0460	2.27	0.29	1.75	0.88
C12H9NO4	231.0532	7.42	1.00	0.75	0.33
C5H6O3	114.0317	0.85	1.00	1.20	0.60
C10H8O5	208.0372	2.40	1.00	0.80	0.50
C8H6O5	182.0215	2.48	1.00	0.75	0.63
C6H6O4	142.0266	0.40	1.00	1.00	0.67
C14H10O2	210.0681	7.86	1.00	0.71	0.14
C12H21NO9S	355.0937	6.51	0.33	1.75	0.75
C9H16O6S	252.0668	4.10	0.33	1.78	0.67
C11H17NO8	291.0954	2.94	0.50	1.55	0.73
C9H5NO5	207.0168	3.90	1.00	0.56	0.56
C7H13NO9S	287.0311	2.70	0.22	1.86	1.29
C13H8O3	212.0473	7.04	1.00	0.62	0.23
C8H16O7S	256.0617	0.76	0.14	2.00	0.88
C18H13NO6	339.0743	7.86	1.00	0.72	0.33
C15H25NO7S	363.1352	8.09	0.57	1.67	0.47
C9H8O5S	228.0092	2.45	1.00	0.89	0.56
C9H7NO3	177.0426	3.32	1.00	0.78	0.33
C9H7NO	145.0528	2.22	1.00	0.78	0.11
C8H6O3	150.0317	1.11	1.00	0.75	0.38
C5H11NO8S	245.0205	0.85	0.13	2.20	1.60
C5H9NO7S	227.0100	3.12	0.29	1.80	1.40
C13H7NO4	241.0375	7.84	1.00	0.54	0.31
C6H11NO8S	257.0205	2.77	0.25	1.83	1.33
C13H8O4	228.0423	7.86	1.00	0.62	0.31
C5H5NO3	127.0269	1.03	1.00	1.00	0.60
C10H11NO3	193.0739	7.88	1.00	1.10	0.30
C7H7NO2	137.0477	2.34	1.00	1.00	0.29
C10H11NO6	241.0586	5.33	1.00	1.10	0.60
C9H20O3S	208.1133	7.15	0.00	2.22	0.33
C7H13NO8S	271.0362	2.82	0.25	1.86	1.14
C11H18O4	214.1205	6.72	0.75	1.64	0.36
C14H13NO3S	275.0616	3.09	1.00	0.93	0.21
C10H9NO4	207.0532	7.69	1.00	0.90	0.40
C13H8O3	212.0473	7.51	1.00	0.62	0.23
C8H7NO3	165.0426	1.28	1.00	0.88	0.38
C15H25NO8S	379.1301	7.65	0.50	1.67	0.53
C7H11NO9S	285.0155	1.58	0.33	1.57	1.29
C7H4N2O3	164.0222	3.97	1.00	0.57	0.43
C10H12O5S	244.0405	4.97	1.00	1.20	0.50
C9H10O5S	230.0249	2.54	1.00	1.11	0.56
C11H10O4	206.0579	3.17	1.00	0.91	0.36
C9H20O4S	224.1082	6.18	0.00	2.22	0.44
C10H9NO4	207.0532	4.82	1.00	0.90	0.40

7 Appendix

C8H15NO9S	301.0468	2.33	0.22	1.88	1.13
C20H14N2O5	330.0827	6.72	1.00	0.70	0.05
C12H24O6S	296.1294	7.01	0.17	2.00	0.50
C9H6O6	210.0164	1.84	1.00	0.67	0.67
C11H17NO8	291.0954	3.23	0.50	1.55	0.73
C11H8O2	172.0524	3.83	1.00	0.73	0.18
C14H11NO2S	257.0510	2.43	1.00	0.79	0.14
C14H9NO3	239.0582	8.22	1.00	0.64	0.21
C9H7NO4	193.0375	6.74	1.00	0.78	0.44
C9H7NO4	193.0375	1.33	1.00	0.78	0.44
C9H14O7S	266.0460	1.28	0.43	1.56	0.78
C11H18N2O4S	274.0987	2.36	1.00	1.64	0.36
C15H8O4	252.0423	5.24	1.00	0.53	0.27
C10H10O4	194.0579	2.79	1.00	1.00	0.40
C9H9NO6	227.0430	2.97	1.00	1.00	0.67
C8H12N4O11	340.0503	7.18	0.45	1.50	1.38
C7H9NO8S	267.0049	2.45	0.50	1.29	1.14
C4H4N2O2	112.0273	2.06	1.00	1.00	0.50
C18H16O6	328.0947	8.16	1.00	0.89	0.33
C8H11NO5S	233.0358	0.59	0.80	1.38	0.63
C13H10O2	198.0681	7.97	1.00	0.77	0.15
C7H6O2	122.0368	0.83	1.00	0.86	0.29
C8H9NO5S	231.0201	2.72	1.00	1.13	0.63
C10H19NO9S	329.0781	1.38	0.22	1.90	0.90
C19H12O4	304.0736	8.03	1.00	0.63	0.21
C8H13NO9S	299.0311	3.00	0.33	1.63	1.13
C14H10O3	226.0630	7.88	1.00	0.71	0.21
C13H26O5S	294.1501	7.63	0.20	2.00	0.38
C6H12O6S	212.0355	2.52	0.17	2.00	1.00
C11H8N2O5	248.0433	8.17	1.00	0.73	0.45
C11H16O5	228.0998	3.27	0.80	1.45	0.45
C6H11NO9S	273.0155	0.96	0.22	1.83	1.50
C7H6O4S	185.9987	1.37	1.00	0.86	0.57
C10H9NO4	207.0532	4.52	1.00	0.90	0.40
C6H10O5S	194.0249	0.59	0.40	1.67	0.83
C9H6O4	178.0266	2.95	1.00	0.67	0.44
C8H7NO	133.0528	2.29	1.00	0.88	0.13
C7H9NO9S	282.9998	3.20	0.44	1.29	1.29
C7H16O5S	212.0718	1.89	0.00	2.29	0.71
C9H15NO8	265.0798	3.10	0.38	1.67	0.89
C3H2N2O4	130.0015	0.55	1.00	0.67	1.33
C10H16O8S	296.0566	2.72	0.38	1.60	0.80
C23H28N4OS2	440.1705	7.19	1.00	1.22	0.04
C14H9NO2	223.0633	7.60	1.00	0.64	0.14
C9H8O	132.0575	3.09	1.00	0.89	0.11
C8H11NO8S	281.0205	2.98	0.50	1.38	1.00
C10H21NO8S	315.0988	3.79	0.13	2.10	0.80
C9H9NO7S	275.0100	3.72	0.86	1.00	0.78
C5H11NO8S	245.0205	1.09	0.13	2.20	1.60
C4H10O3S	138.0351	0.62	0.00	2.50	0.75
C11H18N2O10	338.0961	7.88	0.40	1.64	0.91
C8H5NO5	195.0168	3.14	1.00	0.63	0.63
C9H17NO7S	283.0726	7.26	0.29	1.89	0.78
C14H10O4	242.0579	6.66	1.00	0.71	0.29
C10H10O6S	258.0198	1.63	1.00	1.00	0.60
C13H6O9	306.0012	2.57	1.00	0.46	0.69
C5H12O4S	168.0456	2.12	0.00	2.40	0.80
C8H5NO6	211.0117	2.56	1.00	0.63	0.75
C9H8O2	148.0524	3.37	1.00	0.89	0.22
C9H8O5S	228.0092	2.76	1.00	0.89	0.56
C7H10O2	126.0681	2.77	1.00	1.43	0.29
C7H10O3	142.0630	0.81	1.00	1.43	0.43
C9H7NO6	225.0273	3.17	1.00	0.78	0.67
C7H8O5	172.0372	1.07	0.80	1.14	0.71
C4H7NO9S	244.9842	0.59	0.22	1.75	2.25
C7H12N2O3	172.0848	2.45	1.00	1.71	0.43
C7H7NO4	169.0375	6.22	1.00	1.00	0.57
C10H17NO4	215.1158	3.60	0.75	1.70	0.40
C8H7NO3	165.0426	6.71	1.00	0.88	0.38
C5H10O6S	198.0198	1.00	0.17	2.00	1.20

7 Appendix

C5H11NO9S	261.0155	0.54	0.11	2.20	1.80
C7H10O2	126.0681	1.21	1.00	1.43	0.29
C11H12N2O4S	268.0518	7.18	1.00	1.09	0.36
C5H3N3O2	137.0225	3.17	1.00	0.60	0.40
C9H11N3OS2	241.0344	0.58	1.00	1.22	0.11
C7H10O2	126.0681	2.06	1.00	1.43	0.29
C14H28O5S	308.1657	7.90	0.20	2.00	0.36
C9H10O3	166.0630	3.34	1.00	1.11	0.33
C15H9NO3S	283.0303	2.92	1.00	0.60	0.20
C14H12O4S2	308.0177	1.21	1.00	0.86	0.29
C10H11NO3	193.0739	2.99	1.00	1.10	0.30
C7H7N3O4	197.0437	5.67	1.00	1.00	0.57
C8H16O5S	224.0718	1.70	0.20	2.00	0.63
C10H19NO7S	297.0882	7.46	0.29	1.90	0.70
C9H18O6S	254.0824	4.30	0.17	2.00	0.67
C9H8O4	180.0423	1.33	1.00	0.89	0.44
C8H7NO7S	260.9943	2.81	0.86	0.88	0.88
C13H8O3	212.0473	6.52	1.00	0.62	0.23
C6H12O6S	212.0355	2.83	0.17	2.00	1.00
C7H12O3	144.0786	1.08	0.67	1.71	0.43
C8H14O6S	238.0511	2.57	0.33	1.75	0.75
C10H17NO8S	311.0675	6.59	0.38	1.70	0.80
C6H5N3O2	151.0382	4.18	1.00	0.83	0.33
C8H8N2O6	228.0382	7.57	1.00	1.00	0.75
C9H5NO5	207.0168	3.18	1.00	0.56	0.56
C12H8O3	200.0473	4.38	1.00	0.67	0.25
C11H18N2O10	338.0961	7.48	0.40	1.64	0.91
C8H8O3	152.0473	6.12	1.00	1.00	0.38
C7H5NO6	199.0117	2.68	1.00	0.71	0.86
C15H8O4	252.0423	7.61	1.00	0.53	0.27
C12H10O3S2	266.0071	1.62	1.00	0.83	0.25
C8H16O6S	240.0668	3.28	0.17	2.00	0.75
C7H5NO2	135.0320	2.65	1.00	0.71	0.29
C13H16O3	220.1099	8.10	1.00	1.23	0.23
C15H12O2	224.0837	8.10	1.00	0.80	0.13
C11H13NO3	207.0895	8.17	1.00	1.18	0.27
C8H16O7S	256.0617	1.01	0.14	2.00	0.88
C11H20O4	216.1362	3.18	0.50	1.82	0.36
C6H14O5S	198.0562	2.11	0.00	2.33	0.83
C7H7N3O4	197.0437	6.90	1.00	1.00	0.57
C9H7NO5	209.0324	3.97	1.00	0.78	0.56
C5H10N2O10	258.0335	2.33	0.20	2.00	2.00
C5H9NO9S	258.9998	1.04	0.22	1.80	1.80
C7H8O4S	188.0143	2.55	1.00	1.14	0.57
C10H7NO4	205.0375	3.09	1.00	0.70	0.40
C8H14O9S	286.0359	1.21	0.22	1.75	1.13
C8H7NO3	165.0426	7.36	1.00	0.88	0.38
C7H7NO4	169.0375	6.61	1.00	1.00	0.57
C11H21NO9	311.1216	2.47	0.22	1.91	0.82
C11H10O5	222.0528	3.57	1.00	0.91	0.45
C10H10O7S	274.0147	2.79	0.86	1.00	0.70
C6H8O4	144.0423	2.52	0.75	1.33	0.67
C10H8N2O3	204.0535	2.96	1.00	0.80	0.30
C19H22O4	314.1518	7.71	1.00	1.16	0.21
C13H13NO3	231.0895	8.36	1.00	1.00	0.23
C9H14O8S	282.0409	1.87	0.38	1.56	0.89
C11H20O8S	312.0879	2.42	0.25	1.82	0.73
C9H10O3	166.0630	7.27	1.00	1.11	0.33
C6H10O	98.0732	3.01	1.00	1.67	0.17
C7H15NO8S	273.0518	1.95	0.13	2.14	1.14
C11H7NO5	233.0324	7.26	1.00	0.64	0.45
C9H10N2O5	226.0590	3.01	1.00	1.11	0.56
C6H5N3O2	151.0382	3.84	1.00	0.83	0.33
C10H10O6S	258.0198	0.76	1.00	1.00	0.60
C12H16O6	256.0947	2.90	0.83	1.33	0.50
C6H6N2O3	154.0378	2.14	1.00	1.00	0.50
C15H10O3	238.0630	7.99	1.00	0.67	0.20
C10H7NO5	221.0324	5.77	1.00	0.70	0.50
C11H6O3	186.0317	6.57	1.00	0.55	0.27
C18H10O3	274.0630	7.99	1.00	0.56	0.17

7 Appendix

C11H11NO4	221.0688	8.04	1.00	1.00	0.36
C11H18O8S	310.0722	2.68	0.38	1.64	0.73
C11H12O3	192.0786	3.47	1.00	1.09	0.27
C9H11N3OS2	241.0344	0.88	1.00	1.22	0.11
C7H11NO8S	269.0205	4.53	0.38	1.57	1.14
C13H24OS2	260.1269	3.41	1.00	1.85	0.08
C8H5NO3S	194.9990	7.40	1.00	0.63	0.38
C11H22N2O8S	342.1097	8.31	0.25	2.00	0.73
C14H10O5	258.0528	3.66	1.00	0.71	0.36
C10H17NO9S	327.0624	6.29	0.33	1.70	0.90
C9H8N2O2	176.0586	6.69	1.00	0.89	0.22
C14H28O3	244.2038	8.23	0.33	2.00	0.21
C10H20O5S	252.1031	3.82	0.20	2.00	0.50
C8H5NO6	211.0117	3.02	1.00	0.63	0.75
C9H7NO4	193.0375	2.34	1.00	0.78	0.44
C7H16O5S	212.0718	1.44	0.00	2.29	0.71
C16H10O4	266.0579	7.40	1.00	0.63	0.25
C10H10N2O2	190.0742	7.93	1.00	1.00	0.20
C12H25NO8S	343.1301	6.90	0.13	2.08	0.67
C10H9NO	159.0684	2.64	1.00	0.90	0.10
C10H9NO4	207.0532	2.81	1.00	0.90	0.40
C8H7N3O5	225.0386	6.01	1.00	0.88	0.63
C6H8O6S	208.0042	1.15	0.50	1.33	1.00
C15H23NO8S	377.1144	7.38	0.63	1.53	0.53
C8H6N2O5	210.0277	7.33	1.00	0.75	0.63
C11H11NO4	221.0688	6.95	1.00	1.00	0.36
C8H6N2O5	210.0277	6.93	1.00	0.75	0.63
C12H20O3	212.1412	8.41	1.00	1.67	0.25
C15H30O5S	322.1814	8.18	0.20	2.00	0.33
C12H21NO9S	355.0937	5.20	0.33	1.75	0.75
C12H18O5	242.1154	5.03	0.80	1.50	0.42
C6H7NO3	141.0426	2.46	1.00	1.17	0.50
C14H20O6	284.1260	3.10	0.83	1.43	0.43
C10H9NO3	191.0582	4.40	1.00	0.90	0.30
C14H12O4	244.0736	7.21	1.00	0.86	0.29
C7H13NO6	207.0743	3.10	0.33	1.86	0.86
C10H13NO4	211.0845	7.88	1.00	1.30	0.40
C9H7NO6	225.0273	3.67	1.00	0.78	0.67
C14H28O6S	324.1607	7.70	0.17	2.00	0.43
C10H11NO6	241.0586	4.15	1.00	1.10	0.60
C14H22O6	286.1416	3.15	0.67	1.57	0.43
C9H11NO5	213.0637	4.31	1.00	1.22	0.56
C9H6N2O3	190.0378	4.42	1.00	0.67	0.33
C16H10O4S	298.0300	7.53	1.00	0.63	0.25
C9H5NO5	207.0168	2.54	1.00	0.56	0.56
C13H26O6S	310.1450	7.40	0.17	2.00	0.46
C11H11NO4	221.0688	6.42	1.00	1.00	0.36
C8H12O9S	284.0202	1.07	0.33	1.50	1.13
C8H13NO8	251.0641	2.42	0.38	1.63	1.00
C6H6N2O2	138.0429	0.92	1.00	1.00	0.33
C7H6N2O4	182.0328	3.45	1.00	0.86	0.57
C7H14O4	162.0892	2.40	0.25	2.00	0.57
C9H11NO5	213.0637	3.29	1.00	1.22	0.56
C8H6N2O5	210.0277	3.40	1.00	0.75	0.63
C11H13NO5	239.0794	4.53	1.00	1.18	0.45
C20H30O4	334.2144	8.13	1.00	1.50	0.20
C10H10O6S	258.0198	1.03	1.00	1.00	0.60
C10H12O11S	340.0100	3.01	0.45	1.20	1.10
C9H18O5S	238.0875	2.74	0.20	2.00	0.56
C12H13NO4	235.0845	7.56	1.00	1.08	0.33
C6H6N2O6	202.0226	3.72	0.83	1.00	1.00
C8H8O	120.0575	3.28	1.00	1.00	0.13
C9H19NO7	253.1162	6.77	0.14	2.11	0.78
C10H17N3O3	227.1270	3.11	1.00	1.70	0.30
C8H13NO8	251.0641	0.82	0.38	1.63	1.00
C13H23NO10S	385.1043	4.77	0.30	1.77	0.77
C5H9NO9S	258.9998	0.74	0.22	1.80	1.80
C12H15NO3	221.1052	8.35	1.00	1.25	0.25
C4H5N3O2	127.0382	1.06	1.00	1.25	0.50
C14H20O5	268.1311	3.23	1.00	1.43	0.36

7 Appendix

C11H8O2	172.0524	5.12	1.00	0.73	0.18
C6H12O4S	180.0456	7.34	0.25	2.00	0.67
C16H14O4	270.0892	7.51	1.00	0.88	0.25
C10H9NO5	223.0481	5.82	1.00	0.90	0.50
C17H10O2	246.0681	7.61	1.00	0.59	0.12
C16H14O2S	270.0714	1.34	1.00	0.88	0.13
C10H12O3	180.0786	7.89	1.00	1.20	0.30
C15H26O4	270.1831	8.14	0.75	1.73	0.27
C9H11NO4	197.0688	6.58	1.00	1.22	0.44
C10H10O7S	274.0147	0.95	0.86	1.00	0.70
C12H12O4	220.0736	7.71	1.00	1.00	0.33
C7H7NO	121.0528	3.18	1.00	1.00	0.14
C11H8O2	172.0524	6.74	1.00	0.73	0.18
C12H8O2	184.0524	5.15	1.00	0.67	0.17
C13H18O6	270.1103	2.99	0.83	1.38	0.46
C13H24N4O6S2	396.1137	8.49	0.67	1.85	0.46
C13H9NO	195.0684	4.52	1.00	0.69	0.08
C10H20O6S	268.0981	4.94	0.17	2.00	0.60
C20H13N3O3S	375.0678	8.24	1.00	0.65	0.15
C7H7NO	121.0528	1.02	1.00	1.00	0.14
C15H30O10	370.1839	8.47	0.10	2.00	0.67
C4H8O2	88.0524	1.05	0.50	2.00	0.50
C14H8O3	224.0473	6.88	1.00	0.57	0.21
C11H14O6	242.0790	2.99	0.83	1.27	0.55
C12H10O4	218.0579	3.16	1.00	0.83	0.33
C7H6O5	170.0215	1.43	1.00	0.86	0.71
C8H9NO4	183.0532	7.60	1.00	1.13	0.50
C18H14O7	342.0740	7.74	1.00	0.78	0.39
C9H17NO9S	315.0624	4.83	0.22	1.89	1.00
C13H10O3	214.0630	3.90	1.00	0.77	0.23
C10H12O4	196.0736	3.30	1.00	1.20	0.40
C9H11NO4	197.0688	5.71	1.00	1.22	0.44
C14H8O4	240.0423	6.44	1.00	0.57	0.29
C7H10O	110.0732	2.45	1.00	1.43	0.14
C18H32O9S	424.1767	7.44	0.33	1.78	0.50
C18H10O4	290.0579	7.60	1.00	0.56	0.22
C13H11NO4	245.0688	7.97	1.00	0.85	0.31
C12H20N2O2	224.1525	2.88	1.00	1.67	0.17
C14H12O2	212.0837	8.21	1.00	0.86	0.14
C13H10O2	198.0681	7.18	1.00	0.77	0.15
C11H9NO5	235.0481	7.46	1.00	0.82	0.45
C14H13NO4	259.0845	8.12	1.00	0.93	0.29
C14H8O4	240.0423	7.96	1.00	0.57	0.29
C9H6O3	162.0317	3.93	1.00	0.67	0.33
C14H8O3	224.0473	5.86	1.00	0.57	0.21
C11H8O3	188.0473	5.12	1.00	0.73	0.27
C11H13NO6	255.0743	3.61	1.00	1.18	0.55
C6H10N2O3	158.0691	1.06	1.00	1.67	0.50
C9H17NO9S	315.0624	6.32	0.22	1.89	1.00
C11H18N2O4	242.1267	2.86	1.00	1.64	0.36
C14H11NO3S	273.0460	1.21	1.00	0.79	0.21
C13H18O3	222.1256	7.68	1.00	1.38	0.23
C10H13NO5	227.0794	4.00	1.00	1.30	0.50
C18H34O7S	394.2025	8.51	0.29	1.89	0.39
C13H24N2O4	272.1736	1.46	0.75	1.85	0.31
C12H10O3	202.0630	7.17	1.00	0.83	0.25
C12H10O2	186.0681	7.14	1.00	0.83	0.17
C8H7NO6	213.0273	4.71	1.00	0.88	0.75
C13H27NO8S	357.1457	7.63	0.13	2.08	0.62
C10H8N2O6	252.0382	7.81	1.00	0.80	0.60
C10H10N2O2	190.0742	7.58	1.00	1.00	0.20
C11H20O8S	312.0879	3.81	0.25	1.82	0.73
C12H25NO7S	327.1352	8.23	0.14	2.08	0.58
C12H10O2	186.0681	7.54	1.00	0.83	0.17
C11H8O3	188.0473	4.83	1.00	0.73	0.27
C14H8O3	224.0473	4.49	1.00	0.57	0.21
C13H8O3	212.0473	5.75	1.00	0.62	0.23
C10H7NO5	221.0324	3.46	1.00	0.70	0.50
C14H12O2	212.0837	7.76	1.00	0.86	0.14
C9H14O8S	282.0409	2.58	0.38	1.56	0.89

7 Appendix

C9H10O2	150.0681	4.96	1.00	1.11	0.22
C12H10O3	202.0630	7.85	1.00	0.83	0.25
C6H4N2O5	184.0120	6.20	1.00	0.67	0.83
C12H9NO4	231.0532	7.78	1.00	0.75	0.33
C13H10O2	198.0681	7.47	1.00	0.77	0.15
C10H7NO5	221.0324	4.14	1.00	0.70	0.50
C11H20O4	216.1362	3.83	0.50	1.82	0.36
C10H6N2O2	186.0429	3.49	1.00	0.60	0.20
C15H25NO7	331.1631	7.70	0.57	1.67	0.47
C12H13NO4	235.0845	8.25	1.00	1.08	0.33
C14H8O5	256.0372	6.46	1.00	0.57	0.36
C14H11NO4	257.0688	8.35	1.00	0.79	0.29
C16H22O5	294.1467	8.42	1.00	1.38	0.31
C15H15NO4	273.1001	8.28	1.00	1.00	0.27
C14H8O4	240.0423	3.96	1.00	0.57	0.29
C12H8O2	184.0524	5.39	1.00	0.67	0.17
C12H26O4S	266.1552	8.49	0.00	2.17	0.33
C9H16O4	188.1049	3.71	0.50	1.78	0.44
C11H23N3O5	277.1638	2.56	0.40	2.09	0.45
C7H6O2	122.0368	2.72	1.00	0.86	0.29
C4H4O4	116.0110	0.40	0.75	1.00	1.00
C8H6O4	166.0266	2.68	1.00	0.75	0.50
C11H20O4	216.1362	7.06	0.50	1.82	0.36
C6H5NO3	139.0269	3.72	1.00	0.83	0.50
C5H8O4	132.0423	1.06	0.50	1.60	0.80
C8H10O5	186.0528	2.99	0.80	1.25	0.63
C15H22O2	234.1620	8.55	1.00	1.47	0.13
C5H6O4	130.0266	0.62	0.75	1.20	0.80
C9H14O4	186.0892	2.84	0.75	1.56	0.44
C5H8O5	148.0372	0.40	0.40	1.60	1.00
C8H12O4	172.0736	2.43	0.75	1.50	0.50
C3H4O4	104.0110	0.40	0.50	1.33	1.33
C10H10O5	210.0528	3.02	1.00	1.00	0.50
C16H24O5	296.1624	7.88	1.00	1.50	0.31
C3H6O5S	153.9936	0.39	0.20	2.00	1.67
C8H10O5	186.0528	2.27	0.80	1.25	0.63
C9H8O2	148.0524	3.05	1.00	0.89	0.22
C9H8O3	164.0473	3.28	1.00	0.89	0.33
C9H14O5	202.0841	2.65	0.60	1.56	0.56
C7H6O3	138.0317	2.31	1.00	0.86	0.43
C4H6O5	134.0215	0.39	0.40	1.50	1.25
C6H10O5	162.0528	0.48	0.40	1.67	0.83
C9H8O4	180.0423	3.14	1.00	0.89	0.44
C2H4O5S	139.9779	0.39	0.20	2.00	2.50
C6H8O4	144.0423	0.65	0.75	1.33	0.67
C10H8O4	192.0423	3.09	1.00	0.80	0.40
C18H14O8	358.0689	7.44	1.00	0.78	0.44
C5H10O5	150.0528	0.37	0.20	2.00	1.00
C13H20O5	256.1311	3.28	0.80	1.54	0.38
C3H4O2	72.0211	0.40	1.00	1.33	0.67
C10H16O5	216.0998	2.90	0.60	1.60	0.50
C7H7NO3	153.0426	5.95	1.00	1.00	0.43
C10H10O4	194.0579	3.60	1.00	1.00	0.40
C9H16O5	204.0998	2.57	0.40	1.78	0.56
C8H12O3	156.0786	2.85	1.00	1.50	0.38
C7H13NO3	159.0895	2.83	0.67	1.86	0.43
C5H6O5	146.0215	0.39	0.60	1.20	1.00
C3H6O4S	137.9987	0.37	0.25	2.00	1.33
C7H7NO3	153.0426	5.14	1.00	1.00	0.43
C7H10O5	174.0528	0.73	0.60	1.43	0.71
C5H6O3	114.0317	0.40	1.00	1.20	0.60
C6H8O4	144.0423	1.29	0.75	1.33	0.67
C9H18O4	190.1205	4.18	0.25	2.00	0.44
C12H8N2O5	260.0433	8.31	1.00	0.67	0.42
C7H7NO4	169.0375	4.07	1.00	1.00	0.57
C15H22O8	330.1315	3.06	0.63	1.47	0.53
C8H6O3	150.0317	2.61	1.00	0.75	0.38
C8H14O5	190.0841	2.52	0.40	1.75	0.63
C6H8O3	128.0473	0.65	1.00	1.33	0.50
C8H18O4S	210.0926	7.18	0.00	2.25	0.50

7 Appendix

C11H18O4	214.1205	3.19	0.75	1.64	0.36
C10H14O6	230.0790	2.76	0.67	1.40	0.60
C11H18O4	214.1205	3.79	0.75	1.64	0.36
C15H20N2O4S	324.1144	8.49	1.00	1.33	0.27
C11H20O3	200.1412	7.61	0.67	1.82	0.27
C12H9NO3	215.0582	8.09	1.00	0.75	0.25
C18H30O5	326.2093	8.02	0.80	1.67	0.28
C10H13NO4	211.0845	8.16	1.00	1.30	0.40
C7H5NO5	183.0168	3.26	1.00	0.71	0.71
C8H14O	126.1045	3.70	1.00	1.75	0.13
C10H18O4	202.1205	2.93	0.50	1.80	0.40
C18H34O5	330.2406	7.45	0.40	1.89	0.28
C13H24O2S2	276.1218	2.75	1.00	1.85	0.15
C2H4O2	60.0211	2.72	0.50	2.00	1.00
C2H4O2	60.0211	0.41	0.50	2.00	1.00
C7H6N2O3	166.0378	3.44	1.00	0.86	0.43
C3H8O4S	140.0143	0.50	0.00	2.67	1.33
C12H25NO5S	295.1453	4.62	0.20	2.08	0.42
C9H20O4S	224.1082	7.68	0.00	2.22	0.44
C11H24O4S	252.1395	8.26	0.00	2.18	0.36
C6H10O2	114.0681	2.71	1.00	1.67	0.33
C8H16O6S	240.0668	2.88	0.17	2.00	0.75
C11H18O6	246.1103	4.34	0.50	1.64	0.55
C9H16O3	172.1099	3.01	0.67	1.78	0.33
C8H18O3S	194.0977	5.22	0.00	2.25	0.38
C4H6O2	86.0368	0.53	1.00	1.50	0.50
C6H10O2	114.0681	1.23	1.00	1.67	0.33
C7H8O4	156.0423	1.01	1.00	1.14	0.57
C9H11NO3	181.0739	7.87	1.00	1.22	0.33
C6H5NO4	155.0219	3.06	1.00	0.83	0.67
C12H22O4	230.1518	3.74	0.50	1.83	0.33
C12H18O5	242.1154	3.06	0.80	1.50	0.42
C8H16O4	176.1049	1.43	0.25	2.00	0.50
C14H13NO3	243.0895	8.30	1.00	0.93	0.21
C8H7NO3	165.0426	3.19	1.00	0.88	0.38
C7H6O3	138.0317	2.77	1.00	0.86	0.43
C7H10O6	190.0477	0.40	0.50	1.43	0.86
C10H12O3	180.0786	3.13	1.00	1.20	0.30
C11H22O4	218.1518	7.55	0.25	2.00	0.36
C9H12O4	184.0736	2.77	1.00	1.33	0.44
C9H12O3	168.0786	2.75	1.00	1.33	0.33
C6H8O3	128.0473	2.34	1.00	1.33	0.50
C15H15NO2S	273.0823	3.70	1.00	1.00	0.13
C6H12O4	148.0736	1.22	0.25	2.00	0.67
C10H11NO5	225.0637	3.53	1.00	1.10	0.50
C13H20O6	272.1260	3.06	0.67	1.54	0.46
C14H5NO2S	251.0041	2.68	1.00	0.36	0.14
C14H27NO4	273.1940	7.78	0.50	1.93	0.29
C7H5NO5	183.0168	2.95	1.00	0.71	0.71
C8H7NO6	213.0273	3.35	1.00	0.88	0.75

Table S4.3.7 Molecular formulas of organic compounds detected in α -pinene SOA in ESI⁻ mode.

Formula [M]	Neutral mass (Da)	RT (min)	MCR	H/C	O/C
C9H14O4	186.0892	2.96	0.75	1.56	0.44
C9H14O4	186.0892	0.37	0.75	1.56	0.44
C8H12O4	172.0736	0.36	0.75	1.50	0.50
C10H16O5	216.0998	3.39	0.60	1.60	0.50
C10H16O4	200.1049	0.37	0.75	1.60	0.40
C10H16O3	184.1099	3.48	1.00	1.60	0.30
C8H12O4	172.0736	2.53	0.75	1.50	0.50
C8H14O4	174.0892	0.36	0.50	1.75	0.50
C10H14O5	214.0841	0.36	0.80	1.40	0.50
C10H16O4	200.1049	2.72	0.75	1.60	0.40
C19H28O7	368.1835	7.21	0.86	1.47	0.37

7 Appendix

C10H14O4	198.0892	0.36	1.00	1.40	0.40
C8H14O3	158.0943	2.92	0.67	1.75	0.38
C8H12O5	188.0685	3.28	0.60	1.50	0.63
C11H18O6	246.1103	2.71	0.50	1.64	0.55
C7H10O4	158.0579	3.37	0.75	1.43	0.57
C9H14O3	170.0943	0.38	1.00	1.56	0.33
C4H4O3	100.0160	0.36	1.00	1.00	0.75
C9H14O3	170.0943	3.09	1.00	1.56	0.33
C4H8O2	88.0524	0.35	0.50	2.00	0.50
C8H12O3	156.0786	0.38	1.00	1.50	0.38
C9H14O3	170.0943	7.71	1.00	1.56	0.33
C11H18O7	262.1053	3.06	0.43	1.64	0.64
C8H14O5	190.0841	2.44	0.40	1.75	0.63
C8H12O3	156.0786	2.87	1.00	1.50	0.38
C18H26O6	338.1729	7.51	1.00	1.44	0.33
C4H6O2	86.0368	0.36	1.00	1.50	0.50
C7H8O4	156.0423	0.36	1.00	1.14	0.57
C10H14O4	198.0892	7.14	1.00	1.40	0.40
C20H32O7	384.2148	6.76	0.71	1.60	0.35
C17H26O8	358.1628	4.90	0.63	1.53	0.47
C20H32O7	384.2148	6.97	0.71	1.60	0.35
C9H14O5	202.0841	1.68	0.60	1.56	0.56
C10H16O5	216.0998	7.76	0.60	1.60	0.50
C20H30O8	398.1941	7.85	0.75	1.50	0.40
C20H32O7	384.2148	8.08	0.71	1.60	0.35
C5H8O2	100.0524	0.36	1.00	1.60	0.40
C6H8O2	112.0524	0.36	1.00	1.33	0.33
C8H12O5	188.0685	2.87	0.60	1.50	0.63
C9H12O4	184.0736	0.36	1.00	1.33	0.44
C7H10O3	142.0630	0.37	1.00	1.43	0.43
C7H14O4	162.0892	2.94	0.25	2.00	0.57
C7H8O3	140.0473	0.37	1.00	1.14	0.43
C19H28O5	336.1937	8.02	1.00	1.47	0.26
C7H12O2	128.0837	0.36	1.00	1.71	0.29
C20H30O8	398.1941	7.52	0.75	1.50	0.40
C19H30O5	338.2093	8.09	1.00	1.58	0.26
C6H10O2	114.0681	0.36	1.00	1.67	0.33
C18H26O8	370.1628	7.72	0.75	1.44	0.44
C10H14O3	182.0943	3.81	1.00	1.40	0.30
C8H14O2	142.0994	0.37	1.00	1.75	0.25
C21H34O9	430.2203	7.13	0.56	1.62	0.43
C20H32O9	416.2046	7.49	0.56	1.60	0.45
C19H30O5	338.2093	6.99	1.00	1.58	0.26
C7H8O3	140.0473	2.99	1.00	1.14	0.43
C3H6O	58.0419	0.37	1.00	2.00	0.33
C8H14O6	206.0790	2.34	0.33	1.75	0.75
C21H34O9	430.2203	7.66	0.56	1.62	0.43
C8H10O4	170.0579	3.27	1.00	1.25	0.50
C19H32O8	388.2097	7.39	0.50	1.68	0.42
C7H14O3	146.0943	2.59	0.33	2.00	0.43
C7H10O2	126.0681	0.36	1.00	1.43	0.29
C19H30O6	354.2042	7.41	0.83	1.58	0.32
C19H28O6	352.1886	7.81	1.00	1.47	0.32
C17H26O8	358.1628	6.30	0.63	1.53	0.47
C8H10O4	170.0579	0.37	1.00	1.25	0.50
C19H32O8	388.2097	7.22	0.50	1.68	0.42
C7H8O2	124.0524	0.37	1.00	1.14	0.29
C9H12O3	168.0786	0.36	1.00	1.33	0.33
C11H16O6	244.0947	3.31	0.67	1.45	0.55
C20H32O11	448.1945	7.53	0.45	1.60	0.55
C21H36O9	432.2359	8.15	0.44	1.71	0.43
C9H12O4	184.0736	2.92	1.00	1.33	0.44
C19H28O6	352.1886	7.53	1.00	1.47	0.32
C16H26O7	330.1679	4.13	0.57	1.63	0.44
C20H32O6	368.2199	8.31	0.83	1.60	0.30
C10H16O7	248.0896	3.00	0.43	1.60	0.70
C19H32O6	356.2199	7.62	0.67	1.68	0.32
C8H12O2	140.0837	0.36	1.00	1.50	0.25
C11H20O8	280.1158	2.47	0.25	1.82	0.73
C18H26O7	354.1679	6.75	0.86	1.44	0.39

7 Appendix

C7H12O5	176.0685	0.89	0.40	1.71	0.71
C18H28O9	388.1733	5.60	0.56	1.56	0.50
C14H20O8	316.1158	3.15	0.63	1.43	0.57
C17H28O5	312.1937	7.47	0.80	1.65	0.29
C19H28O4	320.1988	8.47	1.00	1.47	0.21
C18H28O5	324.1937	7.90	1.00	1.56	0.28
C16H24O8	344.1471	4.73	0.63	1.50	0.50
C16H24O6	312.1573	6.33	0.83	1.50	0.38
C11H18O8	278.1002	3.43	0.38	1.64	0.73
C20H32O6	368.2199	7.78	0.83	1.60	0.30
C16H26O6	314.1729	8.60	0.67	1.63	0.38
C16H28O6	316.1886	8.38	0.50	1.75	0.38
C9H14O5	202.0841	0.36	0.60	1.56	0.56
C10H16O5	216.0998	0.36	0.60	1.60	0.50
C7H10O4	158.0579	0.36	0.75	1.43	0.57
C5H8O3	116.0473	0.36	0.67	1.60	0.60
C5H8O4	132.0423	0.35	0.50	1.60	0.80
C3H4O4	104.0110	0.35	0.50	1.33	1.33
C8H12O5	188.0685	0.36	0.60	1.50	0.63
C8H14O3	158.0943	0.37	0.67	1.75	0.38
C9H16O5	204.0998	0.35	0.40	1.78	0.56
C4H4O4	116.0110	0.36	0.75	1.00	1.00
C4H6O4	118.0266	0.35	0.50	1.50	1.00
C7H12O4	160.0736	0.36	0.50	1.71	0.57
C6H8O4	144.0423	0.36	0.75	1.33	0.67
C4H6O3	102.0317	0.37	0.67	1.50	0.75
C7H10O5	174.0528	0.36	0.60	1.43	0.71
C5H6O4	130.0266	0.36	0.75	1.20	0.80
C6H8O3	128.0473	0.37	1.00	1.33	0.50
C10H18O5	218.1154	0.36	0.40	1.80	0.50
C9H16O4	188.1049	2.99	0.50	1.78	0.44
C7H12O3	144.0786	0.36	0.67	1.71	0.43

Table S4.3.8 Molecular formulas of organic compounds detected in β -pinene SOA in ESI⁻ mode.

Formula [M]	Neutral mass (Da)	RT (min)	MCR	H/C	O/C
C9H14O4	186.0892	2.96	0.75	1.56	0.44
C9H14O4	186.0892	0.37	0.75	1.56	0.44
C8H12O4	172.0736	0.36	0.75	1.50	0.50
C10H16O4	200.1049	0.37	0.75	1.60	0.40
C10H16O3	184.1099	3.48	1.00	1.60	0.30
C8H12O4	172.0736	2.53	0.75	1.50	0.50
C8H14O4	174.0892	0.36	0.50	1.75	0.50
C10H14O5	214.0841	0.36	0.80	1.40	0.50
C10H16O4	200.1049	2.72	0.75	1.60	0.40
C19H28O7	368.1835	7.21	0.86	1.47	0.37
C10H14O4	198.0892	0.36	1.00	1.40	0.40
C8H14O3	158.0943	2.92	0.67	1.75	0.38
C8H12O5	188.0685	3.28	0.60	1.50	0.63
C11H18O6	246.1103	2.71	0.50	1.64	0.55
C4H4O3	100.0160	0.36	1.00	1.00	0.75
C4H8O2	88.0524	0.35	0.50	2.00	0.50
C8H12O3	156.0786	0.38	1.00	1.50	0.38
C8H14O5	190.0841	2.44	0.40	1.75	0.63
C8H12O3	156.0786	2.87	1.00	1.50	0.38
C18H26O6	338.1729	7.51	1.00	1.44	0.33
C4H6O2	86.0368	0.36	1.00	1.50	0.50
C7H8O4	156.0423	0.36	1.00	1.14	0.57
C17H26O8	358.1628	4.90	0.63	1.53	0.47
C20H30O8	398.1941	7.85	0.75	1.50	0.40
C20H32O7	384.2148	8.08	0.71	1.60	0.35
C5H8O2	100.0524	0.36	1.00	1.60	0.40
C6H8O2	112.0524	0.36	1.00	1.33	0.33
C9H12O4	184.0736	0.36	1.00	1.33	0.44
C7H10O3	142.0630	0.37	1.00	1.43	0.43

7 Appendix

C7H14O4	162.0892	2.94	0.25	2.00	0.57
C7H8O3	140.0473	0.37	1.00	1.14	0.43
C19H28O5	336.1937	8.02	1.00	1.47	0.26
C7H12O2	128.0837	0.36	1.00	1.71	0.29
C19H30O5	338.2093	8.09	1.00	1.58	0.26
C6H10O2	114.0681	0.36	1.00	1.67	0.33
C18H26O8	370.1628	7.72	0.75	1.44	0.44
C8H14O2	142.0994	0.37	1.00	1.75	0.25
C19H30O5	338.2093	6.99	1.00	1.58	0.26
C7H8O3	140.0473	2.99	1.00	1.14	0.43
C3H6O	58.0419	0.37	1.00	2.00	0.33
C8H14O6	206.0790	2.34	0.33	1.75	0.75
C19H32O8	388.2097	7.39	0.50	1.68	0.42
C7H14O3	146.0943	2.59	0.33	2.00	0.43
C7H10O2	126.0681	0.36	1.00	1.43	0.29
C19H30O6	354.2042	7.41	0.83	1.58	0.32
C19H28O6	352.1886	7.81	1.00	1.47	0.32
C17H26O8	358.1628	6.30	0.63	1.53	0.47
C8H10O4	170.0579	0.37	1.00	1.25	0.50
C9H12O3	168.0786	0.36	1.00	1.33	0.33
C11H16O6	244.0947	3.31	0.67	1.45	0.55
C9H12O4	184.0736	2.92	1.00	1.33	0.44
C16H26O7	330.1679	4.13	0.57	1.63	0.44
C8H12O2	140.0837	0.36	1.00	1.50	0.25
C7H12O5	176.0685	0.89	0.40	1.71	0.71
C14H20O8	316.1158	3.15	0.63	1.43	0.57
C17H28O5	312.1937	7.47	0.80	1.65	0.29
C18H28O5	324.1937	7.90	1.00	1.56	0.28
C16H24O8	344.1471	4.73	0.63	1.50	0.50
C16H24O6	312.1573	6.33	0.83	1.50	0.38
C11H18O8	278.1002	3.43	0.38	1.64	0.73
C16H26O6	314.1729	8.60	0.67	1.63	0.38
C16H28O6	316.1886	8.38	0.50	1.75	0.38
C8H12O4	172.0736	2.76	0.75	1.50	0.50
C20H32O9	416.2046	7.67	0.56	1.60	0.45
C8H12O5	188.0685	8.28	0.60	1.50	0.63
C8H12O4	172.0736	8.54	0.75	1.50	0.50
C9H14O4	186.0892	8.24	0.75	1.56	0.44
C14H20O7	300.1209	7.62	0.71	1.43	0.50
C18H30O9	390.1890	7.36	0.44	1.67	0.50
C18H28O6	340.1886	7.52	0.83	1.56	0.33
C7H10O5	174.0528	8.25	0.60	1.43	0.71
C19H30O6	354.2042	7.22	0.83	1.58	0.32
C18H28O5	324.1937	7.37	1.00	1.56	0.28
C9H14O3	170.0943	7.94	1.00	1.56	0.33
C10H18O6	234.1103	6.07	0.33	1.80	0.60
C6H10O3	130.0630	8.23	0.67	1.67	0.50
C4H6O4	118.0266	8.20	0.50	1.50	1.00
C5H8O3	116.0473	8.22	0.67	1.60	0.60
C19H32O6	356.2199	8.17	0.67	1.68	0.32
C17H26O7	342.1679	7.49	0.71	1.53	0.41
C9H14O3	170.0943	3.11	1.00	1.56	0.33
C20H32O10	432.1995	8.24	0.50	1.60	0.50
C8H14O6	206.0790	8.27	0.33	1.75	0.75
C7H10O4	158.0579	1.88	0.75	1.43	0.57
C6H8O4	144.0423	3.42	0.75	1.33	0.67
C9H14O3	170.0943	0.39	1.00	1.56	0.33
C7H12O3	144.0786	8.33	0.67	1.71	0.43
C6H10O2	114.0681	8.43	1.00	1.67	0.33
C8H14O4	174.0892	3.46	0.50	1.75	0.50
C6H8O3	128.0473	8.30	1.00	1.33	0.50
C5H8O2	100.0524	3.42	1.00	1.60	0.40
C9H14O5	202.0841	2.51	0.60	1.56	0.56
C7H12O3	144.0786	3.27	0.67	1.71	0.43
C8H14O6	206.0790	3.15	0.33	1.75	0.75
C19H32O8	388.2097	7.61	0.50	1.68	0.42
C10H16O5	216.0998	3.04	0.60	1.60	0.50
C10H14O6	230.0790	0.35	0.67	1.40	0.60
C10H18O6	234.1103	7.98	0.33	1.80	0.60
C19H32O7	372.2148	8.31	0.57	1.68	0.37

7 Appendix

C8H14O4	174.0892	8.63	0.50	1.75	0.50
C17H26O8	358.1628	3.15	0.63	1.53	0.47
C17H26O8	358.1628	8.22	0.63	1.53	0.47
C7H12O5	176.0685	7.96	0.40	1.71	0.71
C6H10O5	162.0528	0.62	0.40	1.67	0.83
C6H10O5	162.0528	8.73	0.40	1.67	0.83
C13H22O6	274.1416	7.78	0.50	1.69	0.46
C19H32O6	356.2199	7.93	0.67	1.68	0.32
C15H24O7	316.1522	6.71	0.57	1.60	0.47
C20H30O9	414.1890	7.27	0.67	1.50	0.45
C19H32O8	388.2097	7.87	0.50	1.68	0.42
C7H10O3	142.0630	8.23	1.00	1.43	0.43
C20H30O7	382.1992	8.21	0.86	1.50	0.35
C16H26O10	378.1526	4.35	0.40	1.63	0.63
C19H32O7	372.2148	7.98	0.57	1.68	0.37
C8H14O5	190.0841	1.50	0.40	1.75	0.63
C19H30O5	338.2093	8.43	1.00	1.58	0.26
C18H30O6	342.2042	8.32	0.67	1.67	0.33
C20H32O9	416.2046	3.90	0.56	1.60	0.45
C13H20O7	288.1209	8.11	0.57	1.54	0.54
C10H14O4	198.0892	8.17	1.00	1.40	0.40
C11H20O6	248.1260	3.09	0.33	1.82	0.55
C11H20O7	264.1209	2.61	0.29	1.82	0.64
C9H14O5	202.0841	0.36	0.60	1.56	0.56
C10H16O5	216.0998	0.36	0.60	1.60	0.50
C7H10O4	158.0579	0.36	0.75	1.43	0.57
C5H8O3	116.0473	0.36	0.67	1.60	0.60
C5H8O4	132.0423	0.35	0.50	1.60	0.80
C3H4O4	104.0110	0.35	0.50	1.33	1.33
C8H12O5	188.0685	0.36	0.60	1.50	0.63
C8H14O3	158.0943	0.37	0.67	1.75	0.38
C9H16O5	204.0998	0.35	0.40	1.78	0.56
C4H4O4	116.0110	0.36	0.75	1.00	1.00
C3H6O3	90.0317	0.36	0.33	2.00	1.00
C4H6O4	118.0266	0.35	0.50	1.50	1.00
C7H12O4	160.0736	0.36	0.50	1.71	0.57
C6H8O4	144.0423	0.36	0.75	1.33	0.67
C4H6O3	102.0317	0.37	0.67	1.50	0.75
C2H4O3	76.0160	0.34	0.33	2.00	1.50
C7H10O5	174.0528	0.36	0.60	1.43	0.71
C5H6O4	130.0266	0.36	0.75	1.20	0.80
C6H10O4	146.0579	0.36	0.50	1.67	0.67
C6H8O3	128.0473	0.37	1.00	1.33	0.50
C10H18O5	218.1154	0.36	0.40	1.80	0.50
C7H12O3	144.0786	0.36	0.67	1.71	0.43
C8H14O4	174.0892	3.21	0.50	1.75	0.50

Table S4.3.9 Molecular formulas of organic compounds detected in limonene SOA in ESI⁻ mode.

Formula [M]	Neutral mass (Da)	RT (min)	MCR	H/C	O/C
C9H14O4	186.0892	0.37	0.75	1.56	0.44
C8H12O4	172.0736	0.36	0.75	1.50	0.50
C10H16O4	200.1049	0.37	0.75	1.60	0.40
C8H14O4	174.0892	0.36	0.50	1.75	0.50
C10H14O5	214.0841	0.36	0.80	1.40	0.50
C10H14O4	198.0892	0.36	1.00	1.40	0.40
C8H14O3	158.0943	2.92	0.67	1.75	0.38
C8H12O5	188.0685	3.28	0.60	1.50	0.63
C11H18O6	246.1103	2.71	0.50	1.64	0.55
C7H10O4	158.0579	3.37	0.75	1.43	0.57
C4H4O3	100.0160	0.36	1.00	1.00	0.75
C4H8O2	88.0524	0.35	0.50	2.00	0.50
C8H12O3	156.0786	0.38	1.00	1.50	0.38
C9H14O3	170.0943	7.71	1.00	1.56	0.33
C18H26O6	338.1729	7.51	1.00	1.44	0.33

7 Appendix

C4H6O2	86.0368	0.36	1.00	1.50	0.50
C7H8O4	156.0423	0.36	1.00	1.14	0.57
C20H30O8	398.1941	7.85	0.75	1.50	0.40
C20H32O7	384.2148	8.08	0.71	1.60	0.35
C5H8O2	100.0524	0.36	1.00	1.60	0.40
C6H8O2	112.0524	0.36	1.00	1.33	0.33
C9H12O4	184.0736	0.36	1.00	1.33	0.44
C7H10O3	142.0630	0.37	1.00	1.43	0.43
C7H8O3	140.0473	0.37	1.00	1.14	0.43
C19H28O5	336.1937	8.02	1.00	1.47	0.26
C7H12O2	128.0837	0.36	1.00	1.71	0.29
C19H30O5	338.2093	8.09	1.00	1.58	0.26
C6H10O2	114.0681	0.36	1.00	1.67	0.33
C18H26O8	370.1628	7.72	0.75	1.44	0.44
C8H14O2	142.0994	0.37	1.00	1.75	0.25
C3H6O	58.0419	0.37	1.00	2.00	0.33
C7H10O2	126.0681	0.36	1.00	1.43	0.29
C19H28O6	352.1886	7.81	1.00	1.47	0.32
C17H26O8	358.1628	6.30	0.63	1.53	0.47
C8H10O4	170.0579	0.37	1.00	1.25	0.50
C7H8O2	124.0524	0.37	1.00	1.14	0.29
C9H12O3	168.0786	0.36	1.00	1.33	0.33
C20H32O6	368.2199	8.31	0.83	1.60	0.30
C19H32O6	356.2199	7.62	0.67	1.68	0.32
C8H12O2	140.0837	0.36	1.00	1.50	0.25
C11H20O8	280.1158	2.47	0.25	1.82	0.73
C18H28O5	324.1937	7.90	1.00	1.56	0.28
C20H32O6	368.2199	7.78	0.83	1.60	0.30
C20H32O9	416.2046	7.67	0.56	1.60	0.45
C18H28O6	340.1886	7.52	0.83	1.56	0.33
C7H10O5	174.0528	8.25	0.60	1.43	0.71
C19H30O6	354.2042	7.22	0.83	1.58	0.32
C9H14O3	170.0943	0.39	1.00	1.56	0.33
C19H32O8	388.2097	7.61	0.50	1.68	0.42
C10H14O6	230.0790	0.35	0.67	1.40	0.60
C17H26O8	358.1628	3.15	0.63	1.53	0.47
C6H10O5	162.0528	0.62	0.40	1.67	0.83
C20H30O7	382.1992	8.21	0.86	1.50	0.35
C10H14O4	198.0892	8.17	1.00	1.40	0.40
C11H20O6	248.1260	3.09	0.33	1.82	0.55
C11H20O7	264.1209	2.61	0.29	1.82	0.64
C9H14O4	186.0892	3.25	0.75	1.56	0.44
C10H16O4	200.1049	3.04	0.75	1.60	0.40
C10H16O3	184.1099	3.89	1.00	1.60	0.30
C19H30O5	338.2093	7.48	1.00	1.58	0.26
C8H12O3	156.0786	2.62	1.00	1.50	0.38
C10H14O4	198.0892	2.92	1.00	1.40	0.40
C10H14O4	198.0892	7.64	1.00	1.40	0.40
C10H16O5	216.0998	2.57	0.60	1.60	0.50
C10H14O4	198.0892	8.55	1.00	1.40	0.40
C9H16O4	188.1049	3.31	0.50	1.78	0.44
C8H14O2	142.0994	3.25	1.00	1.75	0.25
C10H18O6	234.1103	3.54	0.33	1.80	0.60
C8H12O5	188.0685	1.39	0.60	1.50	0.63
C11H20O5	232.1311	3.88	0.40	1.82	0.45
C10H14O6	230.0790	3.15	0.67	1.40	0.60
C9H14O5	202.0841	0.36	0.60	1.56	0.56
C10H16O5	216.0998	0.36	0.60	1.60	0.50
C7H10O4	158.0579	0.36	0.75	1.43	0.57
C5H8O3	116.0473	0.36	0.67	1.60	0.60
C5H8O4	132.0423	0.35	0.50	1.60	0.80
C3H4O4	104.0110	0.35	0.50	1.33	1.33
C8H12O5	188.0685	0.36	0.60	1.50	0.63
C8H14O3	158.0943	0.37	0.67	1.75	0.38
C9H16O5	204.0998	0.35	0.40	1.78	0.56
C4H6O4	118.0266	0.35	0.50	1.50	1.00
C7H12O4	160.0736	0.36	0.50	1.71	0.57
C6H8O4	144.0423	0.36	0.75	1.33	0.67
C4H6O3	102.0317	0.37	0.67	1.50	0.75
C7H10O5	174.0528	0.36	0.60	1.43	0.71

7 Appendix

C5H6O4	130.0266	0.36	0.75	1.20	0.80
C6H10O4	146.0579	0.36	0.50	1.67	0.67
C6H8O3	128.0473	0.37	1.00	1.33	0.50
C10H18O5	218.1154	0.36	0.40	1.80	0.50
C7H12O3	144.0786	0.36	0.67	1.71	0.43
C8H14O4	174.0892	3.21	0.50	1.75	0.50

Table S4.3.10 Molecular formulas of organic compounds detected in isoprene SOA in ESI⁻ mode.

Formula [M]	Neutral mass (Da)	RT (min)	MCR	H/C	O/C
C6H14O7	198.0740	0.39	0.00	2.33	1.17
C6H14O6	182.0790	0.37	0.00	2.33	1.00
C5H6O3	114.0317	0.66	1.00	1.20	0.60
C6H14O8	214.0689	0.39	0.00	2.33	1.33
C3H6O2	74.0368	0.40	0.50	2.00	0.67
C5H6O4	130.0266	0.38	0.75	1.20	0.80
C5H8O4	132.0423	0.40	0.50	1.60	0.80
C4H6O3	102.0317	0.43	0.67	1.50	0.75
C2H2O4	89.9953	2.07	0.50	1.00	2.00
C4H6O5	134.0215	0.38	0.40	1.50	1.25
C6H10O5	162.0528	0.48	0.40	1.67	0.83
C3H4O3	88.0160	0.37	0.67	1.33	1.00
C3H4O2	72.0211	0.38	1.00	1.33	0.67
C5H6O5	146.0215	0.38	0.60	1.20	1.00
C4H6O2	86.0368	0.86	1.00	1.50	0.50
C5H8O4	132.0423	1.18	0.50	1.60	0.80
C4H8O2	88.0524	0.48	0.50	2.00	0.50
C6H10O5	162.0528	0.82	0.40	1.67	0.83
C4H6O2	86.0368	0.39	1.00	1.50	0.50
C14H6O2	206.0368	0.38	1.00	0.43	0.14
C5H12O4	136.0736	0.36	0.00	2.40	0.80
C5H12O5	152.0685	0.37	0.00	2.40	1.00
C17H26O4	294.1831	8.05	1.00	1.53	0.24
C7H16O7	212.0896	0.36	0.00	2.29	1.00
C11H22O8	282.1315	2.74	0.13	2.00	0.73
C5H12O6	168.0634	0.39	0.00	2.40	1.20
C11H22O8	282.1315	0.95	0.13	2.00	0.73
C4H8O3	104.0473	0.58	0.33	2.00	0.75
C14H6O	190.0419	0.40	1.00	0.43	0.07
C8H12O3	156.0786	2.61	1.00	1.50	0.38
C5H12O7	184.0583	0.46	0.00	2.40	1.40
C5H8O3	116.0473	0.81	0.67	1.60	0.60
C9H14O4	186.0892	2.51	0.75	1.56	0.44
C2H4O2	60.0211	0.39	0.50	2.00	1.00
C5H8O3	116.0473	0.38	0.67	1.60	0.60
C6H8O5	160.0372	0.63	0.60	1.33	0.83
C2H2O3	74.0004	0.37	0.67	1.00	1.50
C7H12O5	176.0685	1.48	0.40	1.71	0.71
C5H4O4	128.0110	0.39	1.00	0.80	0.80
C11H22O8	282.1315	2.38	0.13	2.00	0.73
C5H12O4	136.0736	2.73	0.00	2.40	0.80
C4H6O3	102.0317	2.76	0.67	1.50	0.75
C7H12O5	176.0685	2.47	0.40	1.71	0.71
C14H22O4	254.1518	7.79	1.00	1.57	0.29
C4H6O	70.0419	0.73	1.00	1.50	0.25
C7H12O4	160.0736	3.00	0.50	1.71	0.57
C6H8O4	144.0423	0.96	0.75	1.33	0.67
C13H4O	176.0262	0.35	1.00	0.31	0.08
C5H10O3	118.0630	0.82	0.33	2.00	0.60
C5H12O4	136.0736	2.52	0.00	2.40	0.80
C8H12O4	172.0736	1.47	0.75	1.50	0.50
C10H14O5	214.0841	2.73	0.80	1.40	0.50
C8H16O8	240.0845	0.74	0.13	2.00	1.00
C2H4O2	60.0211	0.63	0.50	2.00	1.00
C11H20O8	280.1158	1.23	0.25	1.82	0.73

7 Appendix

C7H10O5	174.0528	0.82	0.60	1.43	0.71
C7H8O5	172.0372	0.38	0.80	1.14	0.71
C13H20O2	208.1463	7.99	1.00	1.54	0.15
C6H12O5	164.0685	0.97	0.20	2.00	0.83
C10H12O4	196.0736	2.80	1.00	1.20	0.40
C5H4O3	112.0160	3.22	1.00	0.80	0.60
C10H18O9	282.0951	1.14	0.22	1.80	0.90
C10H18O8	266.1002	0.78	0.25	1.80	0.80
C3H6O2	74.0368	2.88	0.50	2.00	0.67
C10H16O5	216.0998	3.74	0.60	1.60	0.50
C11H20O10	312.1056	0.87	0.20	1.82	0.91
C3H6O2	74.0368	2.53	0.50	2.00	0.67
C12H22O9	310.1264	3.02	0.22	1.83	0.75
C6H8O6	176.0321	1.09	0.50	1.33	1.00
C11H22O9	298.1264	0.63	0.11	2.00	0.82
C4H8O2	88.0524	3.00	0.50	2.00	0.50
C3H6O	58.0419	0.45	1.00	2.00	0.33
C9H10O4	182.0579	2.69	1.00	1.11	0.44
C4H6O3	102.0317	6.20	0.67	1.50	0.75
C10H16O7	248.0896	3.02	0.43	1.60	0.70
C9H16O6	220.0947	2.89	0.33	1.78	0.67
C4H4O3	100.0160	0.43	1.00	1.00	0.75
C8H12O7	220.0583	1.65	0.43	1.50	0.88
C9H14O5	202.0841	2.98	0.60	1.56	0.56
C10H18O6	234.1103	2.74	0.33	1.80	0.60
C9H16O6	220.0947	0.69	0.33	1.78	0.67
C11H22O7	266.1366	2.54	0.14	2.00	0.64
C8H12O5	188.0685	2.53	0.60	1.50	0.63
C4H6O	70.0419	0.40	1.00	1.50	0.25
C7H10O3	142.0630	1.44	1.00	1.43	0.43
C7H10O7	206.0427	0.93	0.43	1.43	1.00
C10H14O6	230.0790	3.05	0.67	1.40	0.60
C10H20O6	236.1260	2.78	0.17	2.00	0.60
C9H18O8	254.1002	0.81	0.13	2.00	0.89
C7H10O6	190.0477	2.11	0.50	1.43	0.86
C5H10O2	102.0681	2.83	0.50	2.00	0.40
C23H28O8	432.1784	8.02	1.00	1.22	0.35
C11H22O9	298.1264	2.55	0.11	2.00	0.82
C9H14O7	234.0740	2.70	0.43	1.56	0.78
C9H18O3	174.1256	7.51	0.33	2.00	0.33
C4H10O7	170.0427	0.39	0.00	2.50	1.75
C7H8O5	172.0372	1.23	0.80	1.14	0.71
C7H8O3	140.0473	0.05	1.00	1.14	0.43
C8H12O5	188.0685	0.83	0.60	1.50	0.63
C11H18O8	278.1002	2.51	0.38	1.64	0.73
C7H12O3	144.0786	0.07	0.67	1.71	0.43
C3H4O2	72.0211	2.90	1.00	1.33	0.67
C16H28O11	396.1632	2.89	0.27	1.75	0.69
C9H16O7	236.0896	0.91	0.29	1.78	0.78
C6H6O5	158.0215	0.38	0.80	1.00	0.83
C3H4O	56.0262	0.38	1.00	1.33	0.33
C9H18O8	254.1002	2.79	0.13	2.00	0.89
C8H16O5	192.0998	0.90	0.20	2.00	0.63
C11H22O9	298.1264	2.82	0.11	2.00	0.82
C6H12O4	148.0736	0.56	0.25	2.00	0.67
C10H16O5	216.0998	2.85	0.60	1.60	0.50
C8H12O6	204.0634	2.68	0.50	1.50	0.75
C6H14O5	166.0841	0.40	0.00	2.33	0.83
C4H4O2	84.0211	0.38	1.00	1.00	0.50
C7H12O5	176.0685	1.84	0.40	1.71	0.71
C11H18O9	294.0951	1.09	0.33	1.64	0.82
C8H14O5	190.0841	0.89	0.40	1.75	0.63
C8H14O5	190.0841	0.83	0.40	1.75	0.63
C5H4O3	112.0160	0.39	1.00	0.80	0.60
C9H14O5	202.0841	1.09	0.60	1.56	0.56
C14H26O10	354.1526	2.88	0.20	1.86	0.71
C16H30O11	398.1788	2.89	0.18	1.88	0.69
C5H10O2	102.0681	0.68	0.50	2.00	0.40
C11H22O3	202.1569	7.00	0.33	2.00	0.27
C6H14O7	198.0740	2.42	0.00	2.33	1.17

7 Appendix

C9H12O5	200.0685	2.79	0.80	1.33	0.56
C9H16O4	188.1049	2.60	0.50	1.78	0.44
C8H12O3	156.0786	2.90	1.00	1.50	0.38
C6H12O5	164.0685	2.99	0.20	2.00	0.83
C11H18O8	278.1002	0.69	0.38	1.64	0.73
C7H8O4	156.0423	1.04	1.00	1.14	0.57
C8H10O4	170.0579	1.95	1.00	1.25	0.50
C16H28O11	396.1632	2.68	0.27	1.75	0.69
C9H18O3	174.1256	5.23	0.33	2.00	0.33
C6H6O4	142.0266	0.40	1.00	1.00	0.67
C5H6O2	98.0368	0.39	1.00	1.20	0.40
C11H22O10	314.1213	0.94	0.10	2.00	0.91
C10H18O7	250.1053	2.55	0.29	1.80	0.70
C5H8O2	100.0524	0.41	1.00	1.60	0.40
C7H16O8	228.0845	0.78	0.00	2.29	1.14
C12H22O9	310.1264	2.45	0.22	1.83	0.75
C8H6O3	150.0317	3.86	1.00	0.75	0.38
C10H16O6	232.0947	0.69	0.50	1.60	0.60
C9H10O3	166.0630	4.15	1.00	1.11	0.33
C12H20O9	308.1107	2.74	0.33	1.67	0.75
C4H10O5	138.0528	0.47	0.00	2.50	1.25
C10H20O7	252.1209	0.98	0.14	2.00	0.70
C16H28O10	380.1682	2.95	0.30	1.75	0.63
C6H14O8	214.0689	0.94	0.00	2.33	1.33
C16H30O11	398.1788	2.64	0.18	1.88	0.69
C8H10O4	170.0579	1.23	1.00	1.25	0.50
C14H28O3	244.2038	8.63	0.33	2.00	0.21
C7H12O8	224.0532	0.73	0.25	1.71	1.14
C9H8O4	180.0423	0.14	1.00	0.89	0.44
C11H24O9	300.1420	2.43	0.00	2.18	0.82
C6H12O7	196.0583	0.98	0.14	2.00	1.17
C10H22O9	286.1264	0.73	0.00	2.20	0.90
C13H24O10	340.1369	2.75	0.20	1.85	0.77
C4H6O	70.0419	2.95	1.00	1.50	0.25
C19H16O3	292.1099	0.41	1.00	0.84	0.16
C9H16O4	188.1049	3.30	0.50	1.78	0.44
C6H6O4	142.0266	1.38	1.00	1.00	0.67
C8H10O4	170.0579	2.63	1.00	1.25	0.50
C11H18O7	262.1053	1.12	0.43	1.64	0.64
C11H24O9	300.1420	1.35	0.00	2.18	0.82
C6H10O5	162.0528	2.74	0.40	1.67	0.83
C10H20O3	188.1412	7.98	0.33	2.00	0.30
C14H24O10	352.1369	2.69	0.30	1.71	0.71
C4H4O5	132.0059	0.37	0.60	1.00	1.25
C10H20O9	284.1107	0.88	0.11	2.00	0.90
C11H18O9	294.0951	2.46	0.33	1.64	0.82
C14H26O10	354.1526	2.58	0.20	1.86	0.71
C3H6O	58.0419	2.56	1.00	2.00	0.33
C4H8O5	136.0372	6.58	0.20	2.00	1.25
C7H8O4	156.0423	0.66	1.00	1.14	0.57
C2H2O2	58.0055	0.37	1.00	1.00	1.00
C5H6O5	146.0215	0.94	0.60	1.20	1.00
C10H18O8	266.1002	1.56	0.25	1.80	0.80
C14H28O12	388.1581	0.61	0.08	2.00	0.86
C4H10O6	154.0477	0.35	0.00	2.50	1.50
C11H22O7	266.1366	0.64	0.14	2.00	0.64
C10H18O6	234.1103	1.32	0.33	1.80	0.60
C7H10O6	190.0477	2.37	0.50	1.43	0.86
C4H8O	72.0575	0.41	1.00	2.00	0.25
C10H14O8	262.0689	1.63	0.50	1.40	0.80
C8H14O6	206.0790	2.31	0.33	1.75	0.75
C9H14O8	250.0689	1.20	0.38	1.56	0.89
C11H18O9	294.0951	2.62	0.33	1.64	0.82
C2H4O2	60.0211	3.63	0.50	2.00	1.00
C8H10O5	186.0528	0.72	0.80	1.25	0.63
C9H12O5	200.0685	0.83	0.80	1.33	0.56
C9H12O4	184.0736	2.19	1.00	1.33	0.44
C7H12O6	192.0634	1.20	0.33	1.71	0.86
C7H8O6	188.0321	0.74	0.67	1.14	0.86
C12H22O9	310.1264	0.91	0.22	1.83	0.75

7 Appendix

C11H24O8	284.1471	0.85	0.00	2.18	0.73
C4H4O	68.0262	0.39	1.00	1.00	0.25
C10H18O6	234.1103	0.62	0.33	1.80	0.60
C14H24O9	336.1420	2.56	0.33	1.71	0.64
C8H10O3	154.0630	0.03	1.00	1.25	0.38
C8H12O8	236.0532	0.97	0.38	1.50	1.00
C12H22O10	326.1213	2.28	0.20	1.83	0.83
C6H8O2	112.0524	1.09	1.00	1.33	0.33
C10H14O6	230.0790	0.75	0.67	1.40	0.60
C10H16O5	216.0998	1.05	0.60	1.60	0.50
C12H20O9	308.1107	0.84	0.33	1.67	0.75
C6H12O8	212.0532	2.36	0.13	2.00	1.33
C9H12O5	200.0685	1.23	0.80	1.33	0.56
C11H22O7	266.1366	2.13	0.14	2.00	0.64
C6H14O8	214.0689	2.35	0.00	2.33	1.33
C3H6O	58.0419	1.40	1.00	2.00	0.33
C4H4O	68.0262	0.73	1.00	1.00	0.25
C16H32O2	256.2402	9.24	0.50	2.00	0.13
C2H4O3	76.0160	0.38	0.33	2.00	1.50
C4H6O4	118.0266	0.56	0.50	1.50	1.00
C5H8O5	148.0372	0.43	0.40	1.60	1.00
C3H6O4	106.0266	0.37	0.25	2.00	1.33
C3H4O4	104.0110	0.38	0.50	1.33	1.33
C5H6O4	130.0266	0.63	0.75	1.20	0.80
C6H8O4	144.0423	0.66	0.75	1.33	0.67
C4H4O4	116.0110	0.41	0.75	1.00	1.00
C7H12O4	160.0736	0.93	0.50	1.71	0.57
C8H12O4	172.0736	2.54	0.75	1.50	0.50

Table S4.3.11 Molecular formulas of organic compounds detected in naphthalene SOA in ESI⁻ mode.

Formula [M]	Neutral mass (Da)	RT (min)	MCR	H/C	O/C
C5H6O3	114.0317	0.66	1.00	1.20	0.60
C3H6O2	74.0368	0.40	0.50	2.00	0.67
C5H6O4	130.0266	0.38	0.75	1.20	0.80
C5H8O4	132.0423	0.40	0.50	1.60	0.80
C4H6O3	102.0317	0.43	0.67	1.50	0.75
C4H6O5	134.0215	0.38	0.40	1.50	1.25
C6H10O5	162.0528	0.48	0.40	1.67	0.83
C3H4O3	88.0160	0.37	0.67	1.33	1.00
C3H4O2	72.0211	0.38	1.00	1.33	0.67
C5H6O5	146.0215	0.38	0.60	1.20	1.00
C4H6O2	86.0368	0.39	1.00	1.50	0.50
C17H26O4	294.1831	8.05	1.00	1.53	0.24
C2H4O2	60.0211	0.39	0.50	2.00	1.00
C5H8O3	116.0473	0.38	0.67	1.60	0.60
C2H2O3	74.0004	0.37	0.67	1.00	1.50
C5H4O4	128.0110	0.39	1.00	0.80	0.80
C7H12O4	160.0736	3.00	0.50	1.71	0.57
C7H10O5	174.0528	0.82	0.60	1.43	0.71
C7H8O5	172.0372	0.38	0.80	1.14	0.71
C13H20O2	208.1463	7.99	1.00	1.54	0.15
C3H6O	58.0419	0.45	1.00	2.00	0.33
C9H10O4	182.0579	2.69	1.00	1.11	0.44
C4H4O3	100.0160	0.43	1.00	1.00	0.75
C4H6O	70.0419	0.40	1.00	1.50	0.25
C23H28O8	432.1784	8.02	1.00	1.22	0.35
C7H8O5	172.0372	1.23	0.80	1.14	0.71
C3H4O2	72.0211	2.90	1.00	1.33	0.67
C6H6O5	158.0215	0.38	0.80	1.00	0.83
C3H4O	56.0262	0.38	1.00	1.33	0.33
C4H4O2	84.0211	0.38	1.00	1.00	0.50
C5H4O3	112.0160	0.39	1.00	0.80	0.60
C11H22O3	202.1569	7.00	0.33	2.00	0.27
C6H6O4	142.0266	0.40	1.00	1.00	0.67

7 Appendix

C5H6O2	98.0368	0.39	1.00	1.20	0.40
C5H8O2	100.0524	0.41	1.00	1.60	0.40
C10H20O3	188.1412	7.98	0.33	2.00	0.30
C4H4O5	132.0059	0.37	0.60	1.00	1.25
C2H2O2	58.0055	0.37	1.00	1.00	1.00
C8H10O5	186.0528	0.72	0.80	1.25	0.63
C4H4O	68.0262	0.39	1.00	1.00	0.25
C4H4O	68.0262	0.73	1.00	1.00	0.25
C8H6O4	166.0266	2.62	1.00	0.75	0.50
C8H6O3	150.0317	2.68	1.00	0.75	0.38
C7H6O3	138.0317	3.59	1.00	0.86	0.43
C9H8O4	180.0423	3.33	1.00	0.89	0.44
C10H8O4	192.0423	3.13	1.00	0.80	0.40
C9H8O3	164.0473	3.10	1.00	0.89	0.33
C10H8O5	208.0372	3.30	1.00	0.80	0.50
C9H6O4	178.0266	2.92	1.00	0.67	0.44
C9H8O5	196.0372	2.81	1.00	0.89	0.56
C9H8O3	164.0473	2.54	1.00	0.89	0.33
C7H6O4	154.0266	2.66	1.00	0.86	0.57
C10H8O4	192.0423	3.83	1.00	0.80	0.40
C7H6O3	138.0317	2.83	1.00	0.86	0.43
C9H6O3	162.0317	2.49	1.00	0.67	0.33
C9H8O2	148.0524	3.13	1.00	0.89	0.22
C9H6O5	194.0215	2.70	1.00	0.67	0.56
C9H18O3	174.1256	6.95	0.33	2.00	0.33
C6H10O4	146.0579	1.78	0.50	1.67	0.67
C10H10O6	226.0477	2.49	1.00	1.00	0.60
C9H8O4	180.0423	1.45	1.00	0.89	0.44
C9H6O5	194.0215	0.87	1.00	0.67	0.56
C10H8O5	208.0372	2.42	1.00	0.80	0.50
C8H6O5	182.0215	1.16	1.00	0.75	0.63
C6H8O5	160.0372	1.03	0.60	1.33	0.83
C8H6O2	134.0368	1.94	1.00	0.75	0.25
C3H4O5	120.0059	0.42	0.40	1.33	1.67
C7H6O	106.0419	2.68	1.00	0.86	0.14
C6H6O3	126.0317	0.38	1.00	1.00	0.50
C7H6O4	154.0266	2.20	1.00	0.86	0.57
C10H8O3	176.0473	3.50	1.00	0.80	0.30
C5H4O3	112.0160	2.93	1.00	0.80	0.60
C8H8O	120.0575	3.10	1.00	1.00	0.13
C9H8O5	196.0372	0.83	1.00	0.89	0.56
C6H4O5	156.0059	0.75	1.00	0.67	0.83
C9H6O4	178.0266	0.83	1.00	0.67	0.44
C8H6O5	182.0215	2.01	1.00	0.75	0.63
C10H8O7	240.0270	0.62	1.00	0.80	0.70
C9H6O3	162.0317	3.06	1.00	0.67	0.33
C9H6O3	162.0317	3.31	1.00	0.67	0.33
C5H6O	82.0419	0.38	1.00	1.20	0.20
C9H10O2	150.0681	0.10	1.00	1.11	0.22
C8H6O6	198.0164	0.99	1.00	0.75	0.75
C11H12O7	256.0583	2.25	0.86	1.09	0.64
C12H24O3	216.1725	8.32	0.33	2.00	0.25
C9H8O5	196.0372	1.83	1.00	0.89	0.56
C5H6O2	98.0368	0.69	1.00	1.20	0.40
C10H10O5	210.0528	1.66	1.00	1.00	0.50
C8H8O	120.0575	2.53	1.00	1.00	0.13
C8H8O4	168.0423	1.14	1.00	1.00	0.50
C11H14O6	242.0790	0.63	0.83	1.27	0.55
C10H10O4	194.0579	1.24	1.00	1.00	0.40
C2H2O4	89.9953	0.37	0.50	1.00	2.00
C3H2O5	117.9902	0.36	0.60	0.67	1.67
C10H6O4	190.0266	3.25	1.00	0.60	0.40
C3H2O4	101.9953	0.34	0.75	0.67	1.33
C6H6O8	206.0063	0.36	0.50	1.00	1.33
C5H4O5	144.0059	0.36	0.80	0.80	1.00
C10H6O5	206.0215	2.88	1.00	0.60	0.50
C6H6O7	190.0114	0.36	0.57	1.00	1.17
C7H6O2	122.0368	2.71	1.00	0.86	0.29
C4H6O4	118.0266	0.36	0.50	1.50	1.00
C8H8O8	232.0219	0.36	0.63	1.00	1.00

7 Appendix

C7H8O7	204.0270	0.36	0.57	1.14	1.00
C8H6O5	182.0215	0.96	1.00	0.75	0.63
C6H4O6	172.0008	0.38	0.83	0.67	1.00
C8H6O4	166.0266	2.13	1.00	0.75	0.50
C7H6O7	202.0114	0.37	0.71	0.86	1.00
C8H6O7	214.0114	0.69	0.86	0.75	0.88
C10H6O5	206.0215	3.45	1.00	0.60	0.50
C5H6O5	146.0215	0.63	0.60	1.20	1.00
C4H2O4	113.9953	0.36	1.00	0.50	1.00
C7H6O6	186.0164	0.61	0.83	0.86	0.86
C5H4O6	160.0008	0.36	0.67	0.80	1.20
C8H6O8	230.0063	1.14	0.75	0.75	1.00
C7H6O5	170.0215	0.99	1.00	0.86	0.71
C8H8O7	216.0270	0.38	0.71	1.00	0.88
C5H4O4	128.0110	0.69	1.00	0.80	0.80
C6H4O7	187.9957	0.36	0.71	0.67	1.17
C10H8O5	208.0372	2.04	1.00	0.80	0.50
C8H6O6	198.0164	0.68	1.00	0.75	0.75
C10H6O6	222.0164	2.81	1.00	0.60	0.60
C9H6O4	178.0266	2.07	1.00	0.67	0.44
C9H6O8	242.0063	2.61	0.88	0.67	0.89
C9H8O4	180.0423	2.72	1.00	0.89	0.44
C10H8O5	208.0372	1.18	1.00	0.80	0.50
C7H6O3	138.0317	3.09	1.00	0.86	0.43
C10H6O7	238.0114	2.57	1.00	0.60	0.70
C5H6O3	114.0317	0.39	1.00	1.20	0.60
C6H4O5	156.0059	0.37	1.00	0.67	0.83
C6H8O5	160.0372	0.38	0.60	1.33	0.83
C8H6O4	166.0266	1.34	1.00	0.75	0.50
C6H6O5	158.0215	0.59	0.80	1.00	0.83
C8H6O6	198.0164	2.58	1.00	0.75	0.75
C5H4O4	128.0110	1.48	1.00	0.80	0.80
C8H6O5	182.0215	2.82	1.00	0.75	0.63
C9H6O7	226.0114	2.73	1.00	0.67	0.78
C9H8O6	212.0321	2.41	1.00	0.89	0.67
C7H6O5	170.0215	1.31	1.00	0.86	0.71
C11H12O5	224.0685	2.49	1.00	1.09	0.45
C9H6O7	226.0114	0.40	1.00	0.67	0.78
C8H6O3	150.0317	0.85	1.00	0.75	0.38
C10H8O5	208.0372	0.73	1.00	0.80	0.50
C10H6O6	222.0164	2.59	1.00	0.60	0.60
C9H8O5	196.0372	4.16	1.00	0.89	0.56
C6H4O4	140.0110	0.37	1.00	0.67	0.67
C6H6O	94.0419	3.59	1.00	1.00	0.17
C8H8O3	152.0473	2.93	1.00	1.00	0.38
C10H10O4	194.0579	3.68	1.00	1.00	0.40
C10H8O6	224.0321	2.49	1.00	0.80	0.60
C8H8O6	200.0321	0.38	0.83	1.00	0.75
C9H6O3	162.0317	3.92	1.00	0.67	0.33
C9H6O5	194.0215	3.23	1.00	0.67	0.56
C10H6O6	222.0164	3.64	1.00	0.60	0.60
C4H2O5	129.9902	0.35	0.80	0.50	1.25
C11H8O6	236.0321	2.76	1.00	0.73	0.55
C7H6O2	122.0368	0.85	1.00	0.86	0.29
C9H8O6	212.0321	0.57	1.00	0.89	0.67
C9H8O2	148.0524	3.83	1.00	0.89	0.22
C6H8O4	144.0423	0.38	0.75	1.33	0.67
C6H4O6	172.0008	0.75	0.83	0.67	1.00
C10H8O6	224.0321	1.70	1.00	0.80	0.60
C9H8O6	212.0321	1.57	1.00	0.89	0.67
C7H4O6	184.0008	0.38	1.00	0.57	0.86
C9H4O5	192.0059	2.97	1.00	0.44	0.56
C10H10O5	210.0528	0.58	1.00	1.00	0.50
C10H8O2	160.0524	5.48	1.00	0.80	0.20
C6H4O5	156.0059	1.08	1.00	0.67	0.83
C19H12O5	320.0685	7.47	1.00	0.63	0.26
C10H8O7	240.0270	2.55	1.00	0.80	0.70
C11H8O6	236.0321	2.51	1.00	0.73	0.55
C8H4O7	211.9957	1.34	1.00	0.50	0.88
C6H6O4	142.0266	0.69	1.00	1.00	0.67

7 Appendix

C8H6O8	230.0063	0.58	0.75	0.75	1.00
C11H12O7	256.0583	1.96	0.86	1.09	0.64
C8H8O5	184.0372	0.40	1.00	1.00	0.63
C10H6O8	254.0063	2.68	1.00	0.60	0.80
C9H6O7	226.0114	2.41	1.00	0.67	0.78
C10H6O7	238.0114	2.94	1.00	0.60	0.70
C6H6O3	126.0317	0.78	1.00	1.00	0.50
C9H8O	132.0575	3.12	1.00	0.89	0.11
C3H2O2	70.0055	0.36	1.00	0.67	0.67
C8H8O4	168.0423	2.32	1.00	1.00	0.50
C5H2O5	141.9902	0.39	1.00	0.40	1.00
C9H10O4	182.0579	1.16	1.00	1.11	0.44
C6H4O4	140.0110	0.73	1.00	0.67	0.67
C10H8O3	176.0473	4.08	1.00	0.80	0.30
C8H6O2	134.0368	2.96	1.00	0.75	0.25
C11H10O7	254.0427	2.79	1.00	0.91	0.64
C10H6O6	222.0164	3.14	1.00	0.60	0.60
C11H12O6	240.0634	0.95	1.00	1.09	0.55
C11H14O6	242.0790	1.19	0.83	1.27	0.55
C5H2O4	125.9953	0.36	1.00	0.40	0.80
C9H6O7	226.0114	0.89	1.00	0.67	0.78
C10H6O5	206.0215	1.72	1.00	0.60	0.50
C7H6O	106.0419	0.85	1.00	0.86	0.14
C10H8O7	240.0270	1.82	1.00	0.80	0.70
C11H10O7	254.0427	1.09	1.00	0.91	0.64
C10H10O4	194.0579	2.94	1.00	1.00	0.40
C9H6O3	162.0317	1.15	1.00	0.67	0.33
C10H10O7	242.0427	2.45	0.86	1.00	0.70
C11H10O6	238.0477	2.72	1.00	0.91	0.55
C10H8O7	240.0270	2.92	1.00	0.80	0.70
C8H4O6	196.0008	0.36	1.00	0.50	0.75
C11H8O3	188.0473	5.57	1.00	0.73	0.27
C7H4O5	168.0059	1.23	1.00	0.57	0.71
C7H8O4	156.0423	0.38	1.00	1.14	0.57
C9H8O	132.0575	3.51	1.00	0.89	0.11
C11H10O5	222.0528	2.97	1.00	0.91	0.45
C13H8O6	260.0321	4.66	1.00	0.62	0.46
C11H12O7	256.0583	1.04	0.86	1.09	0.64
C9H8O2	148.0524	4.08	1.00	0.89	0.22
C7H4O5	168.0059	0.37	1.00	0.57	0.71
C6H4O3	124.0160	0.36	1.00	0.67	0.50
C9H10O4	182.0579	1.60	1.00	1.11	0.44
C9H10O5	198.0528	0.76	1.00	1.11	0.56
C5H4O2	96.0211	0.38	1.00	0.80	0.40
C9H6O3	162.0317	1.49	1.00	0.67	0.33
C11H10O6	238.0477	1.04	1.00	0.91	0.55
C5H4O3	112.0160	0.78	1.00	0.80	0.60
C6H6O2	110.0368	1.87	1.00	1.00	0.33
C6H6O2	110.0368	0.38	1.00	1.00	0.33
C11H8O4	204.0423	3.20	1.00	0.73	0.36
C10H10O3	178.0630	3.26	1.00	1.00	0.30
C14H10O8	306.0376	2.82	1.00	0.71	0.57
C11H10O5	222.0528	2.40	1.00	0.91	0.45
C6H6O2	110.0368	2.65	1.00	1.00	0.33
C7H8O	108.0575	3.33	1.00	1.14	0.14
C9H6O2	146.0368	1.18	1.00	0.67	0.22
C9H10O2	150.0681	2.82	1.00	1.11	0.22
C10H6O4	190.0266	1.65	1.00	0.60	0.40
C8H4O6	196.0008	2.35	1.00	0.50	0.75
C10H6O9	270.0012	2.79	0.89	0.60	0.90
C12H8O6	248.0321	2.90	1.00	0.67	0.50
C4H2O3	98.0004	0.37	1.00	0.50	0.75
C16H10O4	266.0579	3.26	1.00	0.63	0.25
C7H4O5	168.0059	0.57	1.00	0.57	0.71
C9H18O3	174.1256	7.50	0.33	2.00	0.33
C7H6O5	170.0215	2.66	1.00	0.86	0.71
C7H4O6	184.0008	1.19	1.00	0.57	0.86
C7H4O6	184.0008	0.80	1.00	0.57	0.86
C10H10O4	194.0579	0.96	1.00	1.00	0.40
C8H4O4	164.0110	0.61	1.00	0.50	0.50

7 Appendix

C6H2O5	153.9902	0.32	1.00	0.33	0.83
C9H4O7	223.9957	2.54	1.00	0.44	0.78
C15H10O4	254.0579	7.58	1.00	0.67	0.27
C15H10O8	318.0376	3.07	1.00	0.67	0.53
C9H6O2	146.0368	3.17	1.00	0.67	0.22
C10H6O5	206.0215	4.57	1.00	0.60	0.50
C7H4O6	184.0008	2.38	1.00	0.57	0.86
C6H6O2	110.0368	3.05	1.00	1.00	0.33
C6H6O	94.0419	1.15	1.00	1.00	0.17
C16H10O5	282.0528	5.51	1.00	0.63	0.31
C8H6O	118.0419	2.47	1.00	0.75	0.13
C16H24O8	344.1471	3.53	0.63	1.50	0.50
C3H2O3	86.0004	0.36	1.00	0.67	1.00
C18H12O9	372.0481	3.10	1.00	0.67	0.50
C8H4O5	180.0059	1.97	1.00	0.50	0.63
C12H10O6	250.0477	2.90	1.00	0.83	0.50
C10H8O2	160.0524	5.14	1.00	0.80	0.20
C3H2O	54.0106	0.37	1.00	0.67	0.33
C17H12O7	328.0583	3.26	1.00	0.71	0.41
C7H4O3	136.0160	1.28	1.00	0.57	0.43
C11H8O5	220.0372	3.14	1.00	0.73	0.45
C17H14O10	378.0587	3.01	1.00	0.82	0.59
C13H10O6	262.0477	2.99	1.00	0.77	0.46
C12H10O7	266.0427	2.57	1.00	0.83	0.58
C13H10O7	278.0427	2.80	1.00	0.77	0.54
C4H4O4	116.0110	3.04	0.75	1.00	1.00
C12H10O7	266.0427	2.79	1.00	0.83	0.58
C14H10O9	322.0325	2.76	1.00	0.71	0.64
C14H10O6	274.0477	3.12	1.00	0.71	0.43
C7H6O	106.0419	2.06	1.00	0.86	0.14
C7H4O4	152.0110	0.38	1.00	0.57	0.57
C5H4O	80.0262	0.38	1.00	0.80	0.20
C15H10O9	334.0325	2.93	1.00	0.67	0.60
C8H10O3	154.0630	1.62	1.00	1.25	0.38
C6H6O	94.0419	2.37	1.00	1.00	0.17
C15H12O7	304.0583	3.03	1.00	0.80	0.47
C15H10O6	286.0477	3.39	1.00	0.67	0.40
C10H12O5	212.0685	0.96	1.00	1.20	0.50
C11H6O7	250.0114	2.79	1.00	0.55	0.64
C14H12O8	308.0532	2.98	1.00	0.86	0.57
C4H2O	66.0106	0.37	1.00	0.50	0.25
C5H6O6	162.0164	2.74	0.50	1.20	1.20
C12H12O6	252.0634	2.92	1.00	1.00	0.50
C8H4O5	180.0059	0.42	1.00	0.50	0.63
C8H6O8	230.0063	2.83	0.75	0.75	1.00
C8H4O9	243.9855	0.54	0.78	0.50	1.13
C14H10O8	306.0376	2.58	1.00	0.71	0.57
C18H36O5	332.2563	8.00	0.20	2.00	0.28
C9H18O3	174.1256	5.21	0.33	2.00	0.33
C7H4O4	152.0110	1.32	1.00	0.57	0.57
C10H6O8	254.0063	0.74	1.00	0.60	0.80
C11H8O4	204.0423	4.03	1.00	0.73	0.36
C2H4O2	60.0211	2.96	0.50	2.00	1.00
C4H2O	66.0106	2.68	1.00	0.50	0.25
C11H6O7	250.0114	2.85	1.00	0.55	0.64
C11H12O4	208.0736	5.82	1.00	1.09	0.36
C10H10O8	258.0376	2.67	0.75	1.00	0.80
C10H12O5	212.0685	1.30	1.00	1.20	0.50
C12H10O7	266.0427	0.96	1.00	0.83	0.58
C9H6O9	258.0012	0.84	0.78	0.67	1.00
C8H10O6	202.0477	1.00	0.67	1.25	0.75
C4H4O	68.0262	2.43	1.00	1.00	0.25
C12H12O7	268.0583	0.67	1.00	1.00	0.58
C7H8O	108.0575	2.11	1.00	1.14	0.14
C8H10O4	170.0579	0.75	1.00	1.25	0.50
C20H18O10	418.0900	2.27	1.00	0.90	0.50
C9H10O7	230.0427	2.63	0.71	1.11	0.78
C8H8O	120.0575	1.16	1.00	1.00	0.13
C9H4O7	223.9957	1.03	1.00	0.44	0.78
C7H8O5	172.0372	1.82	0.80	1.14	0.71

7 Appendix

C3H4O	56.0262	1.47	1.00	1.33	0.33
C9H8O4	180.0423	3.24	1.00	0.89	0.44
C6H6O6	174.0164	0.36	0.67	1.00	1.00
C10H8O5	208.0372	3.32	1.00	0.80	0.50
C10H6O3	174.0317	3.76	1.00	0.60	0.30
C8H6O6	198.0164	1.25	1.00	0.75	0.75
C8H8O7	216.0270	0.37	0.71	1.00	0.88
C10H10O5	210.0528	2.98	1.00	1.00	0.50
C8H4O4	164.0110	2.79	1.00	0.50	0.50
C7H6O3	138.0317	4.17	1.00	0.86	0.43
C8H6O7	214.0114	1.37	0.86	0.75	0.88
C10H6O4	190.0266	3.61	1.00	0.60	0.40
C2H4O3	76.0160	2.88	0.33	2.00	1.50
C7H6O2	122.0368	2.96	1.00	0.86	0.29
C10H8O6	224.0321	0.92	1.00	0.80	0.60
C9H6O4	178.0266	3.51	1.00	0.67	0.44
C7H6O2	122.0368	2.37	1.00	0.86	0.29
C10H10O4	194.0579	3.28	1.00	1.00	0.40
C9H6O6	210.0164	1.33	1.00	0.67	0.67
C10H6O4	190.0266	4.32	1.00	0.60	0.40
C10H6O3	174.0317	2.76	1.00	0.60	0.30
C11H12O5	224.0685	2.96	1.00	1.09	0.45
C11H10O7	254.0427	2.78	1.00	0.91	0.64
C6H4O6	172.0008	1.03	0.83	0.67	1.00
C5H2O5	141.9902	0.37	1.00	0.40	1.00
C8H8O2	136.0524	2.11	1.00	1.00	0.25
C9H6O6	210.0164	2.83	1.00	0.67	0.67
C12H14O5	238.0841	3.46	1.00	1.17	0.42
C11H10O8	270.0376	3.07	0.88	0.91	0.73
C10H10O4	194.0579	4.38	1.00	1.00	0.40
C8H8O2	136.0524	2.78	1.00	1.00	0.25
C16H10O4	266.0579	3.44	1.00	0.63	0.25
C18H10O8	354.0376	3.48	1.00	0.56	0.44
C11H6O6	234.0164	3.23	1.00	0.55	0.55
C18H12O4	292.0736	7.66	1.00	0.67	0.22
C10H8O8	256.0219	2.85	0.88	0.80	0.80
C12H10O5	234.0528	2.81	1.00	0.83	0.42
C13H10O5	246.0528	3.06	1.00	0.77	0.38
C12H8O5	232.0372	3.82	1.00	0.67	0.42
C16H10O9	346.0325	3.04	1.00	0.63	0.56
C13H10O3	214.0630	6.83	1.00	0.77	0.23
C7H8O3	140.0473	0.37	1.00	1.14	0.43
C10H8O2	160.0524	7.62	1.00	0.80	0.20
C8H4O5	180.0059	2.95	1.00	0.50	0.63
C11H8O3	188.0473	7.80	1.00	0.73	0.27
C7H6O	106.0419	3.05	1.00	0.86	0.14
C8H8O5	184.0372	1.50	1.00	1.00	0.63
C14H10O6	274.0477	3.43	1.00	0.71	0.43
C18H12O4	292.0736	7.22	1.00	0.67	0.22
C10H10O7	242.0427	3.19	0.86	1.00	0.70
C11H6O5	218.0215	2.81	1.00	0.55	0.45
C8H6O8	230.0063	2.32	0.75	0.75	1.00
C12H8O5	232.0372	3.03	1.00	0.67	0.42
C16H12O6	300.0634	3.16	1.00	0.75	0.38
C15H12O7	304.0583	3.17	1.00	0.80	0.47
C9H4O5	192.0059	2.76	1.00	0.44	0.56
C14H10O7	290.0427	3.28	1.00	0.71	0.50
C18H12O5	308.0685	7.88	1.00	0.67	0.28
C9H6O2	146.0368	4.32	1.00	0.67	0.22
C18H16O7	344.0896	3.84	1.00	0.89	0.39
C11H6O6	234.0164	2.86	1.00	0.55	0.55
C14H12O7	292.0583	2.86	1.00	0.86	0.50
C17H12O6	312.0634	6.41	1.00	0.71	0.35
C6H6O5	158.0215	0.95	0.80	1.00	0.83
C16H14O9	350.0638	2.97	1.00	0.88	0.56
C11H8O6	236.0321	3.15	1.00	0.73	0.55
C18H12O7	340.0583	3.73	1.00	0.67	0.39
C13H10O7	278.0427	2.49	1.00	0.77	0.54
C9H10O5	198.0528	3.31	1.00	1.11	0.56
C16H10O4	266.0579	4.06	1.00	0.63	0.25

7 Appendix

C6H6O2	110.0368	0.93	1.00	1.00	0.33
C11H8O5	220.0372	3.56	1.00	0.73	0.45
C19H16O9	388.0794	3.09	1.00	0.84	0.47
C14H10O5	258.0528	3.34	1.00	0.71	0.36
C18H12O10	388.0430	3.02	1.00	0.67	0.56
C17H14O8	346.0689	3.00	1.00	0.82	0.47
C15H10O7	302.0427	3.26	1.00	0.67	0.47
C17H10O6	310.0477	6.67	1.00	0.59	0.35
C18H12O4	292.0736	8.17	1.00	0.67	0.22
C11H8O3	188.0473	7.34	1.00	0.73	0.27
C19H12O4	304.0736	6.99	1.00	0.63	0.21
C19H14O7	354.0740	4.21	1.00	0.74	0.37
C9H10O2	150.0681	3.68	1.00	1.11	0.22
C17H12O5	296.0685	5.44	1.00	0.71	0.29
C16H10O4	266.0579	7.40	1.00	0.63	0.25
C15H12O6	288.0634	3.06	1.00	0.80	0.40
C17H12O10	376.0430	2.98	1.00	0.71	0.59
C16H12O7	316.0583	3.16	1.00	0.75	0.44
C13H8O7	276.0270	3.13	1.00	0.62	0.54
C17H10O6	310.0477	7.29	1.00	0.59	0.35
C19H10O6	334.0477	7.33	1.00	0.53	0.32
C12H8O6	248.0321	3.19	1.00	0.67	0.50
C16H10O5	282.0528	3.07	1.00	0.63	0.31
C18H12O3	276.0786	7.93	1.00	0.67	0.17
C14H12O7	292.0583	2.78	1.00	0.86	0.50
C18H16O8	360.0845	2.12	1.00	0.89	0.44
C15H10O9	334.0325	2.78	1.00	0.67	0.60
C6H14O6	182.0790	0.03	0.00	2.33	1.00
C9H18O3	174.1256	6.59	0.33	2.00	0.33
C16H10O7	314.0427	3.48	1.00	0.63	0.44
C8H4O6	196.0008	2.62	1.00	0.50	0.75
C11H14O6	242.0790	1.69	0.83	1.27	0.55
C7H8O	108.0575	2.97	1.00	1.14	0.14
C11H10O4	206.0579	6.28	1.00	0.91	0.36
C18H12O9	372.0481	3.40	1.00	0.67	0.50
C19H12O4	304.0736	7.74	1.00	0.63	0.21
C17H12O6	312.0634	6.83	1.00	0.71	0.35
C11H10O4	206.0579	2.96	1.00	0.91	0.36
C18H12O6	324.0634	7.15	1.00	0.67	0.33
C16H10O7	314.0427	3.13	1.00	0.63	0.44
C13H12O7	280.0583	3.03	1.00	0.92	0.54
C12H12O7	268.0583	2.79	1.00	1.00	0.58
C18H10O9	370.0325	3.09	1.00	0.56	0.50
C9H6O2	146.0368	6.99	1.00	0.67	0.22
C18H12O11	404.0380	3.02	1.00	0.67	0.61
C13H8O8	292.0219	3.20	1.00	0.62	0.62
C18H14O7	342.0740	5.31	1.00	0.78	0.39
C9H4O6	208.0008	2.33	1.00	0.44	0.67
C19H14O11	418.0536	3.02	1.00	0.74	0.58
C19H12O5	320.0685	6.93	1.00	0.63	0.26
C10H6O3	174.0317	1.01	1.00	0.60	0.30
C12H12O6	252.0634	2.79	1.00	1.00	0.50
C10H8O2	160.0524	6.91	1.00	0.80	0.20
C4H6O3	102.0317	1.23	0.67	1.50	0.75
C12H8O6	248.0321	7.27	1.00	0.67	0.50
C16H12O6	300.0634	3.51	1.00	0.75	0.38
C14H12O8	308.0532	2.38	1.00	0.86	0.57
C20H12O6	348.0634	7.33	1.00	0.60	0.30
C11H8O2	172.0524	6.87	1.00	0.73	0.18
C15H12O5	272.0685	7.19	1.00	0.80	0.33
C6H6O7	190.0114	0.71	0.57	1.00	1.17
C10H6O6	222.0164	0.57	1.00	0.60	0.60
C14H12O6	276.0634	2.99	1.00	0.86	0.43
C19H18O9	390.0951	2.14	1.00	0.95	0.47
C6H4O7	187.9957	0.60	0.71	0.67	1.17
C16H10O10	362.0274	3.04	1.00	0.63	0.63
C13H12O6	264.0634	3.06	1.00	0.92	0.46
C13H8O7	276.0270	2.85	1.00	0.62	0.54
C16H14O7	318.0740	2.97	1.00	0.88	0.44
C14H8O7	288.0270	3.00	1.00	0.57	0.50

7 Appendix

C18H1007	338.0427	3.75	1.00	0.56	0.39
C17H16O10	380.0743	2.71	1.00	0.94	0.59
C20H14O5	334.0841	7.51	1.00	0.70	0.25
C12H8O8	280.0219	2.93	1.00	0.67	0.67
C16H10O4	266.0579	7.94	1.00	0.63	0.25
C12H8O5	232.0372	7.35	1.00	0.67	0.42
C17H14O8	346.0689	3.35	1.00	0.82	0.47
C12H8O3	200.0473	5.52	1.00	0.67	0.25
C13H8O4	228.0423	5.40	1.00	0.62	0.31
C16H10O5	282.0528	4.77	1.00	0.63	0.31
C10H8O2	160.0524	3.45	1.00	0.80	0.20
C15H10O3	238.0630	7.36	1.00	0.67	0.20
C8H16O3	160.1099	3.03	0.33	2.00	0.38
C8H4O5	180.0059	2.46	1.00	0.50	0.63
C6H4O5	156.0059	2.78	1.00	0.67	0.83
C19H18O8	374.1002	3.83	1.00	0.95	0.42
C5H4O4	128.0110	3.10	1.00	0.80	0.80
C18H12O11	404.0380	2.72	1.00	0.67	0.61
C14H10O9	322.0325	1.21	1.00	0.71	0.64
C12H8O3	200.0473	2.95	1.00	0.67	0.25
C14H12O9	324.0481	2.44	1.00	0.86	0.64
C12H14O7	270.0740	2.17	0.86	1.17	0.58
C18H14O5	310.0841	6.84	1.00	0.78	0.28
C15H14O7	306.0740	3.04	1.00	0.93	0.47
C17H10O6	310.0477	4.26	1.00	0.59	0.35
C8H4O5	180.0059	2.45	1.00	0.50	0.63
C4H8O5	136.0372	6.84	0.20	2.00	1.25
C4H2O6	145.9851	0.38	0.67	0.50	1.50
C18H12O7	340.0583	4.65	1.00	0.67	0.39
C9H16O3	172.1099	3.62	0.67	1.78	0.33
C3H2O	54.0106	2.67	1.00	0.67	0.33
C11H12O7	256.0583	3.23	0.86	1.09	0.64
C6H6O5	158.0215	2.61	0.80	1.00	0.83
C6H6O6	174.0164	2.88	0.67	1.00	1.00
C14H8O7	288.0270	3.28	1.00	0.57	0.50
C9H6O2	146.0368	2.68	1.00	0.67	0.22
C6H6O5	158.0215	2.98	0.80	1.00	0.83
C17H10O8	342.0376	3.23	1.00	0.59	0.47
C16H8O8	328.0219	6.47	1.00	0.50	0.50
C7H8O5	172.0372	2.45	0.80	1.14	0.71
C6H12O6	180.0634	7.47	0.17	2.00	1.00
C12H14O8	286.0689	2.74	0.75	1.17	0.67
C19H16O9	388.0794	1.89	1.00	0.84	0.47
C14H14O8	310.0689	2.94	1.00	1.00	0.57
C14H14O8	310.0689	2.94	1.00	1.00	0.57
C14H10O7	290.0427	2.54	1.00	0.71	0.50
C5H6O5	146.0215	2.62	0.60	1.20	1.00
C12H12O7	268.0583	2.57	1.00	1.00	0.58
C13H10O5	246.0528	3.35	1.00	0.77	0.38
C10H10O8	258.0376	2.69	0.75	1.00	0.80
C9H8O6	212.0321	3.63	1.00	0.89	0.67
C15H10O6	286.0477	7.62	1.00	0.67	0.40
C4H4O2	84.0211	0.74	1.00	1.00	0.50
C13H10O9	310.0325	2.56	1.00	0.77	0.69
C11H8O3	188.0473	6.66	1.00	0.73	0.27
C10H12O6	228.0634	0.84	0.83	1.20	0.60
C7H12O4	160.0736	0.92	0.50	1.71	0.57
C18H12O8	356.0532	1.86	1.00	0.67	0.44
C13H14O8	298.0689	0.90	0.88	1.08	0.62
C10H6O7	238.0114	0.77	1.00	0.60	0.70
C9H10O9	262.0325	0.84	0.56	1.11	1.00
C8H10O4	170.0579	0.49	1.00	1.25	0.50
C9H10O8	246.0376	0.99	0.63	1.11	0.89
C9H10O8	246.0376	0.99	0.63	1.11	0.89
C10H8O2	160.0524	4.37	1.00	0.80	0.20
C7H8O	108.0575	1.41	1.00	1.14	0.14
C12H6O4	214.0266	4.70	1.00	0.50	0.33
C12H8O8	280.0219	2.50	1.00	0.67	0.67
C15H14O7	306.0740	2.80	1.00	0.93	0.47
C17H16O9	364.0794	2.16	1.00	0.94	0.53

7 Appendix

C7H6O9	234.0012	0.84	0.56	0.86	1.29
C7H14O3	146.0943	0.73	0.33	2.00	0.43
C17H12O5	296.0685	3.48	1.00	0.71	0.29
C7H6O6	186.0164	2.74	0.83	0.86	0.86
C13H12O9	312.0481	0.74	0.89	0.92	0.69
C17H14O10	378.0587	0.96	1.00	0.82	0.59
C6H6O7	190.0114	1.03	0.57	1.00	1.17
C3H2O2	70.0055	2.83	1.00	0.67	0.67
C9H8O10	276.0117	0.79	0.60	0.89	1.11
C10H10O8	258.0376	2.29	0.75	1.00	0.80
C10H4O5	204.0059	1.34	1.00	0.40	0.50
C12H12O8	284.0532	2.59	0.88	1.00	0.67
C7H6O8	218.0063	0.88	0.63	0.86	1.14
C7H8O10	252.0117	0.91	0.40	1.14	1.43
C14H12O9	324.0481	0.58	1.00	0.86	0.64
C3H4O2	72.0211	4.22	1.00	1.33	0.67
C8H4O8	227.9906	1.11	0.88	0.50	1.00
C9H10O3	166.0630	1.55	1.00	1.11	0.33
C16H14O10	366.0587	0.82	1.00	0.88	0.63
C7H14O3	146.0943	8.72	0.33	2.00	0.43
C5H4O	80.0262	0.76	1.00	0.80	0.20
C8H4O6	196.0008	1.96	1.00	0.50	0.75
C7H4O6	184.0008	1.79	1.00	0.57	0.86
C8H6O6	198.0164	8.82	1.00	0.75	0.75
C7H8O2	124.0524	0.02	1.00	1.14	0.29
C7H12O4	160.0736	8.82	0.50	1.71	0.57
C5H8O5	148.0372	0.43	0.40	1.60	1.00
C3H6O4	106.0266	0.37	0.25	2.00	1.33
C3H4O4	104.0110	0.38	0.50	1.33	1.33
C4H4O4	116.0110	0.41	0.75	1.00	1.00
C8H8O2	136.0524	3.14	1.00	1.00	0.25

D. List of related publications and presentations

Peer-reviewed publications:

Zhang Y., Wang K., Tong H.J., Huang R.J., and Hoffmann T.: The maximum carbonyl ratio (MCR) as a new index for the structural classification of secondary organic aerosol components. *Rapid Commun. Mass Spectrom.*, **2021**, 35, e9113.

Wang K., Huang, R. J., Brüggemann M., Zhang, Y., Yang L., Ni H. Y., Guo J., Han J. J., Bilde M., Glasius M., and Hoffmann T.: Urban organic aerosol composition in Eastern China differs from North to South: Molecular insight from a liquid chromatography-Orbitrap mass spectrometry study. *Atmos. Chem. Phys.*, **2021**, 21, 9089-9104.

Tong H. J., Liu F. B., Filippi A., Wilson J., Arangio A. M., Zhang. Y., Yue S. Y., Lelieveld S., Shen F. X., Keskinen H. K., Li J., Chen H. X., Zhang T., Hoffmann T., Fu P. Q., Brune W. H., Petäjä T., Kulmala M., Yao M. S., Berkemeier T., Shiraiwa M., and Pöschl U.: Reactive species formed upon interaction of water with fine particulate matter from remote forest and polluted urban air. *Atmos. Chem. Phys.*, under review, **2021**.

Tong H. J., Zhang. Y., Filippi A., Wang T., Li C. P., Liu F. B., Leppla D., Kourtchev I., Wang K., Keskinen H. K., Levula J. T., Arangio A. M., Shen F. X., Ditas F., Martin S. T., Artaxo P., Godoi R. H. M., Yamamoto C. I., Souza R. A. F., Huang, R. J., Berkemeier T., Wang Y. S., Su H., Cheng Y. F., Pope F. D., Fu P. Q., Yao M. S., Pöhlker C., Petäjä T., Kulmala M., Andreae M. O., Shiraiwa M., Pöschl U., Hoffmann T., and Kalberer M.: Radical formation by fine particulate matter associated with highly oxygenated molecules. *Environ. Sci. Technol.*, **2019**, 53, 21, 12506-12518.

Wang K., Zhang Y., Huang R. J., Wang M., Ni H. Y., Kampf C., Cheng Y. F., Bilde M., Glasius M., and Hoffmann T.: Molecular characterization and source identification of atmospheric particulate organosulfates using ultrahigh resolution mass spectrometry. *Environ. Sci. Technol.*, **2019**, 53, 11, 6192-6202.

Wang K., Zhang Y., Huang R. J., Cao, J. J., and Hoffmann T.: UHPLC- Orbitrap mass spectrometric characterization of organic aerosol from a central European city (Mainz, Germany) and a Chinese megacity (Beijing). *Atmos. Environ.*, **2018**, 189, 22-29.

Presentations:

Zhang Y., Wang K., Tong H. J., and Hoffmann, T.: H₂O₂ formation by PM_{2.5} associated with highly oxygenated molecules. *European Aerosol Conference*, online, September 2020, post presentation.

Zhang. Y., Wang K., Lelieveld S., Ren H., Li L. J., Yue S. Y., Fu P. Q., Pöschl U., and Tong H. J., and Hoffmann T.: Organic chemical composition by Orbitrap MS and oxidative potential of particulate aerosols. *Asian Aerosol Conference*, Hong Kong, China, May 2019, oral presentation.

Zhang. Y., Wang K., Lelieveld S., Ren H., Li L. J., Yue S. Y., Fu P. Q., Pöschl U., Hoffmann T., and Tong H. J.: Organic chemical composition and oxidative potential of Beijing PM_{2.5}. *American Geophysical Union Joint International Network in Geoscience Meeting*, Xi'an, China, October 2018, oral presentation.

E. Acknowledgements

In this section, I would like to thank all the people, who supported, guided and accompanied me during the time of my PhD studies:

First, I would like to thank my supervisor Prof. Dr. Thorsten Hoffmann for giving the opportunity to work on this diversified and exciting research project. I sincerely appreciate his continuous supports and the freedom to pursue own research goals. Especially, the discussions with him not only inspire me on the academic research but also positively influence my view on the science. I am also very thankful for the possibility to participate in research cooperation, Sino-European school, international conferences, workshops and scientific seminars.

I also like to thank Dr. Haijie Tong and Prof. Ulrich Pöschl from Max Planck Institute for Chemistry (MPIC) for the possibility to participate in several exciting research projects and giving great ideas on my project. I am very thankful for the valuable cooperation and all the great support during my PhD studies.

Thanks to Prof. Rujin Huang from Chinese Academy of Sciences in Xi'an, Prof. Pingqing Fu from Tianjin University and Assoc. Prof. Fangxia Shen from Beihang University for providing the aerosol samples. I like to thank Kai Wang for the help on PhD position application, the suggestion on analytical method development, the help on Orbitrap instrument operation, and advices on manuscript preparation. I also like to thank Denis Leppla for the suggestion on data processing. Moreover, I would like to thank Alexander Filippi, Steven Lelieveld, Fobang Liu in MPIC for many productive cooperations and the help on the experiments in MPIC.

Special thanks to all current and former members of the workgroup Hoffmann for the productive working environment and a great time, as well as my friends in Mainz for making my life more colorful.

Finally, I would like to thank my family, close friends for their ongoing support all the time. Last but not least, I deeply thank my husband Kai Wang for his love, encouragement and support all the time.

F. Curriculum vitae

Personal Information

Name: Yun Zhang
Date of birth: 09 January 1991
Place of birth: Tianjin, China

Education

02/2017–06/2021 Ph.D, Atmospheric Chemistry
Institute of Inorganic Chemistry and Analytical Chemistry
Johannes Gutenberg University Mainz, Germany
Workgroup of Prof. Dr. Thorsten Hoffmann

09/2013–07/2015 Master of Science, Analytical Chemistry in Pesticide Science
China Agricultural University, China
Workgroup of Prof. Dr. Hongyan Zhang

09/2009–07/2013 Bachelor of Science, Chemistry
China Agricultural University, China

Awards & Achievements

07/2017–07/2020 Scholarship of the China Scholarship Council (CSC)

06/2015 Outstanding graduate award for master students

12/2014 National scholarship for graduate students

06/2013 Outstanding graduate award for bachelor students